Wissenschaftszentrum Weihenstephan für Ernährung, Landnutzung und Umwelt

Lehrstuhl für Experimentelle Genetik

Molecular impact of metformin on hepatocellular metabolism

Caroline Leonie Muschet

Vollständiger Abdruck der von der Fakultät Wissenschaftszentrum Weihenstephan für Ernährung, Landnutzung und Umwelt der Technischen Universität München zur Erlangung des akademischen Grades eines

Doktors der Naturwissenschaften

genehmigten Dissertation.

Vorsitzender: Prof. Dr. Wilfried Schwab

Prüfer der Dissertation:

1. apl. Prof. Dr. Jerzy Adamski
2. Prof. Dr. Michael Rychlik

Die Dissertation wurde am 28. 12. 2016 bei der Technischen Universität München eingereicht und durch die Fakultät Wissenschaftszentrum Weihenstephan für Ernährung, Landnutzung und Umwelt am 10. 05. 2017 angenommen.

Table of contents

ABSTRACT **IV**

ZUSAMMENFASSUNG **V**

ABBREVIATIONS **VII**

1. INTRODUCTION **1**

1.1. Diabetes mellitus **1**
1.1.1. Definition and classification of type 2 diabetes 1
1.1.2. Epidemiology of T2D 2
1.1.3. T2D and the hepatocellular carcinoma 2
1.1.4. Treatment of T2D 3
1.2. Metformin **4**
1.2.1. Chemical properties 4
1.2.2. Pharmacokinetics 4
1.2.3. Hepatocellular metformin transport 4
1.2.4. The core signal transduction pathway of molecular metformin action 6
1.2.5. Metformin and metabolism 7
1.2.6. Metformin and the hepatocellular carcinoma 9
1.3. Tracking biology with instrumental analytics: Cell culture metabolomics **10**
1.3.1. Metabolomics 10
1.3.2. Cell culture metabolomics 11
1.4. Aim of the thesis **13**

2. MATERIAL AND METHODS **14**

2.1. Mammalian cell lines **14**
2.2. Chemicals, reagents, media, supplements, solutions and solvents **14**
2.3. Consumables **15**
2.4. Kits **15**
2.5. Equipment **15**
2.6. Software and servers **16**
2.7. Cultivation and storage of mammalian cell lines **17**
2.7.1. Thawing 17
2.7.2. Cultivation 17
2.7.3. Differentiation 18
2.7.4. Storage 18
2.8. Cell harvest and metabolite extraction **18**
2.9. Fluorescence based DNA quantification and cell number determination of metabolomics samples **19**
2.9.1. Development and optimization of the fluorescence based DNA quantification assay 19
2.9.2. Optimized fluorescence based DNA quantification and cell number determination 21
2.9.3. Generation of standard curves 21
2.10. Optimization and validation of cell culture metabolomics **22**
2.10.1. Targeted cell culture metabolomics 22
2.10.2. Non-targeted cell culture metabolomics 22
2.11. Elucidation of hepatocellular metformin transport **23**
2.11.1. Design of the experimental setup 23
2.11.2. Inhibition of metformin transporters 24
2.12. Transporter expression analyses in mammalian cell lines **24**
2.12.1. RNA isolation 24
2.12.2. cDNA synthesis 25
2.12.3. Polymerase chain reaction (PCR) 25
2.13. Elucidation of the impact of glucose and metformin on the hepatocellular metabolome **26**
2.13.1. Determination of the optimal metformin concentration 26
2.13.2. Pre-evaluation of the impact of the glucose concentration on the hepatocellular metabolome. 27
2.13.3. Elucidaton of the impact of glucose and metformin on the hepatocellular metabolome. 28

2.14. LC-MS/MS based metformin quantification 31
2.14.1. Validation of the LC-MS/MS based metformin quantification method 32
2.15. Targeted metabolomics analyses 34
2.16. Non-targeted metabolomics analyses 35
2.17. Calculations, statistical analyses and data evaluation 36
2.17.1. Calculation of validation parameters of analytical methods 37
2.17.2. Normalization of MS measurements 37
2.17.3. Calculation of kinetic parameters 38
2.17.4. Assessment of chemical similarity 38
2.17.5. Statistics 39
2.18. Nomenclature 40

3. RESULTS 41
3.1. Validation of the LC-MS/MS based metformin quantification method 41
3.1.1. General parameters of the LC-MS/MS based metformin quantification method 42
3.1.2. The LC-MS/MS based metformin quantification method for cell culture matrices 46
3.2. Development, optimization and implementation of a fast, fluorescence based DNA quantification method for cell number determination in metabolomics samples 49
3.2.1. Development and optimization of the fluorescence-based DNA quantification method 50
3.2.2. Assessing the applicability of the optimized fluorescence-based DNA quantification method to cell culture metabolomics 53
3.3. Optimization and validation of cell culture metabolomics 57
3.3.1. Targeted cell culture metabolomics 57
3.3.2. Non-targeted cell culture metabolomics 63
3.4. Elucidation of the hepatocellular metformin transport 70
3.4.1. Design of the experimental setup 70
3.4.2. Characteristics of the hepatocellular metformin transport 73
3.4.3. Expression analyses and inhibition studies of potential metformin transporters 74
3.5. Elucidation of the impact glucose and metformin on the cellular metabolome 81
3.5.1. The experimental setup 81
3.5.2. Impact of metformin and glucose concentration on the hepatocellular metabolism 87
3.5.3. The impact of the glucose concentration on the metabolome of THLE-2 cells 92
3.5.4. The impact of the glucose concentration on the metabolome of Hep G2 cells 92
3.5.5. The impact of metformin on the metabolome of THLE-2 cells cultivated at a physiological glucose concentration 93
3.5.6. The impact of metformin on the metabolome of Hep G2 cells cultivated at a physiological glucose concentration 93
3.5.7. The impact of metformin on the metabolome of THLE-2 cells cultivated at a diabetic glucose concentration 94
3.5.8. The impact of metformin on the metabolome of Hep G2 cells cultivated at a diabetic glucose concentration 95

4. DISCUSSION 98
4.1 Method development, optimization, validation and implementation 98
4.1.1. LC-MS/MS based metformin quantification method 98
4.1.2. Fluorometric DNA based cell number determination method 100
4.1.3. Optimization of cell harvest and sample preparation for cell culture metabolomics 101
4.2. Looking for the needle in the haystack – hepatocellular metformin transport 104
4.3. Elucidation of the impact of glucose and metformin on the cellular metabolome 109
4.3.1. Glucose - the metabolic trigger? The impact of the glucose concentration on the hepatocellular metabolism 109
4.3.2. The impact of metformin on the hepatocellular metabolism at physiological glucose conditions 114
4.3.1. The impact of metformin on the hepatocellular metabolism at diabetic glucose conditions 118

5. REFERENCES 124
ACKNOWLEDGEMENTS 144
INDEX OF FIGURES 145
INDEX OF TABLES 146
APPENDIX 147
Expression analysis of potential metformin transporters in mammalian cell lines 147

Precision of the analyte concentration of targeted cell culture metabolomics (5 x 10^5 cells) **148**
Impact of metformin and glucose concentration on the hepatocellular metabolism **149**
List of metabolites above the LOD and/or the LLOQ for cells and cell culture supernatant, measured with targeted metabolomics 149
List of compounds and their HMDB IDs, covered by non-targeted metabolomics 153
Elucidation of the impact of glucose and metformin in the hepatocellular metabolism: Statistics 159
Publications and presentations **178**
Publications 178
Submitted publications 178
Master´s Thesis 178
Presentations 178
Poster presentations 178

Abstract

Type 2 diabetes (T2D) is a complex metabolic disorder characterized by a dysfunctional glucose homeostasis, which has become a major challenge in modern society and health care. The elucidation of its metabolic traits and implications is a vital prerequisite for the successful prevention and treatment of this disease. In this context, the anti-hyperglycaemic drug metformin has been established as an effective treatment of T2D for decades. However, its cellular and metabolic mode of action is still not completely understood. Further, there is growing evidence that metformin might have a potential as a cancer chemopreventive. In both, glucose homeostasis and metformin action, the liver plays a key role. Hence, the aim of this study is to analyze the hepatocellular metformin transport and metabolic action by using a global metabolomics-based approach.

The cell culture model system was chosen, because it allows for changing single parameters and monitoring their complex consequences in a tightly controlled setting. The first step was the development and optimization of a number of methods, which were vital to the realization of the study. An LC-MS/MS based metformin quantification method was developed and validated for cell culture matrices. Further, a fast and robust method for the normalization of metabolomics data from cell culture samples was developed and established. In addition, protocols for targeted and non-targeted cell culture metabolomics were adapted, optimized and partially validated.

The hepatocellular metformin transport was assessed by performing expression analyses in a number of cell lines and inhibitor studies targeting potential metformin transporters in Hep G2 cells. The hepatocellular metformin transport was found to consist of a saturable and a non-saturable component, indicating the coexistence of active and passive transport mechanisms. Further, the obtained results hinted at the potential role of the novel organic cation/carnitine/zwitterion transporter 1 (OCTN1), the plasma membrane monoamine transporter (PMAT) and the thiamine transporter 2 (THTR-2) in the hepatocellular metformin transport.

Although it is well known that metformin has a beneficial effect on the glucose metabolism, the impact of the available glucose concentration on the metformin action remains to be elucidated. To extent the understanding of the relationship between glucose and metformin in a diabetes and cancer related context, the liver cell line THLE-2 and the hepatoma cell line Hep G2 were cultivated at a physiological and a diabetic glucose concentration and treated with metformin. Then, targeted and non-targeted metabolomics analyses were performed. Glucose and metformin action were found to be strongly cell type specific. Whereas THLE-2 cells showed only a minor response, the elevation of the exogenous glucose concentration strongly affected the metabolome of the hepatoma cell line Hep G2. Metformin treatment correlated with a vast array of metabolic alterations. Among the affected pathways were the glutathione metabolism, the polyamine synthesis, the one-carbon metabolism, the glucose and glutamate metabolism, the lipid and the branched-chain amino acid metabolism. Interestingly, the drug-induced metabolic dysregulations strongly differed between the liver and the hepatoma cell line. In addition, the glucose concentration had an impact on the metabolic response to metformin treatment.

In conclusion, the results obtained in course of this study hint at the participation of a number of transporters in the hepatocellular metformin transport. Glucose as well as metformin action were found to differ between immortalized liver cells and hepatoma cells. Further, the relationship between glucose and metformin is dynamic and bidirectional.

Zusammenfassung

Typ 2 Diabetes (T2D) ist eine komplexe, von einer Dysfunktion der Glukosehomeostase gekennzeichnete, Stoffwechselstörung, die zu einer erheblichen Herausforderung der modernen Gesellschaft und des Gesundheitswesens geworden ist. Die Aufklärung ihrer metabolischen Merkmale und Auswirkungen ist eine grundlegende Voraussetzung für die erfolgreiche Prävention und Behandlung dieser Krankheit. In diesem Zusammenhang ist das anti-hyperglykämische Medikament Metformin seit Jahrzehnten als effektive Behandlung für T2D etabliert. Dennoch ist seine zelluläre und metabolische Wirkweise nach wie vor nicht vollständig geklärt. Zudem gibt es vermehrt Belege dafür, dass Metformin Potential in der Krebs-Chemoprävention haben könnte. Die Leber spielt sowohl in der Glukosehomeostase als auch in der Metforminwirkung eine entscheidende Rolle. Daher ist das Ziel dieser Studie die Analyse des hepatozellulären Metformintransportes und der metabolischen Wirkweise mittels eines umfassenden Metabolomics-basierten Ansatzes.

Das Zellkulturmodell wurde gewählt, da es es ermöglicht einzelne Parameter zu verändern und die komplexen Konsequenzen in einer streng kontrollierten Umgebung zu beobachten. Der erste Schritt war die Entwicklung und Optimierung einer Anzahl von Methoden, die grundlegend für die Umsetzung dieser Studie waren. Eine LC-MS/MS-basierte Metforminquantifizierungsmethode wurde entwickelt und für Zellkulturmatrizes validiert. Des Weiteren wurde eine schnelle und robuste Methode zur Normalisierung von Metabolomics-Datensätzen von Zellkulturproben entwickelt und etabliert. Zudem wurden Protokolle für targeted und non-targeted Zellkulturmetabolomics adaptiert, optimiert und teilweise validiert.

Der hepatozelluläre Metformintransport wurde mittels Expressionsanalysen in mehreren Zelllinien und Inhibitorstudien, die potentielle Metformintransporter in Hep G2 Zellen adressierten, untersucht. Der hepatozelluläre Metformintransport besteht aus einer sättigbaren und einer sättigungsfreien Komponente, was auf die Koexistenz von aktiven und passiven Transportmechanismen hindeutet. Zudem weisen die Ergebnisse auf eine mögliche Rolle des organischen Kationen/Carnitintransporters 1 (OCTN1), des Plasmamembran Monoamin-Transporters (PMAT) und des Thiamintransporters 2 (THTR-2) im hepatozellulärem Metformintransport hin.

Obwohl es bekannt ist, dass Metformin einen positiven Effekt auf den hepatozellulären Glukosemetabolismus ausübt, ist der Einfluss, den die verfügbare Glukosekonzentration auf die Metforminwirkung hat, bis dato ungeklärt. Um das Verständnis der Beziehung zwischen Glukose und Metformin im Zusammenhang mit Diabetes und Krebs zu erweitern, wurden die Leberzelllinie THLE-2 und die Leberkarzinomzelllinie Hep G2 bei einer physiologischen und einer diabetischen Glukosekonzentration kultiviert und mit Metformin behandelt. Daraufhin wurden targeted und non-targeted Metabolomicsanalysen durchgeführt. Die Glukose- und die Metforminwirkung waren stark zelltypspezifisch. Während THLE-2 Zellen nur eine geringfügige Antwort zeigten, hatte die Erhöhung der exogenen Glukosekonzentration einen großen Einfluss auf das Metabolom der Leberkarzinomzelllinie Hep G2. Die Metforminbehandlung korrelierte mit einer Vielzahl an metabolischen Änderungen. Unter den beinflussten Stoffwechselwegen befanden sich der Glutathion-Stoffwechsel, die Polyaminsynthese, der Ein-Kohlenstoff-Metabolismus, der Glukose- und Glutamat-Stoffwechsel, der Lipidmetabolismus und der Stoffwechsel verzweigtkettiger Aminosäuren. Die medikamenten-induzierten metabolischen Dysregulationen unterschieden sich stark zwischen der Leber- und der Leberkarzinomzelllinie. Zudem hatte die Glukosekonzentration

einen Einfluss auf die, durch die Metforminbehandlung hervorgerufene, metabolische Antwort.

Zusammenfassend lässt sich feststellen, dass die Ergebnisse dieser Studie darauf hinweisen, dass mehrere Transporter am hepatozellulären Metformintransport beteiligt sind. Sowohl die Glukose- als auch die Metforminwirkung unterschieden sich in immortalisierten Leberzellen und in Leberkarzinomzellen. Zudem ist die Beziehung zwischen Glukose und Metformin dynamisch und bidirektional.

Abbreviations

ACC	Acetyl-CoA carboxylase
ADMA	Asymmetric dimethylarginine
ADP	Adenosine diphosphate
α-AAA	alpha-amino adipic acid
AMP	Adenosine monophosphate
AMPD	Adenosine monophosphate deaminase
AMPK	AMP-activated protein kinase
ARE	Asymptotic relative efficiency
ASP^+	4-(4-Dimethylaminostyryl)-1-Methylpyridinium
ATP	Adenosine triphosphate
AUC	Area under the curve
CAT	Cationic amino acid transporter
CHT	Choline high-affinity transporter
CoA	Coenzyme A
cps	Counts per second
CPT	Carnitine palmitoyltransferase
CV	Coefficient of variation
DMEM	Dulbecco´s modified eagle medium
DMSO	Dimethyl sulfoxide
EC_{50}	Half maximal effective concentration
EDTA	Ethylenediaminetetraacetic acid
EMA	European Medicines Agency
ESI	Electrospray ionization
FA2H	Fatty acid 2-hydroxylase
FBS	Fetal bovine serum
FDA	Food and Drug Administration
FIA	Flow injection analysis
G6Pase	Glucose-6-phosphatase
GLUT	Glucose transporter
GSH	Glutathione (reduced)
GSSG	Glutathione (oxidized)
H1	Sum of hexoses
H_2O	Dihydrogen monoxide / water
HMDB	Human metabolome database
HPLC	High-performance liquid chromatography
IC_{50}	Half maximal inhibitory concentration
Inf	Infinite
IS	Internal standard
KEGG	Kyoto encyclopedia of genes and genomes
K_M	Michaelis constant
LC	Liquid chromatography
LKB1	Liver kinase B1
LOD	Lower limit of detection
LLOQ	Lower limit of quantification
MATE	Multi drug extrusion protein
MPP^+	1-methyl-4-phenylpyridinium
MRM	Multiple reaction monitoring
MS	Mass spectrometry
MSI	metabolomics standards initiative
MTT	Methylthiazolyldiphenyl-tetrazolium bromide
OCT	Organic cation transporter
OCTN	Novel organic cation/carnitine/zwitterion transporter
OXPHOS	Oxidative phosphorylation
m/z	Mass-to-charge ratio

n	Sample size per group
N	Total sample size
NA	Not available
PBS	Phosphate balanced saline
PCR	Polymerase chain reaction
PEPCK	Phosphoenolpyrovate carboxykinase
PMAT	Plasma membrane monoamine transporter
R^2	Coefficient of determination
rpm	Revolutions per minute
RT	Room temperature
RX	Organic halide
SAM	S-adenosylmethionine
SAH	S-adenosylhomocystein
SD	Standard deviation
SDMA	Symmetric dimethylarginine
SEM	Standard error of the mean
SERT	Serotonin reuptake transporter
SLC	Solute carrier
SMPDB	Small molecule pathway database
SOP	Standard operating procedure
T2D	Type 2 diabetes mellitus
TCA	Tricarboxylic acid cycle
TEA	Tetraethylammonium
THTR	Thiamine transporter
T_m	Melting temperature
Total DMA	Total dimethylarginine
ULOQ	Upper limit of quantification
U-test	Wilcoxon-Mann-Whitney test
x g	Times gravity

1. Introduction

1.1. Diabetes mellitus

Diabetes mellitus has been described as early on as 1,550 B.C. in the Ebers papyrus [1]. However, the term "diabetes" was introduced by Aretaeus of Cappadocia [1], [2]. It originates from the greek word "diabaino", which in translation means "run through" and refers to the polyuric character of the disease [1]–[3]. The term "mellitus" (honey), being of Latin origin, was coined in the 17th century by the British physician Thomas Willis and refers to the sweetness of the urine of the patients [1], [4]. About a century later, his landsman, the physician Matthew Dobson, could attribute the sweet taste to the excessive presence of sugar in the urine and blood of a patient [1], [4]. In 1788, Thomas Cawley first established a link between diabetes and pancreatic dysfunction [4]. In 1890, this link was firmly established by Joseph Freiherr von Mering and Oskar Minkowski [5]. In 1936, Sir Harold Percival Himsworth first described two different types of diabetes mellitus, an insulin sensitive and an insulin-insensitive one [6]. The first generally accepted systematic categorization of diabetes mellitus was published in 1979 by the National Diabetes Data Group [7], [8].

1.1.1. Definition and classification of type 2 diabetes

The term diabetes mellitus summarizes a plethora of metabolic diseases, which are characterized by hyperglycemia [8], [9]. This dysregulation of the glucose household is caused by dysfunctional insulin secretion and/or action [8], [9]. According to the American Diabetes Association, there are four different types of diabetes mellitus: type 1 diabetes, type 2 diabetes mellitus, gestational diabetes mellitus and other specific types [9]. The last type summarizes a broad range of different subtypes, namely, genetic defects of β-cell function (e.g. MODY1-6), genetic defects in insulin action, diseases of the exocrine pancreas, endocrinopathies, drug and chemical induced and infection induced diabetes, uncommon forms of immune-mediated diabetes and other genetic syndromes, which are sometimes associated with diabetes [9].

Type 2 diabetes mellitus (T2D) is characterized by gradually developing hyperglycemia in combination with relative insulin deficiency [9]. In detail, the hyperglycemia develops slowly, and the early stages of the disease are often not noticed by the patient. The insulin levels are normal or slightly elevated. However, if the elevated glucose levels are taken into account, the insulin levels should be far higher. This indicates a defective insulin secretion due to β-cell dysfunction. Further, the dysfunctional insulin secretion cannot compensate for the insulin resistance [9]. Insulin resistance is characterized by the resistance to the insulin-stimulated glucose uptake, which might be counteracted by chonically elevated levels of insulin secretion by the β-cells, termed hyperinsulinemia [10]. If this compensation does not suffice, the result is a deterioration of the glucose household. It is a hallmark of impaired glucose tolerance and T2D [10]. Nonetheless, insulin treatment is not required for

survival [9]. The predominant symptoms of T2D are excessive thirst, frequent urination, blurred vision and weight loss [11].

T2D is correlated with obesity, an increased percentage of abdominal fat, lack of physical activity, previous gestational diabetes, age and genetic factors [9]. In this regard, sedentary behaviour has been associated with an increased risk for developing T2D [12]. In detail, Hu *et al.* showed that watching TV for 2 h per day increased the T2D risk by 14% and the same time span spent sitting at work increased the T2D risk by 7% [12]. However, when the same period was spent with standing or walking around at home, the T2D risk was reduced by 12% and 1 h per day of brisk walking reduced the risk by 34% [12]. In addition, Shai *et al.* demonstrated that a 5 unit increase in BMI correlated with a relative risk of 1.55 to 2.36 for T2D diabetes in women [13]. Further, the analysis of the data from more than 73,000 women of the Nurses´ Health Study cohort showed that the precence of a family history of diabetes increased the relative risk to 2.27 [14]. However, participants with a family history of diabetes tended to have a higher BMI, which accounted for 21.1% of the observed association [14]. Based on the meta-analysis of 20 studies, an increased relative risk of 7.43 was determined for women, who suffered from gestational diabetes during pregnancy, when compared to women with a normoglycaemic pregnancy [15].

1.1.2. Epidemiology of T2D

In 2015, the estimated number of people with diabetes amounted to 415 million [11]. Consequently, diabetes exhibits a global prevalence of 8.8% [11]. The IDF Diabetes Atlas (7^{th} edition, 2015) [11] lists 215.2 million men and 199.5 million women, suffering from diabetes in 2015. However, the number of undiagnosed cases is estimated to amount to 193 million people [11]. T2D is the prevalent form of diabetes and accounts for approx. 90 - 95% of all diabetic incidents [9], [11]. Not surprisingly, diabetes and related complications have become a massive burden for modern health care. In 2015, 673 billion USD were spent on the treatment of diabetes in patients with an age of 20 to 79 years [11]. All in all, it has been estimated that 12% of the global health expenditure is spent on diabetes [11]. Further, with being responsible for 14.5% of the global all-cause mortality within the age group of 20 to 79 years, diabetes has become one of the leading causes of death [11].

1.1.3. T2D and the hepatocellular carcinoma

The link between diabetes and cancer has been established for decades. In detail, diabetic patients face an in part strongly increased risk for liver, pancreatic, endometrial, colon, rectum, bladder, and breast cancer [16]. Further, diabetes significantly increases the risk of developing chronic liver disease as well as hepatocellular carcinoma [17]. In case of the hepatocellular carcinoma, El-Serag *et al.* showed that the risk more than doubles from an incidence rate of 0.87 to 2.39 per 10,000 person-years [17]. This increased risk was shown to be independent of other major risk factors, such as alcoholic liver disease, demographic features or viral hepatitis [17].

Primary liver cancer does present a massive burden in modern society. As discussed by El-Serag *et al.*, it is the 5th most common form of cancer and ranks 3rd regarding cancer mortality [18]. The authors further illustrate that the hepatocellular carcinoma is responsible for 85 - 90% of incidences of primary liver cancer. Interestingly, the number of incidences depends on the geographic region, with more than 80% of cases being observed in sub-Saharan Africa and in Eastern Asia. Not surprisingly, approx. 70 - 90% of hepatocellular carcinoma occurances have a history of chronic liver disease and cirrhosis. The risk factors are region dependent. However, prominent risk factors are chronic hepatitis B, hepatitis C, heavy, prolonged alcohol consumption, toxic exposures, obesity and diabetes [18].

1.1.4. Treatment of T2D

Life style intervention as well as pharmacotherapy have been recommended for the management and treatment of T2D [19], [20]. Although, there is no uniformly applicable approach, regarding nutrition therapy, it is nonetheless characterized by a number of hallmarks. For obese T2D patients weight loss, induced by a reduction of calorie intake, has been recommended [19]. In addition, the sodium uptake should be reduced, alcohol consumption kept at a minimum and a well-balanced healthy diet should be established [19]. These interventions aim at an improvement of the glycaemic control, blood pressure and dyslipidemia [19]. Regarding pharmacotherapy, the applied drugs belong to different compound classes and exhibit different modes of action. Compounds, used for treatment of T2D, are categorized as follows: biguanides, sulfonylureas, meglitinides, thiazolidinediones, alpha-glucosidase-inhibitors, incretin-based therapies, insulin, insulin-analogues [20] and sodium glucose cotransporter 2 inhibitors [21]. Sulfonylureas and meglitinides increase pancreatic insulin secretion [22], [23]. Thiazolidinediones act as insulin sensitizers [24]. Alpha-glucosidase-inhibitors impact the glucose household by delaying the carbohydrate uptake in the gut [25]. Dipeptidyl peptidase-4 inhibitors and glucagon-like peptide-1 receptor agonists (incretin-based therapies) lead to an elevation of the glucose-dependent insulin secretion [26] and have been shown to exhibit a beneficial impact on inflammatory and oxidative stress related mechanisms [27]. Sodium glucose cotransporter 2 inhibitors inhibit the renal reabsorption of glucose and thereby, exhibit a beneficial effect on the glucaemic control [21].

However, metformin - a biguanide - is considered the gold standard in T2D treatment [28]. It is used in combination with life style intervention as monotherapy and in combinational therapy with sulfonylureas, thiazolidinediones and insulin [28]. The main biguanides used in T2D treatment have been metformin, buformin and phenformin [29]. The most potent of this set was found to be phenformin, followed by buformin and finally, metformin [30]. In the US, Great Britain and France, phenformin was withdrawn in 1977 due to its association with severe metabolic acidosis [31]. Up to 1978, over 300 cases of phenformin induced lactic acidosis have been reported in literature [32].

1.2. Metformin

1.2.1. Chemical properties

Metformin (1,1-Dimethylbiguanide) belongs to the class of biguanides (**Figure 1**) and is a hydrophilic base (pK_1: 2.8 - 3.1 and pK_2: 13.9) [33], [34], that is strongly dominated by its monoprotonated cationic form at physiological pH [34].

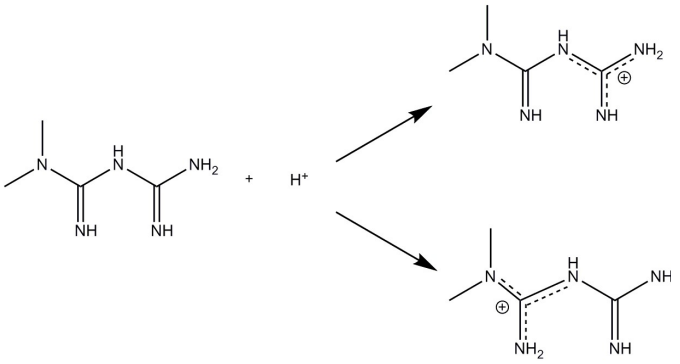

Figure 1: Metformin and its monoprotonated forms.
Left: Neutral form. Right: Monoprotonated forms. These forms are prevalent at a physiological pH. The monoprotonated form displayed in the upper right corner is the one with the lowest energy. It is proposed to be the dominant monoprotonated form [34].

1.2.2. Pharmacokinetics

Metformin is absorbed via the stomach, the duodenum, the jejunum and the ileum. The duodenum was identified as the major uptake side [35], [36]. However, it is hypothesized, that the complete intestine is necessary to take up the drug in sufficient amounts [35]. It is not metabolized by humans [37] and does not bind to plasma proteins [38]. The oral bioavailability averages around 50 - 60% [38], [39] and the biological half-life was found to be 2.8 h [37]. In case of an oral administration of the drug, the plasma concentration and urinary excretion rate peak after about 2 h [39]. 30 - 35% of the unchanged drug were recovered in the urine, whereas, the faecal recovery rate accounted for appox. 30% [39].

1.2.3. Hepatocellular metformin transport

It has been illustrated that the hepatocellular metformin transport consists of a saturable and a non-saturable component [40], which indicates a coexistence of passive and active transport mechanisms. In addition, the metformin uptake is strongly tissue dependent [41]. It was shown that the liver strongly accumulates the drug, when compared to plasma levels of the inferior vena cava and the hepatic portal vein [41]. Further, the metformin response to metformin treatment has been linked to the expression of a number of transporters, and transporter polymorphisms have been shown to correlate with an altered response [42]–[47]. Two common features of the reported metformin transporters are that they belong to the SLC transporter family (**Table 1**) and many of them are known to exhibit a broad, partially overlapping, substrate spectrum [48]–[54].

To the best of my knowledge, the up to now reported metformin transporters, are, the organic cation transporter 1 (OCT1), the organic cation transporter 2 (OCT2) [55], [56], the organic cation transporter 3 (OCT3) [56], [57], the novel organic carnitine/cation/zwitterion transporter 1 (OCTN1) [45], the plasma membrane monoamine transporter (PMAT), the serotonine (reuptake) transporter (SERT) [56] and the thiamine transporter 2 (THTR-2) [48]. The choline high-affinity transporter CHT has also been proposed to be involved in cellular metformin transport [56]. However, the experimental data, supporting this hypothesis, is yet

too weak to secure its position among the set of reported metformin transporters. **Table 1** lists the reported (potential) metformin transporters, their encoding genes and K_M values for the drug.

Organic cation transporters. The most prominent metformin transporters are the OCTs. Especially the role of OCT1 in metformin transport and action has been extensively studied [47], [58], [59]. Further, it was the first identified member of the SLC22 family [60]. However, not only OCT1 but also OCT2 and OCT3 have been shown to be capable of metformin transport [55], [57]. They are polyspecific, bidirectional uniporters [50]. For OCT3 it was shown, that the cation transport is pH dependent and driven by an electrogenic gradient [54]. The metformin transport by OCT1-3 is characterized by a rather low affinity for the drug (**Table 1**). In case of hepatic metformin transport and action, OCT1 has been identified as a major player [47], [58]. Not surprisingly, OCT1 displays the highest relative expression levels in liver, if compared to the other reported (potential) metformin transporters OCT2, OCT3, OCTN1, SERT, PMAT and CHT [61]–[63].

Novel organic carnitine/cation/zwitterion transporter 1. The OCTN1 transporter has been shown to be capable of metformin transport, and its involvement in the gastrointestinal absorption of the drug has been suggested [45]. It is a pH dependent, sodium independent, bidirectional uniporter with a broad substrate spectrum [52], [64]. Expression of OCTN1 has been reported for a broad range of tissues, with the highest levels being detected in the kidney, the bone marrow, the trachea and the spinal cord [63]. The expression levels, detected in the liver, were found to be approximately a 100 times lower than the ones in the kidney [63]. However, the kidney expression levels of OCT2 were 5 times higher than the ones of OCTN1 [63].

Plasma membrane monoamine transporter. Another member of the set of reported metformin transporters is PMAT [42], [56]. Its transport is pH dependent [42] and bidirectional [51]. It possesses a broad substrate spectrum [51], [65] and an ubiquitous expression pattern [63]. The highest relative expression levels were found in the spinal cord and the brain [63]. Its hepatic levels were decisively lower than the ones of OCT1, OCT3 and OCTN1 [63]. The K_M of PMAT for metformin transport is similar to the ones of OCT1-3, THTR-2 and MATE1-2 (**Table 1**).

Serotonin (reuptake) transporter. In 2015, Han *et al.* proposed the involvement of SERT in the cellular uptake of metformin [56]. Although, in principle capable of metformin transport [56], its affinity for the drug is profoundly lower than the affinities of the other metformin transporters (**Table 1**). SERT belongs to the neurotransmitter:sodium symporter family and requires sodium, potassium and/or chloride ion gradients for the transport of serotonin [66]. It is strongly expressed in the lung, where its expression levels surpass the ones of OCT1-3, OCTN1, PMAT and CHT [63]. It has also been reported, to be expressed in the liver; however, at far lower levels compared to the lung [63].

Thiamine transporter 2. The most recent addition to the set of reported metformin transporters is THTR-2. In November 2015, Liang *et al.* demonstrated the capability of THTR-2 to transport metformin [48]. The focus of the study laid on the gastrointestinal transport of the drug. The metformin uptake mechanism of this transporter is pH and electrochemical gradient-dependent [48]. Interestingly, hepatic and intestinal expression of THTR-2 has been documented [48]. However, the hepatic expression levels of OCT1 exceed the ones of THTR-2 [48]. The reported K_M of THTR-2 is lower than the one of OCT1 (**Table 1**).

Multidrug and toxin extrusion proteins. The multidrug and toxin extrusion proteins MATE1 and MATE2-K have been shown to be capable of metformin transport [53]. These proteins are antiporters, mediating the proton-driven exchange of their substrates [53], [67]. They exhibit a broad substrate spectrum and, as their name already indicates, a number of their substrates are drugs [53]. MATE1 has been found to be responsible for the excretion of toxic compounds [68]. In accordance, it has been linked to the renal clearance of metformin [43]. In addition, MATE1 was shown to be expressed in the liver and kidney [68], which renders MATE1 an interesting target for the elucidation of hepatic metformin transport/excretion.

Table 1: List of reported (potential) human metformin transporters and their K_M values for metformin.

Transporter	Gene	K_M [mM]
OCT1	*SLC22A1*	1.47 ± 0.19 [55]; 3.1 ± 0.3 [56]
OCT2	*SLC22A2*	0.99 ± 0.03 [55]; 0.6 ± 0.1 [56]
OCT3	*SLC22A3*	2.47 ± 0.36 [57]; 2.6 ± 0.2 [56]
OCTN1	*SLC22A4*	NA
PMAT	*SLC29A4*	1.32 [42]
SERT	*SLC6A4*	4.0 ± 0.5 [56]
CHT	*SLC5A7*	NA
THTR-2	*SLC19A3*	1.15 ± 0.20 [48]
MATE1	*SLC47A1*	0.78 [53]
MATE2-K	*SLC47A2*	1.98 [53]

1.2.4. The core signal transduction pathway of molecular metformin action

Metformin acts as a weak, reversible and non-competitive inhibitor of complex I of the mitochondrial electron transport chain (**Figure 2**) [69]. This inhibition is concentration dependent [69], [70], and might be tissue dependent as well. For example, the drug does not exhibit a significant impact on complex I activity in skeletal muscle fibres of T2D patients [70]. Nonetheless, a significant reduction of complex I activity was observed, when rat hepatoma cells were treated with a physiological metformin concentration [71]. These inconsistent observations might be caused by the different experimental setups or model organisms. However, another explanation might be the tissue dependent accumulation of the drug. In orally metformin treated mice, the hepatic drug concentration was found to be 4 to 8 times higher than the concentration detected in skeletal muscle [41].

Although complex I is regarded as the primary cellular target of metformin action [69], [71], other mechanisms have been introduced as well [72], [73]. In 2011, Ouyang *et al.* proposed the AMP deaminase (AMPD) as molecular target of metformin [72]. AMPD deaminates adenosine monophosphate (AMP) to inosine monophosphate (IMP) and ammonia. In

accordance with their hypothesis, they observed decreased ammonia levels in metformin treated L6 myotubes [72]. Further, the siRNA knockdown of AMPD diminished the impact of the drug on glucose uptake [72]. Another molecular target of metformin, proposed in 2013, is the hexokinase [73], [74]. The hexokinase catalyses the first step of the glycolysis (glucose to glucose-6-phosphate) [75]. Metformin inhibits the hexokinase isoforms I and II [73], [74].

The inhibition of complex I and hexokinase I and II leads to a significantly elevated AMP/ATP ratio [73], [76], which is one of the major building blocks of the molecular metformin action. This decrease in the energy status of the cell correlates with the activation of the AMP-activated protein kinase (AMPK) [76]. In accordance, the metformin induced inhibition of AMPD correlated with an activation of AMPK [72].

AMPK is a major check point of metabolic control, by upregulating catabolic pathways while downregulating anabolic pathways, proliferation and cell growth [77]. Its activation requires its phsophorylation at α-Thr172 [78]. The phosphorylation is mediated either by the liver kinase B1 (LKB1) or the Ca^{2+}/calmodulin-dependent protein kinase [78], [79]. However, only LKB1 activity is dependent on the energy status [79]. Hence, the core signal transduction of metformin action seems to consist of a LKB1-AMPK dependent cascade (**Figure 2**).

Despite the evidence for a signal transduction of metformin action via LKB1 and AMPK, Foretz *et al.* showed that metformin inhibits hepatic gluconeogenesis by an LKB1-AMPK independent mechanism, which is mediated by the cellular energy status, proposing an alternative route of metformin action [80]. This once more highlights that even the very core signal transduction pathway of molecular metformin action is still controversial.

1.2.5. Metformin and metabolism

Metformin and the glucose metabolism. There is ample reason for metformin being referred to as an anti-hyperglycaemic drug [73], [81]. It does effectively lower the blood glucose levels in T2D patients [81]; and one of the core mechanisms of metabolic metformin action is the inhibition of hepatic gluconeogenesis [71], [80] and simultaneous promotion of glucose utilization [71]. Fulgencio *et al.* showed that treatment of rat hepatocytes with metformin correlated with decreased levels of the gluconeogenetic genes glucose-6-phosphatase (G6Pase) and phosphoenolpyrovate carboxykinase (PEPCK) [82]. In addition, the expression of genes of the hepatic glycolysis was found to be upregulated (glucokinase and liver-type pyruvate kinase) [82]. At first sight, these observations perfectly fit into the overall picture. However, Foretz *et al.* observed that the forced expression of gluconeogenic genes (PEPCK and G6Pase) did not rescue the metformin-mediated decrease in hepatic glucose production, indicating that the metformin-related inhibition of gluconeogenesis acts independent of the transcription levels of gluconeogenetic genes [80]. As mentioned above, the authors suggested a mechanism of metformin action, which relies on the impact of the drug on the cellular energy status [80]. Further, metformin has been reported to stimulate glucose

transport [72]. Metformin increases the glucose uptake by the liver, by promoting the translocation of the glucose transporter 1 (GLUT1) to the plasma membrane (**Figure 2**) [83]. In addition, metformin significantly elevates the insulin-associated translocation of GLUT4 [84]. The effect of metformin on the glucose metabolism is closely connected to its impact on insulin action [84], [85]. Metformin is known to be an insulin-sensitizing agent [85]. It exhibits a beneficial effect on insulin resistance [81], [86], which is a hallmark of T2D [11]. In addition, it has been shown to alter hepatocellular insulin receptor signalling [86]. In detail, metformin treatment does correlate with increased hepatocellular insulin receptor and insulin receptor substrate 2 activation [83]. Further, Lord *et al.* observed that metformin treatment increases the number of low affinity insulin receptors in erythrocytes of obese T2D patients [85].

Metformin, glucose and cancer. Beside the beneficial effect of metformin on the glucose metabolism (**Figure 2**), the relationship of metformin and glucose is far more dynamic. While assessing the potential of metformin as an anti-cancer drug, the bidirectional character of the relationship between glucose and metformin was addressed [87]. Cancer cells exhibit special alterations of the glucose-associated metabolism ("Warburg effect") [88]. They heavily rely on aerobic glycolysis for ATP production [88]. Consequently, glucose has the potential to elevate breast cancer aggressiveness [87]. High glucose concentrations increase proliferation, decrease apoptosis and promote pro-oncogenic signalling in breast cancer cells [87]. Hence, using an anti-hyperglycaemic drug for the prevention or treatment of cancer seems intriguing [88]. Indeed, metformin leads to apoptosis and reduced tumour cell proliferation [87]. Further, Wahdan-Alaswad *et al.* demonstrated that it induces a partial S-phase arrest; whichs extent depends on the glucose concentration [87]. Interestingly, the authors further showed that increasing the available glucose concentration reduces metformin efficacy in terms of apoptosis and cell cycle arrest. Transcriptomics analysis illustrates that, when cells, cultivated at a glucose concentration of 5 mM, are treated with metformin, the majority of differentially regulated genes belong to cellular processes, cell killing and cell proliferation mechanisms. Whereas, when the cells are cultivated at a glucose concentration of 17 mM, metformin treatment predominantly dysregulates genes participating in cell proliferation and metabolic processes [87].

Metformin and the lipid metabolism. Beside its impact on the glucose metabolism, metformin treatment has also been reported to correlate with an increase in fatty acid oxidation in skeletal muscle L6 cells [72]. Metformin treatment leads to an activation of hepatic AMPK, which, in turn, reduces acetyl-CoA carboxylase (ACC) activity [89]. ACC catalyzes the synthesis of malonyl-CoA, an inhibitor of mitochondrial fatty acid oxidation, and precursor of fatty acid synthesis [81]. In accordance, metformin was found to elevate fatty acid oxidation and to reduce the expression of lipogenic genes in primary rat hepatocytes (**Figure 2**) [89].

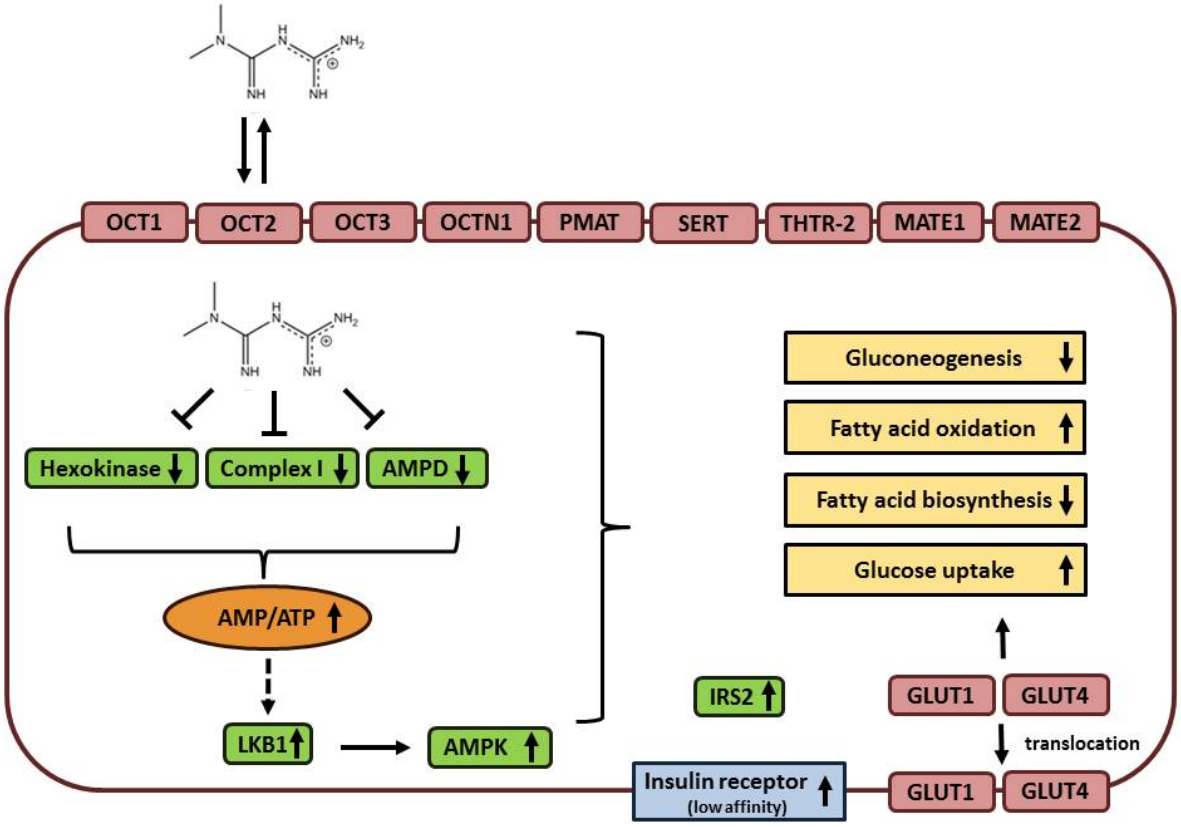

Figure 2: Metformin transport into the cell and action inside the cell.
The figure presents an overview of the major hallmarks of cellular metformin action. Further, transporters, which are capable of translocating the drug, are depicted. Broken arrows depict correlations.

1.2.6. Metformin and the hepatocellular carcinoma

Metformin is the first-line treatment of T2D [81]. However, research, conducted within the last couple of years, opened new perspectives for the application of this drug in other diseases [90]. Metformin is not only a potent anti-diabetic drug [81], but also has a diabetes-preventive effect [91]. In addition, a number of potential other indications have arisen [81], [90]. In this regard, cancer has become one of the major foci [87], [92]–[95]. Evidence has been presented that metformin might be an effective cancer chemopreventive [95] and an anti-cancer drug [93]. Benefitial effects of metformin treatment have been reported in context with pancreatic cancer [96], prostate cancer [97], breast cancer [98], and the hepatocellular carcinoma [95].

Whereas, T2D patients have an increased risk of developing the hepatocellular carcinoma [99], metformin treatment does reduce this risk [99], [100]. In detail, Zhang *et al.* conducted a meta-analysis of three cohort and four case-control studies and found the hepatocellular carcinoma risk in diabetic patients to be significantly reduced, when they were treated with metformin [100]. Chen *et al.* shed some light on the molecular impact of metformin on the hepatocellular carcinoma [95]. They showed that metformin inhibits the

proliferation of hepatoma cell lines (Hep G2 and Hep 3B) and induces a cell cycle arrest in the G0/G1 phase. Its mechanism of action was shown to be LKB1-AMPK dependent [95]. However, a comprehensive, detailed understanding of the molecular mechanisms, responsible for this beneficial effect, has not yet been achieved.

1.3. Tracking biology with instrumental analytics: Cell culture metabolomics

1.3.1. Metabolomics

Metabolites are defined as small molecules, partaking in biological networks [101], representing functional activities, transient effects and end points of cellular regulatory processes [102], [103]. The term metabolome summarizes the metabolites present in a system of interest [101]. Metabolomics aims to provide a comprehensive fingerprint of the metabolic state of the system of interest by the qualitative and quantitative measurement of metabolites [101], [102].

In principle, there are two metabolomics approaches: non-targeted and targeted metabolomics [103]. Non-targeted metabolomics aims at the unbiased profiling of the metabolome [103]. The measured metabolite set is not defined *a priori* and potentially a couple of hundred to about a thousand compounds can be detected in a single run [103]. However, only relative quantification is possible [103]. Further, although in theory unbiased [103], the measured metabolite set depends on a number of parameters [104]. In case of targeted metabolomics, a pre-defined set of up to approx. 200 compounds is analysed [103], [105]. Absolute quantification is possible, and a very high throughput can be accomplished [103]. Both, targeted and non-targeted metabolomics, have been successfully applied in a T2D associated context [106], [107]. Especially their application to biomarker discovery has yielded very promising results and perspectives [107], [108]; such as the identification of predictors for impaired glucose tolerance and T2D [108], and the provision of biomarkers for the early assessment of the success of drug treatment [109].

Metabolomics generates a wealth of information [103], [104], [110]. However, to ensure the reliability and reproducibility of the obtained results, the development, standardization, validation and documentation of analytical methods is of crucial importance [110], [111]. Sources of biological and analytical variation have to be assessed and minimized [110]. Within the last years, massive efforts to elucidate the sources of variation and to standardize protocols and methods have been undertaken [110], [112]. Regarding modern bioanalytics, the Food and Drug Administration (FDA) and the European Medicines Agency (EMA) provide detailed instructions for the requirements and performance of methods [111], [113]. In the field of metabolomics, the metabolomics standards initiative (MSI) has been initiated in 2005 [114]. The MSI provides guidelines on the minimal reporting standards for metabolomics studies, and thereby, endeavors to meet the need for standardization in a scientific field, which is rapidly growing [114]. These standards aim to increase the reproducibility, applicability and availability of the obtained data [111], [113], [114].

1.3.2. Cell culture metabolomics

Cell culture metabolomics is a very powerful tool to unravel alterations in the cellular metabolome and characterize and monitor metabolic disease and drug action [115]. It allows for the evaluation of complex metabolic phenotypes, by providing an imprint of the metabolic state of the observed cellular system [115]. In principle, cell culture metabolomics consists of a number of steps: the cell harvest, the quenching of the metabolism, the metabolite extraction, normalization and subsequent analyses [115]. Each of these hallmarks does provide a number of challenges and requires optimization for the individual experimental setup.

As discussed by Halama *et al.*, for cell harvest, there are two major approaches, which depend on the cell line characteristics (suspension or adherent cells) [115]. In case of suspension cells, the cells can be separated from the cell culture supernatant by centrifugation or filtration, which should be followed by a washing step. With adherently growing cells, the cell layer has to be detached from the cell culture surface. This migh be achieved enzymatically (e.g. trypsinization) or mechanically (scraping). Both procedures allow for an implemented washing step [115]. However, the harvesting method has a pronounced impact on the measured metabolic fingerprint [116], [117]. Trypsinization offers the possibility to count the cells during the harvesting procedure [115]. However, it leads to a massive loss of small polar compounds [117], [118] and does not quench the cellular metabolism immediately [116]. By scraping the cells in extraction solvent, one might avoid these bottlenecks, but forfeits the possibility to count the cells during the harvesting procedure [115].

The efficient extraction of metabolites is a vital prerequesite for the conduction of comrehensive metabolomics analyses [119]. In this context, the composition [118], pH and temperature of the extraction solvent might be adjusted [119]. Ser *et al.* showed that supplementing the extracton solvent with the, frequently used, additive formic acid does not have a pronounced impact on the metabolite recovery [119]. In addition, the temperature (-80 °C vs. 4 °C) had only a very minor effect [119]. However, the extraction solvent composition does have a pronounced influence on the recovered metabolite pattern [118]. Regarding the overall performace of the metabolite extraction, methanol:H_2O based extraction solvents have been recommended [115], [120].

The implementation of a reliable and effective normalization procedure provides one of the major challenges in cell culture metabolomics [121]. In case of suspension cells and adherently growing cells, detached by trypsinization, the cell number can be counted and used for normalization [115]. Another possibility to normalize data, obtained from adherent cell cultures, is the parallelization of the experiment, where one approach is used for metabolomics analyses, and the other for cell number determination [115]. However, this approach requires the cultivation of additional samples [115], rendering it ineffective. Further, instrinsic parameters of the analytical system, such as the total ion current [122] or matrix-induced ion suppression [123], have been suggested. However, analytical parameters,

such as the drying gas temperature, might have a pronounced impact [123]. In addition, with the matrix-induced ion suppression method, the relationship between the signal reduction and the cell concentration was found to be non-linear [123]. A promising approach is the application of marker molecules. For this role, DNA, proteins [121] as well as "housekeeping metabolites" [124] have been suggested. Although, the utilization of housekeeping metabolites might sound interesting, throughout validation of their performance, given the experimental setup and conditions, is required to ensure their eligibility as molecular marker. Silva *et al.* compared the suitability of the total protein content, the DNA content and the cell count for normalization purposes [121]. In this regard, DNA emerged as the most applicable molecular marker [121]. However, the suggested protocol does require a time-consuming DNA extraction step [121], which does call for further optimization.

The analytical properties of cell culture derived samples can differ from the ones of other matrices [123]. Further, different cell concentrations can display different analytical properties [123]. Hence, the applied harvesting and sample preparation protocols and analytical methods should be tailored and validated for their application to cell culture metabolomics.

1.4. Aim of the thesis

The aim of this study is to extent our knowledge of the mechanisms and transporters involved in the hepatocellular metformin transport. Further, a comprehensive understanding of the impact of metformin on the hepatocellular metabolome should be established and the bidirectional relationship of metabolic glucose and metformin action will be elucidated.

Hence, the development, optimization and (partial) validation of methods, especially for cell culture metabolomics and metformin quantification, is the first and a very crucial step in this study. First, a LC-MS/MS based metformin quantification method has to be developed. Second, reliable cell harvesting methods for non-targeted and targeted metabolomics have to be established. Third, the development of a normalization procedure for cell culture metabolomics samples is a crucial prerequisite for metabolomics experiments.

Regarding the hepatocellular metformin transport, the first step will be the profiling of transpors in the cell system of interest. Then, the set of transporters, potentially involved in metformin transport, will be narrowed down by inhibitor studies.

To elucidate the impact of metformin and glucose on the hepatocellular metabolism and to understand the complexity of their relationship, a cell culture metabolomics approach will be applied. Two cell lines, an immortalized liver cell line and a hepatocellular carcinoma cell line, will be analyzed upon different treatments with targeted and non-targeted metabolomics. This approach allows studying metformin and glucose action in a T2D and a cancer-associated context.

2. Material and Methods

2.1. Mammalian cell lines

3T3-L1 (murine)	ATCC (Wesel, Germany)
COS-1 (african green monkey)	ATCC (Wesel, Germany)
HEK293 (human)	DSMZ (Braunschweig, Germany)
Hep G2 (human)	DSMZ (Braunschweig, Germany)
Hepa1-6 (murine)	DSMZ (Braunschweig, Germany)
HK-2 (human)	ATCC (Wesel, Germany)
THLE-2 (human)	ATCC (Wesel, Germany)
SGBS (human)	kindly provided by Prof. Dr. med. Wabitsch [125]

2.2. Chemicals, reagents, media, supplements, solutions and solvents

0.05% Trypsin - 0.53 mM EDTA	Life Technologies (Darmstadt, Germany)
3-isobutyl-1-methylxanthine	Sigma-Aldrich (Steinheim, Germany)
4´,6-Diamidino-2-phenylindole dilactate	Sigma-Aldrich (Steinheim, Germany)
Acetonitrile	Sigma-Aldrich (Steinheim, Germany)
Ammonium acetate	Sigma-Aldrich (Steinheim, Germany)
Biotin	Sigma Aldrich (Hamburg, Germany)
Biozym DNA Agarose	Biozym Scientific GmbH (Oldendorf, Germany)
Bovine collagen type I	BD Biosciences (Heidelberg, Germany)
Bovine pituitary extract	Life Technologies (Darmstadt, Germany)
Bovine serum albumin	Sigma-Aldrich (Hamburg, Germany)
Chloroform	Sigma-Aldrich (Seelze, Germany)
Cimetidine	Sigma-Aldrich (Steinheim, Germany)
CM-H2DCFDA	Invitrogen (Eugene, USA)
Desipramine Hydrochloride	Sigma-Aldrich (Steinheim, Germany)
Dexamethasone	Sigma-Aldrich (Steinheim, Germany)
D-Glucose Monohydrate	AppliChem (Darmstadt, Germany)
Dimethylsulfoxid	Carl Roth GmbH + Co. KG (Karlsruhe, Germany)
DMEM, High Glucose	Life Technologies (Darmstadt, Germany)
DMEM, [-] D-Glucose	Life Technologies (Darmstadt, Germany)
DMEM F-12 HAM	Sigma-Aldrich (Hamburg, Germany)
Ethanol	Merck (Darmstadt, Germany)
FBS Gold	PAA Laboratories GmbH (Pasching, Austria)
FBS Superior	Biochrom GmbH, (Berlin, Germany)
Fibronectin	Sigma Aldrich (Hamburg, Germany)
Formic acid	Sigma-Aldrich (Steinheim, Germany)
Hoechst 33342 (10 mg/mL in H_2O)	Life Technologies (Darmstadt, Germany)
Human recombinant epidermal growth factor	Life Technologies (Darmstadt, Germany)
Hydrogen peroxide	Merck (Darmstadt, Germany)
Insulin solution human	Sigma-Aldrich (Steinheim, Germany)
K-SFM	Life Technologies (Darmstadt, Germany)
L-alanine	Aldrich Chemical Company Inc. (Milwaukee, USA)
L-arginine	Aldrich Chemical Company Inc. (Milwaukee, USA)
L-carnitine hydrochloride	Sigma-Aldrich (Steinheim, Germany)
L-glutamic acid	Aldrich Chemical Company Inc. (Milwaukee, USA)
L-glutamine	Aldrich Chemical Company Inc. (Milwaukee, USA)
L-isoleucine	Aldrich Chemical Company Inc. (Milwaukee, USA)
L-leucine	Aldrich Chemical Company Inc. (Milwaukee, USA)
L-phenylalanine	Aldrich Chemical Company Inc. (Milwaukee, USA)
Metformin hydrochloride	Sigma-Aldrich (Steinheim, Germany)
Methanol	AppliChem (Darmstadt, Germany)
Midori Green Advance DNA stain	Nippon Genetics Europe GmbH (Düren, Germany)

O-acetyl-L-carnitine hydrochloride	Sigma-Aldrich (Steinheim, Germany)
Paroxenthine hydrochloride hemihydrate	Sigma-Aldrich (Steinheim, Germany)
Panthothenate	Sigma Aldrich (Hamburg, Germany)
Phenformin hydrochloride	Sigma-Aldrich (Steinheim, Germany)
Phenylisothiocyanate	Sigma-Aldrich (Steinheim, Germany)
Phosphoethanolamine	Biochrom (Berlin, Germany)
Quinidine anhydrous	Sigma-Aldrich (Steinheim, Germany)
Taq polymerase	In house (produced and kindly provided by Gabriele Zieglmeier)
Thiazolylblue	Carl Roth GmbH + Co. KG (Karlsruhe, Germany)
TRIzol Reagent	Invitrogen (Carlsbad, USA)

2.3. Consumables

12-well plate	Corning Incorporated (Corning, USA)
6-well plate	Corning Incorporated (Corning, USA)
96 well plate (F96, black, flat-bottom)	Nunc, Thermo Fisher Scientific (Schwerte, Germany)
96 deep well plate	Thermo Fisher Scientific (Roskilde, Denmark)
96-well 350 µL PCR plate	Sarstedt (Nümbrecht, Germany)
Cell culture flasks 25 cm^3	Greiner Bio-One GmbH (Frickenhausen, Germany)
Cell culture flasks 75 cm^3	Greiner Bio-One GmbH (Frickenhausen, Germany)
Cell scraper 25 cm	Sarstedt (Nümbrecht, Germany)
CryoTube Vials	Thermo Fisher Scientific (Roskilde, Denmark)
Micro tubes 0.5 ml, PP	Sarstedt (Nümbrecht, Germany)
Micro tubes 2 ml, PP	Sarstedt (Nümbrecht, Germany)
Precellys Glass Beads (0.5 mm)	peqlab Biotechnologie GmbH (Erlangen, Germany)
Pre-slid silicon map	Fisher Scientific (Rochester, USA)

2.4. Kits

Absolute*IDQ* p180 Kit	BIOCRATES LIFE SCIENCES AG (Innsbruck, Austria)
Newborn screening kit	ChromSystems (Gräfelfing, Germany)
RevertAid First Strand cDNA Synthesis Kit	Thermo Fisher Scientific (Schwerte, Germany)
RNeasy Mini Kit	Qiagen (Hilden, Germany)
BEGM BulletKit	Lonza (Basel, Switzerland)
MycoAlert™ Mycoplasma Detection Kit	Lonza (Basel, Switzerland)

2.5. Equipment

Mass spectrometer

4000 QTRAP System	Sciex Germany GmbH (Darmstadt, Germany)
API 4000 System	Sciex Germany GmbH (Darmstadt, Germany)
LTQ XL™ linear ion trap mass spectrometer	Thermo Fisher Scientific (Dreieich, Germany)

Autosampler and (U)HPLC systems

Prominence HPLC System	Shimadzu (Duisburg, Germany)
Agilent 1200 Series HPLC	Agilent Technologies Deutschland GmbH & Co. KG (Böblingen, Germany)
HT PAL autosampler	CTC Analytics AG (Zwingen, Switzerland)
Acquity UPLC system	Waters GmbH (Eschborn, Germany)

(U)HPLC columns

AJ0-4286 SecurityGuard™	Phenomenex (Aschaffenburg, Germany)
Ultra AQ C18 3 µm 50 x 2.1 mm	Restek Corporation (Bellefonte, USA)
XDB-C18 3 µm, 3 x 100 mm	Agilent Technologies Deutschland GmbH & Co. KG (Böblingen, Germany)

ACQUITY UPLC BEH C18 1.7 µm 2.1 mm X 100 mm	Waters GmbH (Eschborn, Germany)

Absorbance, fluorescence and luminescence reader

GloMax Multi Detection System	Promega (Mannheim, Germany)
Safire^2	Tecan (Männedorf, Swizerland)
NanoDrop 1000 Spectrophotometer	Thermo Fisher Scientific (Wilmington, U.S.A.)

Evaporation devices

TurboVap 96	Biotage (Uppsala, Sweden)
Ultravap nitrogen evaporator	Porvair Sciences (Wrexham, UK)

General wet-lab equipment

Cellometer® Auto T4 Plus	peqlab Biotechnologie GmbH (Erlangen, Germany)
Cryolys	peqlab Biotechnologie GmbH (Erlangen, Germany)
Hamilton Microlab STAR™ workstation	Hamilton Bonaduz AG (Bonaduz, Switzerland)
Pecellys 24 homogenizer	peqlab Biotechnologie GmbH (Erlangen, Germany
ThermoALPS Sealer	ThermoFisher Scientific (Munich, Germany)

2.6. Software and servers

Analyst® version 1.5.2 and 1.6	Sciex Germany GmbH (Darmstadt, Germany)
AxioVision LE	Carl Zeiss Microscopy GmbH (Jena, Germany)
Met*IDQ*™ Boron 10.811	BIOCRATES LIFE SCIENCES AG (Innsbruck, Austria)
R 3.1.2	http://www.R-project.org/ , [126]
RStudio Version 0.98.1078	RStudio Inc. (Boston, USA)
PathVisio 3.2.2.	Founded by: Department of Bioinformatics at Maastricht University and the Gladstone Institutes; Core developers: Kutmon M., Bohler A., Melius J., Nunes N., Kelder T., van Iersel M., Hanspers K. and Pico A.; [127], [128]
ChemoView	Sciex Germany GmbH (Darmstadt, Germany)
Primer-BLAST	http://www.ncbi.nlm.nih.gov/tools/primer-blast/ , [129]

2.7. Cultivation and storage of mammalian cell lines

In this project, human and murine cell lines were cultivated, stored and harvested. For cell lines of human origin, the cell line identities were confirmed by the cell line authentication service provided by DSMZ. For the other mammalian cell lines, the organism of origin could be confirmed. Further, the cells were tested for potential mycoplasma contaminations on a regular basis, using the MycoAlert™ Mycoplasma Detection Kit. All cell lines were cultivated at humidified conditions, at 37 °C and 5% CO_2. Depending on the experimental setting, the hexose concentrations and FBS content varied. The FBS supplier and lot numbers were kept constant within one and between connected experiments.

2.7.1. Thawing

Cryo-conserved cell suspensions were thawed in a water bath (37 °C) and immediately transferred to 10 mL growth medium and centrifuged at 500 x g for 5 min. The supernatant was discarded, and the cells were resuspended in growth medium and transferred to a cell culture flask for cultivation.

2.7.2. Cultivation

Hep G2, HEK293, HeLa, Hepa1-6, COS-1 and 3T3-L1 (preadipocytes). In case of the cell lines Hep G2, HEK293, Hepa1-6, HeLa, COS-1 and 3T3-L1 preadipocytes, DMEM High Glucose, supplemented with L-Glutamine and 10% FBS, was used for cultivation. For sub-cultivation, 0.05% Trypsin-EDTA was used for cell detachment. Then, at least three times the volume of the Trypsin-EDTA solution of growth medium, supplemented with 10% FBS, was added, and the cells were split at an appropriate ratio into new culture vessels.

SGBS (preadipocytes). SGBS preadipocytes were cultivated in DMEM F-12 HAM supplemented with 10% FBS, 33 µM biotin and 17 µM panthothenate. For passaging, 0.05% Trypsin-EDTA was used. After cell detachment, at least three times the volume of the Trypsin-EDTA solution of growth medium, supplemented with 10% FBS, was added, and the cell solution was transferred into a tube and centrifuged for 5 min at 500 x g. The supernatant was discarded, and the cells were resuspended in fresh growth medium. Then, the cells were split at an appropriate ratio into new culture vessels.

THLE-2. Cultivation of THLE-2 cells was performed as recommended by the ATCC. Shortly, THLE-2 cells were cultivated, using the BEGM BulletKit (Lonza, Basel, Switzerland). Gentamycin-amphotericin B and epinephrine, which are provided by the kit, were not added to the medium. Further, the medium was supplemented with 5 ng/mL human recombinant epidermal growth factor, 70 ng/mL phosphoethanolamine and 10% FBS. The culturing flasks and plates were pre-coated with 0.01 mg/mL fibronectin, 0.03 mg/mL bovine collagen type I and 0.01 mg/mL bovine serum albumin in BEBM medium. For sub-cultivation, 0.05% Trypsin-EDTA was used to detach the cells. Then, at least three times the volume of the Trypsin-EDTA solution of 0.1% Soybean Trypsin Inhibitor in PBS was added,

and the cell suspension was transferred into a tube and centrifuged for 10 min at 500 x g. Then, the supernatant was discarded; the cells were resuspended in fresh growth medium and split at appropriate ratios into new culture vessels.

HK-2. The cultivation of this cell line was performed by Dr. Janina Tokarz. HK-2 cells were cultivated as recommended by the ATCC. In brief, K-SFM, supplemented with 5 ng/mL human recombinant epidermal growth factor and 0.05 ng/mL bovine pituitary extract, was used as culturing medium. For sub-cultivation, the cells were detached with a 0.05% Trypsin-EDTA solution. Then, at least three times the volume of the Trypsin-EDTA of growth medium was added, and the cell suspension was centrifuged for 10 min at 500 x g. After centrifugation, the supernatant was discarded, and the cells were resuspended in fresh growth medium and split at appropriate ratios into new culture vessels.

2.7.3. Differentiation

3T3-L1 cells were differentiated as described previously [130]. In brief, the cells were cultivated, as described above, until confluency was reached. Then, the cells were cultivated for two additional days. At day 0, the medium was removed, and the differentiation was started by cultivating the cells in DMEM High Glucose, supplemented with L-Glutamine, 0.5 mM 3-isobutyl-1-methylxanthine, 1 µg/mL dexamethasone and 10 mg/mL insulin. At day 4, the medium was exchanged for DMEM High Glucose, supplemented with L-Glutamine and 10 mg/mL insulin. The cells were harvested at day 12 [130].

2.7.4. Storage

For cryo-preservation, 1 x 10^6 to 2 x 10^6 cells/mL were suspended in growth medium with 5% (THLE-2) or 10% (all other cell lines) DMSO, frozen at -80 °C (-1 °C/min) and stored in liquid nitrogen.

2.8. Cell harvest and metabolite extraction

Depending on the experimental setting and subsequent analyses, cells were harvested with two different methods.

Trypsinization. This harvesting method was generally used for the generation of cell pellets for RNA isolation (section **2.12.1**), generation of DNA-standard curves, for the optimization of the fluorescence based DNA and cell number quantification (section **2.9**).
The cells were enzymatically detached, as described in the previous cultivation section, (**2.7.2**). Then, the cells were transferred to a Falcon Tube and centrifuged at 500 x g for 5 min. The supernatant was discarded, and the cells were resuspended in PBS (37 °C) and counted with the Cellometer® Auto T4 Plus. The required cell number was aliquoted into 0.5 mL Micro tubes. Next, the cells were centrifuged at 500 x g and RT for 5 min, and the PBS was discarded. The pellets were snap-frozen and stored at -80 °C. Prior to analysis, metabolite extraction was achieved by adding 80 mg of glass beads (0.5 mm) and either

300 µL of 87.5% (v/v) methanol, for targeted metabolomics and metformin quantification, or 500 µL of 80% (v/v) methanol, spiked with internal standards, for non-targeted metabolomics, to the frozen pellets. Then, the lysates were homogenized with a Precellys24, linked to a Cryolys module, at 5,500 rpm and 4 °C, for two times 25 s with a 5 s break.
Scraping. This harvesting method was used for targeted and non-targeted metabolomics analysis and is compatible with the Hoechst assay (section **2.9**) and the LC-MS/MS based metformin quantification (section **2.14**). The cell layer was washed twice with PBS (37 °C). Then 200 µL (targeted metabolomics and LC-MS/MS based metformin quantification) or 400 µL (non-targeted metabolomics) of methanol extraction solvent, pre-cooled on dry ice, were added to the well (12- or 6-well plates), and the cell layer was scraped. The extraction solvent composition depended on the experimental setting and subsequent analyses (targeted metabolomics: 87.5% methanol:H_2O (v/v); non-targeted metabolomics: 80% methanol:H_2O (v/v) plus internal standards). The homogenate was transferred to Micro tubes, and the wells were washed with another 100 µL of pre-cooled methanolic extraction solvent, which were also transferred to the according Micro tube. The homogenates were stored at -80 °C. Prior to analysis, the homogenates were homogenized with a Precellys 24 homogenization device, linked to a Cryolys module, at 5,500 rpm and 4 °C, for two times for 25 s with a 5 s break.

2.9. Fluorescence based DNA quantification and cell number determination of metabolomics samples

2.9.1. Development and optimization of the fluorescence based DNA quantification assay

The development and the first optimization steps of the assay were performed by me. For the final optimization steps, namely the optimization of the Hoechst 33342 concentration and the sample volume, as well as the generation of standard curves, Dr. Janina Tokarz joined the project. The cultivating, sampling and the DNA measurements of THLE-2 and HK-2 cells were performed by Dr. Janina Tokarz, and the according data was kindly provided.

All cell homogenates, used during the development and optimization of the DNA based cell number quantification assay, were generated, using trypsinized cells, processed as described in section **2.8**. If not stated otherwise, all samples were throughoutly vortexed, prior to application to the 96-well plate and mixed by pipetting. All measurements were performed top-down, without lid in a black flat-bottom 96-well plate. The measurements were conducted using the GloMax Multi Detection System with an UV filter (λ_{Ex} 365 nm, λ_{Em} 410-460 nm). All cell numbers are provided as cell number per sample.

Optimization of the incubation time. The Hoechst 33342 stock solution (10 mg/mL in H_2O) was diluted in PBS to a final concentration of 0.2 µg/mL. 80 µL of this Hoechst dilution were dispensed into the wells of a black 96-well plate. 20 µL of the vigorously vortexed Hep G2 cell homogenate (5 x 10^5 cells) was added to the well and mixed by pipetting. 20 µL of PBS served as blank sample. The samples as well as the blank samples were applied in triplicates.

Then, the plate was incubated at RT in the dark. After 5, 10, 15, 30, 45 and 60 min of incubation, the samples were measured.

Optimization of the incubation temperature. For this optimization step, Hep G2 cell homogenates, containing 5 x 10^5 cells, were used (n per cell number = 3). As it became evident, that the initially applied Hoechst concentration of 0.2 µL/mL was too low, the Hoechst 33342 stock solution (10 mg/mL in H_2O) was diluted in PBS to a final concentration of 2 µg/mL, and 80 µL were dispensed into the wells of three 96-well plates. Then, 20 µL of the vortexed samples were added to the wells and mixed by pipetting. Each sample was applied to each plate once. 87.5% methanol in H_2O (v/v) served as blank sample, which was applied six times to each plate. Then, the plates were incubated at 4 °C, RT or 37 °C for 30 min in the dark and measured.

Testing for plate effects. To test for potential plate effects, Hep G2 homogenates, containing different cell numbers within the range of 1 x 10^5 to 8 x 10^5 cells per sample, were used. The Hoechst stock was diluted to a final concentration of 2 µg/mL, and 80 µL were pipetted into the wells of the 96-well plates. Then, 20 µL of sample/blank were added. The plates were incubated for 30 min at RT in the dark and measured. Each sample was applied to each of the two plates once. The sample size per cell number was 5. 87.5% methanolic extraction solvent was used as blank and was applied five times to each plate.

Optimization of the Hoechst concentration. This step has been previously published in Muschet *et al.* [117]. To optimize the Hoechst concentration, the Hoechst 33342 stock was diluted in PBS to the final concentrations of 0.2, 2.0, 10.0, 20.0, and 30.0 µg/mL. 80 µL of these dilutions were pipetted into the wells of a 96-well plate. Then, 20 µL of vortexed sample were added and mixed by pipetting. The optimization was performed with four different cell lines: Hep G2, THLE-2, SGBS and HK-2. The cell number per sample was fixed at 5 x 10^5 cells. Six cell homogenates were used for each cell line and Hoechst concentration. 87.5% methanol in H_2O (v/v) was used as blank sample. The plates were incubated at RT for 30 min in the dark [117].

Optimization of the sample volume. This optimization step has been published in Muschet *et al.* [117]. Optimization of the sample volume was done, using four different cell lines (Hep G2, THLE-2, SGBS and HK-2) and a fixed cell number of 5 x 10^5 cells per sample. Six cell homogenates were used per cell line and sample volume. To ensure that the dye concentration in the well remained constant at 20 µg/mL, while the applied sample volume was modified, the Hoechst 33342 stock was diluted in PBS to the final concentrations of 16.8, 17.8, 18.8, 20.0, 21.3, 22.9, 26.7, and 32.0 µg/mL. Then, to achieve a final total volume of 100 µL/well, either, 95, 90, 85, 80, 75, 70, 60, or 50 µL of Hoechst solution were added to the wells of a black 96-well plate. Finally, the corresponding sample volume (5, 10, 15, 20, 25, 30, 40 or 50 µL) was added. As blanks, the according volumes of 87.5% methanol in H_2O (v/v) were used. Then, the plates were incubated for 30 min at RT in the dark [117].

Precision. To test the precision of the optimized fluorometric method in combination with the optimized cell harvesting method, 7.5 x 10^4 to 2.5 x 10^6 THLE-2, Hep G2, SGBS and HK-2 cells per well were seeded into 12-well plates and incubated until full attachment was achieved (4 - 16 h, n per cell number = 6). Then, the cells were harvested by the optimized scraping method for targeted metabolomics (section **2.8**). The cell number was determined, using the optimized fluorescence based DNA quantification (section **2.9.2**), and the precision was calculated according to **Equation (2**) (section **2.17.1**).

Impact of the extraction solvent composition. To test whether the composition of the extraction solvent has an impact on the obtained fluorescent signal, samples, containing 5 x 10^5 HEK293 cells, were generated by trypsinization, as described in section **2.8**. Then, 300 µL extraction solvent with different methanol contents (60%, 80% and 100% methanol/H_2O, v/v) were added to the pellets. Each group consisted of 3 samples (n = 3). The samples were homogenized, and DNA quantification was performed, using the optimized parameters listed in section **2.9.2**.

2.9.2. Optimized fluorescence based DNA quantification and cell number determination

The optimized assay, which was used for normalization of metabolomics samples and the inhibitor studies, has been previously published in Muschet *et al.* [117]. It consisted of the following steps: The Hoechst 33342 stock solution was diluted in PBS to a final concentration of 20 µg/mL. 80 µL/well were dispensed into a black, flat-bottom 96-well plate. The sample was vigorously vortexed, and 20 µL/well were applied to the plate and mixed by pipetting. 20 µL of the according methanolic extraction solvent (87.5% methanol, or 80% methanol supplemented with internal standards) were used as blanks. Then, the plate was incubated for 30 min at RT in the dark. The measurement was performed with the GloMax Multi Detection System with an UV filter (λ_{Ex} 365 nm, λ_{Em} 410 - 460 nm) [117]. Cell numbers were calculated, using slope and intercept of the linear equation of the according standard curve (section **2.9.3**).

2.9.3. Generation of standard curves

To generate the standard curves, the cells of the respective cell lines were cultivated as described in section **2.7** and detached via trypsinization and homogenized as described in section **2.8**. Then, fluorescence based DNA quantification, using the optimized method described in section **2.9.2**, was conducted. Cell numbers within the range of 1 x 10^4 to 1 x 10^7 cells per sample were used. The sample size (n) per cell number ranged between 3 and 6. For data evaluation, linear regression analysis of the measured fluorescent signals [rfu] to the applied cell numbers was performed.

2.10. Optimization and validation of cell culture metabolomics

2.10.1. Targeted cell culture metabolomics

For optimization and partial validation of cell culture metabolomics, the Absolute*IDQ* p180 Kit was used. If not stated otherwise, the sample volume for targeted cell culture metabolomics with the Absolute*IDQ* p180 Kit was 10 µL.

Precision. 5 x 10^5 and 1 x 10^6 Hep G2 cells were seeded into 12-well plates (n = 6) and incubated over night. Then, the cells were harvested by scraping, according to the protocol for targeted metabolomics described in section **2.8**.

Accuracy and matrix effects. 5 x 10^5 Hep G2 cells per well were seeded into a 12-well plate and cultivated for 48 h. Then, the cells were harvested and processed as described in section **2.8**. The cells of five wells were scraped using methanolic extraction solvent (87.5%, v/v). The cells of the remaining five wells were scraped using methanolic extraction solvent (87.5%, v/v), spiked with different concentrations of amino acids. The amino acids and their respective concentrations are listed in **Table 2**. As control, pure extraction solvent (87.5% methanol, v/v) as well as spiked extraction solvent were used.

Table 2: List of spiked amino acids and their respective concentrations.

Amino acids	Concentration [mM]
L-alanine	0.4
L-arginine	0.1
L-glutamic acid	0.2
L-glutamine	0.3
L-isoleucine	0.1
L-leucine	0.1
L-phenylalanine	0.05

Sample volume. 5 x 10^5 and 1 x 10^6 Hep G2 cells were seeded into two wells of a 6-well plate and cultivated over night. The cells were harvested and processed according to the scraping protocol described in section **2.8**. Then, targeted metabolomics analysis was performed; using differing sample volumes (10, 20 or 30 µL). In case of 20 µL and 30 µL, the sample volume was applied in steps of 10 µL, with an evaporation step with nitrogen in between.

2.10.2. Non-targeted cell culture metabolomics

Optimization of the extraction solvent composition. Hep G2 and HEK293 cells were seeded into 6-well plates at a density of 1 x 10^6 cells per well. They were cultivated over night, and harvested by scraping as described in section **2.8**. The cells were either scraped in extraction solvent containing 60%, 80% or 100% methanol. The extraction solvent contained internal standards to monitor the extraction efficiency (performed by Dr. Anna Artati). For each extraction solvent group (60%, 80% and 100%), six samples were collected (n = 6). With two tested cell lines, this amounted to a total sample number of N = 36.

Within-run precision. To test the precision of the non-targeted metabolomics platform for cell culture derived samples, one sample was analyzed multiple times within on one plate.

Therefore, HEK293 cells were seeded into a 6-well plate at a density of 1 x 10^6 cells per well. The cells were cultivated over night and harvested by scraping in 80% methanolic extraction solvent, spiked with internal standards, according to the procedure described in section **2.8**. Four wells were pooled into one 2 mL Micro tube, amounting to a total sample volume of approximately 2 mL. This sample was analyzed five times, using non-targeted metabolomics (section **2.16**). The technical replicates were measured on the same plate and within the same batch.

Precision of the harvesting protocol and non-targeted metabolomics. To test the precision and reproducibility of non-targeted cell culture metabolomics, six identical samples were prepared and measured. HEK293 cells were seeded into a 6-well plate at a density of 1 x 10^6 cells per well. The cells were cultivated over night and harvested by scraping in 80% methanolic extraction solvent, spiked with internal standards, as described in section **2.8**. Non-targeted metabolomics analysis was performed as described in section **2.16**. The biological replicates (n = 6) were measured on the same plate and within the same batch.

2.11. Elucidation of hepatocellular metformin transport

If not stated otherwise, metformin was solved and diluted in H_2O. Further, Hep G2 cells, treated with vehicle, were used as negative controls. The cells were harvested according to the scraping protocol used for metformin quantification and targeted metabolomics (section **2.8**). Metformin quantification was performed as described in section **2.14**, and the cell numbers of the cell homogenates were determined, using the optimized fluorescence-based DNA quantification method (section **2.9.2**). Calculation of the cell numbers was done, using a standard curve of the same cell line. Further, the measured metformin concentrations of the cell homogenates were normalized to a reference cell number of 1 x 10^6 cells per sample by means of **Equation (7)** (section **2.17.2**).

2.11.1. Design of the experimental setup

Determination of the incubation time. 2.5 x 10^5 cells per well were seeded into 12-well plates and cultivated over night in medium, supplemented with 10% FBS, to allow for uniform cell attachment. Then, the cells were treated with 2 mM metformin, which was spiked into the supernatant (0.4%, v/v), and further cultivated. The cells were harvested 2, 4, 8, 24, 48 and 72 h post treatment by scraping (section **2.8**). The sample size per group was 6. Further, cells treated with vehicle and harvested after 72 h (n = 3) were used as controls.

Evaluation of fetal bovine serum (FBS) withdrawal. 1 x 10^5 cells were seeded into 12-well plates and cultivated in culturing medium, supplemented with 10% FBS, for 24 h. Then, the cells were washed twice with 2 mL PBS (37 °C), and medium without FBS was added to the wells. The cells were harvested after 0, 12, 24, 36, 48 and 72 h by scraping (section **2.8**), and the cell number of the cell homogenates was determined as described in section **2.9.2**. The sample size per group was 4.

Elucidation of metformin transport. 2.5 x 10^5 cells were seeded into the wells of 12-well plates and cultivated for 24 h in medium, supplemented with 10% FBS, to allow for uniform attachment. Then, the medium was withdrawn, the cells were washed twice with 2 mL PBS (37 °C), and the cells were cultivated for another 24 h in medium without FBS. The cells were treated with 0 (vehicle), 1 µM, 5 µM, 10 µM, 50 µM, 100 µM, 500 µM, 1 mM, 2 mM, 5 mM or 10 mM of metformin, which was spiked into the supernatant (1%, v/v), and cultivated for 4 h. The sample size per group was 6.

2.11.2. Inhibition of metformin transporters

For inhibitor studies, 2.5 x 10^5 Hep G2 cells per well were seeded into 12-well plates and cultivated for 24 h in DMEM, supplemented with 10% FBS. To monitor the pH, phenol red supplemented medium was used. The cells were washed twice with PBS (37 °C) and cultivated for another 24 h in medium without FBS. Then, metformin and the according inhibitor were spiked into the medium. Metformin without inhibitor served as control and solvent without metformin and the according inhibitor was used as vehicle. If not listed otherwise (**Table 3**), the metformin concentration was kept at 50 µM. The concentrations of the inhibitors varied and are listed in **Table 3**. Depending on the polarity of the according inhibitor, either H_2O or DMSO was used as solvent. The cells were incubated for 4 h and scraped in 300 µL 87.5% methanolic extraction solvent (section **2.8**). The sample size per group was 6.

Table 3: List of inhibitors, their concentrations and the according vehicle.

Inhibitor	Concentration [µM]	Solvent
L-Carnitine	50, 500 and 5,000	H_2O
L-Acetylcarnitine	50, 500 and 5,000	H_2O
Quinidine	50 (with 50 µM metformin) and 1,000 (with 2,000 µM metformin)	DMSO
ASP^+	50, 500 and 5,000	H_2O
Desipramine	200	H_2O
Cimetidine	5	DMSO
Paroxentine	0.0001, 0.06, 0.1, 0.6, 2 and 50	DMSO
L-Arginine	50, 500, 5,000	H_2O

In case of desipramine, the aforementioned parameters had to be altered, because the compound proved to be too toxic for the standard cell number and incubation time. 2 x 10^6 cells were seeded into the wells of 6-well plates. The incubation time was shortened to 2 h.

2.12. Transporter expression analyses in mammalian cell lines

2.12.1. RNA isolation

RNA isolation of mammalian cells was based on a previously described protocol [131]. The RNA isolation procedure contained a DNA digestion step to avoid contamination by genomic DNA.

In detail, 1 mL TRIzol Reagent per 5 x 10^5 – 1 x 10^6 cells was added to the frozen cell pellet (approx. 4 x 10^6 cells). Then, the cells were homogenized at RT using a syringe and a 20G

needle. 2:10 (v/v) volumes of chloroform was added to the homogenized cell suspension, which was subsequently vortexed for 15 sec and incubated for 3 min at RT. The sample was centrifuged for 15 min at 4 °C and 21,900 x g. The clear supernatant was transferred into a new tube, and 0.53 volumes of ethanol were added, while being vortexed slowly. The solution was applied to a RNAeasy spin column, supplemented with a 2 mL collection tube, in 700 µL steps. Further, processing steps, including the digestion of residual genomic DNA, were done according to the manufacturer's instructions of the RNAeasy Mini Kit (RNAeasy® Mini Handbook, Fourth Edition. Qiagen, Hilden, Germany).

The RNA concentration was determined using a NanoDrop 1000. Quantification was performed according to the manufacturer´s instructions (NanoDrop 1000 Spectrophotometer V3.7 User´s Manual. Thermo Fisher Scientific, Wilmington, U.S.A.).

2.12.2. cDNA synthesis

Reverse transcription of the isolated RNA to cDNA was performed according to the protocol described earlier [131]. Minor adaptions, which are listed in the following paragraph, were made.

Briefly, 1.5 µg of total RNA were transcribed using the RevertAid First Strand cDNA Synthesis Kit. cDNA synthesis was performed according to the manufacturer´s instructions.

However, a different Oligo-dT_{18} primer, designed and kindly provided by Dr. Janina Tokarz, was used (5'-TTTTTTTTTTTTTTTTTTVN-3') in a final concentration of 0.5 µM. This anchored Oligo-dT_{18} primer binds to the junction of the poly-A tail with the mRNA; thereby, avoiding the reverse transcription of the poly-A tail [131].

2.12.3. Polymerase chain reaction (PCR)

A variety of human cell lines (Hep G2, THLE-2, HEK293 and SGBS) were tested for their expression of reported and potential metformin transporters.

For primer design the Primer-BLAST tool [129] (http://www.ncbi.nlm.nih.gov/tools/primer-blast/) was applied. Primers were designed to span at least one exon-exon junction to avoid contamination by off-target amplification of genomic DNA. Further, the primer had to exceed a size of 300 bp and to have an approximate estimated melting temperature of 60 to 64 °C. The amplification of splice variants was desired, since the aim of the approach was to determine, whether the tested cell lines express the screened transporters.

For the PCR, cDNA of the according cell lines was used as template and human β-actin as positive control. H_2O served as negative control. The PCR mastermix composition for a single approach is listed in **Table 4**. The PCR conditions are listed in **Table 5**.

Table 4: PCR mastermix composition for a single reaction.

Reagent	Volume [µL]	
	Standard	**OCT1 and OCT3**
H_2O	13.2	13.2
10 x buffer*	2.0	2.0
dNTPs (0.2 mM)	2.0	2.0
Forward primer (10 µM)	1.0	0.5
Reverse primer (10 µM)	1.0	0.5
cDNA template	0.5	1.0
Tag polymerase	0.3	0.3

*10 x buffer: 100 mM Tris-HCl (pH = 9), 500 mM KCl, 15 mM $MgCl_2$

Table 5: PCR conditions used in transporter expression analyses.

Number of cycles	Time [min]	Temperature [°C]
1	5.0	95
35 (Transporters)	0.5	95
30-35 (β-actin)	0.5	Primer dependent
40 (OCT1 and OCT3)	1.0	72
1	5.0	72

As OCT1 and OCT3 expression was not detectable in the tested human cell lines, when the standard conditions (**Table 4**: Standard, 35 cycles) were used, the composition of the PCR mastermix and the cycle number had to be altered (**Table 4**: OCT1 and OCT3, 40 cycles). The annealing temperature was set to approx. 3 °C below the melting temperature of the according primers. The primers and their melting temperatures (T_m) are listed in the appendix (**Table S-1**).

For the separation of PCR products by agarose gel electrophoresis, 6 x loading puffer (15% Ficoll 400, 0.25% bromophenol blue, 0.25% xylene cyanol FF) was added to the respective PCR reaction, and 20 µL were loaded onto a TBE (108 g Tris, 55 g boric acid, 9.3 g EDTA in 1 l H_2O) gel, containing 1.8% agarose and 25 µL/L Midori Green Advanced. For separation, a constant electric field of 100-120 V was applied. Detection was performed at a wavelength of 254 nm.

2.13. Elucidation of the impact of glucose and metformin on the hepatocellular metabolome

2.13.1. Determination of the optimal metformin concentration

This experimental setup was described in detail earlier [130]. 1.5 x 10^5 Hep G2 cells were seeded into the wells of 12-well plates and cultivated for 24 h in DMEM High Glucose, supplemented with 10% FBS. Then, the cells were treated either with vehicle (H_2O) or 500 µM, 2 mM or 5 mM metformin, which was spiked into the cell culture superanatant, and cultivated for another 24 h. The sample size per group was 5. The experiment was conducted thrice (N = 15). The cells were harvested by scraping, using 300 µL 87.5% methanolic (methanol:H_2O, v/v) extraction solvent, and homogenized [130].

Targeted metabolomics. Targeted metabolomics analysis was performed using the Absolute*IDQ* p180 Kit as described in section **2.15**. The analyzed sample volume was 10 µL [130].

Determination of the DNA concentration of cell culture homogenates. This method was described in detail earlier [130]. In brief, the samples were strongly vortexed and 2 µL were placed on a NanoDrop 1000. Then, the DNA concentration was determined, using the DNA detection mode. Extraction solvent (87.5% methanol:H_2O, v/v) served as blank [130].

Data evaluation. The data, obtained with targeted metabolomics, was normalized for plate effects (**Equation (6)**, section **2.17.2**). Then, normalization to the mean DNA concentration, using the means of the DNA concentrations of the groups, was performed according to **Equation (7)** (section **2.17.2**). Non-parametric pairwise comparisons of all metformin conditions vs. the vehicle (H_2O) treated controls were performed using the Wilcoxon-Mann-Whitney test (U-test). Correction for multiple testing was done using the Benjamini-Hochberg method.

Methylthiazolyldiphenyl-tetrazolium bromide (MTT) assay. The applied assay was described in detail earlier [130]. In brief, 2.0 x 10^4 Hep G2 cells were seeded into the wells of 96-well plates and cultivated for 24 h in 200 µL DMEM High Glucose supplemented with 10% FBS. Then, the cells were treated with either, vehicle (H_2O) or 500 µM, 2 mM or 5 mM metformin (n = 8), which was spiked into the cell culture supernatant, and incubated for another 24 h [130].

Then, the MTT assay was performed. In case of the negative control wells, the cell culture supernatant was withdrawn, and the wells were washed with 200 µL PBS. To diminish the viability, the cells were incubated for 10 to 15 min in absolute ethanol. After incubation, the ethanol was discarded, and the wells were washed with PBS. Then 200 µL cell culture supernatant was added to the wells. Further, wells with viable cells, but without MTT and wells with DMSO, added after the incubation step with MTT, served as additional negative controls. For the assay, 5 mg/mL MTT were dissolved in PBS, and 10 µL of this solution were added to the according wells. The plates were incubated at 37 °C for 2 h. After the incubation, the cell culture supernatants were discarded, and the wells were washed with PBS. 100 µL DMSO were added to each well, and the plates were incubated at RT for 40 min, while being shaken. Then, the absorbance was measured, using the Safire^2 plate reader. The parameters were set as follows: Measurement λ: 570 nm, reference λ: 630 nm, excitation bandwidth: 5 nm, number of reads: 10, time between movement and read: 20 µs and temperature: 30-32 °C [130].

2.13.2. Pre-evaluation of the impact of the glucose concentration on the hepatocellular metabolome.

1 x 10^6 Hep G2 cells were seeded into the wells of 6-well plates and cultivated for 24 h to ensure uniform attachment. Then, the cell culture supernatant was exchanged for medium containing either, 0, 5, 11 or 25 mM glucose, and the wells were cultivated for another 24 h. The cells were treated with vehicle (H_2O) or 2 mM metformin, which was spiked into the cell culture supernatant, and incubated for another 24 h. Then, the cells were harvested by scraping (section **2.8**) in 300 µL 80% methanolic (v/v) extraction solvent to conduct targeted

metabolomics with the Newborn screening kit and DNA based cell number determination. The cell number per group was n = 3, the experiment was conducted twice (N = 6).

Targeted metabolomics. Targeted metabolomics was performed using the Newborn screening kit, which covers amino acids and acylcarnitines, as described in section **2.15**.

Cell number determination. For the determination of the cell number, the optimized fluorometric DNA quantification method was used (section **2.9.2**).

Data evaluation. The metabolomics data was normalized to the reference cell number of 1 x 10^6 cells per sample as illustrated by **Equation (7)** (section **2.17.2**). Then, the U-Test was applied for pairwise comparisons of the groups. Correction for multiple testing was performed, using the Benjamini-Hochberg method.

2.13.3. Elucidaton of the impact of glucose and metformin on the hepatocellular metabolome.

1.5 x 10^5 THLE-2 cells per well and 7.5 x 10^5 Hep G2 cells were seeded into the wells of 6-well plates and cultivated for 16 h as described in section **2.7.2** to allow for the uniform attachment of the cells while minimizing proliferation. Then, the supernatant was withdrawn, the cells were washed twice with PBS (37 °C), and growth medium containing either 6 mM or 11 mM glucose was added. The cells were cultivated for another 24 h. Subsequently, the cells were either treated with 2 mM metformin or vehicle (H_2O), which was spiked into the cell culture supernatant, and cultivated for another 24 h. 1 mL cell culture supernatant was collected and immediately placed on dry ice. Cell harvest for metabolomics analyses, metformin quantification and cell number determination was performed using the optimized scraping protocols described in section **2.8**.

Four different types of analyses were conducted: targeted metabolomics, non-targeted metabolomics, LC-MS/MS based metformin quantification and fluorescence based cell number determination.

Targeted metabolomics and LC-MS/MS based metformin quantification. Targeted metabolomics analysis of a subset of the collected samples was performed, using the Absolute*IDQ* p180 Kit (section **2.15**). For cell homogenates, the sample size per group (8 groups) was 6, the experiment was conducted twice (N = 12). These samples were also used for LC-MS/MS based metformin quantification (section **2.14**). The cells were scraped in 300 µL 87.5% methanol. Cell culture supernatants were only collected once. The sample size per group amounted to n = 6.

Non-targeted metabolomics. Non-targeted metabolomics was performed as described in section **2.10.2**. Only cell homogenates were analyzed with this approach. The sample size per group was n = 6. The cells were scraped in 500 µL 80% methanol, spiked with internal standards for extraction monitoring (section **2.8**). Due to the sample volume requirement of this approach, two wells were pooled to generate one sample.

Cell number determination. For all samples, the cell number was determined using the optimized, fluorescence based DNA quantification method, described in section **2.9.2**.

Data evaluation. A number of quality control steps were implemented into the analysis and data evaluation. For targeted as well as non-targeted metabolomics analyses, the samples were randomized. With each type of analysis, quality control samples were applied and used to assess the quality of the analyses and for data evaluation.

Raw data. Based on the results of the partial validation of the targeted metabolomics Absolute*IDQ* p180 Kit for cell culture applications (section **3.3.1**), the peak area (amino acids and biogenic amines) or, if not available, the peak intensity (lipids) was used. In case of non-targeted cell culture metabolomics, the "Original Scale" data provided by Metabolon Inc. was used. Based on the results of the validation of the LC-MS/MS based metformin quantification method (section **2.14.1**), the calculated concentrations were used.

LOD and LLOQ. Based on Römisch-Margl *et al.*, the LOD was set to three times the median of the zero samples [132]. In case of cell homogenates, the zero consisted of extraction solvent (87.5% methanol, two zeros per plate). For cell culture supernatants, PBS was used as zero (two zeros per plate). For considering a compound to be above the LOD, the following criteria had to be fulfilled: ≥ 60% of the samples had to display values above the according LOD threshold and ≥ 50% had to be unequal to 0 or NA. An exception was made for the metformin assay, because half of the samples were below the LOD (vehicle-treated cells) in the first place. The LLOQ was set to five times the median of the zero samples. For considering a compound above the LLOQ, the aforementioned criteria for the LOD were used. Those metabolites passing the LOD and LLOQ criteria are listed in the appendix in **Table S-3**.

Normalization of plate effects. In case of non-targeted metabolomics, the obtained data was already normalized for plate effects. In case of targeted metabolomics analysis of cell culture supernatants, normalization of plate effects was not required, because all samples were measured within a single plate. In case of the cell homogenates measured with targeted metabolomics, the samples had to be measured on two consecutive plates. Hence, normalization of plate effects was performed. For normalization, reference cell samples were used (Hep G2, six pooled samples, 1 x 10^6 cells per sample, applied four times per plate). An exception was ADMA, for which the reference plasma had to be used, because the metabolite level of the reference cells was 0. The applied plate normalization factor was calculated according to **Equation (6)** (section **2.17.2**).

Normlization to cell number. In case of the cell homogenates, normalization to the reference cell number of 1 x 10^6 cells per sample was performed as described in **Equation (7)** (section **2.17.2**). In case of the cell culture supernatants, the metabolite levels of the reference supernatants (medium of the exact same composition but without cells) were subtracted. Then, the metabolite levels of the cell culture supernatant samples were normalized to the cell numbers of the according cell line as described in **Equation (7)** (section **2.17.2**).

Imputation. The histograms in **Figure 3** illustrate, that the higher the cell number, the lower the number of non-detected values (defined as NA or 0, reported by Met*IDQ*). Since higher cell numbers entail less missing values, the missing values are indicative of metabolite levels below the LOD. Therefore, NAs and reported infinite values (Inf) were replaced by the half of the minimum value of the according metabolite (minimum-half imputation) [133]. An infinitive value occurs during normalization, when the initially reported value is 0.

Figure 3: Histograms of the number of non-detected (N. D.) values in samples with different cell numbers.
Different cell numbers of THLE-2 cells and Hep G2 cells were seeded out 12-well plates and harvested after full attachment was achieved (THLE-2: 4 h, Hep G2: 16 h). The difference in the cell number range of the two cell lines originates from the different cell size. For cell harvest and metabolite extraction, the cells were scraped in 300 µL 87.5% methanol per well and homogenized. Then, targeted metabolomics using the Absolute*IDQ* p180 Kit was performed. The sample size per cell number group was 6. The histograms show the sum of non-detected (N. D.) values per cell number. A value was defined as non-detected, if a NA (not available) or 0 was reported by Met*IDQ*.
The data for the THLE-2 cells were kindly provided by Dr. Janina Tokarz.

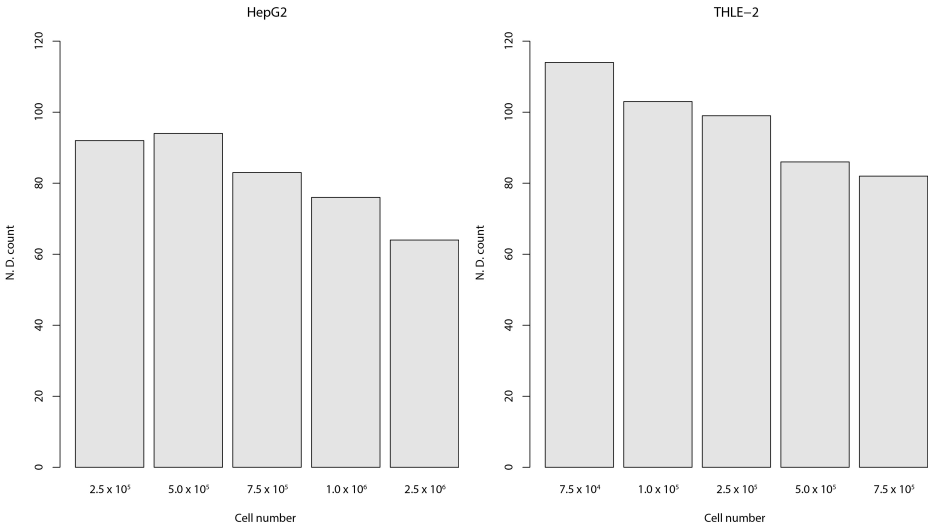

Centering and scaling. To ensure that all assessed compounds exhibit equal importance independent of their order of magnitude (peak area, intensity or concentration), the data was centered and scaled using the autoscaling method as illustrated by **Equation (1)** [134].

Equation (1)

$$\overline{\overline{x_{ij}}} = \frac{x_{ij} - \overline{x_i}}{SD_i}$$

In **Equation (1)**, x_{ij} represents the value to be scaled, $\overline{\overline{x_{ij}}}$ represents the scaled value, $\overline{x_i}$ the mean and SD_i the standard deviation of the compound [134]. The normalized, imputed and scaled data set was used for statistics (section **2.17.5**) and any further analyses.

Enrichment analysis. Discrete quantitative enrichment analysis was performed with MetaboAnalyst 3.0 [133], [135]–[138]. To annotate the metabolites, the HMDB IDs were used (**Table S-4**). If not mentioned otherwise, the default settings of MetaboAnalyst 3.0 were applied. As the data was normalized and scaled prior to analysis, no additional normalization, transformation or scaling was performed. For the metabolite set library the "Pathway-associated metabolite sets" were used.

2.14. LC-MS/MS based metformin quantification

Preparation of standard curves for metformin quantification. 4 µL of metformin stock (**Table 6**), solved in H_2O, was added to 196 µL methanol, spiked with 100 nM phenformin (1:50 dilution, v/v), vortexed and measured. Phenformin was used as internal standard.

In cell culture studies, substance concentrations (molarity) are commonly used to refer to the applied metformin concentrations [40], [86], [95], [139]. Hence, to ensure the conformity and comparability with the cell culture based studies, the method was developed and validated for and applied to, the metformin concentrations will be provided in molar entities. **Table 6** lists the substance and the mass concentrations of the evaluated concentration range.

Table 6: Metformin concentrations used for the evaluation of the linear range and as standard curves for the quantification of metformin in cell culture samples.
The table lists the metformin concentrations used for the evaluation of the linear range. Based on the results of the validation of the metformin method, a subset of these concentrations was chosen for the quantification of metformin in cell homogenates and cell culture supernatants. The concentrations of the stocks are displayed in [nM] and [ng/mL]. In addition, the concentrations on the column (1:50 dilution in methanol spiked with 100 nM phenformin) are listed.

Calibrators

Metformin concentration (stocks) [nM]	Metformin concentration (on the column) [nM]	Metformin concentration (stocks) [ng/mL]	Metformin concentration (on the column) [ng/mL]
0.005	0.0001	0.00065	0.000013
0.05	0.001	0.0065	0.00013
0.25	0.005	0.032	0.00065
0.5	0.01	0.065	0.0013
2.5	0.05	0.32	0.0065
5	0.1	0.65	0.013
25	0.5	3.23	0.065
50	1	6.46	0.13
250	5	32.29	0.65
500	10	64.58	1.29
2,500	50	322.91	6.46
5,000	100	645.82	12.92
10,000	200	1,291.64	25.83
12,500	250	1,614.55	32.29
25,000	500	3,229.09	64.58
37,500	750	4,843.64	96.87
50,000	1,000	6,458.18	129.16
500,000	10,000	64,581.80	1,291.63

Preparation of cell homogenates and cell culture supernatants for metformin quantification. For LC-MS/MS based quantification of metformin, the homogenized cell lysate was diluted 1:50 (v/v) with methanol, spiked with 100 nM phenformin. The dilution was centrifuged for 5 min at RT and 10,000 x g. Then, 150 µL of the clear supernatant were transferred to a 96-deep well plate, which was sealed with a pre-slit silicon mat, for measurement.

The cell culture supernatant was first precipitated by diluting it 1:10 (v/v) with acetonitrile. The dilution was vigorously vortexed for at least 5 s and subsequently centrifuged for 5 min at RT and 10,000 x g. An aliquot of the clear supernatant was diluted 1:50 (v/v) with methanol, spiked with 100 nM phenformin. 150 µL of the dilution were transferred to a 96-deep well plate, which was sealed with a pre-slit silicon mat, for measurement.

LC-MS/MS based metformin quantification. The LC-MS/MS based metformin quantification was conducted as described earlier [109]. However, for cell culture matrices the quantifier and qualifier of phenformin were inversed.

HPLC and instrumental settings. An HPLC Prominence System, with a binary LC-20AB pump and a SIL-20AC autosampler was coupled to a 4000 QTrap triple quadrupole MS, equipped with a turbo spray ion source. For chromatographic analysis, an Ultra AQ C18 3 µm 50 x 2.1 mm column, protected by an AJ0-4286 SecurityGuard^{TM} precolum, was applied. Liquid chromatography was done using isocratic conditions with a flow rate of 0.2 mL/min of 90% B (90% methanol, 10% H_2O, 0.05% formic acid) and 10% A (95% H_2O, 5% methanol) and a run time of 1.5 min. The injection volume was set to 5 µL. The parameter settings for the MS analyses are listed in **Table 7**. The LC-MS system was controlled by the Analyst 1.5.2 software [109].

Table 7: Parameter settings of the mass spectrometer for the metformin quantification method.

	Parameters		
General parameters	Ionization mode	Electrospray ionization (ESI)	
	Ion mode	positive	
	Ion source temperature [°C]	500	
	Curtain gas	15	
	Ion spray voltage	5 500	
	Nebulizing gas	18	
	Drying gas	15	
	Collision gas	6	
Metformin	MRM Quantifier [m/z]	130.1/60.0	
	MRM Qualifier [m/z]	130.1/71.1	
		Quantifier	**Qualifier**
	Declustering potential	35	35
	Entrance potential	8	12
	Collision energy	18	34
	Collision cell exit potential	4	2
	Dwell time [ms]	100	100
Phenformin	MRM Quantifier [m/z]	206.2/60.1	
	MRM Qualifier [m/z]	206.2/105.1	
		Quantifier	**Qualifier**
	Declustering potential	40	40
	Entrance potential	8	8
	Collision energy	31	31
	Collision cell exit potential	6	8
	Dwell time [ms]	150	150

2.14.1. Validation of the LC-MS/MS based metformin quantification method

For the validation of the performance of the method, if applied to eukaryotic cells and their supernatant, cell culture homogenates containing 1 x 10^5 3T3-L1 cells and their supernatants, were used. The 3T3-L1 cells were differentiated to mature adipocytes as described earlier [130] and in section **2.7.3**. As the method allows for different dilution factors, all listed concentrations – if not mentioned otherwise – refer to the final concentrations on the column (**Table 6**).

Specificity. The specificity of the assay was monitored for each experiment and cell line by analyzing vehicle (H_2O or DMSO) treated cells, which were cultivated and prepared in the same way as, and in parallel to, the metformin treated ones.

Linear range, accuracy, precision of multiple preparations and injection precision of the method. For the determination of the limit of detection (LOD), the lower limit of quantification (LLOQ), the upper limit of quantification (ULOQ) and the linear range standard curves were generated. First, a standard curve with 12 calibrators with different concentrations between 0.1 pM and 10 µM (**Table 6**) was measured. The curve was prepared once, and each sample was injected three times to assess the injection precision. The obtained analyte peak areas were normalized to the peak areas of the internal standard (IS). For the calculation of the concentrations, linear regression through zero of the IS normalized analyte areas to the spiked concentrations was performed. The accuracy was calculated as described by **Equation (3)** (section **2.17.1)**, the precision as indicated by **Equation (2) (**section **2.17.1)**. Next, a standard curve containing 15 concentrations within the range of 5 pM to 1 µM (**Table 6**) was generated using a different set of metformin stocks. This standard curve was prepared thrice to assess the precision of multiple preparations, and each one was injected thrice, to reassess the injection precision. The lowest calibrator of the standard cuve, which exhibited an analyte intensity of at least five times the baseline of the blank (methanol without IS) was set as LOD. In addition to this requirement, the deviance of the accuracy of the calibrator, which was defined as LLOQ, had to be within the range of ± 20% [111], [113].

Analyte stability. To evaluate the stability of prepared calibrators, a standard curve was prepared as described above, measured and then stored at -80 °C over night. Before the second measurement, the samples were left in the auto sampler (4 °C) for 1 h to ensure temperature adjustment. Then, the second measurement was conducted, and the samples were again stored at -80 °C. The third measurement was performed after 69 days of storage at -80 °C.

Accuracy and precision of metformin quantification in cell homogenates and cell culture supernatants. For validation of the accuracy and precision, three metformin concentrations within the linear range were spiked 1:10 (v/v) into cell homogenate and cell culture supernatant, thrice. The matrices were then prepared for measurement as described above. The final metformin concentrations were 500 nM, 1,000 nM and 2,000 nM (cell homogenates) and 50 nM, 100 nM and 200 nM (cell culture supernatants). The accuracy was calculated as described in equation **Equation (3)** (section **2.17.1**), the precision as illustrated by **Equation (2)** (section **2.17.1**).

Matrix factor. To assess potential matrix effects, the matrix factors were determined. Three metformin concentrations were spiked three times into cell homogenate, cell culture supernatant, 87.5% methanolic extraction solvent and H_2O. Then, the matrix factor of the analyte and the internal standard were determined using **Equation (4)** (section **2.17.1**) and the IS normalized matrix factor was calculated as described in **Equation (5)** (section **2.17.1**). 87.5% methanolic extraction solvent was used as the reference matrix to determine the peak

area without matrix for cell homogenates; in case of cell culture supernatants, H_2O was used as the reference matrix.

Quality control. The performance of the assay was constantly monitored to assure the reliability of the results regardless of the tested cell line or metformin concentration. To ensure the specificity of the method for all measured matrices, zero samples, which were generated within the same experiment by treating the according cells with vehicle (H_2O or DMSO), were prepared and measured. Additionally, the LOD and LLOQ were checked for each application of the method by measuring a standard curve with a minimum of 11 different concentrations within the range of 5 pM to 1 µM. Based on the recommendation provided by the EMA, a minimum of 6 concentrations had to be within the linear range to assure reliability of the quantification [111].

2.15. Targeted metabolomics analyses

In course of this study two different targeted metabolomics approaches were used: the Newborn screening kit and the Absolute*IDQ* p180 Kit.

Newborn screening kit. Analyses using the Newborn screening kit were performed by Dr. Janina Tokarz and Maria Kugler. Targeted metabolomics of cell homogenates with the Newborn screening kit was performed according to the manufacturer´s instructions ("Arbeitsvorschrift für die LC-MS/MS Bestimmung: MassChrom® Aminosäuren und Acylcarnitine aus Trockenblut (V4.1)," 2011.). The application of the kit to cell homogenates was described earlier [140]. Some minor adaptions were made, which are listed below.

Adaptations. The cell homogenates were centrifuged for 5 min at 4 °C and 11,000 x g. The sample volume used for metabolomics analysis was 10 µL. In contrast to the previously described method [140], the sample was applied directly to a 96-well plate, and not to a filter paper. Hence, the drying of the filters was omitted.

Method. In brief, 10 µL of the centrifuged cell homogenate were pipetted into the well of a 96-well plate. 200 µL of extraction solvent, containing isotopically labelled internal standards, were added and the plate was shaken at 600 rpm for 20 min at RT. The plate was shortly centrifuged, and the liquid was evaporated at 60 °C in a speed-vac centrifuge. 60 µL of derivatization reagent were added, and the plate was placed on a metal block, heated to 72 °C, and incubated for 18 min. Then, the plate was shortly centrifuged, and the liquid was evaporated by placing the plate on the heating block (72 °C). After evaporation, 100 µL of the reconstitution buffer were added, and the plate was shaken at 600 rpm and RT for 10 min. The plate was sealed with ThermoSeal foil using the ThermoALPS Sealer set to 165 °C for 4 s. The FIA-MS/MS measurement was performed with a 4000 QTrap controlled by the Analyst 1.5.2 software. The injection volume was set to 10 µL, the run time to 1.7 min and the flow rate of the mobile phase to 0.1 ml/min. Depending on the analyzed metabolite, different operation modes were applied: neutral loss scan (subset of amino acids, neutral loss: $m/z = 102$), precursor ion scan (free carnitine and acylcarnitines, fragment ion: $m/z = 85$) and

multiple reaction monitoring (subset of amino acids). Primary data evaluation was performed with the ChemoView software [140].

Absolute*IDQ* p180 Kit. Analyses using the Absolute*IDQ* p180 Kit were performed by Dr. Cornelia Prehn, Katharina Faschinger, Andrea Kraume and Silke Becker. Targeted metabolomics of cell homogenates with the the Absolute*IDQ* p180 Kit was performed according to the manufacturer´s instructions (Absolute IDQ ® p180 Kit (BIOCRATES): UM-P180-ABSCIEX-10.). The method consists of a FIA-MS/MS and a LC-MS/MS part. The FIA-MS/MS procedure measures free carnitine (C0), acylcarnitines (C), lysophosphatidylcholines (lysoPC), diacylphosphatidylcholines (PC aa), acylalkylphosphatidylcholines (PC ae), sphingomyelins (SM) and the sum of hexoses (H1) [105]. The LC-MS/MS part measures amino acids and biogenic amines [105]. The application of the kit to different matrices has been previously described [105], [141].

Sample preparation and volume. Depending on the experimental setting, the sample volume for cell homogenates ranged from 10 µL to 30 µL. Prior to their application, the cell homogenates were vigorously vortexed. The applied sample volume for cell culture supernatants was 10 µL. Prior to their application, the supernatants were thawed on wet ice and centrifuged for 5 min at 4 °C and 2,750 x g.

Method. In brief, the internal standards for the LC-MS/MS part were added to the wells of a 96-well filter plate, which was already pre-spiked with the internal standards for the FIA-MS/MS part of the assay. Then, 10 - 30 µL of the sample were added and the liquid was evaporated under nitrogen flow in an Ultravap nitrogen evaporator. If the sample volume exceeded 10 µL, it was applied in 10 µL steps with alterating evaporation steps. The sample was applied manually; all subsequent liquid handling steps were performed with a Hamilton Microlab STAR workstation. Derivatization of amino acids and biogenic amines was performed by incubation with 5% phenylisothiocyanate for 20 min. 300 µL methanol with 5 mM ammonium acetate was added, and the plate was shaken at 450 rpm and RT for 30 min. Then, the plate was centrifuged for 5 min at RT and 500 x g. The liquid was then split into two parts. One part was diluted 1:2 with H_2O for the LC-MS/MS measurement; the second part was diluted 1:6 with BIOCRATES running solvent for the FIA-MS/MS measurement. For the LC-MS/MS analyses, the injection volume was set to 20 µL; for the FIA-MS/MS analyses, it was set to 10 µL. Metabolomics analyses were performed with an API4000 mass spectrometer, coupled to a 1200 Series HPLC, supplied with a HT PAL autosampler. The HPLC system was equipped with a XDB-C18 3 µm, 3 x 100 mm column. The LC-MS system was controlled by the Analyst 1.6 software. Primary data analysis including quality assessment was performed with the Met*IDQ* software package [105].

2.16. Non-targeted metabolomics analyses

The UPLC-MS/MS analyses were performed at the Genome Analysis Center (Helmholtz Zentrum München, Munich, Germany) while the library matching was conducted by Metabolon (Metabolon, Inc., Durham, U.S.A).

Sample preparation and volume. The cell homogenates were centrifuged for 5 min at 4 °C and 11,000 x g, and the clear supernatant was used for analysis. One sample was split, with 105 µL each, in two wells; one well was analyzed in positive, and the other well was analyzed in negative ion mode. A pool of all analyzed cell homogenates and pooled human plasma served as reference matrices. H_2O and methanol were used as controls. In case of the human plasma, 475 µL of 100% methanol, spiked with internal standards for extraction monitoring, were added to 100 µL of human plasma, which was then centrifuged at 11,000 x g and 4 °C for 5 min. 105 µL per well of the clear supernatant were transferred to the 96-well 350 µL PCR plate. In case of the H_2O control, 475 µL of spiked 80% methanolic extraction solvent (v/v) were added, and the sample was centrifuged using the same parameters as with the human plasma and cell homogenates. The reference matrices were applied six times for each ionization mode (105 µL per well). The controls were applied once for each ionization mode (H_2O control: 105 µL, methanol control: 105 µL).

Method. Analyses using non-targeted metabolomics were performed by Dr. Anna Artati, Andrea Kraume and Bianca Eichner. As mentioned above, the sample was applied twice to a 96-well 350 µL PCR plate and dried under nitrogen flow in a TurboVap 96. The wells for the negative ion mode were reconstituted in 50 µL of 6.5 mM ammonium bicarbonate (pH = 8.0) in H_2O. The wells for the positive ion mode were reconstituted in 50 µL of 0.1% formic acid in H_2O. Both reconstitution solvents were spiked with internal standards to monitor the system performance. LC-MS/MS analysis was conducted with a LTQ XL™ linear ion trap mass spectrometer, coupled to an Acquity UPLC system. UPLC separation was performed for the positive and the negative ion mode separately on two separate columns of the same type (ACQUITY UPLC BEH C18 1.7 µm 2.1 mm X 100 mm) according to the method established by Metabolon (Metabolon, Inc., Durham, U.S.A). Applications were previously described in [104], [142]. For the positive ion mode, 0.1% formic acid in H_2O (solvent A) and 0.1% formic acid in methanol (solvent B) were used. For the negative ion mode, 6.5 mM ammonium bicarbonate in H_2O (pH = 8.0) (solvent A) and 6.5 mM ammonium bicarbonate in 95% methanol:H_2O (v/v) (solvent B) were used. A gradient run was performed, starting with 99.5% solvent A and ending with 98% solvent B, within a run time of 11 minutes and with a flow rate of 0.35 mL/min. An *m/z* range of 80 to 1000 was scanned, and alterations between MS and MS/MS scans were done using a dynamic exclusion technique.

2.17. Calculations, statistical analyses and data evaluation

For data evaluation, biostatistics, multivariate analyses and plotting R 3.1.2 [119] was used. The following packages were used: effsize [143], samplesize [144], coin [145], [146], exactRankTests [147], Kendall [148], miscTools [149], plyr [150], lawstat [151], ggplot2 [152], nls2 [153], ChemmineR [154], fmcsR [155], pvclust [156] and pheatmap [157]. For creating pathways and displaying data on nodes PathVisio 3.2.2. [127], [128] was used.

2.17.1. Calculation of validation parameters of analytical methods

Validation parameters were defined and calculated as proposed by the "Guideline on bioanalytical method validation" by the EMA [111] and the "Guidance for Industry: Bioanalytical Method Validation" by the FDA [113].

Precision. The precision is defined as the degree of accordance of scatter of multiple (serial) measurements. It is represented by the coefficient of variation [111], [113]. The precision will be expressed in percent. It is calculated according to **Equation (2)** [111].

Equation (2) $$precision\ (CV)[\%] = \frac{standard\ deviation}{mean} * 100\%$$

Accuracy. The accuracy represents the closeness of the determined value to the true (nominal) value [111] and is calculated according to equation **Equation (3**) [111]:

Equation (3) $$accuracy\ [\%] = \frac{determined\ value}{true\ value} * 100\%$$

Matrix factor. The matrix factor is a representation of matrix effects, which are defined as the alteration in the response as a result of the presence of interfering compounds in the sample (matrix) [111]. The EMA lists two types of matrix factors: the matrix factor of the analyte and internal standard and the matrix factor of the analyte normalized to the matrix factor of the internal standard [111]. The calculation of the matrix factor for the analyte and the internal standard is shown in **Equation (4)** [111]. The calculation of the IS normalized matrix factor is shown in **Equation (5)** [111].

Equation (4) $$matrix\ factor = \frac{peak\ area_{matrix}}{peak\ area_{witho\quad matrix}}$$

Equation (5) $$matrix\ factor_{IS\ normalized} = \frac{matrix\ factor_{analyte}}{matrix\ factor_{internal\ standard}}$$

2.17.2. Normalization of MS measurements

Normalization of plate effects. For the normalization of plate effects the plate normalization factor for each metabolite was calculated using reference samples (**Equation (6)**). Then, the metabolites levels were multiplied with the respective plate normalization factor.

Equation (6) $$Plate\ normalization\ factor = \frac{Median\ compound\ level_{all\ plate}}{Median\ compound\ level_{plate\ x}}$$

Normalization to cell number. Normalization of analyte levels and concentrations to the cell number was performed using **Equation (7)**.

Equation (7) $$analyte_n = \frac{analyte_m * c_n}{c_m}$$

$analyte_n$ is the normalized analyte level or concentration and $analyte_m$ the measured analyte level or concentration. c_m represents the determined cell number and c_n the cell number the analyte is normalized to. If not stated otherwise, the reference cell number (c_n) was 1 x 10^6 and the medians of cell numbers of the according groups were used as c_m.

2.17.3. Calculation of kinetic parameters

Transport kinetics: Michaelis-Menten equation. To assess the kinetics of metformin transport, the Michalis-Menten equation was used (**Equation (8)**). *v* represents the uptake rate, v_{max} the maximum velocity, S the substrate concentration and K_M the Michaelis-Menten constant [40], [158]–[160].

Equation (8)
$$v = \frac{v_{max} * S}{K_M + S}$$

To calculate the parameters, two approaches are possible: the data can be rearranged to become suitable for linear regression (e.g., Lineweaver-Burk plot [161]) or non-linear regression can be performed [162]. The advantages and disadvantages of these approaches are discussed in detail in [162]. In brief, in case of the Lineweaver-Burk transformation, rearrangement of the data leads to a distortion of the error distribution. This can be accounted for by correct weighting during linear regression. However, non-linear regression does not require the rearrangement of the data in the first place, and is considered to be the most accurate approach to model non-linear biological responses [162]. Therefore, based on the Michaelis-Menten equation displayed above, an iterative approach was applied to determine the best fit.

Extended transport kinetics: Michaelis-Menten equation including a non-saturable term. To account for a potential dualilty of drug transport (saturable and non-saturable component), a non-saturable term was added to the Michaelis-Menten equation. This approach has previously been applied to metformin transport studies by Sogame *et al.* [40] and Proctor *et al.* [139]. K_{ns} is the non-satruable component.

Equation (9)
$$v = \frac{v_{max} * S}{K_M + S} + K_{ns} * S$$

Again, based on the **Equation (9)**, an iterative non-linear regression approach was applied to determine the best fit.

2.17.4. Assessment of chemical similarity

Chemical similarity. To assess the similarity of different chemical structures, two different coefficients were used: the Tanimoto coefficient and the overlap coefficient.
The input data (SDF files and SMILES) were retrieved from the Human Metabolome Database (HMDB) [163]–[165] and DrugBank [166].

Tanimoto coefficient. The Tanimoto coefficient is a prominent association coefficient, which is frequently used to assess the similarity of chemical compounds [167]. It is defined by **Equation (10)** [167], [168]:

Equation (10) $$Tanimoto\ coefficient = \frac{c}{a+b-c}$$

a is the number of features of compound *a*, *b* is the number of features of compound *b* and *c* the number of common features [167], [168]. Hence, 1 represents a perfect fit and 0 no overlap of the tested structures. The atom pair descriptors of the tested molecules were used as input. An atom pair descriptor is the shortest bond path between two atoms of a molecule. It is given as the number of atoms on this bond path, including the two terminal atoms [168].

Overlap coefficient. The overlap coefficient was calculated and the overlap was graphically displayed using the fmcsR package [155]. It was calculated as follows:

Equation (11) $$Overlap\ coefficient = \frac{F_a}{F_c}$$

F_a is the number of non-hydrogen atoms of compound a, and F_c is the number of non-hydrogen atoms common to compound *a* and *b*. For matching of the query compound (e.g., metformin) and the target compound structure (e.g., ASP^+) with the fmcsR package [155], the number of tolerated atom mismatches as well as the number of tolerated bond mismatches was set to 0.

2.17.5. Statistics

To test for normal distribution of the data, either the Shapiro test [169] or QQ-plots with 95% confidence intervals were applied. To test for equality of variances the Levene´s test [170] was used. In case of small sample sizes any assessment of a distribution is difficult, as the sample size provides too little information for reliable test statistics [171]. Hence, for experiments with small sample sizes (e.g., inhibitor studies), non-parametric methods were applied per default. In addition, if multiple testing of single parameters was applied (e.g., metabolomics), and a number of parameters did exhibit a non-normal distribution or heteroscedasticity, all parameters were tested, applying non-parametric methods.

An alpha (α) of 0.05 was applied. To test two groups, the Wilcoxon-Mann-Whitney (U-test) test was used [172], [173]. To test more than two groups, the Kruskal-Wallis test [174] was the method of choice. As posthoc test, the U-test was applied, and the results were corrected for multiple testing.

Correction for multiple testing. To adjust for multiple testing, two different methods were used: the Bonferroni correction [175] and the Benjamini-Hochberg method [176]. The selection of the method depended on the aim of the experiment. If controlling the type I error ("false positive") was of utmost importance (e.g., in case of the inhibitor studies in section **3.4**), the conservative Bonferroni correction [175] was used. If avoiding type II errors ("false negative") was prevalent the Benjamini-Hochberg method was applied (e.g., metabolomics analyses of glucose and metformin treated cells in section **3.5**).

The type of applied test, the sample size, the p-value and, if applicable, the method used for correction of multiple testing, will be provided for each experiment.

Cliff´s delta. Cliffs delta is a non-parametric effect size, which represents the overlap of two distributions of scores and takes on a value between -1 and +1 [177]. It is calculated as indicated by **Equation (12)** [177], [178]:

Equation (12) $$Cliff´s\ delta = \frac{\#(x_a > x_b) - \#(x_a < x_b)}{n_a n_b}$$

The terms $\#(x_a > x_b)$ and $\#(x_a < x_b)$ represent the number of times an observation of group a was higher or lower in the dominance matrix as an observation of group b. n indicates the sample size of the according group [177], [178]. The according Cliff´s deltas were calculated using the effsize package [143]. In this study, a positive value represents a relative increase of the "treatment" group compared to the "control" group (e.g., metformin treated cells vs. non-treated controls) and vice versa in case of a negative value.

2.18. Nomenclature

Experimental reporting standards. The sample sizes, listed in the material and methods section, list the complete sample set for the according experimental setup (e.g., the number of samples per group generated for all inhibitor studies). The sample sizes, listed in the figures and tables of the results and discussion sections (**3 Results** and **4 Discussion**), show the sample size of the according experiment after removal of samples which did not pass quality control (e.g., below LOD or outside the 1.5 x interquantile range) or samples with documented problems during sample generation and processing.

Metabolites. For non-targeted metabolomics, the nomenclature used and provided by Metabolon Inc. was adopted. The metabolite names and according HMDB IDs are provided in **Table S-4**. Compounds marked with a "*" were identified but not yet confirmed based on a standard. Compounds starting with an "X - ", followed by numerical values were not identified. In case of the metabolites measured with the targeted metabolomics Absolute*IDQ* p180 Kit, the nomenclature used in this study, full names of potential compounds fitting the according MRM, and, if available, HMDB IDs are provided in the supplemental information of Muschet *et al.* [117]. The metabolite nomenclature illustrated in **Table 8** was based on the nomenclature used by BIOCRATES LIFE SCIENCES AG (Absolute*IDQ*® Kit. Analytical Specifications p180. AS-P180-3. BIOCRATES LIFE SCIENCES AG), Römisch-Margl *et al.* [132] and Zunkunft *et al.* [105].

Table 8: Nomenclature of the metabolites covered by the Absolute*IDQ* p180 Kit.
The table lists the nomenclature of the metabolites, which were covered with the Absolute*IDQ* p180 Kit. *x* indicates the number of carbons and *y* the number of double bonds [132]. Further, DC represents a dicarboxylation, M a methylation and OH a hydroxylation [132]. Metabolites, which are not covered by this specification, are listed in the Abbreviations section and introduced in the text.

Nomenclature: Targeted metabolomics (Absolute*IDQ* p180 Kit)

Abbreviation	Metabolite class	Example(s)
C*x*:*y*	(Acyl)carnitine(s)	C0 Free carnitine C2 Acetylcarnitine
Three-letter code	Amino acids	Ala Alanine
lysoPC a C*x*:*y*	Lysophosphatidylcholines	lysoPC a 24:0 Lysophosphatidylcholine acyl C24:0
PC aa C*x*:*y*	Diacylphosphatidylcholines	PC aa C38:0 Diacylphosphatidylcholine C38:0
PC ae C*x*:*y*	Acylalkylphosphatidylcholines	PC aa C38:0 Diacylphosphatidylcholine C38:0
SM C*x*:*y*	Sphingomyelins	SM C16:0 Sphingomyelin C16:0
H1	Sum of hexoses	

3. Results

3.1. Validation of the LC-MS/MS based metformin quantification method

A crucial prerequisite for the elucidation of metformin uptake and action was the availability of a method for the reliable quantification of metformin in different matrices. Therefore, a MS based metformin quantification method was developed, optimized and validated. The most important criteria during the method development and optimization were the applicability to a wide range of matrices, robustness, high-throughput suitability and satisfactory performance in regard to specificity, accuracy, precision and the linear range. Since this method should be implemented into a platform portfolio, a wide range of matrices, being of vital importance in diabetes research, should be covered: human and murine plasma and serum, murine tissues, cell homogenate and cell culture supernatant. As the major focus of this project was the elucidation of cellular metformin action, cell homogenate and cell culture supernatant will be the focus of this chapter.

The first approach was developed together with the PhD student Sven Zukunft from the same laboratory and was used for the metformin quantification in murine tissues and fluids [179], [180]. However, further optimization was required to ensure the reliable performance of the method in all tested matrices. In short, depending on the matrix, the sample preparation was adapted by adding another precipitation step with acetonitrile and adjusting the sample dilution in methanol. Further, a reversed phase C18 column was added to the HPLC setup to diminish the impact of the matrix on the quantification. In addition, the internal standard was switched from metformin (d6) to phenformin, a commonly used internal standard for metformin quantification [181], [182]. The internal standard was changed due to the instability of the deuterium labelled metformin (d6).

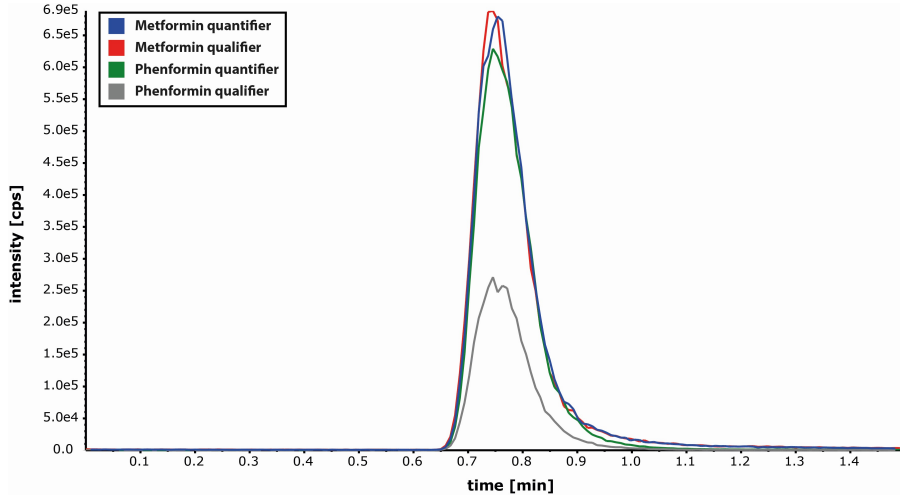

Figure 4: Multiple reaction monitoring (MRM) chromatogram of the optimized LC-MS/MS metformin quantification method using treated Hep G2 cells.
1 x 10^6 Hep G2 cells were treated with 500 µM metformin for 24 h and scraped in 87.5% methanolic extraction solvent. Metformin quantification was performed using the optimized and validated metformin quantification method.

In course of this PhD project, two matrices were of crucial importance, namely, cell homogenate and cell culture supernatant. Therefore, the validation of the method for those two matrices as well as the validation of the method itself will be discussed in the following chapter.

The validation of the optimized LC-MS/MS based metformin quantification method (

Figure 4) was based on the "Guideline on bioanalytical method validation" by the EMA [111] and the "Guidance for Industry: Bioanalytical Method Validation" by the FDA [113]. In course of the validation process specificity, accuracy, precision, stability and the linear range with the LOD, LLOQ as well as the ULOQ, were determined. The simple sample preparation procedure, consisting of a single methanolic dilution for cell homogenates and a precipitation step in acetonitrile, followed by a methanolic dilution step for supernatants, in combination with a 1.5 min runtime, allows for a very high throughput and low variability due to sample preparation or machine performance. However, whereas proteins and DNA are precipitated by methanol or acetonitrile and the subsequent centrifugation step, lipids and other metabolites, which might interfere in the quantification, are not removed. To account for this issue, differentiated 3T3-L1 cells, having a high lipid content [141], [183], were chosen for validation, as this matrix might pose a higher risk for potential interference compared to other cell lines used in this study.

3.1.1. General parameters of the LC-MS/MS based metformin quantification method

General parameters for validation were the specificity, the linear range, with the LOD, LLOQ and the ULOQ, the accuracy and the precision of standard curve preparation as well as the injection precision and the short and long term stability of prepared calibrators.

Specificity. The specificity is defined as the ability of a method to unequivocally measure the analyte in the presence of endo- and exogenous compounds in a matrix [111]. The specificity of the LC-MS/MS based metformin quantification method was constantly monitored by measuring vehicle treated cells (zeros), which were cultivated and processed the same way as the metformin treated cells. No interferences were observed. Further, a second MRM, the so called qualifier, was used as an additional quality control step. The addition of a qualifier allows for the detection of a potential cosscontamination by a coeluting compound having the same MRM [184].

Linear range. Initially, a standard curve with 12 concentrations between 0.1 pM and 10 µM was prepared and measured (**Table 9**). To calculate the metformin concentrations, linear regression analysis of the analyte peak areas (normalized to the IS) to the spiked concentrations was performed. Only concentrations within the range of 0.5 nM and 1,000 nM were used for linear regression analysis to avoid the integration of anchor points. As the integration of the peaks started at the baseline and the zeros did not show any peaks, linear regression through zero was the method of choice. Then, the slope obtained via linear regression was used to calculate the metformin concentration in all measured calibrators.

Further, the accuracy of all concentrations was calculated according to **Equation (3)** (section **2.17.1**). The LOD was defined as the first concentration within the standard curve, with an analyte intensity at least five times higher than the baseline of the according blank (methanol without IS). The LLOQ was defined as the first concentration within the standard curve, with an analyte intensity at least five times higher than the baseline [111], [113] of the blank and a deviation of the accuracy ± 20% [113].

Table 9: Determination of the linear range of the LC-MS/MS based metformin quantification method.
A standard curve with 12 calibrators within the range of 0.1 pM and 10 µM was used to determine the linear range. The table lists the spiked and calculated concentrations, the preliminary LOD and LLOQ, the ULOQ as well as the accuracies of the according concentrations. The standard curve was prepared once and injected thrice. The standard deviations represent the variation of the injections.

Linear range

Spiked metformin concentration [nM]	Calculated metformin concentration ± SD [nM]		Accuracy ± SD [%]	
	Quantifier	Qualifier	Quantifier	Qualifier
0.0001	0.22 ± 0.02	0.03 ± 0.01	215666.67 ± 17214.34	28266.67 ± 12786.84
0.001	0.18 ± 0.01	0.05 ± 0.00	17733.33 ± 1201.39	4806.67 ± 498.93
0.01	0.17 ± 0.02	0.03 ± 0.01	1680.00 ± 186.82	334.33 ± 79.22
0.1	0.24 ± 0.06	0.10 ± 0.04	236.00 ± 55.02	103.20 ± 42.88
0.5	0.64 ± 0.05 (LOD)	0.53 ± 0.04	127.73 ± 10.14	105.87 ± 7.37
1	1.04 ± 0.02 (LLOQ)	0.89 ± 0.04	104.00 ± 1.73	88.60 ± 4.29
5	5.55 ± 0.05	5.33 ± 0.11 (LOD & LLOQ)	111.07 ± 0.99	106.67 ± 2.14
10	11.27 ± 0.15	10.80 ± 0.35	112.67 ± 1.53	108.00 ± 3.46
50	54.57 ± 1.69	54.00 ± 1.54	109.13 ± 3.38	108.00 ± 3.08
100	109.67 ± 3.06	110.00 ± 1.73	109.67 ± 3.06	110.00 ± 1.73
1,000	997.67 ± 13.65	998.67 ± 11.02	99.77 ± 1.37	99.87 ± 1.10
10,000	7806.67 ± 90.74 (ULOQ)	7756.67 ± 70.95 (ULOQ)	78.07 ± 0.91	77.57 ± 0.71

The preliminary LOD was found to be 0.5 nM for the quantifier and 5 nM for the qualifier. The LLOQ was 1 nM for the quantifier and 5 nM for the qualifier. Due to its better performance in case of the LOD and LLOQ, the MRM 130.1/60.0 was chosen as quantifier. The ULOQ was set to 10,000 nM. It should be noted that this concentration did not fulfill the recommendations made by the FDA and EMA, which require an accuracy of 100% ± 15-20% [111], [113]. However, inclusion of this concentration into the linear regression led only to a very minor decrease of the R^2 (from 0.9999 to 0.9996), illustrating that the response curve is still linear.

To verify the determined LOD, LLOQ and the accuracy and to assess the precision of the standard curve, a standard curve with 15 concentrations, within the range of 5 pM to 1 µM, was prepared thrice, using a different set of metformin stock solutions (**Table 10**). The ULOQ was not included into the standard curve, as it strongly contaminated the system and might impact the reevaluation of the LOD and LLOQ. In addition, a closer evaluation of the ULOQ was not necessary, as none of the samples, measured with this method, exhibited concentrations within the range of the ULOQ. The LOD was again defined as the lowest concentration of the standard curve having an intensity of more than five times higher than the baseline of the blanks. The aforementioned LLOQ criteria were extended. In addition to the intensity and accuracy criteria, the precision (CV) had to be below 20% [113]. The

preliminary LOD of the quantifier as well as the preliminary LOD and the LLOQ of the qualifier could be verified (**Table 10**). The LLOQ of the quantifier was found to be slightly lower (0.5 nM). The higher LLOQ of the first approach (**Table 9**) might be caused by the contamination of the system by the highest concentration (the standard curve was injected thrice). All concentrations above the LLOQ showed an accuracy within the recommended range of 100% ± 15% [111], [113] and a CV well below 10% (**Table 10**). As observed for the first standard curve, the R^2 (0.5-1,000 nM) for both, the quantifier and the qualifier, exceeded 0.999, indicating an excellent linear correlation.

Table 10: LOD, LLOQ, accuracy and precision of the LC-MS/MS based metformin quantification method.
A standard curve consisting of 15 calibrators within the range of 5 pM to 1 µM, was prepared thrice (n = 3). The preliminary LOD and LLOQ were confirmed. The table lists the calculated metformin concentrations, accuracies and precisions. The precision is represented by the coefficient of variation [%]. The standard deviations represent the variation of the multiple preparations.

Standard curve

Spiked metformin concentrations [nM]	Calculated metformin concentration ± SD [nM]		Accuracy ± SD [%]		Precision (CV) [%]	
	Quantifier	Qualifier	Quantifier	Qualifier	Quantifier	Qualifier
0.005	0.13 ± 0.03	0.13 ± 0.02	2564.74 ± 682.14	2666.59 ± 493.17	26.60	18.49
0.01	0.11 ± 0.05	0.15 ± 0.06	1074.18 ± 514.67	1465.21 ± 582.79	47.91	39.78
0.05	0.08 ± 0.02	0.13 ± 0.03	156.08 ± 36.35	266.13 ± 58.45	23.29	21.96
0.1	0.18 ± 0.02	0.16 ± 0.02	179.27 ± 21.46	161.03 ± 15.13	11.97	9.40
0.5	0.56 ± 0.04 (LOD & LLOQ)	0.48 ± 0.02	112.12 ± 8.89	95.88 ± 4.27	7.93	4.45
1	1.15 ± 0.04	0.97 ± 0.03	115.16 ± 4.12	96.78 ± 3.37	3.58	3.48
5	4.77 ± 0.09	4.18 ± 0.10 (LOD & LLOQ)	95.49 ± 1.84	83.56 ± 1.99	1.93	2.38
10	10.23 ± 0.30	9.04 ± 0.25	102.29 ± 2.98	90.43 ± 2.53	2.91	2.79
50	48.82 ± 1.28	44.55 ± 1.20	97.64 ± 2.55	89.11 ± 2.40	2.62	2.69
100	106.14 ± 1.87	97.32 ± 1.49	106.141 ± 1.87	97.32 ± 1.49	1.76	1.53
200	200.08 ± 6.75	183.42 ± 5.96	100.04 ± 3.38	91.71 ± 2.98	3.37	3.25
250	251.08 ± 4.58	228.55 ± 4.64	100.43 ± 1.83	91.42 ± 1.86	1.82	2.03
500	497.13 ± 4.92	459.79 ± 4.13	99.43 ± 0.98	91.96 ± 0.83	0.99	0.90
750	757.29 ± 19.79	698.17 ± 16.01	100.97 ± 2.64	93.09 ± 2.13	2.61	2.29
1,000	995.12 ± 2.56	910.55 ± 5.95	99.51 ± 0.26	91.05 ± 0.59	0.26	0.65

In conclusion, the linear range (quantification range [113]) of the quantifier was found to be 0.5 nM to 10,000 nM. For the quantification of metformin in cell homogenates, standard curves with ≥ 10 calibrators within the range of 5 pM to 10 µM were used. The inclusion of concentrations below and close to the determined LOD allowed for the monitoring of the LOD and LLOQ, which was of crucial importance for the lateron conducted inhibitor studies (section **3.4.3**). As recommended by the FDA and EMA, at least six concentrations had to be within the linear range of the method [111], [113].

Injection precision. To determine the injection precision of the method, the standard curves used for determination of the linear range were injected thrice. The CVs are listed in **Table 11**. In conclusion, the method shows excellent injection reproducibility (quantifier: CVs below 10%) with all concentrations within the linear range (0.5 nM - 10 µM) and both approaches.

Table 11: Injection precision of the LC-MS/MS based metformin quantification method.
The table shows two separate approaches. With the first approach a standard curve, consisting of 12 calibrators with concentrations within the range of 0.1 pM to 10 µM (n = 1) was prepared and injected thrice. With the second approach, three identical standard curves, with calibrators with 15 different concentrations within the range of 5 pM to 1 µM were prepared (n = 3) and each was injected thrice.

Injection precision

	1st approach		2nd approach	
Spiked metformin concentration [nM]	**CV [%] Quantifier**	**CV [%] Qualifier**	**CV ± SD [%] Quantifier**	**CV ± SD [%] Qualifier**
0.0001	8.0	45.2		
0.001	6.8	10.4		
0.005			47.92 ± 38.95	60.31 ± 25.17
0.01	11.1	23.7	46.16 ± 4.66	51.06 ± 18.29
0.05			55.63 ± 26.09	25.26 ± 19.61
0.1	23.3	41.6	37.02 ± 22.03	61.74 ± 16.51
0.5	7.9	7.0	3.93 ± 2.98	16.95 ± 14.56
1	1.7	4.8	5.89 ± 1.47	8.88 ± 3.24
5	0.9	2.0	3.15 ± 1.30	3.39 ± 2.34
10	1.4	3.2	1.63 ± 1.25	3.67 ± 1.34
50	3.1	2.9	1.92 ± 0.67	3.38 ± 0.54
100	2.8	1.6	2.80 ± 0.74	3.10 ± 1.22
200			2.33 ± 0.66	3.71 ± 0.50
250			1.16 ± 0.80	2.34 ± 0.12
500			2.45 ± 0.83	3.35 ± 0.31
750			2.83 ± 0.33	3.21 ± 1.02
1,000	1.4	1.1	2.18 ± 0.13	3.87 ± 0.42
10,000	1.2	0.9		

Analyte stability. The short term and long term stability of prepared calibrators at -80 °C was tested to evaluate whether the calibrators could be stored and re-measured. Therefore, a standard curve with the range of 0.5 nM to 1,000 nM was prepared and measured at day 0, day 1 and day 69 (three injections per calibrator at each time point). The results are shown in **Table 12**. As a normal distribution of the data was not given, the nonparametric Fiedman test (p-value: 9.1×10^{-4}) and the Nemenyi post-hoc test were applied. Although a slight increase in metformin levels after one day of storage was observed, the analyte levels of the samples are not significantly affected by short term storage at -80 °C. The slightly increased analyte levels are most likely caused by the evaporation of methanol during the time in the autosampler. However, over a period of more than two months (**Table 12**: Long term) the metformin concentration decreased significantly to 51- 64% compared to day 0 (Nemenyi post-hoc test: p-value: 5.4×10^{-4}). Therefore, a long term storage of the samples is not possible. But, already prepared calibrators might be stored over night at -80 °C.

Table 12: Short term and long term stability of prepared calibrators.
A standard curve with seven metformin concentrations within the linear range of the assay was prepared and measured thrice. Then the samples were stored at -80 °C and re-measured the next day to assess the short term stability (day 1). Afterwards the samples were stored up to day 69 and re-measured again to test the long term stability (day 69). The stabilities are shown as percentage of controls (concentration at day 0). The table displays the stabilities ± standard deviations.

Stability

Metformin concentration [nM]	**Short term (day 1)**	**Long term (day 69)**
0.5	113.7 ± 6.3	64.0 ± 1.0
1	114.4 ± 3.5	61.0 ± 3.0

5	107.1 ± 1.7	53.6 ± 1.0
10	107.1 ± 1.4	53.3 ± 1.6
Metformin concentration [nM]	**Short term (day 1)**	**Long term (day 69)**
50	107.8 ± 0.2	52.2 ± 1.2
100	106.4 ± 1.4	51.8 ± 1.2
1,000	110.6 ± 1.5	51.4 ± 0.8

3.1.2. The LC-MS/MS based metformin quantification method for cell culture matrices

For this study, the method was validated for cell homogenates and cell culture supernatants. In this context, accuracy, precision and matrix effects were tested.

Precision. To assess the precision of the method in regard to cell homogenates and cell culture supernatants, three concentrations within the linear range and with relevance to the application of the method to cell culture metabolomics studies, were spiked into either cell homogenates or supernatants of differentiated 3T3-L1 cells, thrice. The validated concentration range on the column is 10 x higher for the cell homogenates than for cell culture supernatants (**Table 13**) due to the 10 x higher dilution factor, caused by the additional acetonitrile precipitation step, required for the analysis of cell culture supernatants (section **2.14**). Further, the concentration range was fitted to the expected concentration range of the cell homogenates, used for the elucidation of the impact of glucose and metformin on the hepatocellular metabolism (section **3.5**). The finally measured concentration range of this experiment was found to be 200-1,200 nM; thereby fitting the expectations quite well. As illustrated by the CVs in **Table 13**, the method shows a very high precision for cell homogenates. In case of cell culture supernatants, the precision was found to be lower as indicated by a higher CV. However, the CV is below the 15% threshold recommended by the EMA [111] and the FDA [113].

Table 13: Precision (CV) of the LC-MS/MS based metformin quantification method in cell homogenates and cell culture supernatants.
Three analyte concentrations were spiked into cell homogenates of differentiated 3T3-L1 cells and the according supernatants (n = 3). The samples were prepared, measured and evaluated as described in section **2.14.1**.

Precision		
Spiked metformin concentration [nM]	**CV [%] Quantifier**	**CV [%] Qualifier**
Cell homogenates		
500	0.73	2.51
1,000	6.63	4.36
2,000	1.57	1.97
Cell culture supernatants		
50	13.29	13.10
100	13.51	13.01
200	3.57	6.38

Accuracy. The accuracy was assessed by quantifying the metformin concentration in cell homogenates and cell culture supernatants, spiked with three different drug concentrations. Quantification was achieved by using a standard curve, which was prepared by diluting the according stocks 1:50 (v/v) in methanol, spiked with phenformin as internal standard (section **2.14**). Then, the deviation of the quantified metformin concentrations from the true

values was calculated as shown in **Equation (3)** (section **2.17.1**). The results are listed in **Table 14**. For all tested concentrations and both matrices, the quantifier yielded better accuracies than the qualifier, confirming the choice of this MRM as quantifier. Further, the quantifier fulfills the recommendations made by the FDA and EMA of less than ± 15% deviation in accuracy [111], [113] for both matrices. In addition, the very good performance of the method in terms of accuracy, if quantified with a standard curve in IS spiked methanol, shows that the standard curve does not have to be prepared in the matrix.

Table 14: Accuracy of the LC-MS/MS based metformin quantification method in cell homogenates and cell culture supernatants.
Three analyte concentrations were spiked into cell homogenates of differentiated 3T3-L1 cells and the according supernatants (n = 3). The samples were prepared, measured and evaluated as described in section **2.14.1**. The table displays the mean accuracies of the according concentrations ± standard deviation.

Accuracy

Spiked metformin concentration [nM]	Quantifier [%]	Qualifier [%]
Cell homogenates		
500	99.20 ± 0.72	95.80 ± 2.40
1,000	99.20 ± 6.58	95.03 ± 4.15
2,000	102.17 ± 1.61	96.33 ± 1.89
Cell culture supernatants		
50	88.07± 11.70	84.87 ± 11.12
100	87.37 ± 11.81	83.10 ± 10.81
200	93.33 ± 3.33	89.00 ± 5.68

Matrix effects. Potential matrix effects of cell homogenates and cell culture supernatants were assessed by calculating the matrix factor of the analyte and the IS (**Equation (4)**, section **2.17.1**) and the IS normalized matrix factor (**Equation (5)**, section **2.17.1**). As illustrated by the analyte and IS matrix factors as well as the IS normalized matrix factors listed in **Table 15**, neither the cell homogenates nor the cell culture supernatants exhibit a strong impact on the metformin quantification.

Table 15: Matrix factors of the LC-MS/MS based metformin quantification in cell homogenates and cell culture supernatants.
Three metformin concentrations were spiked thrice into cell homogenate, cell culture supernatant, 87.5% methanolic extraction solvent and H_2O (n = 3). The table lists the mean matrix factors ± standard deviations of the analyte (metformin) and the IS (phenformin) and the IS normalized matrix factors for both matrices.

Matrix factors

Spiked metformin concentration [nM]	Matrix factor metformin (Quantifier)	Matrix factor metformin (Qualifier)	Matrix factor phenformin	IS normalized matrix factor metformin (Quantifier)	IS normalized matrix factor metformin (Qualifier)
Cell homogenate					
500	1.08 ± 0.01	1.09 ± 0.02	1.04 ± 0.01	1.04 ± 0.01	1.04 ± 0.01
1,000	1.16 ± 0.07	1.15 ± 0.05	0.99 ± 0.02	1.17 ± 0.07	1.16 ± 0.05
2,000	1.12 ± 0.01	1.05 ± 0.01	0.91 ± 0.02	1.23 ± 0.01	1.16 ± 0.01
Cell culture supernatant					
50	1.25 ± 0.16	1.24 ± 0.16	1.05 ± 0.01	1.20 ± 0.16	1.18 ± 0.15
100	1.13 ± 0.15	1.11 ± 0.14	1.05 ± 0.01	1.07 ± 0.14	1.06 ± 0.13
200	1.02 ± 0.03	1.01 ± 0.06	1.04 ± 0.01	0.98 ± 0.03	0.97 ± 0.06

Outcome. The LC-MS/MS based metformin quantification method, optimized and validated in course of this study, is a robust, fast, accurate and precise method for the quantification of metformin in cell homogenates and cell culture supernatants. The method spans a wide concentration range (pM to μM) and can be regarded as a high-throughput method due to the simple sample preparation procedure and the short run time. In addition, it is highly compatible with other methods, as samples harvested and prepared for metformin quantification can be measured with the targeted and non-targeted methods and assays. Further, it allows for the determination of the cell number with the fluorescence based DNA quantification method, which was developed and optimized in course of this study and will be discussed in the next chapter. This allows for effective experimental designs, because drug, DNA and metabolite quantification can be performed using the same sample.

Limitations and outlook. In future, the method should be validated for a number of different cell lines and cell culture supernatants. To test the robustness of the method in the according matrices, a broader concentration range and a higher number of metformin concentrations should be validated.

3.2. Development, optimization and implementation of a fast, fluorescence based DNA quantification method for cell number determination in metabolomics samples

Since the sample harvest for metformin quantification and metabolomics analyses is identical, the technical bias can be reduced. The sampling procedure consists of a quenching step in methanolic extraction solvent, followed by scraping to detach the cells and collect the cellular material and a subsequent homogenization step (section **2.8**). Consequently, this protocol renders cell counting impossible. As metformin has been reported to impair cell proliferation and introduce apoptosis [87] it can safely be assumed that the cell numbers of the samples with treated cells might be lower than the ones of the controls, which would introduce a technical bias into the analyses. This bias has to be accounted for by means of data normalization to cell number.

Therefore, establishing a reliable normalization method was a crucial prerequisite for the elucidation of hepatocellular metformin uptake and action. Initially, additional wells were cultivated under the same conditions as the ones used for metabolomics analyses and metformin quantification. Then, a DAPI staining of those parallel wells was performed, multiple images per well were taken and the cell number was determined [130]. However, this method has a major drawback. The parallel wells might be representative for the culturing conditions and cellular behavior of the adjoining wells, but it is not possible to account for the loss of cellular material during cell harvest and sample preparation, or the individual variation between the harvested wells. Therefore, a method had to be developed, which allows for the quantification of a cellular marker, which robustly correlates – at best in a linear manner – with the cell number, using cell homogenates in organic solvent. In this regard, the DNA and the protein concentration are promising molecular markers [121]. Silva *et al.* showed that the DNA concentration does outperform the protein concentration as a molecular marker for normalization purposes [121]. The first attempt to determine the cell number by measuring the DNA content of a sample was rather simple: measuring the absorption of the sample with a NanoDrop ($\lambda = 260$ nm, reference $\lambda = 280$ nm) [130]. Although it could be shown that the measured signal linearly correlates with the cell number, and that this method was successfully applied to metabolomics analyses [130], it had two disadvantages. First, the high methanol content of the sample led to fast evaporation of the measured sample volume (2 µL), and often the sample had to be applied multiple times to obtain a valid measurement, which limited the throughput of the method. Second, the method suffered from high between-run variability.

Consequently, a different method for the quantification of DNA in cell homogenates was needed. The requirements for the assay to be developed were: quantification of DNA in organic solvent, absolute quantification of the cell number, high-throughput, low sample volume, low between-run variability and its applicability to a wide range of cell lines. With this final approach, the DNA of the cell homogenates used for metabolomics analyses and drug quantification was stained with the DNA selective dye Hoechst [185]. To allow for the quantification of a high number of samples in a single run, the method was developed to work in a 96-well format. This fluorescence based DNA quantification method removed the

major bottlenecks of previous approaches. It is applicable to the cell homogenates itself, robust and fast.

3.2.1. Development and optimization of the fluorescence-based DNA quantification method

The idea of the fluorescence-based DNA quantification assay was to mix the cell homogenate with a dilution of Hoechst dye, which selectively stains DNA [185]. In course of the development and optimization of the method, multiple parameters were tested. The most crucial parameters were the incubation time, the incubation temperature, the dye concentration, the sample volume and the correlation of the fluorescent signal to the cell number. Robustness of the method was analyzed by its application to a wide range of cell lines with different sizes, culturing conditions and organisms and tissues of origin. In addition, the applicability of the novel normalization method to metabolomics analyses was tested by analyzing the correlation of the metabolite concentrations, measured with a targeted metabolomics approach, to the cell numbers, which were determined with the optimized DNA quantification method.

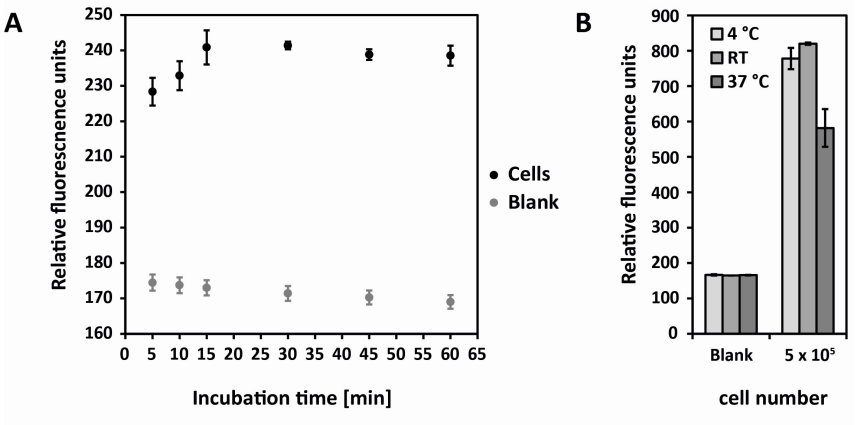

Figure 5: Optimization of the incubation time and incubation temperature of the DNA based cell number quantification method.
A: Optimization of the incubation time. The graph shows the relative fluorescent signal [rfu] to the incubation time response curve. 20 µL of a Hep G2 cell homogenate containing 5 x 10^5 cells were added to 80 µL of Hoechst dilution (0.2 µg/mL in PBS) thirce and incubated at RT in the dark. The plate was measured after an incubation time of 5, 10, 15, 30, 45 and 60 min. **B:** Optimization of the incubation temperature. 20 µL of Hep G2 cell homogenates containing 5 x 10^5 cells (n = 3) were added to 80 µL of Hoechst dilution (2 µg/mL in PBS). The plates were incubated at either, 4 °C, RT or 37 °C, for 30 min in the dark.

Incubation time. The data in **Figure 5A** show that the fluorescent signal increases with the incubation time up to 15 min. After 15 min of incubation, the signal intensity stagnates. As the same sample was measured in triplicate, the standard deviations, displayed in the plot, represent the technical variability of the measurement. The minimum CV, and consequently the highest technical precision, was observed for an incubation time of 30 min (0.4%). Therefore, the incubation time was set to 30 min.

Incubation temperature. Another crucial parameter was the incubation temperature. The same Hep G2 homogenates were applied to three different plates, which were either incubated at 4 °C, RT or 37 °C. For the incubation at RT a climatized room, which keeps the temperature constant during the whole year, was chosen to avoid any subsequent introduction of batch effects due to seasonal changes in temperature. Incubation of the plates at 4 °C or at RT did not affect the signal levels. However, incubation at 37 °C led to reduced signal levels (**Figure 5B**). Based on these results, RT was chosen as the optimal incubation temperature.

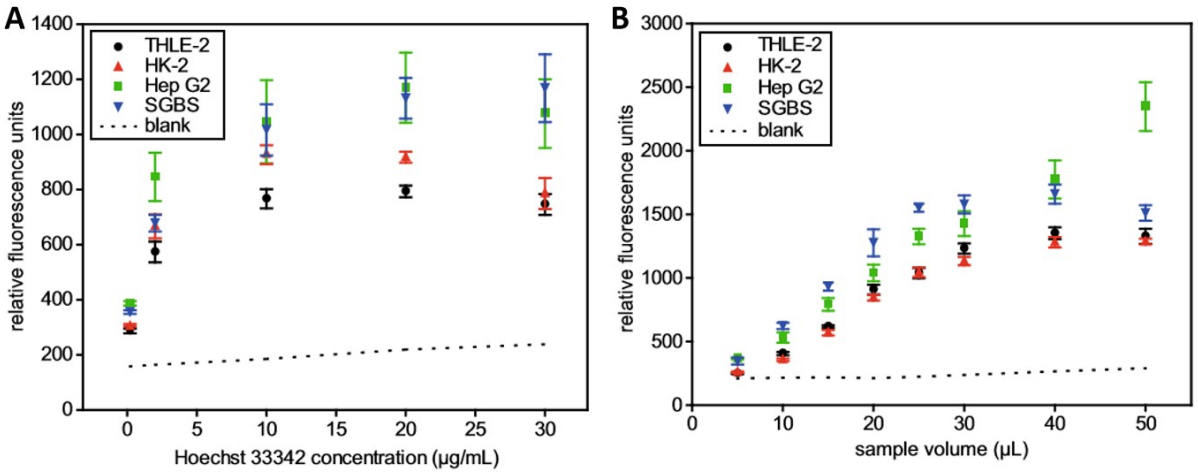

Figure 6: Optimization of the Hoechst 33342 concentration and the sample volume.
A: Fluorescent signal to Hoechst 33342 concentration response curve for four human cell lines. 20 µL of THLE-2, HK-2, Hep G2 and SGBS cell homogenates, containing 5 x 10^5 cells, were added to 80 µL of different Hoechst dilutions. Tested Hoechst concentrations were: 0.2, 2, 10, 20 and 30 µg/mL in PBS (n per cell line and Hoechst concentration = 6). The samples were incubated for 30 min in the dark. **B:** Fluorescent signal to sample volume response curve for four human cell lines. Different sample volumes (5, 10, 15, 20, 25, 30, 40 and 50 µL) of THLE-2, HK-2, Hep G2 and SGBS cell homogenates, containing 5 x 10^5 cells, were added to the respective Hoechst dilutions. The final Hoechst 33342 concentration was 20 µg/mL in PBS. The total volume in the well was 100 µL. The plates were incubated at RT in the dark for 30 min.
The plots have been taken from Muschet *et al.* [117]. The experiments with the THLE-2 and the HK-2 cells were performed by Dr. Janina Tokarz.

Hoechst 33342 concentration. This optimization step has previously been published by Muschet *et al.* [117]. To achieve a maximum of robustness, all further optimization steps were performed with four different cell lines, namely Hep G2 (human hepatocellular carcinoma), THLE-2 (human liver), SGBS (human preadipocyte), HK-2 (human kidney). These cell lines were chosen to cover a broad range of physical properties and tissues of origin. To optimize the Hoechst 33342 concentration, dye concentrations between 0.2 µg/mL and 30 µg/mL were tested. The concentration range was based on the recommendations provided by the manufacturer (Life Technologies, Darmstadt, Germany). For all cell lines, the highest signal intensity was observed with a sample volume of 10 to 20 µL (**Figure 6A**). Further elevation of the Hoechst 33342 concentration correlated with a decrease in fluorescent signal intensity for three out of four cell lines. Thus, the optimal Hoechst 33342 concentration was found to be 20 µg/mL [117].

Sample volume. This optimization step has previously been published by Muschet *et al.* [117]. To determine the optimal sample volume, volumes between 5 and 50 µL were tested. **Figure 6B** demonstrates that three out of four cell lines (THLE-2, HK-2

and SGBS) display a saturation of the response signal at sample volumes above 25 µL. Consequently, the optimal sample volume was found to be 20 µL [117].

Precision. Standard curves of a wide range of cell lines – Hep G2, THLE-2, SGBS, HK-2, HEK293, Hepa1-6, differentiated 3T3-L1, HeLa and COS-1 – were prepared (**Figure 8**) and measured with the optimized DNA quantification method. The standard curves of Hep G2, THLE-2, SGBS and HK-2 were taken from Muschet *et al.* [117].The mean precision of all tested cell lines and cell numbers was found to be 5.52% ± 1.85% (CV ± SD). As the cells were harvested by trypsinization and aliquoted, this CV represents the precision of the assay itself. Consequently, the assay has an excellent precision. However, in context with cell culture metabolomics, the combination of the harvesting method (scraping) with the fluorometric cell number determination is of importance. Therefore, four different cell lines (Hep G2, THLE-2, SGBS and HK-2) were seeded at different cell numbers, incubated until full attachment was given and harvested, using the optimized harvesting protocol for targeted metabolomics (scraping in 300 µL 87.5% methanolic extraction solvent per well and subsequent homogenization). Then, the cell numbers were determined using the optimized DNA based method, and the precision was calculated for each cell line and cell number (**Table 16**). The combination of the DNA assay with this harvesting method vastly decreases the precision. This might be explained by the fact that the harvesting method and extraction solvent was optimized with the aim in mind to achieve the optimal performance of the according metabolomics analyses. The high variation is most likely a result of the scraping step and should be taken into account during the normalization and evaluation of the metabolomics data.

Table 16: Precision of the fluorometric DNA quantification method for cell number determination in combination with the optimized harvesting protocol for targeted metabolomics.
The table lists the seeded cell numbers and the respective CVs of all tested cell lines. Different cell numbers of Hep G2, THLE-2, SGBS and HK-2 cells were seeded into 12-well plates, incubated until full attachment was achieved (4 - 16 h) and harvested using the optimized scraping protocol for targeted metabolomics (n per cell number = 6). Then, the DNA-based fluorometric cell number determination was performed. The different cell number ranges originate from the differences in the cell sizes of the tested cell lines.
THLE-2 and HK-2 cells were cultivated and harvested by Dr. Janina Tokarz. The data was kindy provided.

Precision CV [%]

Seeded cell number	Hep G2	THLE-2	SGBS	HK-2
7.5 x 10^4		6.98	12.03	31.41
1.0 x 10^5		16.46	10.74	18.36
2.5 x 10^5	17.62	17.02	18.32	23.22
5.0 10^5	17.38	21.17	7.83	11.34
7.5 x 10^5	10.97			12.57
1.0 x 10^6	21.78			
2.5 x 10^6	13.12			

Methanol content of the extraction solvent. As the extraction solvents used for targeted and non-targeted metabolomics can have a different methanol concentration, the impact of the methanol content of the metabolomics sample on the fluorescent signal, obtained with the optimized DNA quantification method, was tested. A range of 60% to 100% methanol:H_2O (v/v), which covers the most frequently used extraction solvent compositions in this study, was tested. **Figure 7** illustrates that the methanol content of the extraction solvent does not have a significant impact on the measured fluorescent signal (p-value: 0.992,

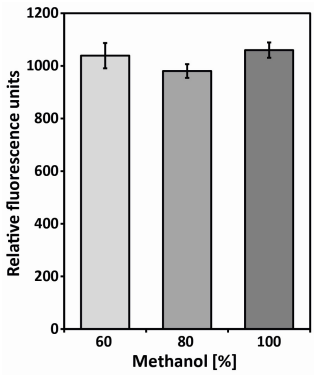

Figure 7: Impact of the methanol content of the extraction solvent on the fluorescent signal of the optimized DNA quantification method.
300 µL of 60%, 80% or 100% methanol:H_2O (v/v) were added to cell pellets (n = 3, N = 9). Then, the samples were homogenized, and the DNA was measured with the optimized fluorescence based quantitation method.

Kruskal-Wallis Test, n = 3). The assay is robust in regard to the methanol concentration (60% - 100%). This allows for a higher flexibility of the harvesting procedure, as the methanol:H_2O ratio can be adjusted to the polarity of the desired metabolite classes (**Figure 13**). In conclusion, signal intensities obtained with samples, harvested according to the protocol for targeted metabolomics (87.5% methanolic extraction solvent), can be compared to those harvested according to the protocol for non-targeted metabolomics (80% methanolic extraction solvent), if the difference in sample volume is taken into account during the calculation of the cell number.

Plate effects. Potential plate effects were tested by applying the same Hep G2 homogenates to separate plates. No significant plate effects were observed (Bonferroni corrected p-values > 0.5, U-Test, n = 5).

3.2.2. Assessing the applicability of the optimized fluorescence-based DNA quantification method to cell culture metabolomics

To provide a reliable basis for the normalization of cell culture metabolomics data to the cell number, two major requirements have to be fulfilled. First, the measured signal of the observed molecular marker (DNA) for normalization has to correlate with the cell number linearly. Second, the cell number has to linearly correlate with the measured signal of the according analyte.

Correlation between fluorescent signal and cell number. To test the correlation between the fluorescent signal and the used cell number, cell homogenates with different cell numbers within the range of 1.0×10^4 to 1.0×10^6 per sample were generated and measured. To test the robustness of the method in regard to the cell line, nine different cell lines with different properties, culturing conditions and organism as well as tissue of origin were tested. All tested cell lines showed excellent linear correlations between the used cell number and the measured fluorescent signal (**Figure 8**).

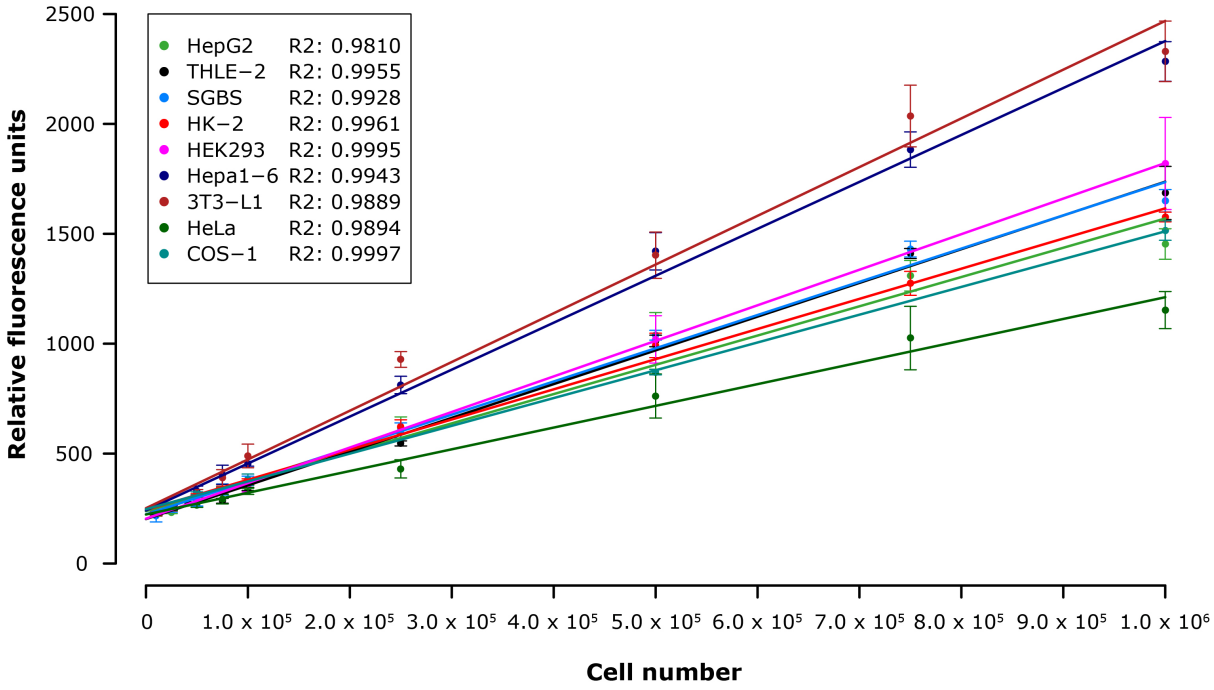

Figure 8: Standard curves for mammalian cell lines with different properties, culturing conditions and organisms and tissues of origin.
Cell homogenates, containing different cell numbers within the range of 1.0×10^4 to 1.0×10^6 cells per sample, of nine different cell lines were generated (n per cell number = 3 - 6), and measured with the optimized fluorescence based DNA quantification method. Linear regression of the fluorescent signal [rfu] to the cell number per sample was performed. The plot shows the mean fluorescent signals ± standard deviations of all cell lines and cell numbers and the result of the linear regression and lists the coefficients of determination (R^2) in the legend.
The data for the THLE-2 and HK-2 cells was kindly provided by Dr. Janina Tokarz. The data for the Hep G2, THLE-2, SGBS and HK-2 have previously been published by Muschet *et al.* [117].

Correlation between cell number and metabolite concentration. This approach has been published by Muschet *et al.* [117]. To test whether the measured metabolite concentration correlates linearly with the used cell number, five different cell numbers of THLE-2, HK-2, SGBS (7.5×10^4 - 7.5×10^5 cells per sample) and Hep G2 (2.5×10^5 - 2.5×10^6 cells per sample) were harvested by trypsinization, and targeted metabolomics analysis using the Absolute*IDQ* p180 Kit was performed. To ensure that the analysis represents the nature of the correlation, and not the performance of the applied metabolomics assay, a validated targeted metabolomics approach was chosen. Only metabolites with ≥ 50% of the samples displaying metabolite concentrations above the LOD of the Absolute*IDQ* p180 Kit provided by BIOCRATES, were included into the data evaluation. After this quality control step, 85 to 114 out of 188 metabolites remained in the data set. Then, linear regression analysis was performed. Excellent linear correlation ($R^2 > 0.9$) was given for 91% to 97% of the metabolites (**Table 17**). **Figure 9** shows that a very small subset of the assessed metabolites displays a negative linear correlation between the measured metabolite concentration and the cell number, which might be caused by increasing matrix effects with increasing cell number. All of them were found to exhibit a very weak correlation between their concentration and the cell number [117].

Table 17: Percentage of metabolites, which display a linear correlation ($R^2 > 0.9$) of their concentration to the cell number.
Modified after Muschet *et al.* [117].

Linear correlation between metabolite concentration and cell number

	Percentage of metabolites with $R^2 > 0.9$ (Number of metabolites above the LOD)
THLE-2	96% (114)
Hep G2	94% (94)
HK-2	91% (85)
SGBS	97% (110)

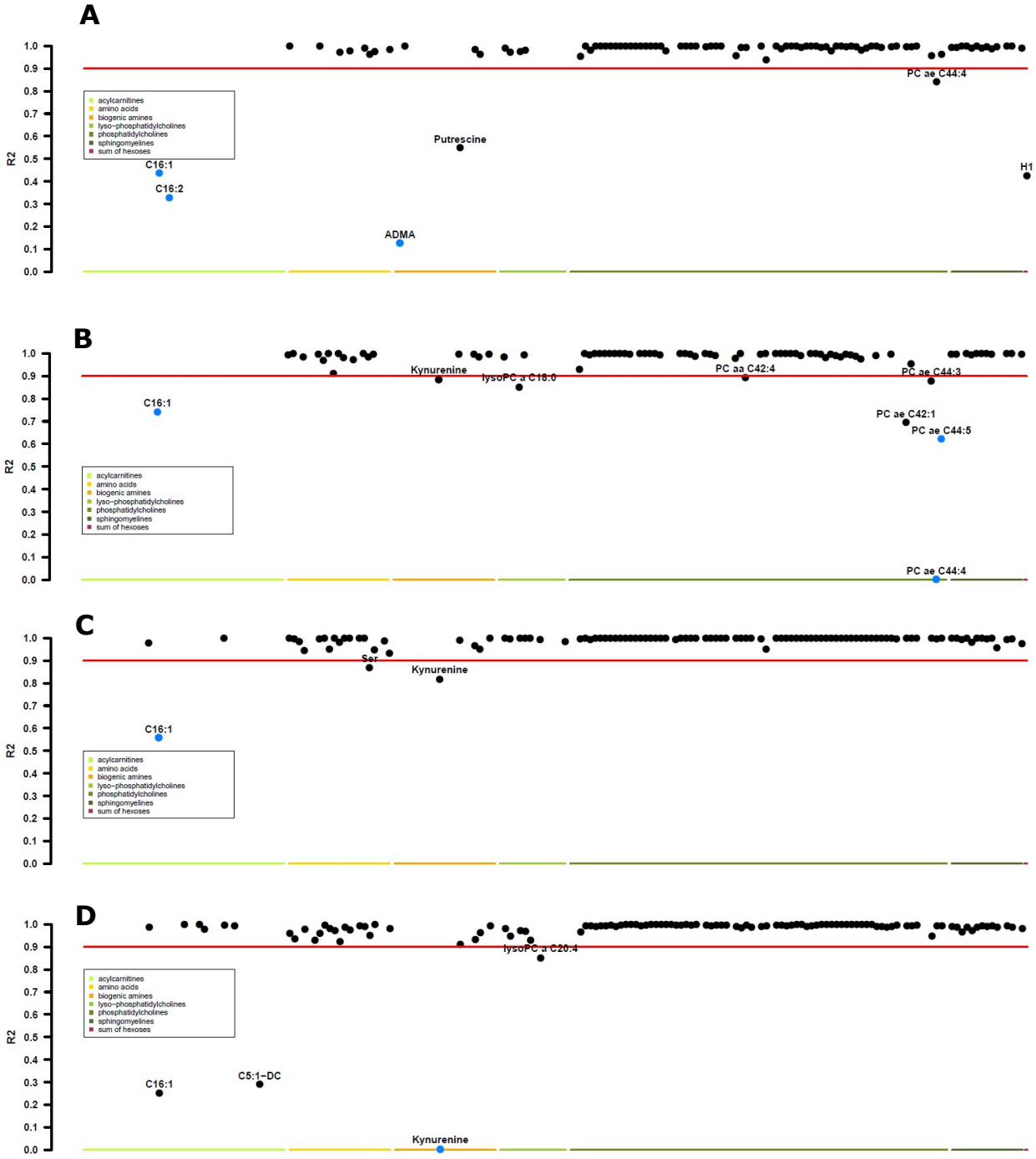

Figure 9: Linear correlation of the metabolite concentration to the cell number for Hep G2, HK-2, SGBS and THLE-2 cells. Each panel shows the R^2 values of all assessed metabolites (dots) of all four cell lines (Hep G2: Panel A, HK-2: Panel B, SGBS: Panel C, THLE-2: Panel D). Metabolites, which did not pass the quality control step, are not represented by a dot. The red line indicates a threshold of 0.9 for R^2 values. Metabolites with a positive linear correlation between their concentration and the cell number are marked by black dots. Metabolites with a negative linear correlation between their concentration and the cell number are marked by blue dots.
Data for THLE-2 and HK-2 cells were kindly provided by Dr. Janina Tokarz. Modified after Muschet *et al.* [117].

Outcome. A fast, robust and versatile fluorometric DNA quantification method for cell number determination of metabolomics samples has been developed and optimized. This method allows for the determination of the cell number of the metabolomics sample itself and, therefore, abolishes the need for the co-cultivation of parallel samples for normalization purposes. Further, all tested cell lines displayed a linear relationship between the cell number and the measured fluorescent signal. In addition, more than 90% of the validly quantified metabolites exhibited a linear correlation between the cell number and their concentration, thereby, proving the eligibility of the cell number as a normalization entity.

Limitations and outlook. A major limitation is the restriction of the method to treatments and culturing conditions, which do not change the karyotype of the analyzed cell lines. Another limitation are those metabolites, which concentrations did not correlate with the cell number in a positive linear fashion. Any observed alteration of their metabolite levels after normalization cannot be attributed to an actual biological effect, but are simply the reflection of a technical bias. This has to be taken into account during the interpretation of the results. Although the mean precision of the DNA based quantification method for cell number determination itself is very good, its precision for samples harvested by scraping is lower than the precision of the LC-MS/MS based metformin quantification method for cell homogenates (**Table 13**) and the precision of a subset of metabolites, quantified with the Absolute*IDQ* p180 Kit (**Figure 10**). Consequently, a sample-wise normalization to the cell number, determined with this method, would increase the variation of the respective analytes instead of diminishing it. However, normalization of differently treated groups is mandatory. To circumvent the errorprone sample-wise normalization to cell number, the median of the according group will be used for normalization.

3.3. Optimization and validation of cell culture metabolomics

3.3.1. Targeted cell culture metabolomics

For targeted cell culture metabolomics, the previously published scraping protocol [141], which is compatible with the Absolute*IDQ* p180 Kit and the Newborn screening kit [140], [141], [186] as well as the LC-MS/MS based metformin quantification method and the fluorescence based DNA quantification method, was adopted. The method was slightly modified [130]. The most crucial modification was the addition of a washing step to ensure complete collection of the sample. Therefore, after scraping the sample, the well is washed with 100 µL of extraction solvent to collect the remaining cellular material [130].

To test the performance and applicability of the adapted harvesting method in combination with the targeted metabolomics approach (Absolute*IDQ* p180 Kit) to cell culture metabolomics, a partial validation was performed. In course of this validation, precision, accuracy and matrix effects were determined. Since the subsequent experiments were to be conducted with liver cell lines (Hep G2 and THLE-2), Hep G2 cell homogenates were used for the validation.

Precision. To test the precision of the targeted cell culture metabolomics approach, Hep G2 cells were harvested and processed according to the adapted protocol for targeted metabolomics analyses (section **2.8**). Then, targeted metabolomics were performed with the Absolute*IDQ* p180 Kit, which allows for the quantification of a wide range of acylcarnitines, amino acids, biogenic amines, lysophosphatidylcholines, diacylphosphatidylcholines, acylalkylphosphatidylcholines, sphingomyelins and the sum of hexoses.

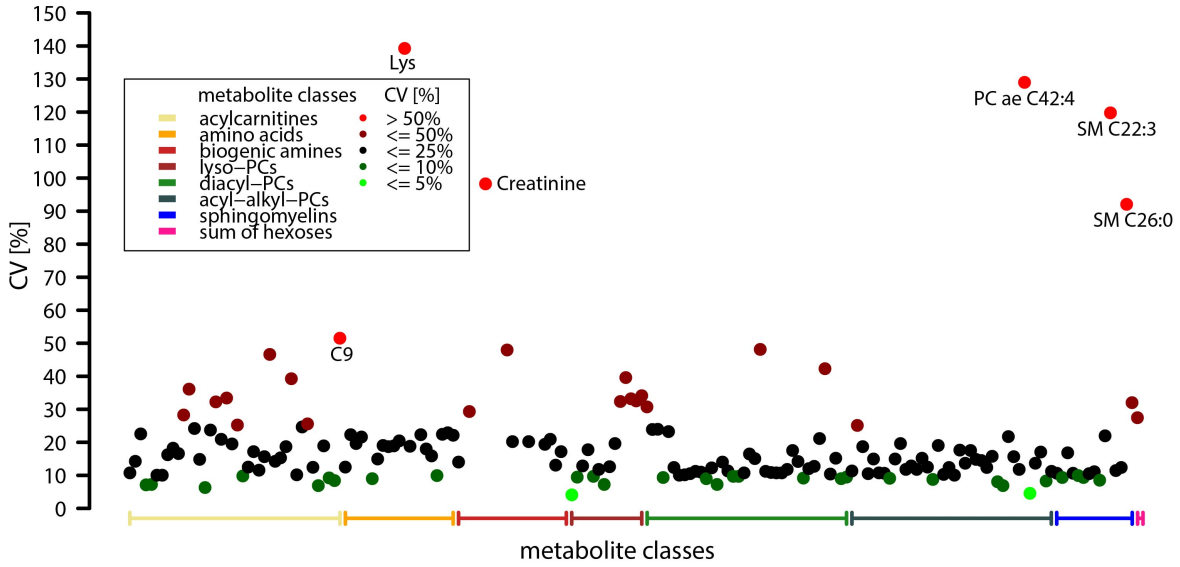

Figure 10: Precision of the analyte concentrations of targeted cell culture metabolomics (1 x 10^6 cells).
1 x 10^6 Hep G2 cells were scraped and processed according to the adapted protocol for targeted cell culture metabolomics (n = 6). Then, targeted metabolomics analysis of 188 metabolites was performed. Analyte concentrations, normalized to the

respective internal standards, were used for the calculation of the CVs. The plot shows the distribution of the CVs of all metabolites, assigned to their respective metabolite classes. Metabolites, which show a CV of above 50%, are named.

Figure 10 displays the distribution of the CVs of all measured metabolites of the samples, containing 1 x 10^6 cells, and **Table 18** lists the according values of the CVs of all tested metabolite classes. The mean CV of all measured metabolites was found to be 19.5% ± 18.95%. The median, which is less prone to outliers [187], was found to be 14.5%. It should be noted that the precision is strongly analyte dependent. The better performance of the median compared to the mean indicates the presence of outliers in the metabolite panel. This is demonstrated by the CV distribution shown in **Figure 10**, which illustrates that the majority of metabolites exhibited a CV below 20% (127 metabolites). Further, 92 metabolites met the 15% criterion, recommended by the FDA [113] and EMA [111]. However, a small number of metabolites (e.g., lysine and creatinine) displayed very high CVs.

Table 18: Precision of the analyte concentrations of targeted cell culture metabolomics (1 x 10^6 cells).
1 x 10^6 Hep G2 cells were harvested and processed according to the adapted protocol for targeted cell culture metabolomics (n=6), and targeted metabolomics of 188 metabolites, belonging to different metabolite classes, was performed. Analyte concentrations, normalized to the respective internal standards, were used for the calculation of the CVs. The table shows the means of the CVs ± standard deviations of the metabolite classes and lists the median of the CVs in brackets.

Precision

Metabolite class (number of measured metabolites in the metabolite class)	**CV [%]** Mean ± SD (Median)
Acylcarnitines (40)	19.17 ± 10.86 (16.44)
Amino acids (21)	24.68 ± 28.06 (19.02)
Biogenic amines (21)	30.06 ± 25.98 (20.22)
Lyso-phosphatidylcholines (14)	19.79 ± 12.00 (15.34)
Diacyl-phosphatidylcholines (38)	14.97 ± 8.86 (11.25)
Acyl-alkylphosphatidylcholines (38)	16.44 ± 19.22 (12.07)
Sphingomyelins (15)	25.77 ± 33.54 (11.05)
Sum of hexoses (1)	27.45

The samples, containing 5 x 10^5 Hep G2 cells (**Figure S-1** and **Table S-2**), slightly outperformed the ones with 1 x 10^6 cells per sample in terms of precision. The mean precision was found to be 15.25% ± 14.19% (CV). However, the general trends and aforementioned conclusions remain unaffected.

Accuracy. To test the accuracy of the targeted cell culture metabolomics approach, seven amino acids with different chemical and physical properties were spiked into the extraction solvent. Those amino acids represent the absolute quantitative metabolite panel (metabolites which concentrations are calculated by means of a standard curve) of the kit (Absolute*IDQ*® Kit. Analytical Specifications p180. AS-P180-3. BIOCRATES LIFE SCIENCES AG). The spiked concentrations were adjusted to the expected concentration range of cell culture derived samples. Then, 5 x 10^5 Hep G2 cells were scraped with either pure or spiked extraction solvent. Pure and spiked extraction solvent without cells served as controls. To determine the accuracies (**Table 19**) of the spiked metabolites, the differences in their concentrations between spiked and non-spiked cell homogenates was calculated and compared to the true value (spiked concentration) using **Equation (3)** (section **2.17.1**).

As shown in **Table 19**, the accuracies of the tested metabolites were found to not deviate more than ± 25% from the true value. For the cell homogenates, only glutamine and phenylalanine displayed accuracy deviations of more than 15%. Further, the accuracies of the amino acids in cell homogenates were slightly higher compared to those in the extraction solvent (**Table 19**). This might be accounted for by the loss of methanol during scraping due to evaporation. In addition, matrix effects might be responsible for this observation.

Table 19: Accuracy of targeted cell culture metabolomics.
5×10^5 Hep G2 cells were either scraped in pure or in spiked extraction solvent (87.5% methanol). For the calculation of the accuracy, the difference in the concentration of the spiked and non-spiked samples were used. The accuracies were calculated using **Equation (3)** (section **2.17.1**). The table lists the mean accuracies ± standard deviation (n = 5) for cells and the accuracies (n = 1) for the extraction solvent control.

	Accuracy [%]	
Metabolite	**Cells**	**Extraction solvent**
Alanine	97.10 ± 5.74	82.75
Arginine	102.64 ± 5.57	85.40
Glutamine	118.72 ± 9.01	98.33
Glutamate	89.60 ± 17.42	87.50
Leucine	107.90 ± 5.13	91.60
Isoleucine	99.80 ± 5.55	85.70
Phenylalanine	123.02 ± 4.73	106.20

Matrix effects. Potential matrix effects were determined by calculating the matrix factors of the analyte and internal standard (**Equation (4)**, section **2.17.1**) and the IS normalized matrix factor (**Equation (5)**, section **2.17.1**) of the seven spiked amino acids. The matrix factors of the analytes showed that the cellular matrix, depending on the metabolite, has no or only a small impact on the measurement of the metabolites (**Table 20**). However, the matrix, indeed, had a negative impact on the peak area of the internal standard (matrix factor IS), which led to an increased IS normalized matrix factor. This impact was strongly metabolite dependent, but reached its observed maximum with > 200% for glutamate. In this context, the good accuracies, which were obtained by using the scraping protocol in combination with the Absolute*IDQ* p180 Kit (**Table 19**), should be interpreted in a different light. The discrepancies between the observed accuracies and IS normalized matrix factors might be explained by the impact of the analyte concentration on the peak area of the internal standard. In general, the higher the analyte concentrations in the calibrators, the smaller was the area of the according internal standard. For the highest analyte concentrations in the standard curves, the peak area of the corresponding IS of the tested amino acids decreased to 28.20% - 80.39% of the peak area of the IS in the calibrator with the lowest concentration of the according metabolite. The decrease of the internal standard peak area led to an overestimation of the analyte concentration as indicated by the IS normalized matrix factor in case of the cell homogenates. Consequently, the decreased IS peak areas in the cell homogenates (due to matrix effects) and the decreased IS peak areas of the (higher) concentrations of the standard curves (due to analyte induced suppression) partly compensate each other. This is further underlined by the accuracies of the extraction solvent, which were mostly found to be below 100%. The only exception was phenylalanine, which was spiked at a lower concentration (50 µM) than the other metabolites (100 µM – 400 µM).

Table 20: Matrix factors of targeted metabolomics analysis of seven amino acids in cell homogenates.
Hep G2 cell homogenates, containing 5 x 10^5 cells (n = 5), and 87.5% methanolic extraction solvent (n = 1) were spiked with seven amino acids with different chemical and analytical properties and measured with the Absolute*IDQ* p180 Kit. Then, the matrix factors of the analytes and internal standards were calculated with **Equation (4)** (section **2.17.1**), and the IS normalized matrix factor was calculated with **Equation (5)** (section **2.17.1**). The table shows the mean matrix factors ± standard deviations.

Matrix factors

	Alanine	Arginine	Glutamine	Glutamate	Leucine	Isoleucine	Phenylalanine
Matrix factor analyte	1.00 ± 0.05	1.00 ± 0.07	1.12 ± 0.04	1.14 ± 0.08	1.08 ± 0.06	1.06 ± 0.06	1.14 ± 0.05
Matrix factor IS	0.68 ± 0.04	0.85 ± 0.05	0.81 ± 0.06	0.82 ± 0.06	0.82 ± 0.06	0.82 ± 0.06	0.90 ± 0.06
IS normalized matrix factor	1.47 ± 0.08	1.19 ± 0.08	1.39 ± 0.05	2.01 ± 0.14	1.31 ± 0.07	1.28 ± 0.07	1.27 ± 0.05

Precision of the analyte signals. On basis of the results, obtained for the matrix effects and the accuracy, the precision was re-evaluated. This time, the analyte signals (peak area for metabolites measured with the LC run; intensity for metabolites measured with FIA) without any normalization to the internal standards were used. The mean precision (CV) was found to be 18.44% ± 25.27% and the median was 12.48%. These values were slightly lower than the according values for the IS-normalized concentrations.The distribution of the CVs is shown in **Figure 11**, and the means and medians of the metabolite classes are listed in **Table 21**. Although the non-IS-normalized analyte peak areas and intensities produced stronger outliers (e.g., total dimethylarginine (total DMA)), all metabolite classes, with the only exception of the biogenic amines, showed a lower mean CV compared to the IS-normalized precisions, which were calculated on basis of the concentrations (**Figure 10**). It should be noted, that the higher mean CV of the biogenic amines might be driven by the very low precision of total DMA. In accordance, the median precision of the peak areas of the biogenic amines is lower than the one of the analyte concentrations.

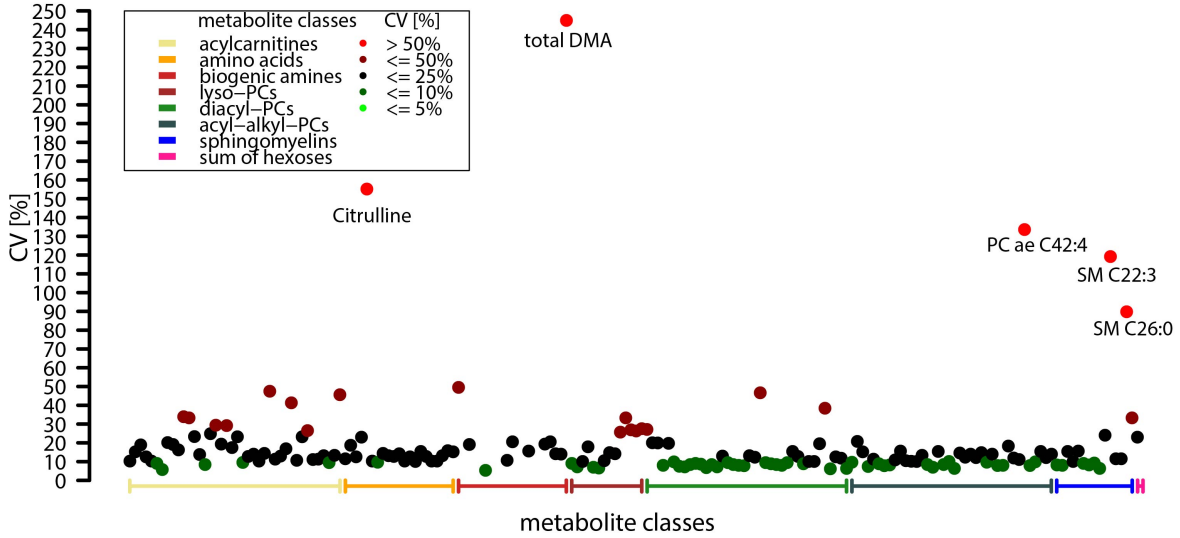

Figure 11: Precision of the analyte signals of targeted cell culture metabolomics.
1 x 10^6 Hep G2 cells were scraped and processed according to the adapted protocol for targeted cell culture metabolomics (n = 6). Then, targeted metabolomics analysis of 188 metabolites was performed. The non-IS-normalized metabolite signals were used for calculation of the precision. The plot shows the distribution of the CVs of all metabolites, assigned to their respective metabolite classes. Metabolites, which show a CV of above 50%, are named.

Table 21: Precision of the analyte signals of targeted cell culture metabolomics.
1 x 10^6 Hep G2 cells were harvested and processed according to the adapted protocol for targeted cell culture metabolomics (n = 6), and targeted metabolomics of 188 metabolites, belonging to different metabolite classes, was performed. The non-IS-normalized analyte signals were used for the calculation of the precision. The table shows the means of the CVs ± standard deviations of the metabolite classes and lists the median of the CVs in brackets.

Precision

Metabolite class (number of measured metabolites in the metabolite class)	**CV [%]**
Acylcarnitines (40)	18.71 ± 10.29 (14.78)
Amino acids (21)	20.04 ± 31.11 (12.78)
Biogenic amines (21)	39.44 ± 69.07 (19.14)
Lyso-phosphatidylcholines (14)	16.93 ± 9.24 (14.50)
Diacyl-phosphatidylcholines (38)	12.70 ± 8.57 (9.40)
Acyl-alkylphosphatidylcholines (38)	14.66 ± 20.08 (11.00)
Sphingomyelins (15)	25.33 ± 33.39 (11.49)
Sum of hexoses (1)	23.07

Sample volume. During the evaluation and partial validation of the Absolute*IDQ* p180 Kit for cell homogenates, it became apparent that the major bottleneck was the low signal intensity, which limited the number of reliably quantified metabolites. To address this bottleneck, the sample volume was optimized. Different volumes were tested: 10 µL, the default volume for plasma, serum and tissues [105], [132], [188]; 20 µL, which was the volume previously suggested for cell culture homogenates [141] and 30 µL. Since the analyte signal was found to be the more reliable entity than the IS-normalized metabolite concentrations, the analyte intensities (FIA metabolites) and peak areas (LC metabolites) were evaluated. As shown in **Figure 12**, increasing the sample volume led to an increase in the signal response for the majority of metabolite classes, namely, amino acids, biogenic amines, phosphatidylcholines and sphingomyelins. Acylcarnitines and the sum of hexoses remained unaffected. However, it should be noted that free carnitine (C0) and the short chain acylcarnitines C2, C3 and C4, indeed, showed a positive correlation between analyte intensity and the applied sample volume. Consequently, the sample volume for targeted cell culture metabolomics was increased to 30 µL.

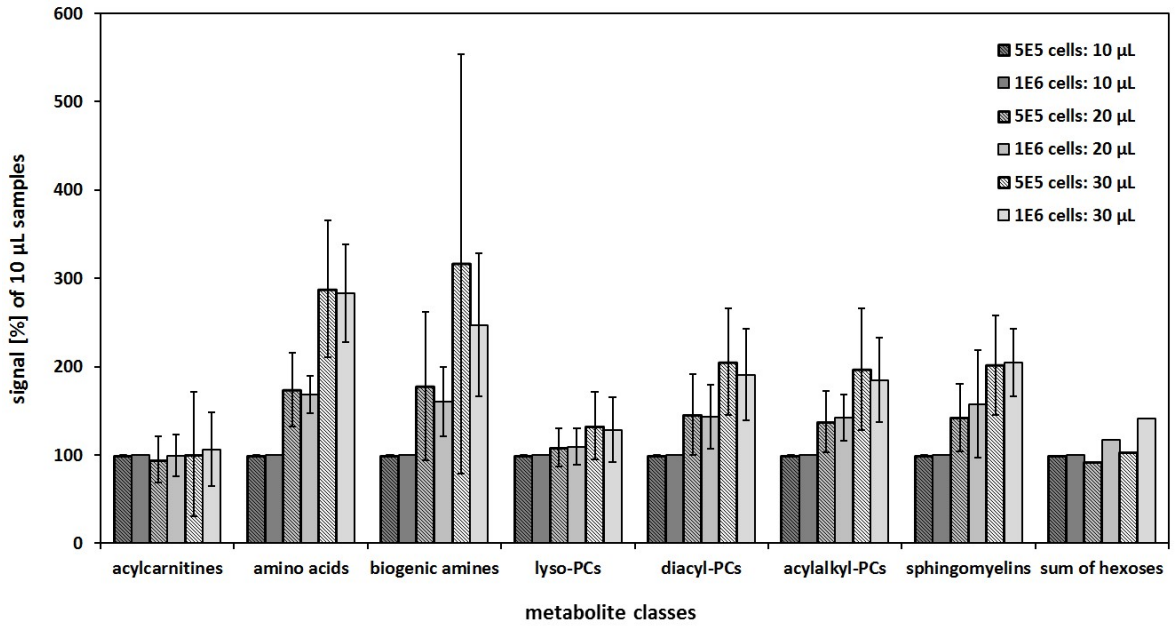

Figure 12: Optimization of the sample volume for targeted cell culture metabolomics.
10 µL, 20 µL and 30 µL of cell homogenates, containing either 5 x 10^5 or 1 x 10^6 cells per sample, were used for targeted cell culture metabolomics (n per cell number = 1). The figure shows the mean signal response (peak area for the metabolites, measured with the LC run; intensity for the metabolites, measured with FIA) for the metabolite classes ± standard deviations. As the 10 µL groups were used as references (100%), no standard deviations could be calculated. In addition, the sum of hexoses is a single entity; hence, no standard deviation could be calculated.

Outcome. The partial validation of the harvesting procedure in combination with the targeted metabolomics approach yielded satisfactory results in terms of accuracy and precision. However, close attention should be given to the metabolite levels and selection. Further, the impact of the matrix and analyte concentration on the internal standards has to be kept in mind during data evaluation.
This harvesting method and the Absolute*IDQ* p180 Kit were used for the elucidation of the impact of glucose and metformin on the cellular metabolome. The results of the validation section formed the basis of the finally used parameters. The sample volume was set to 30 µL. In addition, metabolites, which exhibited concentrations below the LOD and LLOQ, were assessed and reported.

Limitations and outlook. A major limitation of the method is the high number of metabolites below the LOD. Addressing this issue is difficult, as it was found that the number of metabolites above the LOD is strongly cell line dependent (**Table 17**). Optimization for each cell line would strongly diminish the compatibility of the method and the comparability of the results. Another limitation is posed by those metabolites with a very low precision. The validation of the lipid panel and the sum of hexoses for cell homogenates in terms of precision and accuracy needs to be performed in the future. Further, this validation should also be performed for different cell lines and cell culture supernatants.

3.3.2. Non-targeted cell culture metabolomics

To elucidate the impact of metformin and glucose on the hepatocellular metabolism, two cell culture metabolomics approaches were chosen: a targeted and a non-targeted one. For targeted metabolomics with cells, a previously established protocol [141] was adapted, optimized and partially validated. However, a protocol for the non-targeted metabolomics analyses of cell culture samples was not available. The protocol for targeted metabolomics was not applicable, because the sample volume was too low for the non-targeted metabolomics approach [104], [142]. The protocol for non-targeted cell culture metabolomics had to fulfill a number of requirements: the immediate quenching of the cellular metabolism, the potential to identify as many compounds as possible, the possibility to cover metabolites, belonging to different metabolite classes, and with vastly different chemical and analytical properties, the compatibility with the LC-MS/MS based metformin quantification method and the possibility to assess the cell number of the metabolomics sample. Since the harvesting method used for targeted metabolomics fulfilled all aforementioned criteria, this method was adapted to fit the non-targeted metabolomics approach. The extraction solvent volume was increased from 300 µL to 500 µL, the extraction solvent was spiked with internal standards to monitor extraction efficiency, and the optimal extraction solvent composition was determined. The metabolite coverage was tested, and the precision of the metabolomics analysis as well as the precision of the harvesting protocol in combination with the metabolomics analysis was validated.

Optimization of the extraction solvent composition. To test the impact of the methanol content on non-targeted cell culture metabolomics, 1 x 10^6 Hep G2 and HEK293 cells were scraped in extraction solvent, consisting of either 60%, 80% or 100% methanol, spiked with internal standards, and analyzed with the non-targeted metabolomics approach. Library matching was performed by Metabolon (Metabolon, Inc., Durham, U.S.A). The results are shown in **Figure 13**. As expected, the higher the content of the organic solvent (methanol) in the extraction solvent, the higher were the intensities of the identified lipids. However, the results were more complex for the other metabolite classes. The impact of the extraction solvent composition was cell line dependent. For example, whereas, with HEK293 cells, metabolites, belonging to the energy metabolism, carbohydrates, xenobiotics, nucleotides and cofactors and vitamins, displayed their highest intensities with 60% methanol and decreased with increasing methanol content; with Hep G2 cells, they were lowest with 60% methanol and tended to increase with increasing methanol content. In case of Hep G2 cells, the amino acids showed their highest overall intensity with 60% methanol content, which is most likely explained by their polar nature. However, for HEK293 cells, no clear trend was observed for amino acids. The impact of the extraction solvent composition on the absolute number of detected compounds was found to be very low (**Figure 13**). The total number of compounds in all conditions and both cell lines was found to be 156 to 162. In case of HEK293 cells, no dependency on the methanol content could be found. For Hep G2 cells, the number of detected compounds seemed to increase with the methanol content of the extraction solvent

(60% methanol: 156 compounds, 80% methanol: 159 compounds and 100% methanol: 162 compounds).

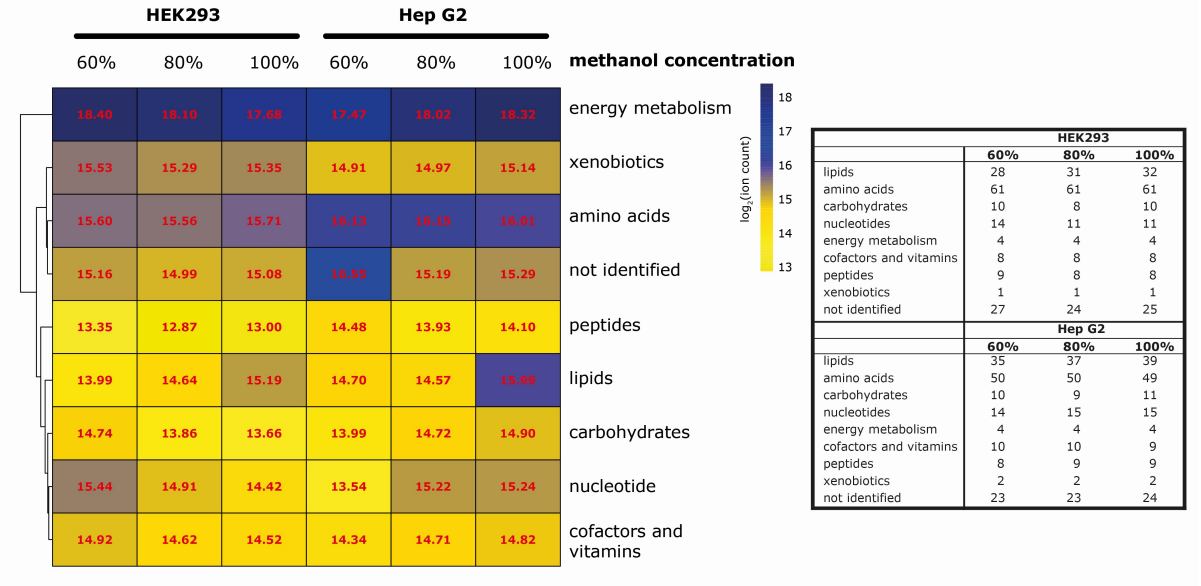

	HEK293		
	60%	80%	100%
lipids	28	31	32
amino acids	61	61	61
carbohydrates	10	8	10
nucleotides	14	11	11
energy metabolism	4	4	4
cofactors and vitamins	8	8	8
peptides	9	8	8
xenobiotics	1	1	1
not identified	27	24	25
	Hep G2		
	60%	**80%**	**100%**
lipids	35	37	39
amino acids	50	50	49
carbohydrates	10	9	11
nucleotides	14	15	15
energy metabolism	4	4	4
cofactors and vitamins	10	10	9
peptides	8	9	9
xenobiotics	2	2	2
not identified	23	23	24

Figure 13: Impact of the extraction solvent composition on non-targeted cell culture metabolomics.
1 x 10^6 Hep G2 and HEK293 cells were harvested with extraction solvent, containing either 60%, 80% or 100% methanol:H_2O (v/v), and non-targeted metabolomics were performed. Left: A heatmap, showing the $\log_2$ values of the median ion counts of the analyzed metabolite classes for the tested extraction solvent compositions and cell lines. Right: The table lists the number of detected metabolites, with the tested conditions. A metabolite was only counted, if it was positively identified (ion count ≠ 0) in more than 50% of the samples (> 3) of the respective group (n = 6).

The methanol content of the extraction solvent was chosen to be set to 80% for four reasons:

First, 80% methanol yielded a satisfactory number of metabolites as well as metabolite intensities for all analyzed compound classes.

Second, 80% methanol allowed for higher flexibility than the 100% methanolic extraction solvent. Although the 100% methanolic extraction solvent yielded higher intensities for lipids and also for other metabolite classes and a slightly higher number of detected compounds, it is very inflexible in regard to the application to other cell lines. If the hepatocellular carcinoma cell line Hep G2 and the embryonic kidney cell line HEK293 are analyzed using non-targeted metabolomics, it becomes apparent that different cell lines display highly different metabolite profiles (**Figure 14**). By using a monophasic, pure organic extraction solvent, one might loose important information on very polar compounds and, thereby, unintendedly and unknowingly introduce a major technical bias into the analysis. This consideration had to be given close attention, because this protocol should serve as a general and robust (standard) operating procedure ((S)OP) for non-targeted metabolomics of a very wide range of cell lines and cell culture conditions, not only for this study, but for the platform in general.

Third, the 80% and 60% methanolic extraction solvents are easier to handle than the 100% methanolic extraction solvent, due to less evaporation and higher surface tension. This might not be of consequence, if a single experimenter is performing the cell culture experiment.

However, it becomes of importance, if multiple labs use the same procedure to collect samples for one or multiple studies. Since these protocols were established to provide general (S)OPs for cell culture samples for the platform as well as a multi-lab approach (Stem cells for Biological Assays of Novel drugs and prediCtive toxiCology (StemBANCC) [189]), those practical considerations had to be taken into account.

Fourth, the usage of 80% methanol reduced the number of freeze-thaw cycles. The detection of very polar compounds and the higher surface tension as well as the decreased evaporation might favor the 60% methanolic extraction solvent. However, samples collected in 60% methanol are frozen at -80 °C, whereas, samples in 80% methanolic extraction solvent do not. Consequently, using 60% methanolic extraction solvent would introduce freeze-thaw cycles, which might result in metabolite degradation [190], [191]. This becomes especially important, if a sample has to be re-measured. Further, the samples are measured with multiple assays (e.g., fluorescence based DNA quantification for cell number determination, metabolomics and metformin quantification). Depending on the analyses, it is challenging or even impossible to conduct all measurements without having to store the sample. As the integrity of the metabolite profile was found to depend on the storage temperature [112], higher temperatures than -80 °C were not considered a suitable option.

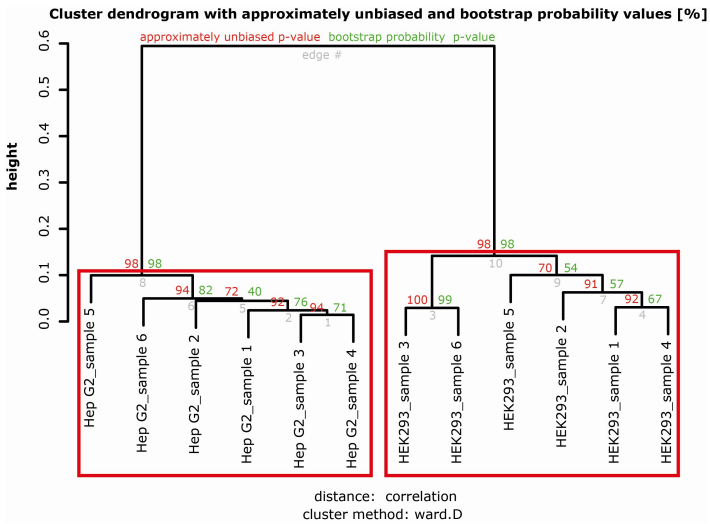

Figure 14: HEK293 and Hep G2 cells exhibit different metabolite profiles.
1 x 10^6 HEK293 and Hep G2 cells were analyzed with non-targeted metabolomics (n = 6, N = 12). Then, unsupervised hierarchical clustering was performed to test whether those two cell lines build separate clusters, based on their metabolite profiles. All common detected compounds were used for analysis. Prior to analysis, the data was glog-transformed and scaled and centered by autoscaling. Hierarchical clustering was performed using the Ward1 method [287] and 10,000 bootstrap replications. The unsupervised hierarchical clustering shows that the cell lines Hep G2 and HEK293 form the two major clusters (approximately unbiased p-value: 0.98), thereby, highlighting that the metabolite profile is cell line dependent. With an approximately unbiased p-value greater than 0.95 (95%), the null hypothesis that the Hep G2 and HEK293 clusters do not exist, is rejected.

Within-run precision. To test the precision of the non-targeted metabolomics analysis for the cell culture matrix, one sample was analyzed five times within the same plate and batch. The technical replicates displayed only slight variations in the absolute number of detected compounds (140 to 144). The distribution of the CVs of all detected metabolites are shown in **Figure 15**. The mean CVs of the metabolite classes and their respective standard deviations are listed in **Table 22**.

Table 22: Precision of the non-targeted metabolomics analysis.
HEK293 cells were harvested and processed according to the protocol for non-targeted cell culture metabolomics. The sample was measured 5 times. The table shows the means of the CVs ± standard deviations of the compound classes. The median of the CVs is listed in brackets.

Precision

Metabolite class	Mean ± SD (median) [%]
Lipids	25.92 ± 19.37 (20.42)
Amino acids	9.45 ± 7.14 (8.34)
Carbohydrates	13.42 ± 6.32 (13.14)
Nucleotides	15.86 ± 6.96 (17.69)
Energy metabolism	8.82 ± 9.64 (5.24)
Cofactors and vitamins	8.46 ± 5.55 (7.84)
Peptides	20.33 ± 9.83 (20.95)
Xenobiotics	5.47 ± 0.68 (5.47)
Not identified	17.39 ± 23.13 (9.60)

Figure 15 as well as **Table 22** illustrate, that the majority of metabolites display very low to medium (≤ 25%) CVs. The mean CV of all detected compounds was found to be 15.09% ± 14.56%. While the mean CV of 15% was acceptable for a non-targeted metabolomics approach, the standard deviation of 14.6% already indicated, what **Figure 15** and **Table 22** show in detail. The reproducibility of the metabolomics results is strongly metabolite class dependent. Many metabolite classes, namely amino acids, metabolites belonging to the energy metabolism, cofactors and vitamins as well as xenobiotics, displayed low CVs, indicating a high precision. Carbohydrates, nucleotides, peptides and all metabolites, which could not be identified by library matching, showed medium CVs, indicating a sufficient precision to yield reproducible results. However, a technical CV of 13% - 20% might mask a small but significant change in the cellular metabolome, caused by biological processes, due to increased variance in the data. This has to be taken into account during the planning of the study design, data evaluation and biostatistics (e.g., type I and type II error). With 26%, lipids display the highest CV out of all metabolite classes (**Table 22**). This might be caused by the heterogeneity of the chemical and physical properties of this huge metabolite class.

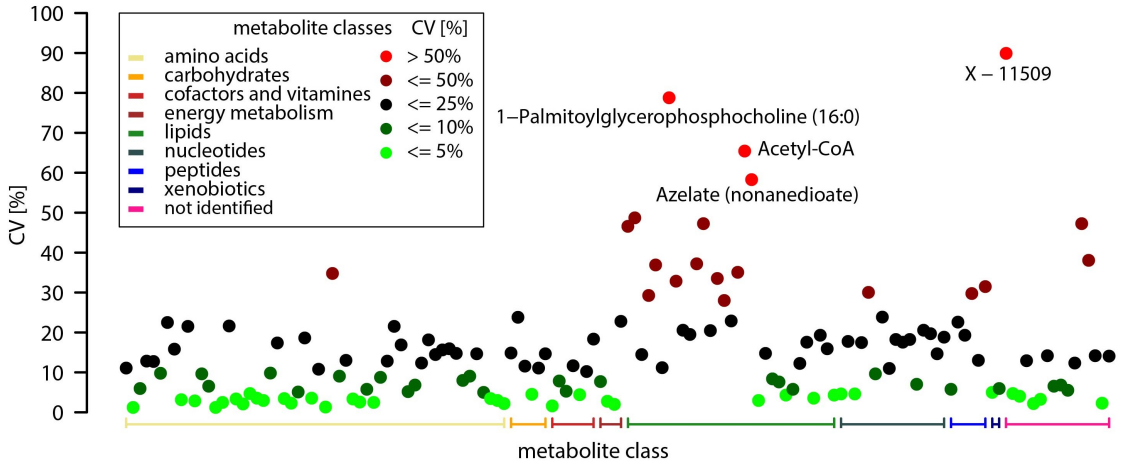

Figure 15: Within-run precision of the non-targeted metabolomics analysis.
A HEK293 cell homogenate, containing 1 x 10^6 cells per 500 µL, was measured five times within the same batch. The plot shows the distribution of the CVs of all metabolites, which are grouped according to their metabolite class. Metabolites with a CV ≥ 50% are highlighted.

Precision of the harvesting protocol and non-targeted metabolomics. To test the precision of the non-targeted cell culture metabolomics approach, six samples of 1 x 10^6 HEK296 and Hep G2 cells were generated as described in section **2.10.2**. Then, non-targeted metabolomics analysis was performed. The cell homogenates were measured within the same batch.

For HEK293 cells, the number of detected compounds was found to be within the range of 149 to 158. Not surprisingly, this range is slightly bigger than the one found for the technical replicates. The mean CV of all detected compounds was found to be 18.01% ± 13.70%. The majority of metabolites had very low to medium CVs (<25%), indicating a good reproducibility of non-targeted cell culture metabolomics, if the samples are measured within the same batch. All metabolite classes exhibited either low or medium CVs (**Table 23**).

In case of Hep G2 cells, the mean CV of all detected compounds was found to be 23.06% ± 19.63%. This indicated a lower precision of samples, containing Hep G2 cells, compared to HEK293 samples. The increased CV might be caused by the stronger adherence of Hep G2 cells to the surface of the wells of cell culture plates, which was observed during cell scraping. This feature of the cells might lead to a higher variability, introduced during detachment of the cells by scraping, and, hence, introduces a higher variability into the results. This hypothesis is underlined by the very high CV found for lipids (**Table 23**). If the cells were not completely detached by scraping, a cell membrane layer, which, inter alia, consists of membrane lipids [192], might remain on the surface of the wells. The variance of the absolute number of detected compounds (151 to 158) was slightly lower for Hep G2 cells compared to HEK293 cells.

Table 23: Precision of the harvesting protocol in combination with non-targeted cell culture metabolomics.
1 x 10^6 HEK293 and Hep G2 cells were harvested and processed according to the protocol for non-targeted cell culture metabolomics (n = 6, N = 12). The table shows the means of the CVs ± standard deviations [%] of the compound classes. The medians of the CVs are listed in brackets. If no standard deviation is given, only one metabolite of the according metabolite class could be measured.

	Precision	
Metabolite class	**HEK293** Mean ± SD (Median) [%]	**Hep G2** Mean ± SD (Median) [%]
Lipids	24.63 ± 15.45 (23.13)	34.08 ± 25.32 (23.62)
Amino acids	14.85 ± 8.87 (13.76)	18.91 ± 13.02 (13.30)
Carbohydrates	20.44 ± 11.85 (22.20)	14.24 ± 5.94 (12.64)
Nucleotides	22.37 ± 25.13 (19.45)	24.47 ± 15.47 (21.72)
Energy metabolism	5.22 ± 2.11 (4.88)	6.55 ± 2.93 (6.22)
Cofactors and vitamins	18.49 ± 11.69 (15.56)	20.03 ± 12.54 (16.69)
Peptides	24.57 ± 12.19 (23.45)	16.24 ± 9.31 (14.37)
Xenobiotics	11.11	8.69 ± 3.45 (8.69)
Not identified	13.91 ± 10.44 (11.70)	25.01 ± 26.65 (19.26)

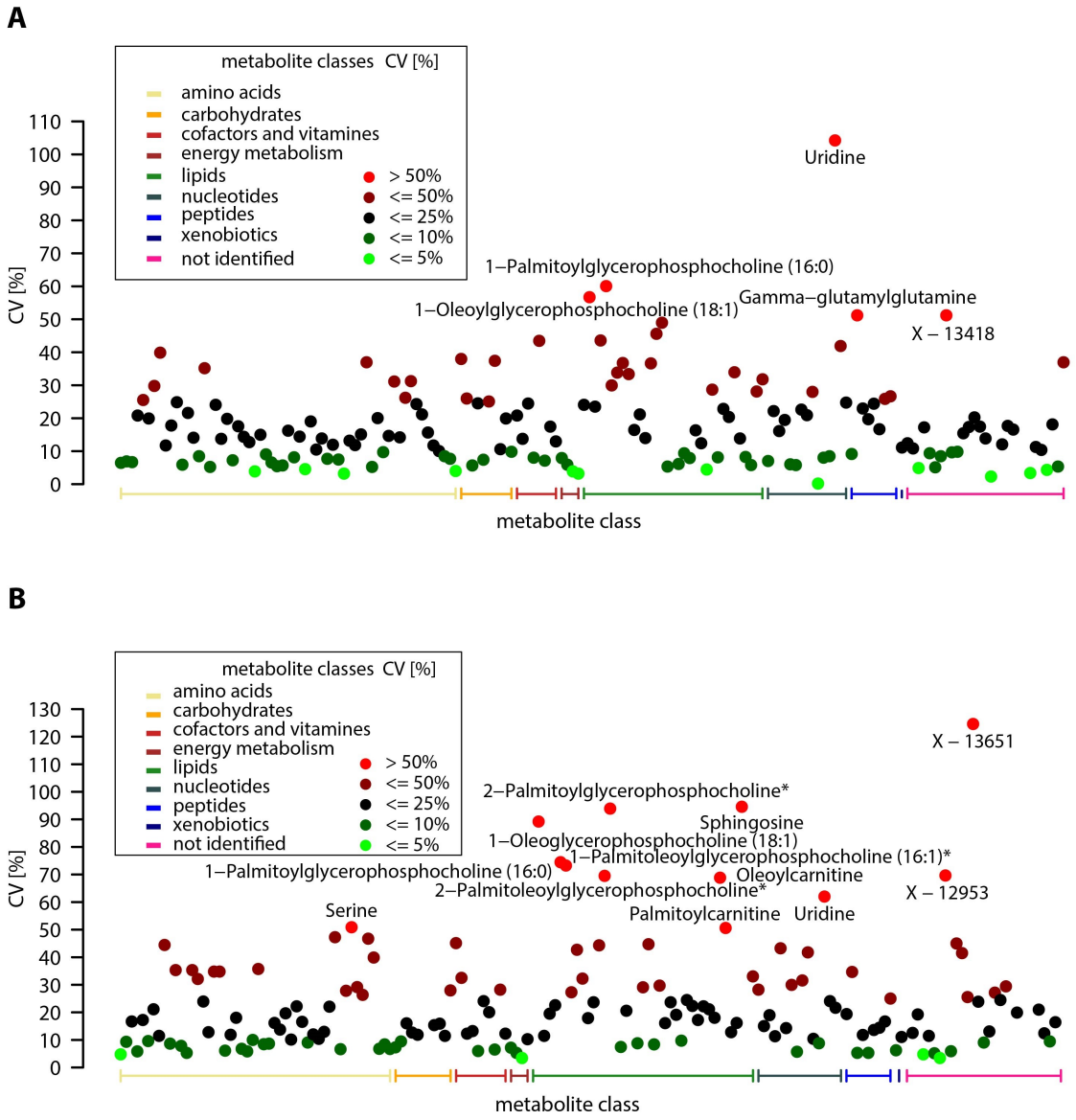

Figure 16: Precision of the harvesting protocol in combination with non-targeted cell culture metabolomics.
1 x 10^6 HEK293 and Hep G2 cells were harvested, processed and measured with the optimized protocol (n = 6). The graphs show the CV distributions for all measured metabolites. Panel A: HEK293 cells. Panel B: Hep G2 cells.

Outcome. The harvesting method for targeted cell culture metabolomics was adapted and modified for non-targeted cell culture metabolomics by adding internal standards for extraction monitoring and increasing the sample volume. Further, the impact of the extraction solvent composition was assessed and the methanol concentration was set to 80%. However, adaption of the methanol content is possible, if the focus lies on a specific metabolite subset (e.g., polar or very non-polar). In addition, the within-run precision and the precision of the harvesting protocol in combination with non-targeted cell culture metabolomics were tested. The protocol is compatible with other assays used in course of this study and performed well in terms of precision.

Limitations and outlook. The low precision of the lipid panel, which comprises one of the major measured metabolite classes, poses a major limitation. Further, a systematic and throughout validation of a range for cell lines, with different physical properties, culturing conditions and tissues and organisms of origin, has to be performed.

3.4. Elucidation of the hepatocellular metformin transport

In recent years, metformin transport and pharmacokinetics have become a rapidly developing field in metformin research [43], [47], [48], [56], [193]–[195]. In this context, studies often focus on the gastrointestinal absorption of the drug [36], [45], [48], [56], [139] and on transporter polymorphisms and their association with altered metformin pharmacokinetics and response [46], [47], [195]. When regarding hepatocellular metformin transport, OCT1 is believed to be the dominant determinant of metformin uptake [81]. However, hepatic metformin transport might not be narrowed down to a single transporter. First, in case of rat hepatocytes, metformin uptake consists of a saturable and a non-saturable component [40]. Second, Han *et al*. showed that cellular metformin transport is driven by a number of different transporters [56]. Third, next to OCT1, a number of other reported metformin transporters (**Table 1**) were found to be expressed in the liver (e.g., THTR-2 [48], OCTN1 [49], MATE1 [49]). Hence, next to OCT1, other mechanisms and transporters have to be involved in the hepatocellular metformin transport. The characterization of the human hepatocellular metformin transport and the identification of potential hepatocellular metformin transporters is a key prerequisite to broaden our understanding of molecular metformin action.

3.4.1. Design of the experimental setup

Incubation time. The optimal incubation time for the metformin treatment was determined by treating Hep G2 cells with 2 mM metformin and harvesting them at different time points between 0 h and 72 h post treatment. The concentration was chosen, since it is elicits a significant metformin response, while having no impact on the morphology of Hep G2 cells (section **3.5.1** and [130]). The metformin concentration and the cell number of the collected cell homogenates were determined. **Figure 17** shows, that the hepatocellular metformin uptake has a strong positive correlation with the incubation time up to 8 h. Then, the metformin uptake enters a plateau.

Consequently, the incubation time for the elucidation of metformin uptake via inhibitor studies was set to four hours. This incubation time ensures that the metformin uptake is within its linear phase. Further, it allows for a relatively high throughput. The harvest of a single sample takes approximately 1 - 2 min. For a sample size of $n = 6$ per group, a treatment (and harvesting) interval of 10 - 15 min per group was chosen. The incubation time of four hours allowed for the assessment of multiple inhibitors and inhibitor concentrations in a single experiment, thus, ensuring a high comparability of the results.

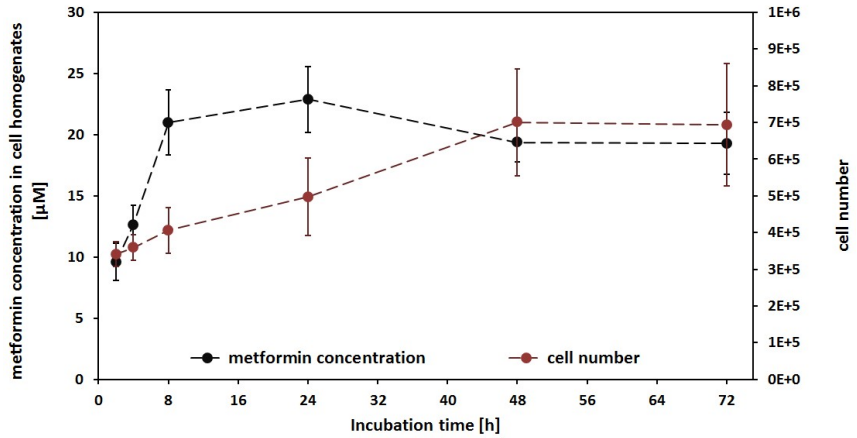

Figure 17: Time course analysis of metformin uptake for the determination of the metformin incubation time.
The plot shows the hepatocellular metformin uptake over time and the cell numbers. 2.5 x 10^5 Hep G2 cells were seeded and cultivated over night to ensure uniform attachement. Then, the cells were treated with 2 mM metformin and incubated for different periods of time (n = 6). Metformin concentrations and cell numbers were measured.

The incubation time for the elucidation of the impact of metformin on the cellular metabolome (section **3.5**) was set to 24 h to allow for sufficient adjustment of the metabolic processes of the cells. At 24 h, a saturation of metformin uptake was reached (**Figure 17**).

Evaluation of fetal bovine serum (FBS) withdrawal. Some of the inhibitors used in this study are endogenous compounds (e.g., carnitine), which might be present in unknown concentrations in the fetal bovine serum with which the culturing medium is supplemented. To obtain a well defined environment for the metformin inhibitor studies and eliminate any potential impacting factors, it was decided to cultivate the cells in FBS-free medium. In this context, the impact of the FBS withdrawal on the cell number was tested. Hep G2 cells were cultivated for up to 72 h in FBS-free growth medium. **Figure 18** shows the cell number to incubation time response curve. After withdrawal of the FBS, the cell number droped slightly. However, after 24 h, the cells had adjusted to the FBS withdrawal and started proliferation. The cell numbers reached a plateau after 48 h.

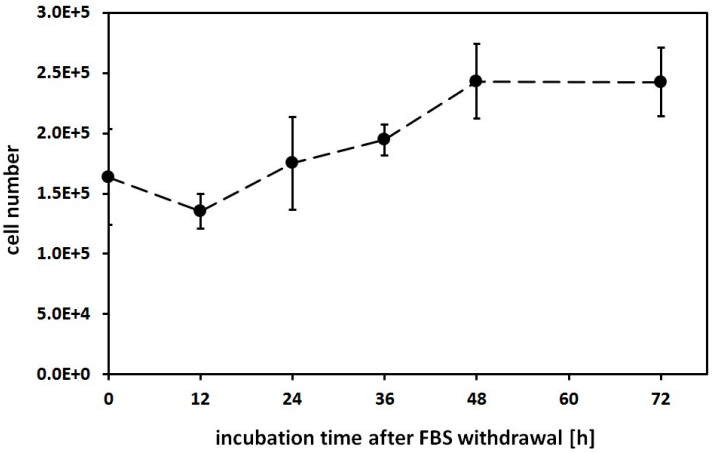

Figure 18: Impact of the FBS withdrawal on the cell number.
1 x 10^5 Hep G2 cells were cultivated for 24 h in growth medium, supplemented with 10% FBS. Then, the cell culture supernatant was withdrawn, the wells were twice washed with PBS, and the cells were cultivated in FBS-free growth medium for up to 72 h. The cells were scraped at the according time points, and the cell numbers were determined using the DNA based cell number quantification method (n = 2 - 4). The plot shows the cell number to incubation time response.

Based on these results, 24 h were chosen as incubation time in

FBS-free growth medium.

Metformin concentration. A crucial parameter for the elucidation of hepatocellular metformin uptake was the drug concentration. The best approach would be to use a physiological concentration. However, defining the physiological metformin concentration is a challenge. First, the prescribed doses range from 500 mg to 3,000 mg daily (Bundesinstitut für Arzneimittel. Gebrauchsinformation: Information für Anwender, Glycophage® 500 mg Filmtabletten (2015)) [196]. Second, the plasma metformin profile is highly time dependent [182], [197]. Third, there are different types of metformin tablets: immediate-release and extended-release tablets [197], [198]. Regarding the plasma metformin concentration-time profile, extended-release tablets display a lower maximum concentration (C_{max}), which is reached at a later timepoint after administration of the drug (higher t_{max}), and broader peaks compared to their immediate-release counterparts [197]. Further, they have been reported to exhibit a higher bioavailability [197]. Fourth, the metformin concentration is strongly tissue dependent [41]. In addition, transporter polymorphisms can alter the response to and pharmacokinetics of metformin [46], [47], [195].

The single oral dose of a 500 mg tablet, given to volunteers, correlated with plasma metformin concentrations within the low µM range [182], [197]. Depending on the type of tablet and the study, a C_{max} of 549 ng/mL - 794 ng/mL (4.35 µM - 6.15 µM) was reached at a t_{max} of 2.4 h - 5.6 h [182], [197]. A similar metformin concentration range was measured, applying the LC-MS/MS based metformin quantification method, optimized and validated in course of this study, to serum samples of metformin treated patients [109]. Additionally, it has to be considered that Wilcock *et al.* showed that the plasma metformin concentration of mice depended on the location the biofluid was taken from [41]. In case of diabetic mice, the plasma metformin concentration of the hepatic portal vein exceeded the one of the inferior vena cava by a factor of 1.3 to 1.7 [41]. Taking a plasma metformin concentration of 6.15 µM, Wilcock *et al.*´s observation of different metformin concentrations in different areas of the circulation and the prescription range into consideration, one would end up with an estimated plasma concentration range in the hepatic portal vein of 8 µM to 363 µM. Finally, a concentration of 50 µM was chosen for the elucidation of hepatocellular metformin uptake. This concentration would - based on

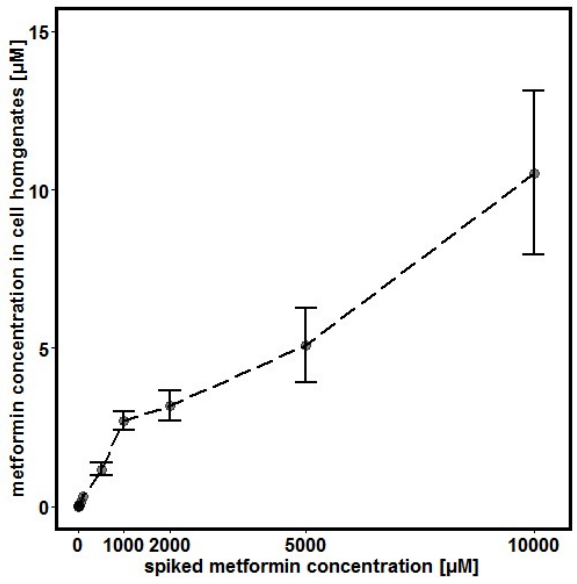

Figure 19: Hepatocellular metformin uptake.
2.5 x 10^5 Hep G2 cells were seeded and cultivated using the optimized parameters (section **2.11.1**). Then, they were treated with different metformin concentrations, within the range of 1 µM to 10 mM, and the metformin concentrations in the cell homogenates were determined (n = 3 - 6).

the assumptions above - equal the plasma concentration of the hepatic portal vein, correlating with a dose of 2,000 mg metformin, 4 h after treatment. Further, 50 µM metformin reflects the plasma metformin concentration range of the hepatic portal vein of normal and diabetic mice (normal: 51.7 µM ± 5.4 µM; diabetic: 61.5 µM ± 8.0 µM) [41].

To test the applicability and eligibility of the chosen metformin concentration to the aim of this study, the hepatocellular metformin uptake was tested. **Figure 19** shows the metformin uptake of Hep G2 cells, which were treated with different metformin concentrations. The metformin uptake was found to be linear up to a treatment concentration of 1 mM. Consequently, the metformin concentration of 50 µM is suitable for the elucidation of the hepatocellular metformin uptake.

3.4.2. Characteristics of the hepatocellular metformin transport

To assess the kinetics of the hepatocellular metformin transport, Hep G2 cells were treated with different concentrations of metformin, and the metformin concentrations of the cell homogenates were measured. Then, two data modelling approaches were applied. First, a Michaelis-Menten model (**Equation (8)**, section **2.17.3**) was fitted to the data (**Figure 20**: Red curve). Second, an extended Michaelis-Menten model was applied (**Figure 20**: Black curve). The second model contained an additional non-saturable component (**Equation (9)**, section **2.17.3**). The extended model (deviance: 48) outperformed the classical Michaelis-Menten model (deviance: 60), indicating that the metformin transport does indeed follow a dual nature.

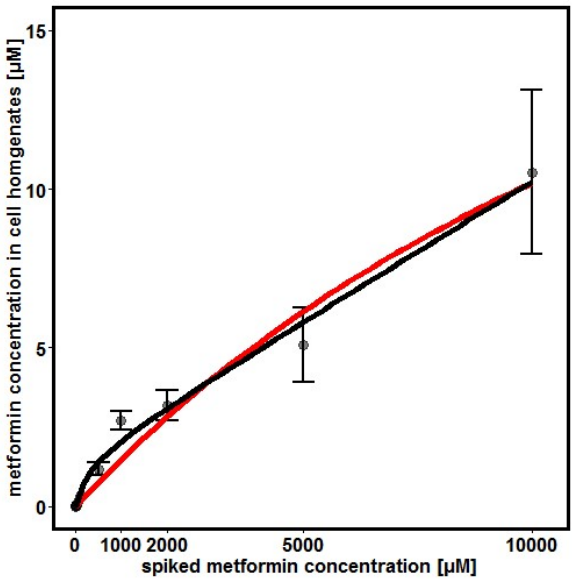

Figure 20: Hepatocellular metformin transport kinetics. 2.5×10^5 Hep G2 cells were seeded and cultivated using the optimized parameters (section **2.11.1**). Then, they were treated with different metformin concentrations, within the range of 1 µM to 10 mM, and the metformin concentrations in the cell homogenates were determined (n = 3 - 6). Then, non-linear regression, based on the Michaelis-Menten equation (**Equation (8)**, section **2.17.3**) and an extended Michaelis-Menten model (**Equation (9)**, section **2.17.3**), were performed. Red curve: Michaelis-Menten; Black curve: Michaelis-Menten, extended to accomodate a non-saturable component.

The lower concentration range seems to be dominated by the saturable component, whereas, at higher metformin concentrations, the linear non-saturable component is predominant. At a metformin concentration of 2 mM a saturation was observed (**Figure 20**). However, with increasing metformin concentrations, the metformin concentration in the cell homogenates still increased.

The obtained K_M value for metformin transport of Hep G2 cells was found to be 280 µM, which is in a comparable order of magnitude as the K_M value reported by Sogame *et al.* for rat hepatocytes (K_M = 404 µM) [40]. The slightly lower K_M found for Hep G2 cells might be due to

differences in the model system and their respective transporter expression profiles.

3.4.3. Expression analyses and inhibition studies of potential metformin transporters

Metformin is a small, polar and hydrophilic compound, which is predominately present in its monoprotonated cationic form at a physiological pH [33], [34]. The drug has been reported to be transported by cation transporters [44], [193], [199], and all reported transporters belong to the SLC family (**Table 1**). These characteristics were assumed to be of crucial importance in the transporter-mediated cellular uptake and excretion of metformin.

Hence, the first step in the elucidation of the transporter-mediated human hepatocellular metformin transport was to test, whether metformin transport in general can be decreased by inhibitors of cation transporters. Futher, based on the aforementioned observations, the study focused on transporters belonging to the SLC family.

To elucidate the role of multiple transporters in the metformin transport with emphasis on the uptake of the drug, a combinational screening approach was taken. First, the expression of reported and potential metformin transporters was assessed. Then, if an expression of the respective transporter was observed, inhibitor studies were conducted. **Table 24** lists the inhibitors and their Tanimoto coefficients and overlap coefficients, if compared to metformin.

Table 24: List of compounds, relevant for the elucidation of transporter-mediated hepatic metformin transport.
The table shows the compounds, their Tanimoto coefficients and their overlap coefficients, if compared to metformin.

Potential inhibitors of metformin transport

Compound	Tanimoto coefficient	Overlap coefficient
ASP^+	0.038	0.444
MPP^+	0.009	0.333
Quinidine	0.013	0.444
Carnitine	0.011	0.444
Acetylcarnitine	0.008	0.444
Paroxetine	0.003	0.333
Cimetidine	0.036	0.667
Desipramine	0.009	0.444
L-Arginine	0.063	0.556

General inhibiton of transporter-mediated metformin uptake. To verify, whether transporters are indeed involved in the human hepatocellular metformin transport, a small cationic compound should be used as competitive inhibitor for all potential metformin transporters present. Two potential compounds were: 1-methyl-4-phenylpyridinium (MPP^+), which is frequently used in metformin transport studies [42], [47], [48] and its analogue 4-(4-dimethylaminostyryl)-1-methylpyridinium (ASP^+), which is used to study cation transporters [200], [201]. Both compounds have been reported to be transported by metformin transporters [42], [47], [48], [193], [200], [201]. As ASP^+ clearly outperformed MPP^+ in terms of its structural similarity to metformin (**Table 24**) and was shown to exhibit a higher correlation in its inhibition profile [202], it was chosen as inhibitor.

The treatment of Hep G2 cells with ASP^+ and metformin in a ratio of 1:1 (v/v, 50 µM) did not significantly alter the metformin uptake (Posthoc: U-Test with Bonferroni correction, p-value: 0.195, n = 6) (**Figure 21**). However, if the ASP^+ concentration was elevated to 500 µM, a significant decrease (Posthoc: U-Test with Bonferroni correction, p-value: 0.006, n = 6) to 59% ± 10% of the control (50 µM metformin) was observed (**Figure 21**). By increasing the ASP^+ concentration to 5 mM, the intracellular metformin levels decreased further to 48% ± 11% (Posthoc: U-Test with Bonferroni correction, p-value: 0.029, n = 4 - 6). These results indicate that metformin is transported into the cells by cation transporters. However, it should be noted that ASP^+ in part quenched the fluorescent signal, measured with the Hoechst assay. Consequently, normalization to the cell number, determined by using the DNA based cell number determination method, would have introduced a technical bias, which would have led to an overestimation of the metformin levels of the ASP^+ treated cells. Therefore, no normalization was performed. Since the treatment with 5 mM ASP^+ correlated with an increased cell detachment during the washing steps of the cell harvest, which is represented by a very high CV (23%), the impact of 5 mM ASP^+ on the hepatocellular metformin uptake might be overestimated.

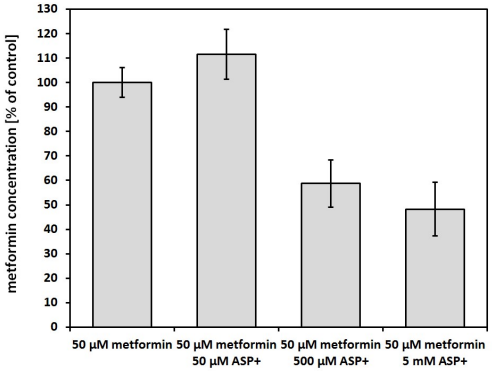

Figure 21: Inhibition of metformin uptake by ASP^+.
2.5×10^5 Hep G2 cells were seeded and cultivated using the optimized parameters described in section **2.11.2**. Then, they were treated 50 µM metformin and varying concentrations of ASP^+ and incubated for 4 h. The metformin concentrations in the cell homogenates were measured. Treatment with ASP^+ significantly inhibited the hepatocellular metformin uptake (Kruskal-Wallis Test: p-value 0.001; n = 4 - 6).

To circumvent the interference of ASP^+ with the DNA based cell number determination method and to reliably repeat the experiment, a second inhibitor of organic cation transporters was chosen, namely, quinidine. Quinidine, which is considered to be a classical inhibitor of organic cation transport [52], has been reported to be a potent inhibitor of the majority of known metformin transporters: OCTN1 [52], OCT1-3 [203], PMAT [51], SERT [204], MATE1 and MATE2-K [205]. As the IC_{50} value for the inhibition of human hepatocellular metformin uptake by quinidine was estimated to be 55 µM [203], treatment of Hep G2 cells with concentrations as high as 1 mM should abolish the active metformin transport completely. To verify the role of transporters in the metformin uptake at physiological concentrations, cells were treated with 50 µM metformin with and without quinidine. To analyze the impact of passive transport at supraphysiological metformin concentrations, cells were treated with 2 mM metformin with and without quinidine.

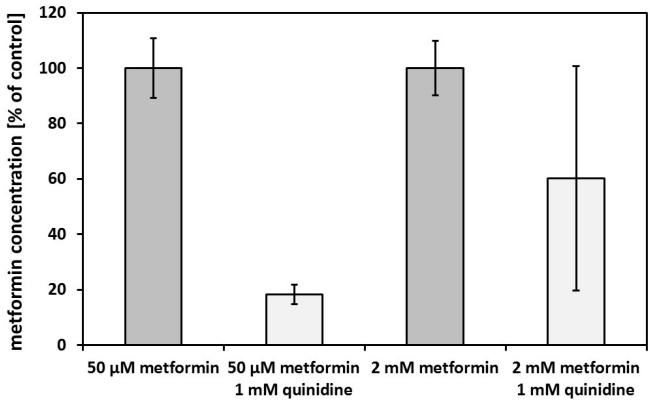

Figure 22: Inhibition of metformin uptake by quinidine.
2.5×10^5 Hep G2 cells were seeded and cultivated using the optimized parameters described in section **2.11.2** (n = 5 - 6). To elucidate the impact of transporters on the hepatocellular metformin transport at physiological conditions, the cells were treated with 50 µM metformin with and without 1 mM quinidine and incubated for 4 h. To elucidate the impact of passive transport at supraphysiological conditions, Hep G2 cells were treated with 2 mM metformin with and without 1 mM quinidine and incubated for 4 h.

As shown in **Figure 22**, the quinidine treatment had a massive impact on the hepatocellular metformin uptake. At physiological metformin concentrations (50 µM), quinidine treatment induced a significant decrease of intracellular metformin levels to 18% ± 4% of the controls (50 µM metformin) (U-Test, p-value: 0.013, Bonferroni correction, n = 5 - 6). These results support the hypothesis that, at physiological concentrations, metformin transport is strongly dominated by transporters. However, the uptake is not completely abolished by quinidine treatment.

In case of the supraphysiological metformin conditions (2 mM metformin), quinidine treatment correlated with a decrease in metformin levels to 60% ± 41% of the control cells. The massive variance originates from the high toxicity of the combinational treatment, which led to a massive cell loss during washing. The change in metformin levels, if compared to control cells, was found to be not significant (U-Test, p-value: 0.276, Bonferroni correction, n = 6). However, the difference in the percentage of imported metformin, when compared to the according controls, between the cells, treated with 50 µM metformin and quinidine, and the cells, treated with 2 mM metformin and quinidine, was found to be significant (U-Test, p-value: 0.026, Bonferroni correction, n = 5 - 6). These results indicate that with increasing metformin concentrations, passive transport becomesmore more pronounced in the hepatocellular metformin uptake.

Organic cation transporters (OCTs). As shown above, the hepatocellular metformin transport, at physiological metformin concentrations, is strongly transporter dependent. One of the transporter subfamilies, closely linked to metformin transport, are the organic cation transporters (OCT1, OCT2 and OCT3, encoded by *SLC22A1*, *SLC22A2* and *SLC22A3*) [44]. Therefore, their expression in human cell lines was analyzed. No detectable OCT2 expression could be found in any of the tested cell lines. In case of OCT1 and OCT3,

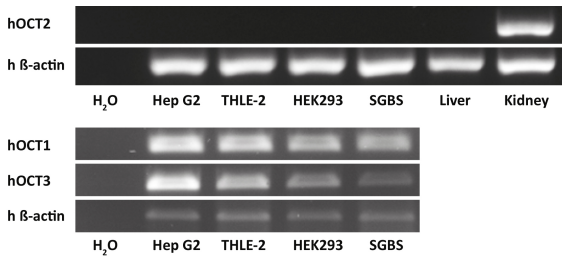

Figure 23: Expression of the organic cation transporters OCT1-3 in human cell lines.
The OCT2 expression was assessed in human cell lines of different tissue origins and human liver and kidney, using the standard PCR conditions (35 cycles, 0.5 µL template). The β-actin control was run with 35 cycles. For OCT1 and OCT3, the cycle number and template volume had to be increased to obtain a detectable signal (40 cycles, 1.0 µL template). The β-actin control was run with 30 cycles.

transcripts could only be observed using very high cycle numbers and template concentrations, indicating very low expression levels (**Figure 23**).

To elucidate the potential impact of the low abundandly expressed OCT1 and OCT3 on the metformin transport of Hep G2 cells, inhibitor studies using paroxetine were conducted. The IC_{50} values of paroxetine for OCT1, OCT2 and OCT3 dependent metformin uptake were reported to be 1.0 µM ± 0.2 µM, 11.0 µM ± 1.2 µM and 6.4 µM ± 1.3 µM (mean ± SD), respectively [56]. Interestingly, no change in intracellular metformin levels was observed, when the cells were treated with 2 µM paroxetine (**Table 25**). Taking the IC_{50} value for OCT1 into consideration, this data suggests, that OCT1 is not involved in the metformin transport of Hep G2 cells. When the cells were treated with 50 µM paroxetine, the intracellular metformin levels decreased to 60.1% ± 9.7%. However, paroxetine-induced inhibition of metformin transport might also be attributed to the plasma membrane monoamine transporter (PMAT) (IC_{50} for paroxetine-mediated inhibition of MPP^+ uptake: 22.46 µM ± 5.68 µM [206]), which was found to be abundandly expressed in Hep G2 cells (**Figure 25**).

Novel organic carnitine/cation/zwitterion transporters (OCTNs). Another transporter subfamily, which has been associated with metformin transport, are the novel organic carnitine/cation/zwitterion transporters [45]. OCTN1 as well as OCTN2 were found to be expressed in human liver tissue [49]. In accordance with these observations, OCTN1 and OCTN2 were found to be expressed in the hepatic cell lines Hep G2 and THLE-2 (**Figure 24**). OCTN1 was found to be low abundant in Hep G2 cells, with higher levels were observed in THLE-2 cells. OCTN2 expression was low in both cell lines. Both transporters are polyspecific and capable of carnitine transport [50], [207] (OCTN1: K_M = 412.6 ± 191 µM, OCTN2: K_M = 3.39 ± 1.16 µM [207]). OCTN1 is capable of metformin transport and has been linked to the gastrointestinal absorption of the drug [45]. Further, it transports quinidine [50] and could, consequently, contribute to the observed quinidine-mediated inhibition of hepatocellular metformin uptake (**Figure 22**). In addition OCTN1 has been shown to be capable of acetylcarnitine transport [64]. However, OCTN2 has been shown to be incapable of metformin transport [56]. To test whether OCTN1 is responsible for the hepatocellular metformin uptake, inhibitor studies using the model substrates carnitine and acetylcarnitine were conducted (**Table 25**).

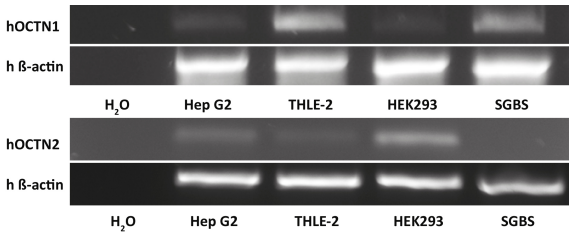

Figure 24: Expression of the novel organic carnitine/cation/zwitterion transporters OCTN1 and OCTN2 in human cell lines.

Carnitine led to a significant (Kruskal-Wallis Test: p-value 7.70 x 10^{-4}, n = 6) decrease of intracellular metformin concentrations. Carnitine concentrations of up to 500 µM led to a pronounced dose-dependent decrease of metformin uptake. However, a further elevation of the inhibitor concentration to 5 mM did not correlate with any additional decrease in metformin levels. Similarly, acetylcarnitine led to a significant reduction of metformin uptake

(Kruskal-Wallis Test: p-value 0.027, n = 4 - 6). However, the inhibition by acetylcarnitine was found to be less pronounced and non-dose dependent. Acetylcarnitine is most likely a less potent inhibitor of the metformin uptake, because it displays a lower structural similarity, as demonstrated by the Tanimoto coefficient, to the drug than carnitine (**Table 24**).

These results indicate that metformin, carnitine and acetylcarnitine share at least one common transporter. The data supports the hypothesis that the OCTN1 transporter is partially responsible for the hepatocellular uptake of the drug.

Table 25: Inhibition of potential metformin transporters involved in the hepatocellular metformin uptake.
Hep G2 cells were deprived of FBS for 24 h. Then, the cells were treated with either vehicle (negative control), 50 µM metformin (control), or with 50 µM metformin plus the according inhibitor. The incubation time was set to 2 h (desipramine) to 4 h. Then, the cells were scraped and LC-MS/MS based metformin quantification and DNA based determination of the cell number were performed. The table lists the inhibition of metformin transport as percent of the controls (50 µM metformin).

Metformin Transporter: Inhibitor studies		
Inhibitor	**Concentration [µM]**	**Percentage of intracellular metformin compared to the controls ± SD [% of control]**
L-Carnitine	50	73.8 ± 6.2
	500	61.6 ± 5.0
	5,000	67.3 ± 6.9
L-Acetylcarnitine	50	77.7 ± 6.4
	500	76.5 ± 4.2
	5,000	77.9 ± 5.4
Paroxetine	0.0001	97.9 ± 7.5
	0.060	100.6 ± 11.0
	0.100	96.6 ± 1.1
	0.600	92.0 ± 6.4
	2	100.3 ± 2.0
	50	60.1 ± 9.7
Desipramine	200	56.8 ± 7.7
Cimetidine	5	91.8 ± 5.3
L-Arginine	50	105.5 ± 3.9
	500	114.5 ± 14.5
	5,000	110.3 ± 6.2

Plasma membrane monoamine transporter (PMAT) and serotonine transporter (SERT). In 2015, Han *et al.* showed that PMAT and SERT are capable of metformin transport and proposed their involvement in the intestinal absorption of the drug [56]. PMAT was found to be expressed in both tested hepatic cell lines, Hep G2 and THLE-2. In addition, Hep G2 cells also expressed SERT (**Figure 25**). Unfortunately, a selective PMAT inhibitor has not yet been reported [56]. To assess, whether PMAT and SERT partake in the hepatocellular metformin uptake, inhibitor studies with paroxetine and desipramine were conducted. This combinational approach for the elucidation of the potential participation of SERT and PMAT in cellular metformin uptake has been proposed and validated by Han *et al.* [56]. The authors suggested a concentration of 0.1 µM paroxetine to inhibit SERT and a concentration of 200 µM desipramine to inhibit OCT1, OCT2, OCT3, SERT, PMAT and MATE1 [56]. With an IC_{50} of 2.01 nM ± 0.36 nM (mean ± SEM) for serotonine uptake, paroxetine is a highly potent SERT inhibitor [66]. For the metformin transport, the IC_{50} of

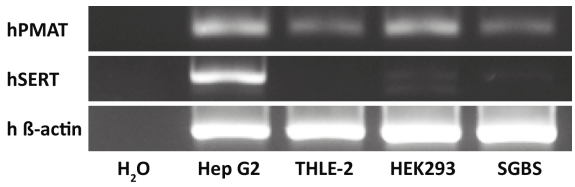

Figure 25: Expression of the plasma membrane monoamine (PMAT) and the serotonine transporter (SERT) in human cell lines.

paroxetine for SERT was reported to be 6.0 nM ± 0.6 nM (mean ± SD) [56]. The IC_{50} for the inhibition of PMAT mediated MPP^+ uptake by paroxetine was found to be 22.46 µM ± 5.68 µM [206]. As to my knowledge, the respective IC_{50} for PMAT mediated metformin uptake has not yet been reported.

Paroxetine treatment with doses up to 2 µM did not induce any changes in the metformin uptake (**Table 25**) (n = 5 - 6, U-Test, Bonferroni corrected). This indicates that SERT, although being expressed (**Figure 25**), is not involved in the metformin transport of Hep G2 cells. The elevation of the dose to 50 µM, which is slightly higher than the double of the IC_{50} for PMAT mediated MPP^+ uptake, induced a significant decrease of the intracellular metformin levels to 60%, compared to those of the controls (U-Test: p-value: 0.011, Bonferroni corrected, n = 6). Desipramine treatment led to a significant decrease of the hepatocellular metformin uptake (U-Test: p-value: 0.002, n = 6), similar in its extend (57%) to the one observed with 50 µM paroxetine. The observed pattern hints at an implication of PMAT in the hepatocellular uptake of the drug.

Multidrug and toxin extrusion protein 1 (MATE1). The MATE1 transporter has been linked to the renal secretion of metformin [43] and its hepatic expression has been reported [68]. In addition, Hilgendorf *et al.* suggested that it might play a role in the hepatocellular excretion of drugs [62]. MATE1 was found to be expressed in both tested hepatic cell lines (**Figure 26**: Hep G2 and THLE-2). Consequently, its potential participation in hepatocellular metformin transport was assessed. Cimetidine is a highly potent MATE1 inhibitor (K_I 1.1 µM ± 0.3 µM for MATE1 dependent tetraethylammonium (TEA) transport [67]; IC_{50} of OCT1, OCT2 and OCT3 mediated metformin transport: 20.9 µM ± 1.4 µM, 16.6 µM ± 1.3 µM, 9.8 µM ± 1.3 µM, respectively [56]; and K_I for PMAT mediated MPP^+ uptake > 500 µM [51]), which has been used for the elucidation of metformin transport [56]. Han *et al.* proposed a concentration of 5 µM cimetidine to selectively inhibit MATE1 [56]. However, the application of this concentration to Hep G2 cells did not elicit significant changes in intracellular metformin levels (**Table 25**). This result indicates that MATE1 is not involved in the hepatocellular metformin transport.

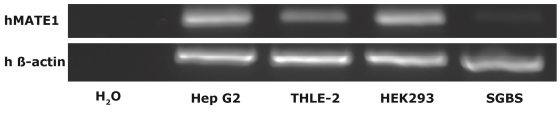

Figure 26: Expression of the multidrug and toxin extrusion protein 1 (MATE1) in human cell lines.
As the expression analyses of OCTN2 (**Figure 24**) and MATE1 were conducted within the same experiment, they share the same β-actin control.

Thiamine transporter 2 (THTR-2). In November 2015, Liang *et al.* demonstrated that THTR-2 is capable of metformin transport [48]. Further, it was found to be expressed in the human liver [48] and in hepatic cell lines (**Figure 27**). Hence, THTR-2 might be involved in the human hepatocellular metformin transport. Consequently, the next step should be the elucidation of the impact of THTR-2 on the hepatocellular metformin transport.

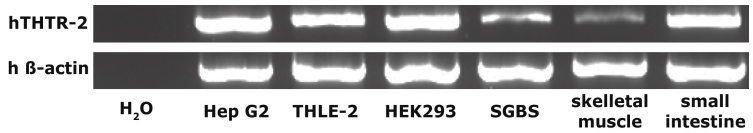

Figure 27: Expression of the thiamine transporter 2 (THTR-2) in human cell lines.
THTR-2 expression of Hep G2, THLE-2, HEK293 and SGBS cells was tested. Human skeletal muscle and small intestine served as positive controls.

Outcome. The obtained results showed that the hepatocellular metformin transport consists of a non-saturable (passive) and a saturable (active) component. At physiological metformin concentrations, metformin transport is dominated by active transport involving a number of potential transporters. The results of the inhibitor studies indicate that OCTN1 and PMAT are potential candidates, responsible for the hepatocellular metformin uptake. In addition, THTR-2 was found to be expressed in all tested human cell lines (**Figure 27**) and, hence, might be a promising candidate.

Limitations and outlook. From a technical point of view, spiking inhibitors into cell culture medium might pose a limitation as the inhibitor might change the pH of the medium. Although, the formulation of the medium is defined, closely resembles physiological conditions and the pH can be monitored by using phenol red, conducting the experiments in a buffer solution would offer the possibility to more stringently define and control the experimental settings. Unfortunately, measuring hepatocellular metformin transport in a buffer solution is not feasible, as it requires trypsinization to detach the adherently growing Hep G2 cells (**Figure 28**). Trypsinization and resuspension in buffer leads to a massive loss of intracellular small polar molecules due to trypsic leakage [117]. Hence, the trypsic leakage might lead to an overestimation of the non-saturable component of metformin transport, thereby diminishing the translational characteristics of the obtained results to physiological conditions.

3.5. Elucidation of the impact glucose and metformin on the cellular metabolome

To understand a disease and to successfully treat it, a broad understanding of the mechanisms, causing and driving it is necessary. Consequently, the elucidation of the cellular and molecular mechanisms of health and disease has become of vital importance in modern health care. In this regard, representative models have to be established and used. Of course, the experimental approach as well as the chosen model strongly depends on the aim of the study.

This study aimed to elucidate the impact of glucose and metformin on the hepatocellular metabolism. In this context, a cell culture based approach in combination with metabolomics analyses was chosen. The application of this approach offers a number of unique opportunities. First, it is possible to assess the intracellular changes as well as the alteration in the cellular secretome. Further, the environmental parameters, which can influence the experimental outcome, are well defined and monitored. Third, this model system offers the possibility to elucidate the response of a single cell type to a specific challenge. Thereby, altered metabolic signatures do not represent an overall change of multiple tissues, as is the case with biofluids or whole organs, but can be attributed to the specific alterations of metabolic pathways in a single cell type.

3.5.1. The experimental setup

The model systems. Two cell lines, THLE-2 and Hep G2 (**Figure 28**), were chosen as model systems to elucidate the impact of the glucose concentration and metformin on the hepatocellular metabolism.

THLE-2. THLE-2 is an immortalized human liver cell line, which was derived from a healthy adult donor [208]. Immortalization was achieved with the Simian virus 40 large tumor antigen [208]. The cell line expresses hepatocyte differentiation markers, retains enzymes involved in the metabolism of xenobiotics and is non-tumorigenic [208]. Thus, this cell line has been used for metabolism-induced toxicology screening [209].

Hep G2. Hep G2 is one of the most frequently used hepatoma cell lines [210] and has successfully been applied to elucidate hepatocellular metformin action [30], [86], [95], [211] and has served as a model for hepatocellular carcinoma [95]. It was derived from the material of the liver tumor biopsy of a 15 year old caucasian male with well differentiated hepatocellular carcinoma [212]. This cell line retains many liver-specific functions [210], such as human plasma protein synthesis [213]. In general, hepatoma cell lines have been frequently used for toxicity studies and to investigate hepatocellular functions [210]. However, the transferability of the obtained results to a “normal, healthy” human liver is difficult to assess, as hepatoma cells exhibit diminished biotransformation activities [210]. Further, in case of Hep G2 cells, the relative expression levels of OCT1-3 strongly differ from those found in the liver [62]. In addition, a number of drug-metabolizing enzymes were found to be differentially expressed, if compared to primary human hepatocytes [214].

Nonetheless, the down-regulation of the expression of drug-metabolizing enzymes [214] is unlikely to affect metformin action on a primary level, as the drug was shown to be not metabolized in humans [37]. A more crucial role might have the cancer associated changes in metabolism. Whereas normal cells use mitochondrial oxidative phosphorylation (OXPHOS) for energy generation, cancer cells strongly rely on aerobic glycolysis [88]. This alteration of the very backbone of the cellular metabolism is referred to as “Warburg effect” [88], and its interaction with metformin might follow a dual nature. First, metformin has been reported to inhibit Complex I of the electron transport chain [69]. Second, it has been shown to alter the cellular glucose metabolism via an inhibition of gluconeogenesis [215] as well as an inhibition of the isoforms I and II of the glycolytic enzyme hexokinase [73].

Figure 28: THLE-2 and Hep G2 cells were cultivated at physiological (6 mM) or diabetic (11 mM) glucose concentrations and treated with metformin or H_2O. The microscopic images show the two cell lines at the time point of harvest (100 x amplification).

Cell line	6 mM glucose control	6 mM glucose 2 mM metformin	11 mM glucose control	11 mM glucose 2 mM metformin
THLE-2	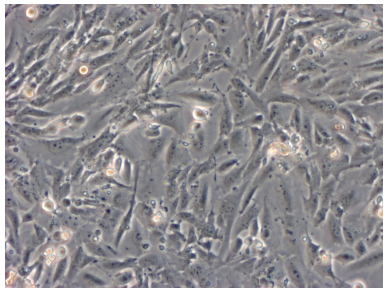	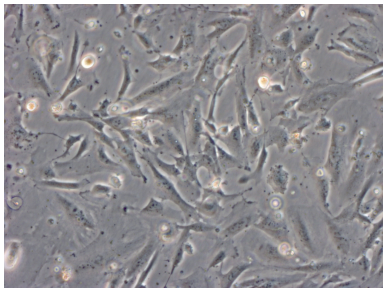	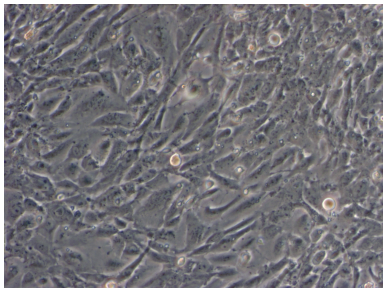	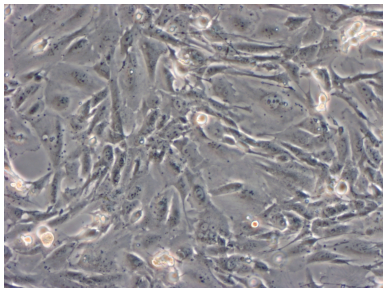
Hep G2	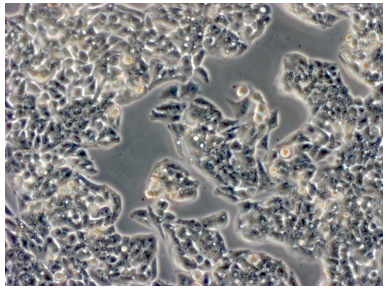	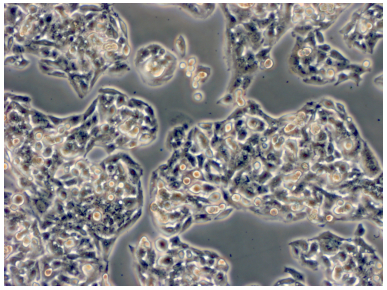	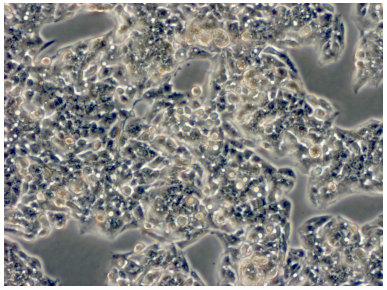	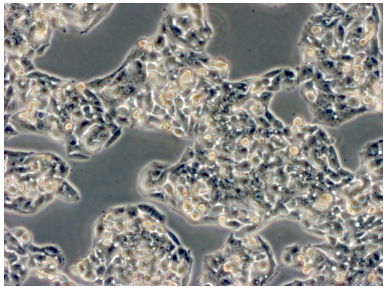

Metformin concentration. The first step was the determination of the optimal metformin concentration for the elucidation of the hepatocellular metformin action in a cell culture based setting, adressing parameters like the viability and the metabolite profile. These experiments were part of my Master´s Thesis [130]. The tested metformin concentrations were 500 µM, 2 mM and 5 mM. The pre-selection of those concentrations was based on the data obtained by Julia Sundermeier, who tested concentrations within the range of 0.1 mM to 50 mM in course of her internship (supervisor: Sven Zukunft) (data not published). The concentrations of 500 µM and 2 mM are within the range of physiological metformin concentrations, measured in the tissues of diabetic and normal mice [41]. However, 5 mM metformin clearly exceeds the physiological range [41]. Nonetheless, metformin concentrations within the low to intermediate mM range are very frequently applied to elucidate (hepato)cellular metformin action and have been shown to elicit characteristic responses [95], [216], [217]. A potential reason might be the lack of response to lower metformin concentrations in short term studies. In detail, when Hep G2 cells were treated with 500 µM metformin for 24 h, the obtained viability was found to be 85% to 95% of the one of the controls. In addition, this metformin concentration did not exhibit a significant impact on the measured metabolite profile of the cells (targeted metabolomics: Absolute*IDQ* p180 Kit, U-Test Benjamini-Hochberg correction, n per group = 15, p-value > 0.05). However, it has been previously reported, that in mice and patients, the application of metformin elicited significant changes in the metabolite profile [106], [218], [219]. For example, blood alanine and valine levels were found to be increased in metformin treated patients with insulin resistance [218]. Although 500 µM might be within the physiological range, it does not elicit physiological responses in a short term cell culture based experiment. Most likely, the incubation time is the reason for the blunted response, as metformin is usually used for long-term intervention [106]. However, these time ranges cannot be applied to a cell culture based setting. Therefore, an alternative route, namely, the elevation of the applied metformin concentration, had to be taken. Treatment of the cells with 2 mM metformin for 24 h led to the significant alteration of the intracellular concentrations of 46 metabolites. A reduction in viability to 76% of the one of the controls was observed. However, this metformin concentration did not alter the morphology of treated Hep G2 and THLE-2 cells (**Figure 28**). A further elevation of the metformin concentration to 5 mM correlated with the significant change of 105 metabolites. However, the viability decreased to as low as 48%. **Figure 29** shows examples of the metformin concentration dependent regulation of intracellular metabolite levels. Consequently, 2 mM was chosen as the optimal metformin concentration to mimic physiological conditions in a short term cell culture based experiment. Although it is not similar to the metformin concentration measured in the liver or the hepatic portal vein, it is still within the physiological range [41]. In addition, as metformin treatment has been linked to significant changes in metabolite levels in mice and in patients [106], [218], [219], it more closely mimics the metabolic response to drug treatment than the 500 µM treatment.

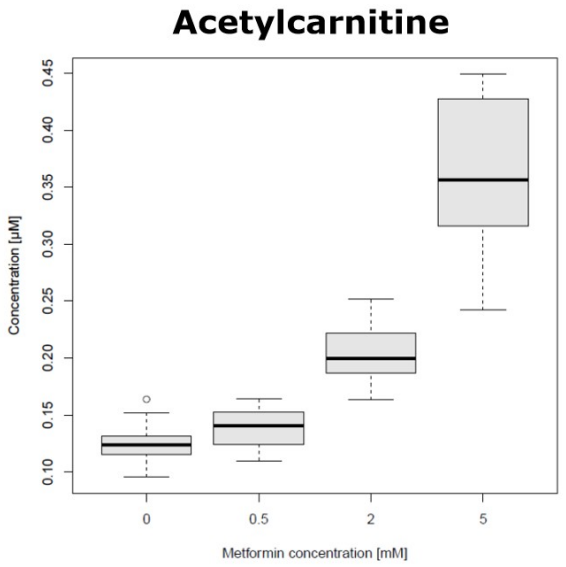
Acetylcarnitine
Concentration [µM]
0.10
0.15
0.20
0.25
0.30
0.35
0.40
0.45
0
0.5
2
5
Metformin concentration [mM]

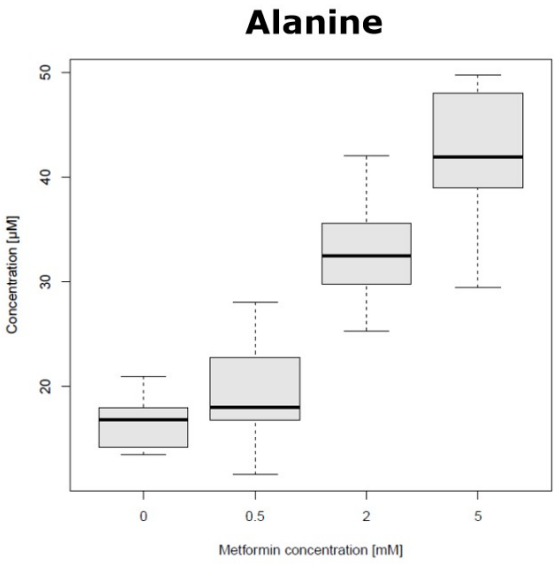
Alanine
Concentration [µM]
20
30
40
50
0
0.5
2
5
Metformin concentration [mM]

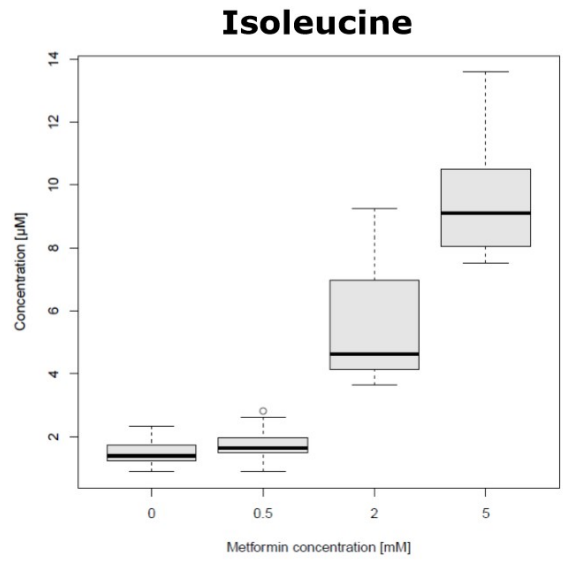
Isoleucine
Concentration [µM]
2
4
6
8
10
12
14
0
0.5
2
5
Metformin concentration [mM]

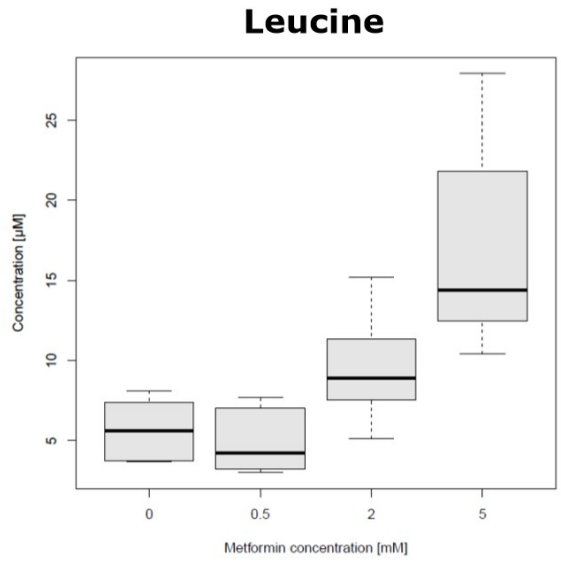
Leucine
Concentration [µM]
5
10
15
20
25
0
0.5
2
5
Metformin concentration [mM]

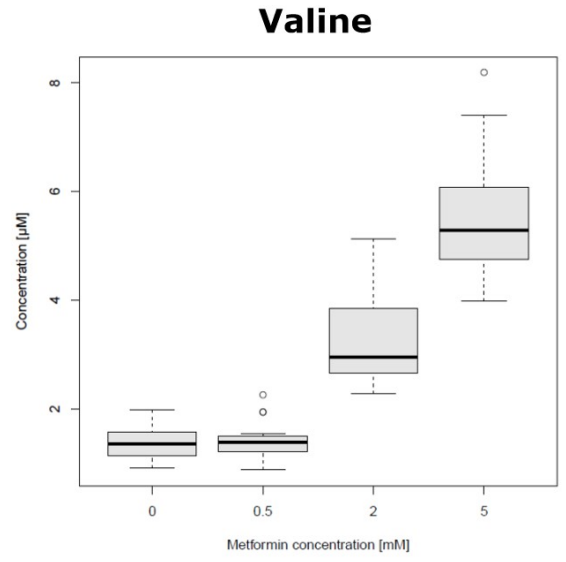
Valine
Concentration [µM]
2
4
6
8
0
0.5
2
5
Metformin concentration [mM]

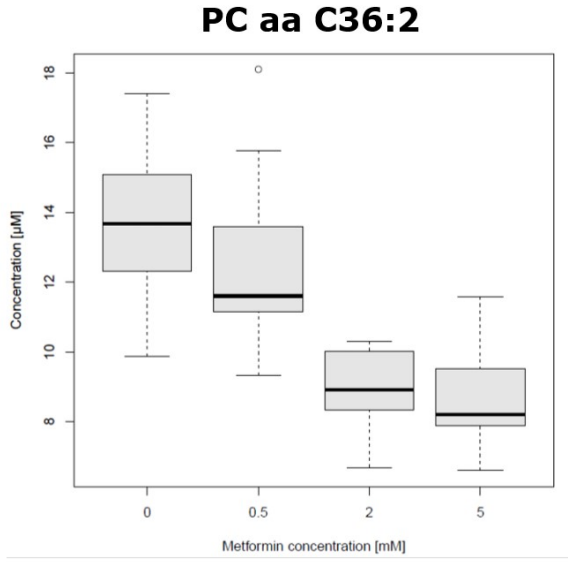
PC aa C36:2
Concentration [µM]
8
10
12
14
16
18
0
0.5
2
5
Metformin concentration [mM]

Figure 29: Metformin concentration dependent regulation of intracellular metabolite concentrations.
1.5 x 10^5 Hep G2 cells were seeded into the wells of 12 well plates and cultivated for 24 h in DMEM High Glucose. Then, the cells were treated with either 500 µM, 2 mM or 5 mM metformin (n per group = 15). Cells treated with vehicle (H_2O) served as controls. Then, the cells were harvested and targeted metabolomics using the Absolute*IDQ* p180 Kit was performed.

Glucose concentration. To evaluate the impact of the glucose concentration on the hepatocellular metabolome and metformin action, three glucose concentrations were tested. Hep G2 cells were cultivated in glucose-free medium, supplemented with either 0, 5, 11 or 25 mM glucose, for 24 h and then treated with either vehicle or 2 mM metformin. Then, targeted metabolomics using the Newborn screening kit was performed. The elevation of the exogenous glucose concentration from 0 to 5 and from 5 to 11 mM had a pronounced impact on the hepatocellular metabolome. However, a further elevation from 11 to 25 mM yielded no significant changes in the measured metabolite concentrations (p-value > 0.05, U-Test: Benjamini-Hochberg corrected). Further, no significant changes in the metabolite levels of the metformin treated cells, cultivated at a glucose concentration of 11 or 25 mM, were observed.

Finally, to assess the impact of the glucose concentration on the hepatocellular metabolome and metformin action, the glucose concentrations of 6 mM (low glucose or physiological glucose condition) and 11 mM (high glucose or diabetic glucose condition) were chosen. The low glucose concentration had to be changed to 6 instead of 5 mM, as the cell culture medium, needed for the cultivation of the THLE-2 cells, could not be obtained with a lower glucose concentration.

When regarded in a physiological context, a 2 h postprandial (after the intake of a meal with at least 75 g carbohydrate content) blood glucose level of below 7.8 mM is representative of an individual (0 - 50 years of age) without diabetes mellitus [220]. Hence, the low glucose concentration of 6 mM mimics a non-diabetic, non-fasting individual. According to the WHO report on the “Definition, Diagnosis and Classification of Diabetes Mellitus and its Complications”, a plasma glucose concentration of ≥ 7.0 mM (fasting) or ≥ 11.1 mM (2 h after 75 g glucose load) is representative for diabetes mellitus [221]. For venous whole blood, the thresholds are given with ≥ 6.1 mM (fasting) and ≥ 10.0 mM (2 h after 75 g glucose load) [221]. Thus, the applied high glucose concentration of 11 mM reflects the glucose concentration of a diabetic, non-treated, non-fasting patient.

3.5.2. Impact of metformin and glucose concentration on the hepatocellular metabolism

To assess the impact of the glucose concentration on the hepatocellular metabolism, THLE-2 and Hep G2 cells were cultivated either at low glucose (6 mM) or high glucose (11 mM) conditions (48 h). Further, to evaluate the impact of metformin, both cell lines were treated with 2 mM metformin or vehicle (H_2O) for 24 h. Then, the cells were harvested using the optimized protocols (section **2.8**). Targeted and non-targeted metabolomics analyses, cell number determination and metformin quantification were performed.

The determined cell numbers of the samples used for targeted metabolomics of both cell lines were lower for the metformin treated cells, when compared to the vehicle treated cells (**Figure 30**). Whereas this observation was significant for Hep G2 cells, for THLE-2 it was not. This hinted at a higher susceptibility of Hep G2 cells to the treatment with the anti-diabetic drug. Further, for Hep G2 cells, an elevation of the glucose level of the culturing medium from 6 mM to 11 mM induced a significant increase in cell number. This could not be observed for THLE-2 cells. Since the differences in the cell number of THLE-2 cells were not significant in the first experiment, it is not surprising, that they were not significant in the second either. **Figure 32** shows the results of the cell count of the sample set, generated for non-targeted metabolomics. Whereas, for the THLE-2 cells the same trend as for the sample set, generated for targeted metabolomics, was not observed (**Figure 30**), the cell

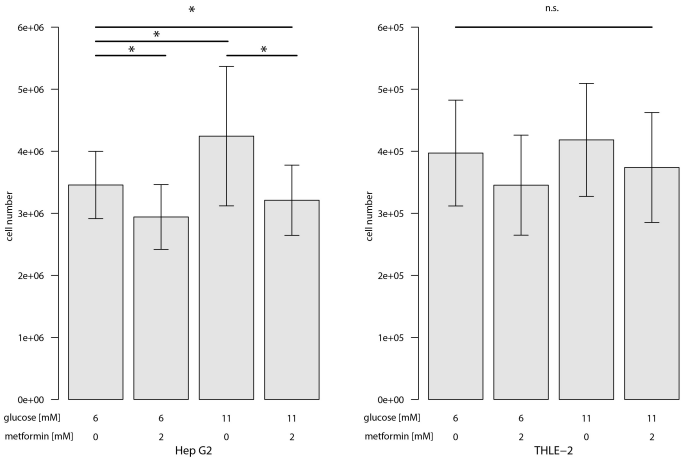

Figure 30: Impact of metformin and glucose concentration on the cell number of Hep G2 and THLE-2 cells in samples for targeted metabolomics.
Hep G2 and THLE-2 cells were cultivated either under low or high glucose conditions and treated with vehicle or metformin (n = 12, N = 96). Then, the cells were harvested for targeted metabolomics analyses, and the cell numbers were determined using the fluorescence based DNA quantification method. The graph shows the cell number per well. Statistical analysis was performed using the Kruskal-Wallis test for comparison of > 2 groups. The U-Test was used for posthoc pairwise comparisons. The obtained p-values were corrected with the Benjamini-Hochberg method for multiple testing. The ateristc indicates a p-value of below 0.05 after correction for multiple testing. n.s.: not significant.

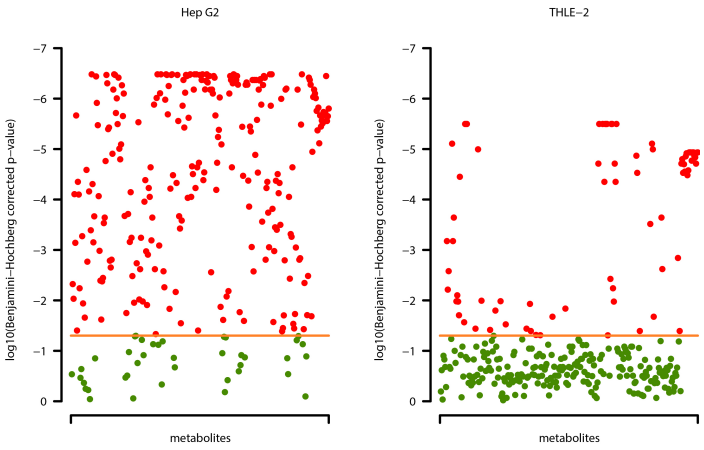

Figure 31: Impact of metformin and glucose concentration on the hepatocellular metabolite profile in samples for targeted metabolomics.
Targeted metabolomics of the Hep G2 and THLE-2 cell homogenates was performed. The plots show the Benjamini-Hochberg adjusted p-values (Kruskal-Wallis Test, n = 12, N = 96) of all measured metabolites in all treatment groups. The p-values of significantly changed metabolites are displayed in red, the non-significant ones in green. The orange lines mark the significance threshold.

numbers of the Hep G2 cell samples showed a similar trend as in the sample set for targeted metabolomics. However, due to the smaller sample size of the non-targeted sample set (n = 6, N = 48), this trend was not significant.

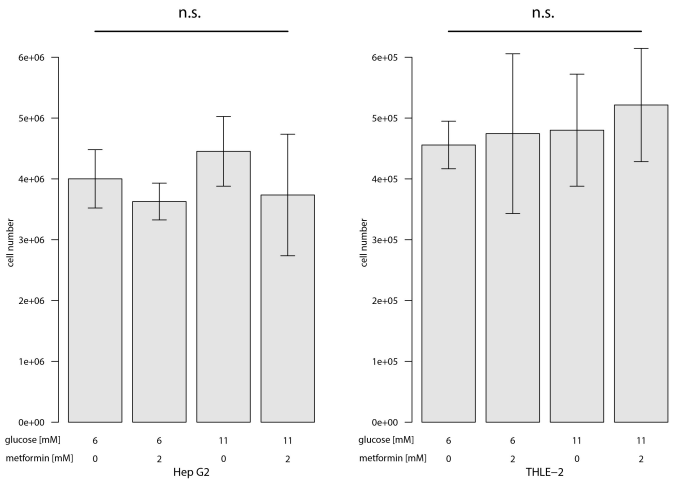

Figure 32: Impact of metformin and glucose concentration on the cell number of Hep G2 and THLE-2 cells in samples fo non-targeted metabolomics.
Hep G2 and THLE-2 cells were cultivated either under low or high glucose conditions and treated with vehicle or metformin (n = 6, N = 48). Then, the cells were harvested for non-targeted metabolomics analyses, and the cell numbers were determined using the fluorescence based DNA quantification method. The graph shows the cell numbers per well. Statistical analysis was performed using the Kruskal-Wallis test. n.s.: not significant.

A similar observation was obtained for the analysis of the impact of metformin treatment and glucose concentration on the hepatocellular metabolome (**Figure 31** and **Figure 33**). In both sample sets, the metabolic response – represented by the number of significantly altered metabolites – was far more pronounced for Hep G2 cells, when compared to THLE-2 cells. Again, the p-values of the non-targeted sample set are higher than those of the targeted sample set. This might be caused by the fact that a different metabolite panel was analyzed. Additionally, the lower samples size as well as the relative metabolite quantification in case of non-targeted metabolomics might impact the experimental outcome.

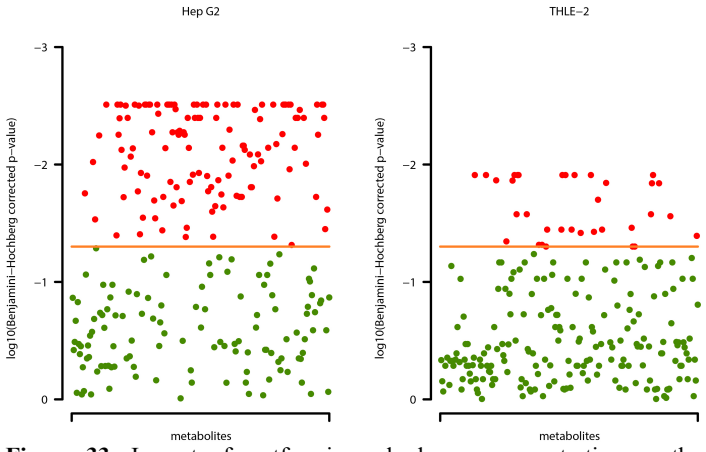

Figure 33: Impact of metformin and glucose concentration on the hepatocellular metabolite profile in samples for non-targeted metabolomics.
Non-targeted metabolomics of the Hep G2 and THLE-2 cell homogenates were performed. The plots show the Benjamini-Hochberg adjusted p-values (Kruskal-Wallis Test, n = 6, N = 48) of all measured metabolites in all treatement groups. The p-values of significantly changed metabolites are displayed in red, the non-significant ones in green. The orange lines mark the significance threshold.

Figure 35 (non-targeted metabolomics) and **Figure 34** (targeted metabolomics) show the metabolic profile of the two liver cell lines, when cultivated at a physiological (low) or a diabetic (high) glucose concentration and subjected to metformin treatment. **Figure 36** shows the impact of the cellular response to the culturing conditions and drug treatment on the cell culture supernatants. For all measured profiles, the two major clusters are based upon the differences between the two cell lines. This already indicated that “normal” liver (THLE-2) and hepatoma (Hep G2) cells indeed exhibit differences in their metabolism and their responses to glucose and metformin.

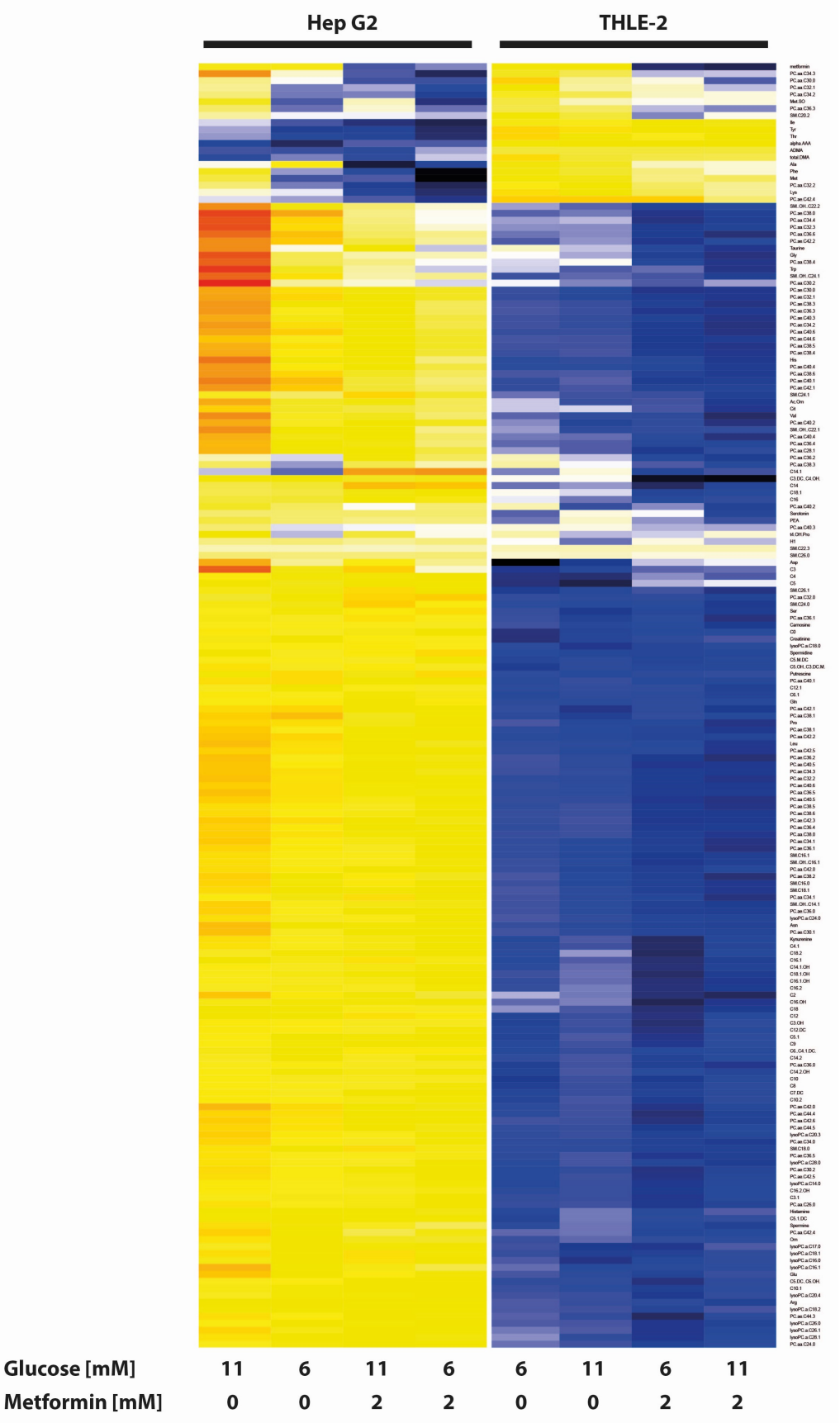

Figure 34: Metabolic profile of metformin- and vehicle-treated THLE-2 and Hep G2 cells, cultivated at different glucose conditions, analyzed with targeted metabolomics. The heatmap shows the metabolic profile of THLE-2 and Hep G2 cells, cultivated at either low glucose or high glucose conditions and with or without metformin treatment. Targeted metabolomics were conducted. The data was corrected for plate effects and normalized to 1 x 10^6 cells. Minimum-half imputation and autoscaling was performed. The heatmap shows the median of the according groups. Clustering of the groups and the metabolites was performed using the manhattan metric [288] and the Ward1 algorithm [287]. The white line separates the two major clusters.

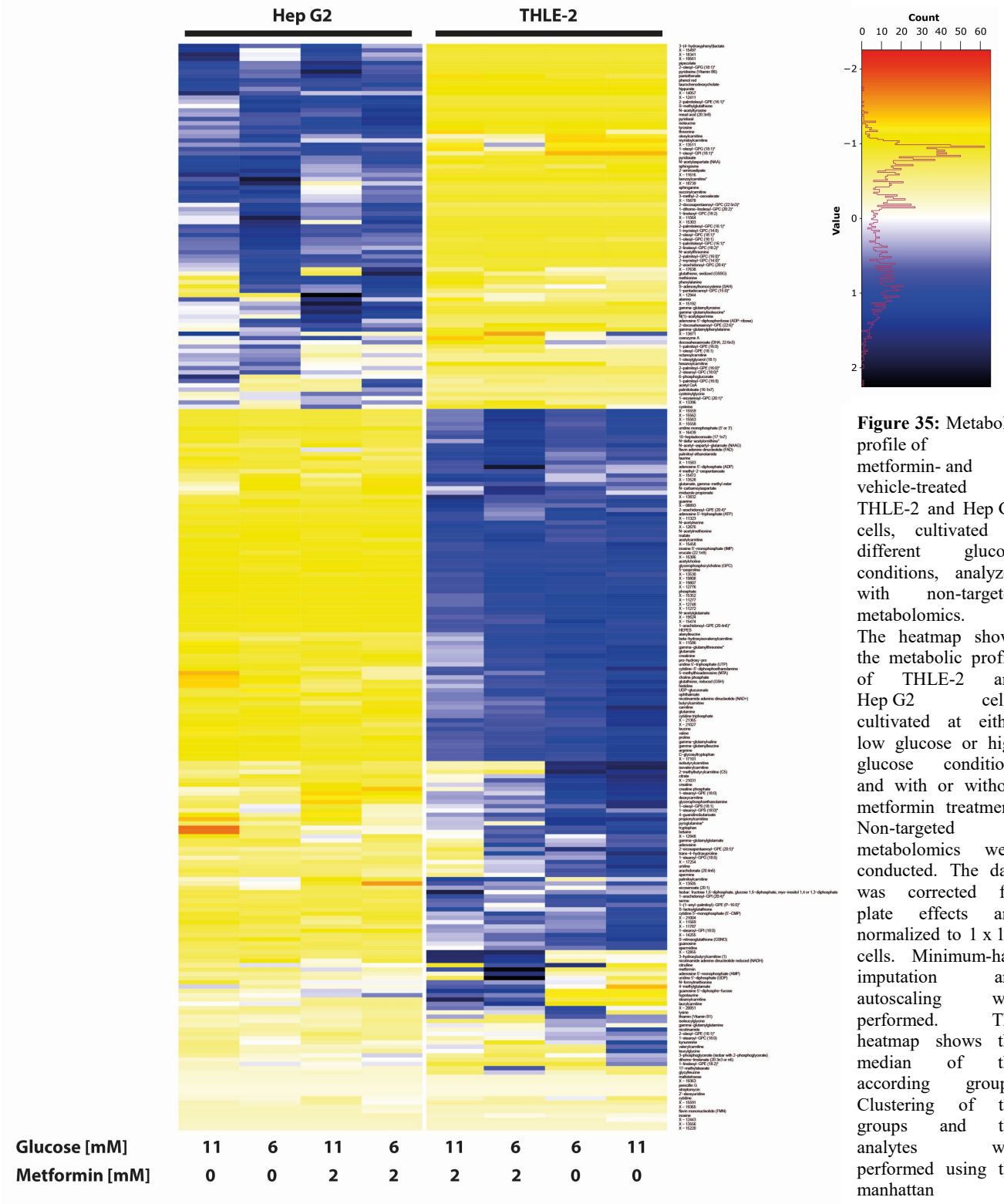

Figure 35: Metabolic profile of metformin- and vehicle-treated THLE-2 and Hep G2 cells, cultivated at different glucose conditions, analyzed with non-targeted metabolomics. The heatmap shows the metabolic profile of THLE-2 and Hep G2 cells, cultivated at either low glucose or high glucose conditions and with or without metformin treatment. Non-targeted metabolomics were conducted. The data was corrected for plate effects and normalized to 1 x 10^6 cells. Minimum-half imputation and autoscaling was performed. The heatmap shows the median of the according groups. Clustering of the groups and the analytes was performed using the manhattan metric [288] and the Ward1 algorithm [287]. The white line separates the two major clusters.

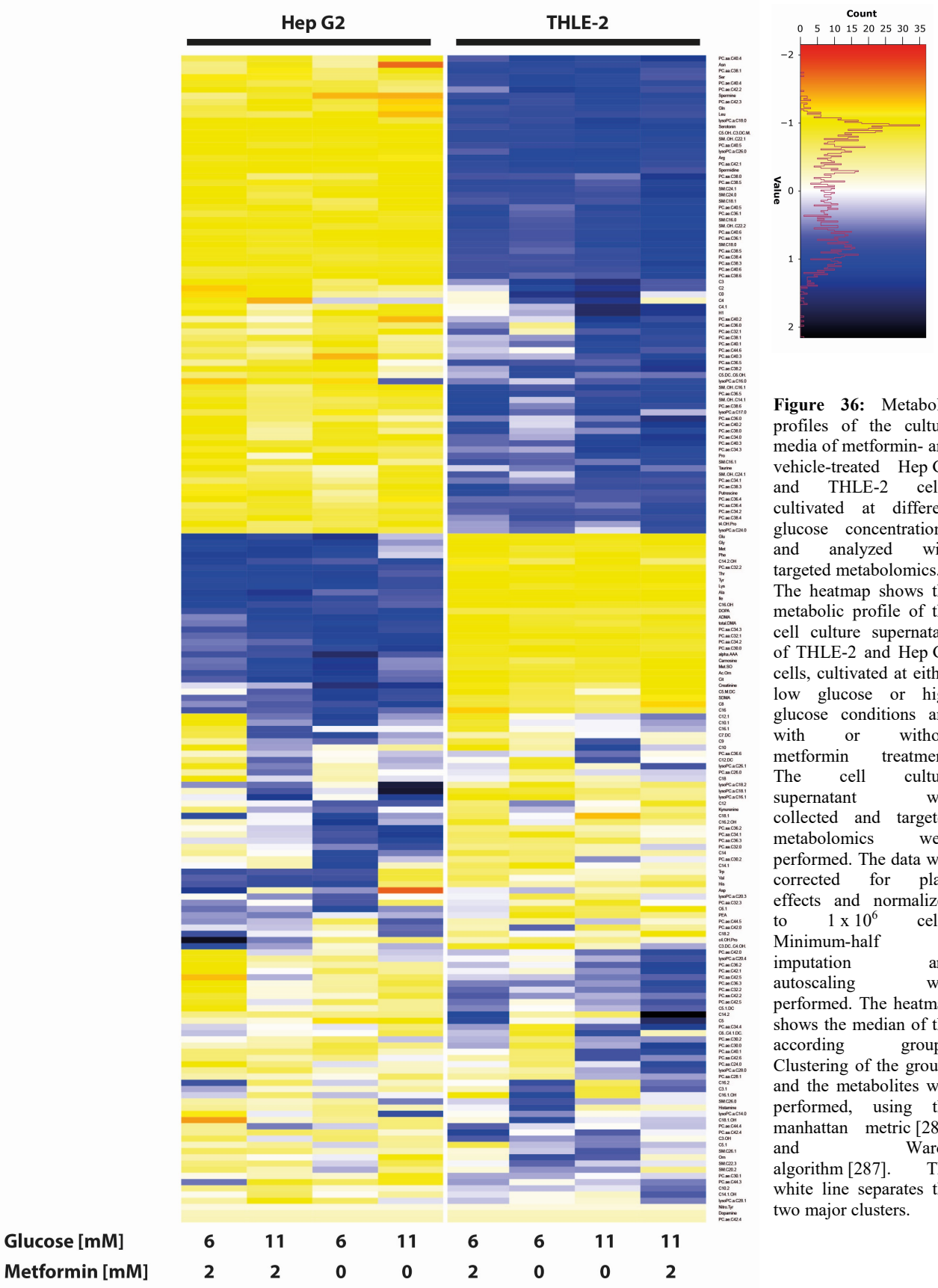

Figure 36: Metabolic profiles of the culture media of metformin- and vehicle-treated Hep G2 and THLE-2 cells, cultivated at different glucose concentrations, and analyzed with targeted metabolomics. The heatmap shows the metabolic profile of the cell culture supernatant of THLE-2 and Hep G2 cells, cultivated at either low glucose or high glucose conditions and with or without metformin treatment. The cell culture supernatant was collected and targeted metabolomics were performed. The data was corrected for plate effects and normalized to 1 x 10^6 cells. Minimum-half imputation and autoscaling was performed. The heatmap shows the median of the according groups. Clustering of the groups and the metabolites was performed, using the manhattan metric [288] and Ward1 algorithm [287]. The white line separates the two major clusters.

3.5.3. The impact of the glucose concentration on the metabolome of THLE-2 cells

The glucose concentration had no pronounced impact on the metabolome of THLE-2 cells. The only significantly altered parameter was the sum of hexoses (H1), which was found to be strongly elevated in the cell homogenates. No pathways were found to be significantly enriched. The p-values of the pairwise comparisons of the applied conditions are listed in **Table S-5**, **Table S-6** and **Table S-7**.

3.5.4. The impact of the glucose concentration on the metabolome of Hep G2 cells

For the hepatoma cell line Hep G2, the hexose concentration was found to vastly alter the cellular metabolome. **Table 26** lists the significantly altered pathways. Not surprisingly, quite a number of hexose associated pathways was found among the significant hits. The amino acid metabolism was strongly affected as well. Interestingly, the glutathione and the pyrimidine metabolism were changed. The list of significantly altered pathways illustrates that the glucose concentration had a massive impact on the very backbone of the metabolism of hepatoma cells. In addition, some acylcarnitines and sphingomyelins and many phosphatidylcholines, measured with targeted metabolomics, were found to be significantly altered.

Table 26: Enriched pathways of Hep G2 cells, cultivated at physiological and high glucose concentrations.
Hep G2 cells were either cultivated with 6 mM or 11 mM glucose. Non-targeted metabolomics was performed. The table shows the results of the enrichment analysis.

Enrichment analysis

Pathway	Total number of compounds	Hits	Fold enrichment	p-value (Benjamini-Hochberg adjusted)
Pyrimidine metabolism	36	9	7.4	4.3E-07
Aspartate metabolism	12	3	8.5	8.6E-07
Ammonia recycling	18	8	7.8	3.3E-06
Methionine metabolism	24	8	8.8	3.4E-06
Betaine metabolism	10	3	9.3	3.8E-06
Malate-aspartate shuttle	8	3	8.2	7.8E-06
Glycolysis	21	4	8.3	7.8E-06
Gluconeogenesis	27	4	8.3	7.8E-06
Mitochondrial electron transport chain	15	4	8.3	7.8E-06
Protein biosynthesis	19	16	8.7	9.9E-06
Phenylalanine and tyrosine metabolism	13	2	9.4	4.4E-05
Nucleotide sugars metabolism	9	1	9.4	8.6E-05
Starch and sucrose metabolism	14	1	9.4	8.6E-05
Urea cycle	20	8	8.0	1.2E-04
Tryptophan metabolism	34	2	8.6	1.2E-04
Histidine metabolism	11	2	8.6	1.6E-04
Glycine, serine and threonine metabolism	26	5	7.1	1.6E-04
Glucose-alanine cycle	12	4	8.3	4.7E-04
Alanine metabolism	6	2	8.3	7.6E-04

Selenoamino acid metabolism	15	1	8.3	8.2E-04
Arginine and proline metabolism	26	6	6.3	1.5E-03
Tyrosine metabolism	38	1	7.2	4.2E-03
Catecholamine biosynthesis	5	1	7.2	4.2E-03
Pentose phosphate pathway	18	1	6.0	1.7E-02
Glutamate metabolism	18	5	5.7	1.8E-02
Glutathione metabolism	10	6	4.2	1.9E-02

3.5.5. The impact of metformin on the metabolome of THLE-2 cells cultivated at a physiological glucose concentration

Metformin treatment of THLE-2 cells, cultivated at a physiological glucose concentration, significantly altered a number of cellular metabolite levels. Especially, metabolites belonging to the acylcarnitine metabolism were found to be strongly affected. Further, the levels of a number of phosphatidylcholines and amino acids, such as aspartate and glycine, were found to be significantly changed (**Table S-5**). The mitochondrial electron transport chain, the glycolysis/gluconeogenesis pathways, the TCA and the glucose-alanine cycle were found to be significantly affected by metformin treatment (**Table 27**). In addition, also the ketone body metabolism, ammonia recycling, the malate-aspartate shuttle and prostacyclin-associated signaling were among the significant hits of the pathway enrichment analysis.

Table 27: Enriched pathways of THLE-2 cells, cultivated at a physiological glucose concentration, and treated with metformin.
THLE-2 cells, cultivated at a physiological glucose concentration, were either treated with vehicle or with 2 mM metformin. Then, non-targeted metabolomics was performed. The table shows the results of the enrichment analysis.

Enrichment analysis

Pathway	Total number of compounds	Hits	Fold enrichment	p-value (Benjamini-Hochberg adjusted)
Ketone body metabolism	10	4	4.7	1.0E-03
Malate-aspartate shuttle	8	3	5.9	1.0E-03
Citric acid cycle	23	9	5.0	1.7E-03
Glycolysis	21	4	5.4	2.0E-03
Gluconeogenesis	27	4	5.4	2.0E-03
Mitochondrial electron transport chain	15	4	5.4	2.0E-03
Glucose-alanine cycle	12	4	4.5	2.4E-03
Ammonia recycling	18	8	3.2	1.5E-02
Intracellular signaling through prostacyclin receptor and prostacyclin	6	2	4.2	4.9E-02

3.5.6. The impact of metformin on the metabolome of Hep G2 cells cultivated at a physiological glucose concentration

Metformin treatment vastly altered the metabolome of hepatoma cells. A very broad spectrum of metabolites and metabolite sums were found to be significantly changed. These results indicated changes in the glucose, phosphatidylcholine and acylcarnitine metabolism, changes in the hydroxylation status of lipids, and changes in the amino acid and polyamine as

well as sphingomyelin metabolism as measured by targeted metabolomics. In addition, based on the non-targeted metabolomics data set, a number of pathways were found to be significantly altered. Next to an alteration of the glucose metabolism and the electron transport chain, the pathway enrichment analysis (**Table 28**) revealed changes in RNA transcription, nucleotide sugar metabolism and protein biosynthesis. Further, the arginine and proline as well as the nicotinate and nicotinamide and the taurine and hypotaurine metabolism were significantly affected.

Table 28: Enriched pathways of Hep G2 cells cultivated, at a physiological glucose concentration, and treated with metformin.
Hep G2 cells, cultivated at a physiological glucose concentration, were either treated with vehicle or with 2 mM metformin. Then, non-targeted metabolomics was performed. The table shows the results of the enrichment analysis.

Enrichment analysis

Pathway	Total number of compounds	Hits	Fold enrichment	p-value (Benjamini-Hochberg adjusted)
Arginine and proline metabolism	26	6	9.6	7.9E-07
RNA transcription	9	6	4.6	2.4E-03
Nicotinate and nicotinamide metabolism	13	2	8.4	2.4E-03
Nucleotide sugars metabolism	9	1	8.4	2.4E-03
Starch and sucrose metabolism	14	1	8.4	2.4E-03
Protein biosynthesis	19	16	4.0	3.6E-03
Taurine and hypotaurine metabolism	7	3	6.3	7.3E-03
Glucose-alanine cycle	12	4	6.0	1.8E-02
Urea cycle	20	8	5.8	1.8E-02
Selenoamino acid metabolism	15	1	6.2	2.5E-02
Alanine metabolism	6	2	6.1	2.5E-02
Glycolysis	21	4	5.2	2.5E-02
Gluconeogenesis	27	4	5.2	2.5E-02
Mitochondrial electron transport chain	15	4	5.2	2.5E-02
Pentose phosphate pathway	18	1	6.0	2.5E-02
Malate-aspartate shuttle	8	3	5.0	2.5E-02
Ammonia recycling	18	8	3.5	4.3E-02

3.5.7. The impact of metformin on the metabolome of THLE-2 cells cultivated at a diabetic glucose concentration

Metformin treated THLE-2 cells, cultivated at high glucose conditions, exhibited a number of significant changes in their metabolite levels. Next to the hits listed in **Table 29**, acylcarnitines, amino acids and metabolites, belonging to the polyamine, the creatinine and the glutathione metabolism were found to be significantly altered. The enrichment analysis showed that in addition to the pathways, which were found to be regulated in metformin-treated THLE-2 cells, cultivated at a physiological glucose concentration (**Table 27**), a number of lipid associated pathways can be found among the significant hits (**Table 29**).

Table 29: Enriched pathways of THLE-2 cells, cultivated at a diabetic glucose concentration, and treated with metformin. THLE-2 cells, cultivated at a diabetic glucose concentration, were either treated with vehicle or with 2 mM metformin. Then, non-targeted metabolomics was performed. The table shows the results of the enrichment analysis.

Pathway	Total number of compounds	Hits	Fold enrichment	p-value (Benjamini-Hochberg adjusted)
Arginine and proline metabolism	26	6	6.2	9.5E-06
Ammonia recycling	18	8	5.2	1.4E-05
Malate-aspartate shuttle	8	3	7.6	1.4E-05
Phospholipid biosynthesis	19	3	5.9	3.9E-05
Glucose-alanine cycle	12	4	6.2	1.4E-04
RNA transcription	9	6	4.8	1.4E-04
Glycolysis	21	4	6.3	2.0E-04
Gluconeogenesis	27	4	6.3	2.0E-04
Mitochondrial electron transport chain	15	4	6.3	2.0E-04
Glutamate metabolism	18	5	6.1	4.6E-04
Citric acid cycle	23	9	5.7	1.4E-03
Oxidation of branched chain fatty acids	14	5	6.1	1.8E-03
Ketone body metabolism	10	4	5.9	1.8E-03
Glycine, serine and threonine metabolism	26	5	3.5	3.6E-03
Histidine metabolism	11	2	5.8	5.5E-03
β-oxidation of very long chain fatty acids	14	4	5.6	5.5E-03
Phenylacetate metabolism	4	1	7.0	7.3E-03
Betaine metabolism	10	3	4.3	1.2E-02
Urea cycle	20	8	3.0	1.3E-02
β-alanine metabolism	13	3	4.9	1.7E-02
Arachidonic acid metabolism	37	1	6.0	1.8E-02
Bile acid biosynthesis	49	2	4.4	2.0E-02
Butyrate metabolism	9	2	4.7	2.4E-02
Insulin signaling	19	3	4.5	2.4E-02
Nucleotide sugars metabolism	9	1	5.5	2.5E-02
Starch and sucrose metabolism	14	1	5.5	2.5E-02
Alanine metabolism	6	2	4.6	2.6E-02
Pyrimidine metabolism	36	10	2.8	3.1E-02
Fatty acid metabolism	29	3	3.3	3.6E-02
Methionine metabolism	24	8	2.4	4.3E-02
Alpha linolenic acid and linoleic acid metabolism	9	3	3.4	4.7E-02
Pantothenate and CoA biosynthesis	10	3	3.4	4.7E-02

3.5.8. The impact of metformin on the metabolome of Hep G2 cells cultivated at a diabetic glucose concentration

Metformin treatment of Hep G2 cells, cultivated in medium with a high glucose concentration, had a pronounced impact on the cellular metabolome. A broad range of acylcarnitines, sphingomyelins, phosphatidylcholines and amino acids were found to be significantly changed upon metformin treatment (**Table S-5** and **Table S-7**). In addition, the hydroxylation and desaturation status of some of the measured lipid species was significantly altered. The pathway enrichment analysis (**Table 30**) illustrates that the response vastly

differed from the one of metformin treated THLE-2 cells, cultivated at the same glucose concentration (section **3.5.7**). In addition, it differed from the data obtained for Hep G2 cells, cultivated at a physiological glucose concentration (section **3.5.6**).

Table 30: Enriched pathways of Hep G2 cells, cultivated at a diabetic glucose concentration, and treated with metformin. Hep G2 cells, cultivated at a diabetic glucose concentration, were either treated with vehicle or with 2 mM metformin. Then, non-targeted metabolomics was performed. The table shows the results of the enrichment analysis.

Enrichment analysis

Pathway	Total number of compounds	Hits	Fold enrichment	p-value (Benjamini-Hochberg adjusted)
Betaine metabolism	10	3	7.8	1.5E-05
Aspartate metabolism	12	3	8.1	1.5E-05
Pyrimidine metabolism	36	9	5.6	1.5E-05
Methionine metabolism	24	8	7.4	1.5E-05
Tryptophan metabolism	34	2	9.5	7.1E-05
Phenylalanine and tyrosine metabolism	13	2	9.4	7.1E-05
Histidine metabolism	11	2	9.3	7.3E-05
Protein biosynthesis	19	16	7.8	7.3E-05
Arginine and proline metabolism	26	6	8.1	1.3E-04
Glycine, serine and threonine metabolism	26	5	6.9	2.0E-04
Intracellular signaling through prostacyclin receptor and prostacyclin	6	2	6.3	2.0E-04
Ammonia recycling	18	8	6.9	5.7E-04
Pantothenate and CoA biosynthesis	10	3	5.7	3.2E-03
Riboflavin metabolism	9	2	6.1	3.5E-03
Glycerol phosphate shuttle	8	2	7.3	4.6E-03
Tyrosine metabolism	38	1	7.2	5.4E-03
Catecholamine biosynthesis	5	1	7.2	5.4E-03
Taurine and hypotaurine metabolism	7	3	5.4	6.9E-03
Sphingolipid metabolism	15	3	6.6	7.1E-03
Vitamin B6 metabolism	10	2	5.5	1.6E-02
Cysteine metabolism	8	2	6.0	1.8E-02
Malate-aspartate shuttle	8	3	4.8	2.1E-02
Glycolysis	21	4	4.8	2.2E-02
Gluconeogenesis	27	4	4.8	2.2E-02
Mitochondrial electron transport chain	15	4	4.8	2.2E-02
Biotin metabolism	4	1	5.5	2.5E-02
Bile acid biosynthesis	49	3	4.3	3.0E-02
Phenylacetate metabolism	4	1	5.0	3.7E-02
Glucose-alanine cycle	12	4	4.2	3.8E-02
Nucleotide sugars metabolism	9	1	4.7	4.4E-02
Starch and sucrose metabolism	14	1	4.7	4.4E-02
Citric acid cycle	23	9	3.1	4.7E-02

Outcome. The metabolic implications of glucose and metformin are vast and complex. Further, the response strongly depends on the assessed cell line and its metabolic features. The implications and potential consequences of those observations will be discussed in detail in section **4.3**.

Limitations and outlook. Next to the limitations, posed by the cell culture model in general, other parameters have to be addressed. Two major limitations, which have been mentioned earlier, are, of course, the drug concentration and the incubation time. In future, promising steps might be a proteomic approach and the elucidation of phosphorylation (enzymatic activation/inactivation) patterns. In addition, the interplay of glucose and metformin, in regard to T2D and cancer, should be addressed in a mouse model to obtain a more complete picture of the potential implications of this relationship in an *in vivo* setting.

4. Discussion

The aim of this study was to elucidate the hepatocellular metformin transport and action. Further, the understanding of the molecular mechanisms, defining the relationship between glucose and metformin, should be extended. The first step was the development, optimization, validation and implementation of methods for cell culture metabolomics and metformin quantification.

4.1 Method development, optimization, validation and implementation

Regarding method development, the aim was to establish a reliable, fast, robust and versatile protocol for cell culture metabolomics, which is applicable to a wide range of scientific questions.

A LC-MS/MS based metformin quantification method was developed, optimized, validated and implemented. A fluorometric DNA-based cell number determination method was developed, optimized, tested for suitability to its application to metabolomics studies, partially validated and established. The established cell harvesting and sample preparation protocol for targeted metabolomics [141] was further optimized and partially validated. Further, adaptions to the protocol were made to ensure its compatibility with the non-targeted metabolomics approach. The protocol for non-targeted metabolomics was optimized and its precision was assessed.

4.1.1. LC-MS/MS based metformin quantification method

The reliable quantification of metformin was one of the major prerequisites to elucidate hepatocellular metformin transport and action.

A number of different approaches for metformin quantification have been published [36], [38], [41], [181], [182]. The methods were either based on radioactivity [38], [41], HPLC [36], [222] or (LC-)MS [181], [182], [223]. These methods have been validated for and/or applied to a limited set of either murine, rat or human biofluids or tissues [36], [38], [41], [181], [182], [223]. However, as to my knowledge, a flexible, versatile, high-throughput feasible method for metformin quantification in cell homogenates, cell culture supernatants, murine tissues and biofluids and human serum and plasma has not yet been established.

The requirements, which had to be met by the method, where defined as follows:

- *Absolute quantification*: Absolute quantification allows for comparison of the results with databases and other publications, which is of crucial importance for mouse models and clinical trials.
- *Applicability to a wide range of matrices*: The method should allow for the comparison of metformin levels in different model systems (cell culture and mouse models) and clinical trials. In this study, the focus lies on cell homogenates and cell culture supernatants.

- *Compatibility with other analysis methods*: To minimize the need for co-culturing and increase the flexibility and precision of the experiments, the metformin quantification method should be compatible with various other analyses, namely, targeted metabolomics (Absolute*IDQ* p180 Kit and the Newborn screening kit), non-targeted metabolomics and DNA-based cell number determination.
- *Low sample volume*: The method should require as low a sample volume as possible to allow conducting multiple analyses (e.g., metabolomics) with the same sample.

Although radioactivity-based methods have successfully been applied to a number of matrices [38], [41], they had several disadvantages. First, the radioactivity of the labelled metformin might have an impact on the metabolome. Second, the compatibility with other analysis methods is not given. Further, an HPLC based approach suffers from low sensitivity [222]. Thus, a HPLC-MS/MS based approach was favored.

LC-MS based metformin quantification has proven to be an efficient approach and is already well established in literature, especially, if applied to human biofluids [181], [182], [223]–[225]. In this regard, Liu *et al.* showed that metformin quantification in human plasma could be reliably conducted using a very similar system (Shimadzu Prominence HPLC system coupled to a Sciex API 4000 triple quadrupole mass spectrometer) and applying ESI in positive ion mode [224]. In addition, the concept of measuring a quantifier and a qualifier has been successfully applied to metformin quantification in whole blood samples [225]. Not surprisingly, the same mass transitions (metformin: *m/z* 130/60 and 130/71, phenformin: *m/z* 206/60 and 206/105), as selected in this study, were chosen [225]. Further, phenformin has already been established as internal standard [182], [223]. In addition, the protein precipitation by acetonitrile, which had to be added in case of the cell culture supernatants (section **2.14**), has been successfully applied in diverse metformin quantification methods, focusing on human plasma [181], [182], [224]. Also, the applicability of reversed phased chromatography using a C18 column has been demonstrated for LC-MS based metformin quantification in human plasma [223]. Hence, an LC-ESI-MS/MS based metformin quantification method was developed and validated for cell homogenates and cell culture supernatants. As deuterated metformin (d6) was observed to be instable, if solved in water, the biguanide phenformin was used as internal standard. To increase the reliablitiy of the measurements, two MRMs were implemented for each, the analyte and the internal standard. To minimize portential matrix effects, the HPLC system was equipped with a C18 column. Further, to allow for a high throughput, the sample preparation procedure was kept as simple as possible.

This study showed that the developed and validated LC-MS/MS based method allows for the absolute quantification of metformin in cell homogenates and cell culture supernatants. Further, it is applicable to metabolomics samples and can be easily integrated into the workflow. It requires only a very low sample volume and is, in this regard, rather flexible, as only the dilution factors, and not the applied sample volumes, are fixed. In addition, a run time of 1.5 min and the very short sample preparation procedure render it high-throughput feasible. As listed in the results section, it meets the FDA [113] and EMA [111] criteria for

bioanalytical method validation in terms of precision and accuracy. However, the simple sample preparation procedure and the isocratic HPLC conditions also pose the major limitation. While proteins are precipitated in course of the sample preparation, other potentially interfering compounds (e.g., lipids) are not removed. Further, the isocratic methanolic HPLC conditions, in combination with a C18 column, are most likely not sufficient to retain polar compounds. Hence, the assay might be susceptible to matrix effects and each new matrix has to be throughoutly validated prior to analysis.

4.1.2. Fluorometric DNA based cell number determination method

The cultivation of cells under different conditions and the treatment with metformin and inhibitiors did have a pronounced impact on the cell number. Thus, for example, the significant reduction of the cell number, due to metformin treatment (**Figure 30**), would lead to erroneous data interpretation. If not adjusted for, the metabolomics analyses of samples with reduced cell numbers would not reflect the metabolic metformin response, but the impact of metformin on the cell number. Hence, a major prerequisite to derive reliable conclusions from inhibitor studies and cell culture metabolomics data was the development of a robust normalization procedure to account for the biological variation.

Basing the method on a reliable molecular marker is one of the most crucial prerequisites for establishing a reliable and robust method for the normalization of cell culture metabolomics data. MS-based markers such as the total signal of a metabolite class [226] or the total ion current [122] were ruled out, because they do not allow for the comparison of different cell lines. Silva *et al.* compared three different normalization approaches: DNA, protein and cell number [121]. The DNA concentration was identified as the most suitable approach. It showed a better correlation to cell number than the protein concentration. Interestingly, it also scored better than the cell number count itself as cell clumps can distort the counting, but do not impact the DNA quantification. However, the proposed DNA quantification procedure does include a labor intensive and very time consuming DNA extraction protocol [121]. This protocol would not have been applicable to studies with larger sample sizes (e.g., Elucidation of the impact of glucose and metformin on the hepatocellular metabolome), without introducing between-day and between-run effects. To account for these effects, additional quality control measures would have to be taken, which would further increase the sample size, time and costs and diminish the reliability of the results. Thus, DNA was chosen as the molecular marker. But a faster, more effective method had to be developed.

The method had to fulfill the following prerequisites:

- *Applicability to metabolomics samples*: To avoid co-culturing, the method should be applicable to the metabolomics samples (cell homogenates in organic solvent). Thereby, the compatibility with different metabolomics analyses and LC-MS/MS based metformin quantification would be ensured.
- *Absolute quantification*: The method should allow for the absolute quantification of the cell number.

- *Applicability to a wide range of cell lines*: The method should be applicable to a wide range of cell lines of different tissues and organisms of origin and with different culturing conditions and physical properties.
- *Low sample volume*: The required sample volume should be as low as possible.
- *Fast*: As some of the experiments of this study did contain higher sample numbers, the assay should be fast and work in a 96-well format.

For this method, the fluorescent, DNA selective Hoechst dye [185] was chosen. The method was established in a 96-well format, does not require any additional sample preparation steps and has an optimal sample volume of 20 µL (**Figure 6B**) and incubation time of 30 min (**Figure 5A**). Hence, the method is fast and easy to perform. It eliminates the need for co-culturing and DNA purification. Further, by using standard curves of the same cell line, the cell number can be determined, which allows for absolute quantification of the cell number of the sample and, consequently, offers the possibility to compare metabolomics data, obtained with different cell lines. However, if a standard curve of the same cell line is not available, the experimenter has to settle for relative quantification. The assay proved to be robust in regard to the methanol concentration of the sample and could be successfully applied to all tested cell lines, independent of the tissue and/or organism of origin. In addition, it requires an acceptable amount of sample. If necessary, the sample volume can be even further decreased with higher cell numbers. However, the relatively low precision, when applied in combination with scraping of adherent cells with methanolic extraction solvent, poses a limitation, which had to be taken into consideration during data evaluation. Further, if compounds, which induce alterations in the cellular DNA content, are applied, a normalization based on DNA might introduce a bias, if treated and non-treated cells are compared. This bias might be avoided by using standard curves of treated and non-treated cells for the cell number determination of the respective groups.

To assess, whether the method is suitable for the normalization of cell culture metabolomics data, two prerequesites had to be met: First, the DNA content had to linearly correlate with the cell number. Second, the cell number had to linearly correlate with the measured analytes. A linear correlation of the fluorometric singal to the cell number ($R^2 > 0.9$) was observed for all tested cell lines (**Figure 8**). In addition, the vast majority of analyzed metabolites above the LOD of all tested cell lines displayed a linear correlation to the cell number (**Table 17** and **Figure 9**). In conclusion, the developed and optimized DNA based cell number determination method presents a effective approach for the normalization of cell culture metabolomics data [117].

4.1.3. Optimization of cell harvest and sample preparation for cell culture metabolomics

Targeted metabolomics. The cell harvesting and sample preparation method, optimized by Dr. Anna Halama [141], was adapted and modified. The procedure used for targeted (and with further adaptions also for non-targeted) metabolomics is effective, flexible, fast and compatible with multiple methods (e.g. Absolute*IDQ* p150 and p180 Kits, Newborn

screening kit, non-targeted metabolomics and the LC-MS/MS based metformin quantification). Further, it allows for an implemented normalization step of the metabolomics sample (fluorometric DNA quantification for cell number determination). Therefore, the major focus of this study was not the optimization, but the validation. Hence, partial validation was performed. The tested parameters were: accuracy, precision and matrix effects.

The assay performed satisfactory in regard to accuracy and presistion. In detail, the precision was found to be strongly metabolite class dependent (**Table 18** and **Table 21**). However, the majority of metabolites displayed a CV of less than 20%. For 6 out of the 7 tested amino acids, the accuracy was found to be within the range of 80%-120%, with phenylalanine being the only exception (123%). Further, excellent matrix factors were observed for the analyte peak areas (1.00 - 1.14). However, a major drawback was the analyte concentration dependent, non-satisfactory performance of the internal standards. The matrix factors of the internal standards ranged from 0.68 to 0.90, which led to in part strongly elevated IS-normalized matrix factors. In accordance with this observation, the precision of the analyte signals did slightly outperform the precision of the IS-normalized analyte concentrations. These results indicate the presence of matrix effects.

Non-targeted metabolomics. Since the metabolite set, which is measured with a non-targeted metabolomics approach, is (per definition) not pre-defined [103], the analyte set cannot be validated in full. However, the design of the non-targeted metabolomics approach allows for stringent quality control (e.g., a number of internal standards to monitor extraction efficiency and the systems performance as well as multiple reference matrices). In course of this study, the applicability of the modified cell harvesting method was tested, the extraction solvent composition was optimized and the precision of the MS analysis as well as the combination of the MS analysis with the harvesting and sample preparation procedure was assessed.

Based on the obtained metabolite patterns (**Figure 13**), and taking practical aspects such as storage and handling into consideration, 80% methanol, spiked with internal standards for extraction monitoring, was chosen as extraction solvent. However, the methanol content can be adjusted to the polarity of the metabolite classes of interest. Not surprisingly, the precision of targeted metabolomics outperformed the precision of non-targeted metabolomics. Fruther, the precision of non-targeted cell culture metabolomics analysis was found to metabolite class and cell line dependent.

A major bottleneck arises from the fact that the metabolite set cannot be fully validated, as it is not known prior to the analysis. Hence, it is possible that patters, arising from an analytical feature (e.g., matrix effects, signal intensities outside the linear range), might be treated as a biological observation or mask metabolic alterations. To avoid erroneous data interpretation, a targeted approach should be applied to verify the results, obtained with non-targeted metabolomics. Further, taking into consideration that the metabolite concentrations linearly correlate with the cell number, the risk of a misinterpretation of the data, obtained with non-targeted metabolomics, might be reduced by analyzing standard curves of the cell lines

of interest, containing different cell numbers. Since this approach would allow for recording the linear range of a broad spectrum of metabolites in a cell line specific manner.

Conclusions. The lack of standardized methods still poses one of the major challenges in metabolomics [110]. To address this bottleneck with cell culture metabolomics, a number of methods have been developed, optimized and (partially) validated in course of this study. These methods allow for the coverage of a very broad range of analytes and, thereby, have the potential to aid the comprehensive understanding of the cellular metabolism. They are applicable to a wide range of cell lines and experimental setups. Their robustness and inter-compatibility allow for obtaining the maximum of information out of a single experiment.

4.2. Looking for the needle in the haystack – hepatocellular metformin transport

Considering, that the varying expression and performance of metformin transporters have been closely linked to altered metformin pharmacokinetics and action [47], [61], [194], [195], [227]–[229], the identification and characterization of metformin transporters has emerged as a vibrant field within recent years [43], [45], [48], [56]. Hence, in course of this project, the hepatocellular metformin uptake has been characterized, and the impact of metformin transporters has been addressed in a cell culture based setting. In this context, the questions which had to be addressed were: Whether active and passive components contribute to the human metformin transport on a cellular level, and which transporters, known to be capable of metformin translocation, might be involved in the hepatocellular transport of the drug.

Consequently, it was first evaluated, whether active and passive transport mechanisms contribute to the hepatocellular metformin transport. The coexistence of transporter-associated and passive transport of drugs is already well known [230]. This coexistence of has been previously suggested in context with the absorption of metformin by the intestine [36]. Further, Sogame *et al.* showed, that the metformin transport in rat hepatocytes, indeed, contains a saturable and a non-saturable component [40]. In this study, the metformin transport curve of Hep G2 cells was found to display similar characteristics (**Figure 20**) as the one observed for rat hepatocytes [40]. Modeling the metformin transport of this cell line (**Figure 20**) and inhibitor studies using quinidine (**Figure 22**), verified that *in vitro* the transport of the drug in human hepatocytes, indeed, possesses a saturable and a non-saturable component. Passive transport is non-saturable [230]. In contrast to passive transport, one of the major characteristics of carrier-mediated transport is its saturability [230]. Thus, the saturable component might be indicative of an active carrier-mediated metformin transport.

However, in the context of the dual nature of metformin uptake, the physiological concentration range should be taken into consideration. In mice, orally treated with 50 mg/kg metformin, the metformin concentrations of plasma as well as the majority of tissues was found to be within the µM range [41]. Only the proximal jejunum, the jejunal-ileal junction and the distal ileum exhibited concentrations within the mM range [41]. The maximum plasma concentration in the hepatic portal vein was found to be 51.7 µM ± 5.4 µM for normal and 61.5 µM ± 8.0 µM for diabetic mice. The maximum hepatic metformin concentration was 182 µM ± 22 µM and 282 µM ± 80 µM respectively [41]. When comparing the drug dosage of the mice [41] to the daily dosages of patients (Bundesinstitut für Arzneimittel. Gebrauchsinformation: Information für Anwender, Glycophage® 500 mg Filmtabletten (2015). [196]), the applied metformin concentration of 50 mg/kg [41] would be within the upper range or, depending on body weight and exact dosage, even exceed the range. Consequently, in human hepatocytes, metformin transport might be driven by active transport mechanisms. This hypothesis is supported by the data obtained with the inhibitor studies with ASP^+ and quinidine (**Figure 21** and **Figure 22**), which indicate that the active transport is the driving force of human hepatocellular metformin transport at physiological concentrations. However, any hypotheses, regarding human metformin pharmacokinetics, have to be considered with care. First, the potential metformin concentration range, the human liver might be subjected to, was derived from a mouse model. Second, the inhibitor studies were

conducted in a closely defined cell culture setting. Interestingly, the inhibitors ASP^+ and quinidine could not completely abolish hepatocellular metformin uptake. Quinidine inhibited more than 80% of the hepatocellular metformin uptake at a physiological concentration (**Figure 22**). There might be three possible explanations for the observed residual metformin uptake. First, this residual metformin uptake might reflect the passive transport rates at physiological conditions. Indeed, by increasing the metformin concentration to 2 mM, the relative intracellular metformin level of quinidine treated Hep G2 cells was elevated to 60% of the controls. Second, the residual metformin uptake might also be indicative of a yet unknown transporter with a very high IC_{50} value for quinidine mediated inhibition of metformin uptake. Third, it should be noted that some of the quinidine did precipitated, after being spiked into the medium. In course of the incubation time, the drug dissolved again. On the contrary, metformin is well soluble in cell culture medium, at the applied concentrations. This could offer another explanation for the observed residual metformin uptake, as the quinidine concentration might not have been 1 mM during the complete duration of the incubation time. Hence, it might be possible that metformin was taken up, before a quinidine concentration, sufficient to block all metformin transporters, was reached. Consequently, based on these observations, the non-saturable component might be overestimated. This possibility should be tested by preconditioning the cells with quinidine, before they are treated with metformin.

For Hep G2 cells, the K_M value of metformin uptake was found to be 280 µM, which is close to the K_M value of 404 µM, reported for rat hepatocytes [40]. However, both K_M values have to be considered with great care. First, no saturation was reached, which might impede the reliability of the estimation of the kinetic parameter. Second, intact Hep G2 cells are a complex system, expressing a multitude of transporters (**Figure 23** - **Figure 37**), capable of the import and export of metformin [42]–[45], [48], [56].

Potential candidates, which have been reported to be capable of metformin transport, were OCT1, OCT2 [55], [56], OCT3 [56], [57], OCTN1 [45], PMAT [56], SERT [56] and THTR-2 [48]. In this context, OCT1 has already been established as a key mediator in hepatocellular metformin transport [199] and strongly dominates the expression profile of hepatic metformin trnasporters (**Table 31**). In addition, the crucial role of OCT2 and OCT3 in metformin transport has been well documented [55], [61], [229]. However, OCT2 is predominantly linked to renal metformin transport [55] and has undetectable [61] or low expression levels in the liver [62]. OCT2 was also not expressed in the tested hepatic cell lines (**Figure 23**). The very low expression of cation transporters, observed in this study, is in accordance with previously published data on Hep G2 cells [62]. In addition, the pattern (expression of OCT1 and OCT3, no expression of OCT2) reflects the hepatic organic cation transporter expression pattern [61]. Regarding the fact, that hepatic OCT1 expression exceeds the expression of the other potential metformin transporters [62], [63] (**Table 31**), any observed metformin transport patterns in cells, showing high OCT1 expression levels, will, by default, be dominated by this, already well characterized, transporter. Hence, Hep G2 cells, with their very low to not detectable OCT expression levels [62] (**Figure 23**), is the ideal model system for the elucidation of the impact of, not yet established, hepatic

metformin transporters. In addition, based on the inhibitor studies, the participation of OCT1 in the metformin uptake of Hep G2 cells could be ruled out. Whether the significant decrease in intracellular metformin levels, upon treatment with 50 µM paroxetine (**Table 25**), can be attributed to an inhibition of OCT3 or PMAT cannot be elucidated with inhibitor studies. First, the IC_{50} values of these transporters for paroxetine-dependent inhibition of cation transport are too similar (OCT3: 6.4 µM ± 1.3 µM for metformin [56], PMAT: 22.46 µM ± 5.68 µM for MPP^+ [206]) to unequivocally determine which transporter might be the driving force. Second, there is no selective PMAT inhibitor yet available [56]. Third, as to my knowledge, there is currently no reported OCT3 inhibitor, for which it was shown, that it is not affecting any of the other (potential) metformin transporters. Only knock-down or knock-out studies can give an unequivocal answer to this question.

Table 31: List of relative hepatic expression levels of reported human metformin transporters.
The hepatic relative expression levels, displayed in this table, were taken from Nishimura *et al.* [63].

Transporter	Gene	Relative expression level
OCT1	*SLC22A1*	2.23
OCT2	*SLC22A2*	$3.67\ 10^{-5}$
OCT3	*SLC22A3*	0.124
OCTN1	*SLC22A4*	2.02×10^{-4}
PMAT	*SLC29A4*	$5.30\ 10^{-5}$
SERT	*SLC6A4*	2.56×10^{-5}
THTR-2	*SLC19A3*	NA
MATE1	*SLC47A1*	NA
MATE2-K	*SLC47A2*	NA

The inhibitor studies with carnitine and acetylcarnitine hinted at OCTN1 being a potential candidate for follow-up experiments. However, due to the polyspecificity of a number of transporters, involved in the metformin transport [49], [50], and the fact that the complete substrate spectrum and/or affinities of them might not yet be known, no final statement can be made. For example, the K_M for the metformin transport of OCTN1 has not yet been reported (2015) [48]. Again, to verify the implication of the OCTN1 transporter in the human hepatocellular metformin transport, the gene has to be knocked-down or knocked-out.

Another transporter, which is capable of transporting metformin [53] and was found to be expressed in the liver [68] and in hepatic cell lines (**Figure 26**), is MATE1. The observed expression profile in human cell lines (**Figure 26**) is in accordance with the fact, that MATE1 is primarily expressed in the liver and kidney [68]. The treatment of Hep G2 cells with the MATE1 inhibitor cimetidine [67] did not induce significant alterations in the intracellular metformin levels, indicating that MATE1 might not partake in the metformin transport of Hep G2 cells. However, this hypothesis should be regarded with care, because the used cimetidine concentration was based on the suggestion made by Han *et al.* [56]. The authors based the selection of their recommended concentration on the K_I (which they refer to as IC_{50}) of MATE1 for TEA transport [56], published by Tsuda *et al.* 2009 [67], and not on the IC_{50} of cimetidine for MATE1 dependent metformin transport, which has, as to my knowledge, not yet been reported. The lack of response might also originate from choosing too low an inhibitor concentration. However, by increasing the cimetidine concentration, the

selectivity of the inhibitor is lost, which is illustrated by the IC_{50} values of cimetidine mediated metformin transport by OCT1-3 (range: 9.8 - 20.9 µM) [56].

One transporter, which remains to be tested for its implication in the hepatocellular metformin transport, is the newly identified THTR-2 [48], which was found to be expressed in the human liver [48] and the tested hepatic cell lines (**Figure 27**). However, conducting inhibitor studies might present a challenge as the model substrate, thiamine, is also transported by MATE1 [231] and OCT1 [232]. Hence, either a selective inhibitor has to be identified or knock-down or knock-out studies have to be conducted.

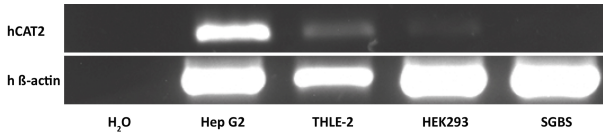

Figure 37: Expression of the cationic amino acid transporter 2 (CAT2) in human cell lines.

Most likely the set of metformin transporters is not yet complete. As early as 1992, Khan *et al.* established a link between metformin transport and the cationic amino acids arginine and lysine [233]. In detail, they observed increased drug levels in arginine and lysine treated NIH-3T3 cells [233]. In accordance, significantly elevated intracellular metformin levels (Kruskal-Wallis test: p-value: 0.031, n = 5 - 6) were detected in arginine treated Hep G2 cells (**Table 25**). These observations hint at a potential role of a cationic amino acid transporter in metformin transport. One potential candidate might be the cationic amino acid transporter 2 (CAT2), which was found to be expressed in both hepatic cell lines (**Figure 37**). Interestingly, the potential link between metformin and cationic amino acid transport [233] as well as the broad overlapping substrate spectra of the reported metformin transporters [231], open up the question whether the impact of metformin on intracellular levels of compounds, with a relatively high structural similarity, is a primary effect - due to its impact on their transport - or a secondary effect of the drug.

Up to this point, the major focus of the search for potential candidates, involved in the hepatocellular metformin transport, was on transporters, which capability for metformin transport has already been reported. However, considering the fact that quite a number of those transporters have been shown to be rather unspecific in their substrate preferences [56], [231] and exhibit relatively low affinities for the drug (**Table 1**), the viewpoint should be broadened. Consequently, the next step should be the identification of not yet reported metformin transporters. This task, however, poses a complex challenge. Limiting the number of potential candidates to a subset, which can be screened by overexpression and knock-down or knock-out experiments, might be the major bottleneck. Interestingly, all reported metformin transporters belong to the SLC family (**Table 31**). Hence, the SLC family might be a suitable starting point. However, the human SLC family consists of more than 300 transporters [234]. Further, their mutual affiliation to this family might be the only feature they have in common. Among the set of reported metformin transporters are uni-, sym- as well as antiporters with very different transport characteristics and expression patterns [50]. Hence, it is not possible to choose potential candidates on basis of their transport type or transport characteristics. Deriving conclusions from evolutionary analyses and classifications might be considered as an alternative approach. However, this approach could be misleading. For example, the SLC22 transporter family comprises of two major clades, the organic cation

transporters (OCT clade) and the organic anion transporters (OAT clade). OCT1-3 and OCTN1-2 belong to two distinct subclades within the major OCT clade [235]. Interestingly, OCT1-3 and OCTN1 have been reported to be capable of metformin transport [45], [55]–[58]. OCTN2 belongs to the same subclade as OCTN1[235] and has a higher sequence similarity to OCTN1 than OCTN1 has to the metformin transporters OCT1-3 [50]. Although OCTN1 has been reported to be capable of metformin transport [45], OCTN2 is not [56]. A, maybe more promising, approach might be the substrate focused one, taken by Liang *et al.* [48]. In 2014, Chen *et al.* showed that OCT1 is a high-capacity transporter for thiamine and, consequently, metformin can serve as a competitive inhibitor for thiamine uptake [232]. Based on this observation, Liang *et al.* hypothesized that thiamine transporters should be capable of metformin transport [48]. Indeed, this assumption did hold true for the thiamine transporter THTR-2. Although THTR-2 proved to be capable of metformin transport, THTR-1 was not [48]. Next to the overlap in the substrate spectra of transporters, the similarity of the substrates to metformin might be worth considering. If the Tanimoto coefficients of more than 41,000 compounds, derived from the HMDB (http://www.hmdb.ca/ [163]–[165], accession date: 03/17/2016), were calculated, a number of interesting candidates were found among the top hits (e.g., top 1%: creatinine, arginine, asymmetric dimethylarginine (ADMA); top 5%: serotonin and thiamine; top 20%: carnitine and acetylcarnitine). Creatinine is a weak organic cation, which, at a physiological pH, exists predominantly in its monoprotonated form. It is transported by OCT2. Interestingly, also the organic anion transporter OAT3 has been reported to be capable of creatinine transport [236]. ADMA and arginine are substrates of OCT2, CAT2 and MATE1[237] and have been linked to metformin transport and action [233], [238]. However, although these substrate candidates were among the top ranking ones, they still had to be picked from a larger set of compounds on basis of *a priori* knowledge, hence, rendering this approach ineffective. A major limitation of this approach is the fact, that the interaction of the transported molecule and the transporter is neglected. In this context, docking studies might be feasible. However, the experimentally verified structural information on human SLC transporters is still scarce [234]. But, high-resolution structures of prokaryotic and eukaryotic homologues are available and might be used for hypothesis generation [234].

Conclusions. To expand our understanding of the human hepatocellular metformin transport a cell culture based approach using the human hepatoma cell line Hep G2 was chosen. The first step of this study was the characterization of the metformin transport of Hep G2 cells. Metformin was taken up via active and passive transport mechanisms. At a physiological concentration, the metformin uptake was dominated by transporters. Consequently, the expression of reported metformin transporters in Hep G2 cells was tested and inhibitor studies were conducted to assess their potential impact on the cellular metformin uptake. In case of Hep G2 cells a participation of OCT1 in the uptake of the drug could be ruled out. However, OCTN1, PMAT and THTR-2 might be promising candidates for continuative studies.

4.3. Elucidation of the impact of glucose and metformin on the cellular metabolome

The aim of this study was the elucidation of the impact of the glucose concentration and metformin treatment on the hepatocellular metabolism. The human liver cell line THLE-2 and the human hepatoma cell line Hep G2 served as model systems. To elucidate the impact of glucose on the cellular metabolism and metformin action, they were cultivated at a physiological and a diabetic glucose concentration. Then, they were treated with metformin and metabolomics analyses were performed. Hence, the cell lines, conditions and analyses, applied in this study, allow for addressing the following questions:

- How does the physiological and diabetic glucose concentration affect the hepatocellular metabolism?
- How does metformin impact the hepatocellular metabolism at physiological and diabetic glucose concentrations?
- What are the differences in the metabolism of liver cells and hepatoma cells?
- Does the impact of the glucose concentration on the cellular metabolism differ when liver cells are compared to hepatoma cells?
- What are the metabolic mechanisms behind the beneficial effect of metformin on the risk and treatment of the hepatocellular carcinoma [93], [95]?

4.3.1. Glucose - the metabolic trigger? The impact of the glucose concentration on the hepatocellular metabolism

To assess the impact of the glucose concentration on the hepatocellular metabolome, THLE-2 and Hep G2 cells were cultivated at physiological (6 mM) and elevated (11 mM) glucose conditions. Then, targeted metabolomics of the cell homogenates and cell culture supernatants was performed. In addition, non-targeted metabolomics of the cell homogenates was done.

THLE-2. Interestingly, THLE-2 cells displayed almost no glucose related response. In detail, only a single parameter was found to be significantly affected. The sum of hexoses (H1) was found to be increased in cells, cultivated at an elevated glucose concentration (**Table S-5**). This observation is in accordance with our understanding of the hepatic glucose response. Ishida *et al.* showed that in dogs the oral administration of glucose correlates with an elevated net hepatic glucose uptake [239]. Nonetheless, the observation made in this study has to be interpreted with care, because the levels of H1 were below the LOD in the measured cell homogenates (**Table S-3**). However, the absence of a significant metabolic change in this cell line might indicate a robustness of the metabolic state of liver cells towards altered glucose availability.

Hep G2. In case of the hepatocellular carcinoma cell line Hep G2, metabolic changes upon increasing the glucose concentration were observed in different areas of the metabolome. As to be expected, the glucose metabolism (glycolysis, gluconeogenesis and the glucose-alanine cycle) as well as the mitochondrial transport chain were found to be significantly affected, if

the exogenous glucose level was increased (**Table 26**). However, the metabolites, on which the pathway enrichment analysis was based, were the same for the glycolysis, the gluconeogenesis and the mitochondrial transport chain, namely, ATP, ADP, NAD and NADH. In addition, it should be taken into account that these metabolic intermediates partake in a large spectrum of reactions [75], [240], [241] and, hence, cannot be regarded as unique markers for the respective pathways. However, including the results of the targeted metabolomics analysis leads to a more distinctive picture. The level of alanine, one of the major amino acid precursors for hepatic gluconeogenesis [242], was found to be significantly increased, which indicates that alanine is not metabolized to glucose. This might strengthen the hypothesis of a glucose-dependent impairment of the hepatic gluconeogenesis in cancer cells. In summary, for Hep G2 cells, the elevation of the extracellular glucose levels correlates with a decreased glucose anabolism.

Further, it should be noted that citrate and malate, which are intermediates of the TCA [241], were found to be significantly elevated, which might indicate an increased flux through the TCA. In addition, the branched chain amino acids (BCAA) valine, leucine and isoleucine were found to be significantly decreased. BCAA degradation relies on a complex interplay of enzymatic reactions, taking place in liver and muscle tissue [243]. Decreased serum BCAA levels have been linked to cirrhosis and the hepatocellular carcinoma [244]. Further, female Wistar rats, bearing the Walker-256 carcinosarcoma, displayed elevated levels of the branched-chain amino acid transaminase [243], which catalyzes the first step of BCAA degradation [243], [245], and branched-chain 2-oxo acid dehydrogenase [243], which catalyzes the second step [243], [245], in liver and muscle tissue [243]. In accordance, Buffalo strain rats with the Morris hepatoma 5123tc showed elevated leucine oxidation [246]. This indicates that the tumor-associated elevation of the BCAA degradation might drain the BCAA pool. Hence, the observed decrease in hepatocellular BCAA levels upon elevation of the exogenous glucose concentration might reflect a glucose-dependent progression of cancer-assossiated metabolic traits. However, whether this hypothesis holds true has to be tested *in vivo*. Further, the applied cell culture based setting does not allow to mimick the interaction between organs and, hence, the observations regarding the BCAA metabolism have to be handled with care.

Next, protein synthesis scored among the significant hits in the pathway enrichment analysis. This observation is explained by a decrease of the majority of amino acids levels (in part significantly) upon increased glucose levels. However, no significant changes of amino acid levels were observed in cell culture media. In conclusion, this indicates a change of protein metabolism and not of amino acid uptake and excretion. Based on these metabolomics data sets, it is impossible to unambiguously distinguish, whether, protein synthesis is elevated, or protein degradation is diminished. Nonetheless, the metabolic consequences can be tracked, and light might be shed on the dimension of the metabolic implications of elevated glucose levels. Protein- and subsequently amino acid degradation lead to the production of inorganic ammonia, which is then further metabolized to urea [247]. The recycling of ammonia as well as the urea cycle were found to be significantly affected (**Figure 38**). In this context, the glutamate levels have to be considered. The transamination of amino acids results in the

generation of glutamate and an α-keto acid [248]. Glutamate undergoes an oxidative deamination, which is catalyzed by the glutamate dehydrogenase and generates α-ketoglutarate and ammonia [248]. Ammonia serves as substrate for the synthesis of carbamoyl phosphate, an urea cycle intermediate, by the mitochondrial carbamyl phosphate synthase I (CPS I) [248]. In addition, glutamate can be converted to N-acetylglutamate, which acts as an allosteric activator of the CPS I [249]. Glutamate was found to be significantly decreased. A decrease of N-acetylglutamate was also present, but was not significant. Even more interestingly, the levels of the intermediates of the urea cycle, covered by the metabolomics analyses, were found to be downregulated. The changes in aspartate, ornithine and citrulline levels were significant. Arginine was also found to be downregulated, but not significantly so. However, creatine, which is synthetizised from glycine (significantly downregulated) and arginine [250], was found to be significantly downregulated. Zhao *et al.* proposed that under low glucose conditions, cells would rely on amino acids for energy production, which should result in an increased urea cycle activity [251]. In addition, they suggested that under high glucose conditions, amino acid metabolization for energy production and gluconeogenesis would be inhibited. However, they focused on the acetylation-mediated regulation of the involved enzymes [251].

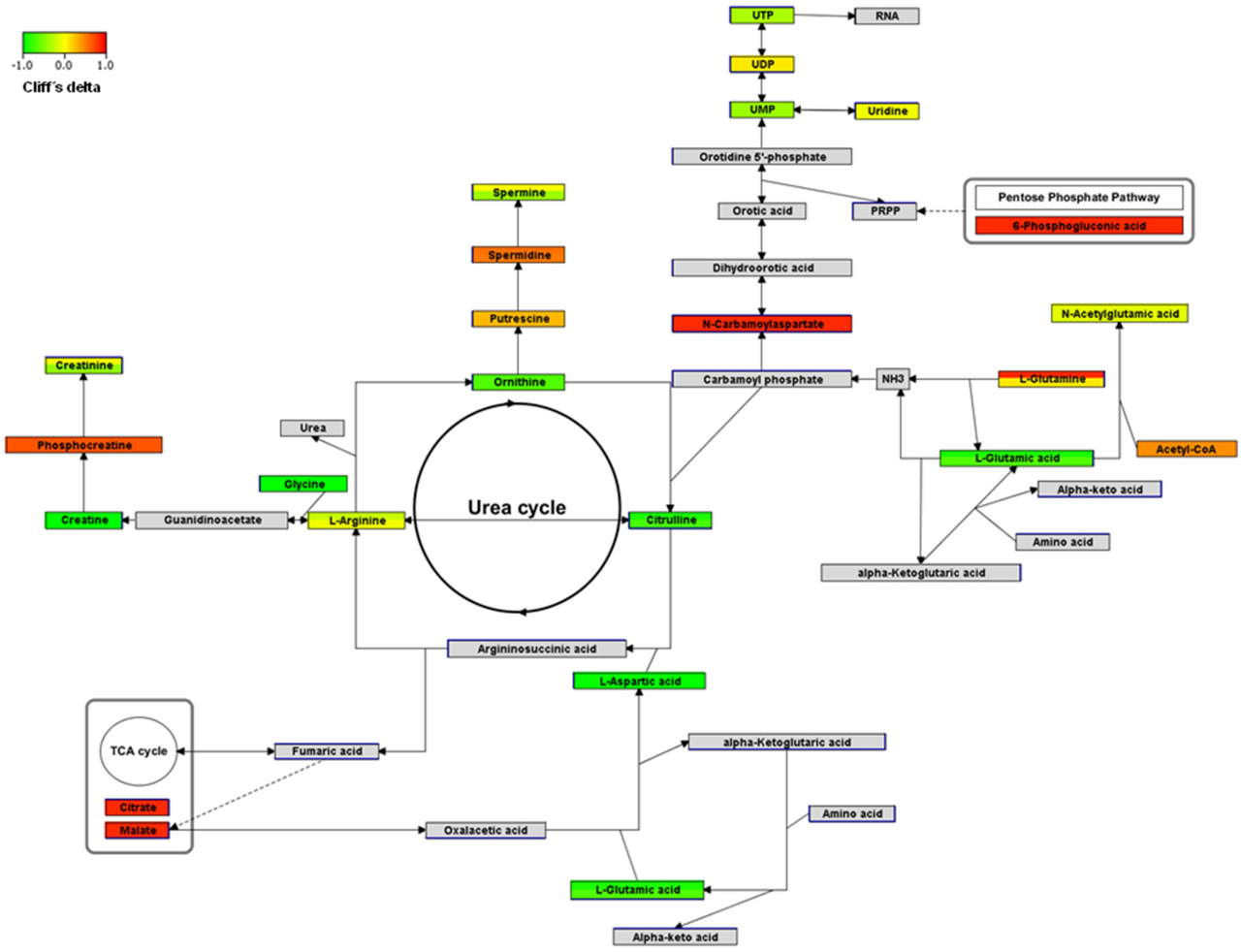

Figure 38: Impact of the glucose concentration on the urea cycle and associated pathways of Hep G2 cells.
The figure shows a schematic overview of the urea cycle and selected associated pathways. Regulations of measured metabolites are represented by the effect size (Cliff´s delta). In case the metabolite was present in the non-targeted and the

targeted dataset, the respective box is horizontally divided (e.g., arginine, creatinine, glutamine, glutamate, citrulline, spermidine and spermine). The upper part represents the effect size, obtained with non-targeted, and the lower part, the one, obtained with targeted metabolomics analyses. Although, the extent of the effect size differed with glutamine, the orientation of the dysregulation (up) was the same in both datasets.
This pathway was designed on the basis of information provided by KEGG [252], [253] and Voet *et al.* [158].

The glutamate metabolism not only represents a link between the amino acid and carbohydrate metabolism [249], but is also related to the glutathione household and the γ-glutamyl cycle [254]. Further, the glutathione metabolism is associated with the folate and the betaine/methionine metabolism (one-carbon metabolism), which in turn is linked to the pyrimidine metabolism [255]. All of these pathways were identified as hits, either being significantly affected pathways (**Table 26**), or their respective metabolites turned out to be significantly altered (**Figure 39**). The pyrimidine metabolism was identified as top hit among the regulated pathways. Pyrimidine synthesis is a prerequisite for cellular proliferation [256]. Inhibitor (N-(phosphonacetyl)-L-aspartate) induced pyrimidine deprivation was shown to correlate with growth inhibition [256]. Further, it could be associated with an antitumor activity in mice with colonic tumor transplants [256]. Analyzing the dysregulation of the pyrimidine metabolism intermediates, correlating with elevated glucose levels, it becomes clear that the first steps of this pathway are upregulated. Namely, glutamine, an amino acid closely linked to cancer [257], and N-carbamoylaspartate were found to be significantly increased. In this context, also 6-phosphogluconate, a pentose phosphate pathway intermediate [258], was found to be significantly elevated. 6-Phosphogluconate is converted to ribose-5-phosphate via ribulose-5-phosphate [258]. Ribose-5-phosphate is the substrate of phosphoribosyl pyrophosphate synthetase, which synthetizes phosphoribosyl pyrophosphate (PRPP) [259]. Phosphoribosyl pyrophosphate in turn is an activator of the cytosolic carbamyl phosphate synthase II (CPS II), which catalyzes the metabolization of glutamine to carbamoyl phosphate [260]. However, interestingly, uridine, and its measured derivatives as well as cytidine and its measured derivatives, were not found to be significantly affected. But, UMP and UTP exhibited negative effect sizes. Cytosine, uracil and thymine and its derivatives were not covered by the metabolomics analyses.

Focussing on the one-carbon metabolism, glycine was found to be significantly decreased. Decreased glycine and lyso-phsophatidylcholine 18:2 levels have been shown to be associated with T2D development [108]. However, it should be noted, that the decrease in lyso-phosphatidylcholine C18:2 levels in Hep G2 cells with high glucose was not significant in the targeted metabolomics dataset. Interestingly, it was found to be significantly regulated in the non-targeted metabolomics dataset (1-linoleyl-GPC 18:2). This might be accounted for by the differences in analysis. With targeted metabolomics, this metabolite was detected in FIA mode, whereas, with non-targeted metabolomics, an additional LC separation step was performed.

Serine levels were not significantly altered. The measured intermediates of the methionine/betaine metabolism displayed decreased levels (methionine, betaine, S-adenosylhomocystein (SAH)). Although, the downregulations of the reduced (GSH) and oxidized (GSSG) glutathione levels were not significant, the reduction of the levels of a number of γ-glutamyl amino acids was significant. Taken together with the significant

downregulation of glutamate and 5-oxoproline, this indicates a downregulation of the γ-glutamyl cycle (**Figure 39**).

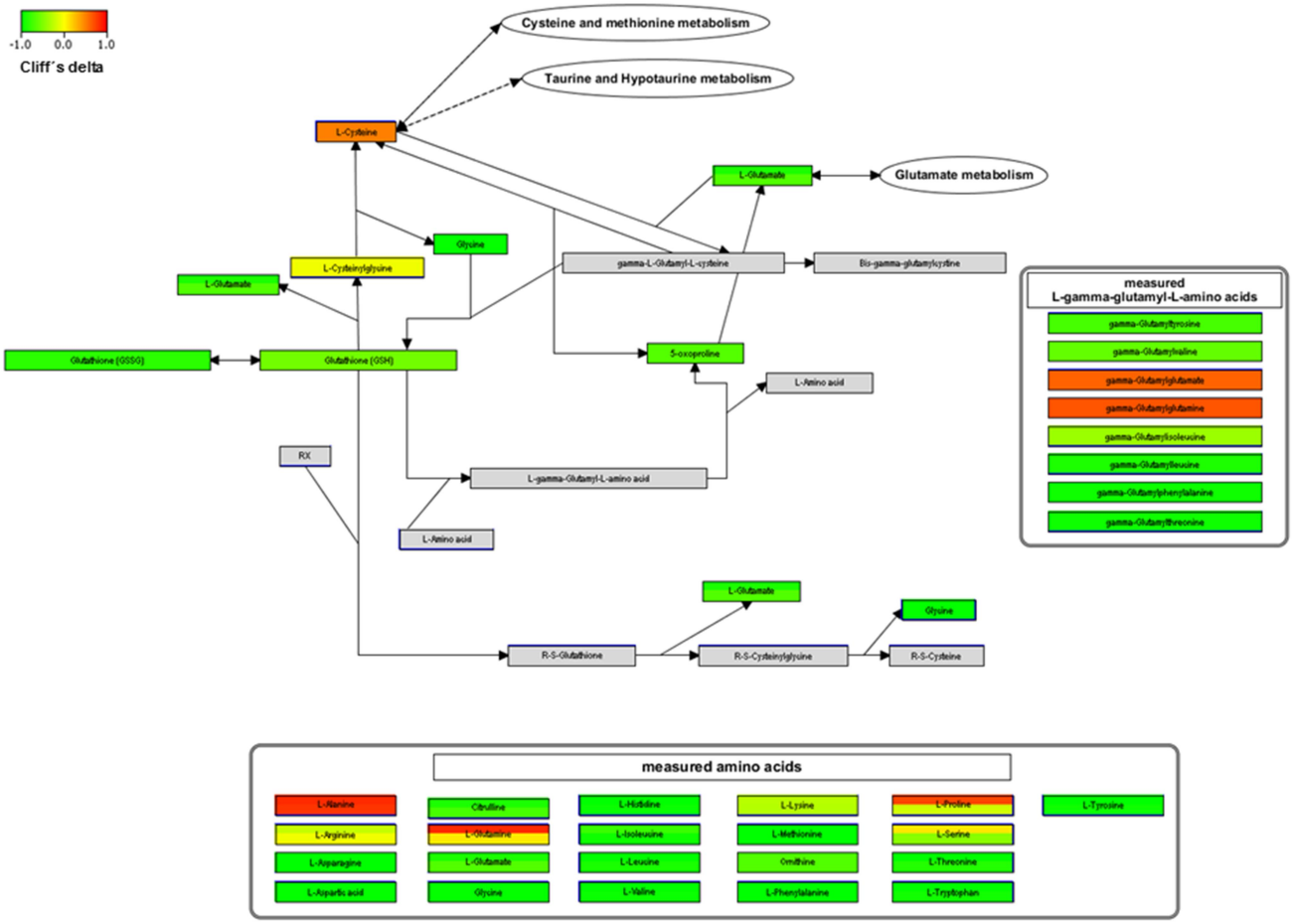

Figure 39: Impact of the glucose concentration on the glutathione metabolism and associated pathways and metabolites of Hep G2 cells.
The figure shows a schematic overview of the glutathione metabolism and selected associated pathways and metabolites. Regulations of measured metabolites are represented by the effect size (Cliff´s delta). In case the metabolite was present in the non-targeted and the targeted dataset, the respective box is horizontally parted. The upper part represents the effect size, obtained with non-targeted, the lower, the one, obtained with targeted metabolomics analysis. In case of proline, the orientation of the dysregulation did differ between the targeted and the non-targeted dataset. Hence, it was not considered for the biological interpretation of the results.
This pathway was designed on basis of information provided by KEGG [252], [253].

Choline phosphate levels as well as the sum of all measured phosphatidylcholines were significantly downregulated. Considering the fact that the choline and the phosphatidylcholine metabolism are closely linked to the methionine/betaine metabolism [261], these results fit into the major picture. Ghoshal *et al.* demonstrated that rats, fed with a methionine-choline deficient diet, displayed a very high prevalence of development of hepatocellular carcinoma (51%) [262]. In this context, the downregulation of the one-carbon and the phosphatidylcholine metabolism might hint at a negative impact of the elevated glucose concentration on carcinogenesis.

Another metabolism, which has to be considered, is the polyamine metabolism. It is closely linked to the methionine metabolism. Spermidine was found to be significantly upregulated.

Kubo *et al.* showed that, after resection for hepatocellular carcinoma, the tumor-free survival rate negatively correlated with the spermidine concentration [263]. Interstingly, when the cells were treated with metformin, spermidine levels were found to be reduced. The possible implications of this observation will be discussed (section **4.3.1**).

4.3.2. The impact of metformin on the hepatocellular metabolism at physiological glucose conditions

To elucidate the impact of metformin on the hepatocellular metabolism at physiological glucose conditions, THLE-2 and Hep G2 cells were cultivated with 6 mM glucose and subsequently treated with either vehicle (H_2O, controls), or 2 mM metformin. Then, the cells were harvested, and targeted and non-targeted metabolomics analyses, and, with the samples, generated for targeted metabolomics, LC-MS/MS based metformin quantification, were performed. In the non-targeted metabolomics sample set, metformin was one of the identified and relatively quantified compounds. Further, the cell numbers were determined. In addition, cell culture supernatants were collected and measured using the targeted metabolomics approach.

THLE-2. Interestingly, the response of THLE-2 cells to metformin was far less pronounced than the response of the hepatoma cell line Hep G2. Not surprisingly, the mitochondrial transport chain as well as the glycolysis/gluconeogenesis and glucose associated pathways were found to be significantly affected. It has previously been reported, that metformin inhibits complex I of the electron transport chain [264]. This alters the AMP/ATP ratio, which leads to an activation of AMPK [76]. It should be noted, that although the change in their levels was not significant, ATP was found to be decreased and AMP was found to be elevated in metformin treated THLE-2 cells. Further, metformin inhibits the hexokinase [73], [74], which catalyzes the first enzymatic step of the glycolysis [75]. In addition, it decreases hepatic gluconeogenesis [80]. In accordance, alanine was found to be elevated (not significant).

However, when focusing on the metabolite profile of THLE-2 cells, subjected to metformin treatment, it is striking, that a number of long and short chain acylcarnitines were significantly elevated. Further, although not significant, the even-chain acylcarnitines were found to be predominantly upregulated as well. In contrast, free carnitine levels were decreased. These (acyl)carnitines partake in the carnitine shuttle and are, consequently, transport forms of fatty acid intermediates of the (even-chain) fatty acid metabolism [265]. Indeed, with the pathway enrichment analysis on basis of the targeted metabolomics data set, the oxidation of very long chain fatty acids was the top hit. A pathway, very closely linked to the β-oxidation, and, consequently, to the acylcarnitine profile, is the hepatic ketogenesis [266], which was the top hit of the enrichment analysis based on the non-targeted data set. However, although the pathway was found to be significantly affected, the single metabolites were not significantly changed. Therefore, no reliable conclusions about the type of dysregulation can be made.

Another interesting aspect of the metformin response of THLE-2 cells, were the significantly elevated glycine levels. However, other metabolites associated with the one-carbon metabolism were not found to be significantly altered.

A fascinating result is the elevation of the cellular alpha-amino adipic acid levels (α-AAA). In 2013, Wang *et al.* showed that strongly elevated plasma α-AAA levels are a potent early biomarker for diabetes [267]. In addition, they demonstrated that α-AAA treated mice exhibited higher α-AAA plasma levels, but lower baseline fasting glucose levels. Further, peak glucose concentrations, after glucose administration, were found to be lower in treated mice. In addition, α-AAA treatment did significantly increase fasting plasma insulin levels [267]. In this context, the observed metformin-mediated elevation of hepatocellular α-AAA levels might represent a not yet reported and elucidated response, which might contribute to the anti-diabetic action of this drug and should be considered for further elucidating experiments.

Hep G2. Interestingly, the α-AAA levels of Hep G2 cells were found to be significantly decreased upon metformin treatment. This is not the only difference in the metabolic metformin response between the liver cell line THLE-2 and the hepatocellular carcinoma cell line Hep G2. Another very striking feature is the difference in their metformin-associated acylcarnitine metabolism. Whereas, in case of the normal liver cell line, the medium and long-chain acylcarnitines, measured with targeted metabolomics, were found to be predominantly elevated, the ones of the hepatocellular carcinoma cell line displayed a more complex response. The saturated and unsaturated long chain acylcarnitine levels were found to be predominantly decreased. In 2016, Yaligar *et al.* showed that the growth of hepatocellular carcinomas correlated with increased acylcarnitine levels in murine livers [268]. Further, patients with hepatocellular carcinoma displayed significantly higher plasma acylcarnitine levels [268]. If considered in this context, the negative regulation of acylcarnitine levels by metformin might be of interest in its application as supplementary treatment for hepatocellular carcinoma, as suggested by Petrushev *et al.* [93]. Interestingly, the levels of the hydroxylated acylcarnitines increased in metformin treated Hep G2 cells. However, from an analytical point of view, any interpretation of patterns regarding these metabolites is difficult, because they were below the LOD (**Table S-3**). Nonetheless, when considered in a greater context, it provides a consistent picture. Namely, the sum of hydroxylated sphingomyelins did significantly increase as well (all cellular hydroxylated sphingomyelins were above the LOD and LLOQ). These results indicate a metformin-dependent change in the hydroxylation status of hepatocellular carcinoma cells. One potential mechanism might be the elevated hydroxylation of fatty acids by the fatty acid 2-hydroxylase (FA2H), which are then incorporated into a wide range of different lipid species [269]. FA2H has been shown to be a negative modulator of the cell cycle in the rat schwannoma cell line D6P2T [270], which is a subclone of an ethylnitrosourea-induced rat peripheral nervous system tumor line [271]. Further, the overexpression of FA2H as well as the treatment of mammalian cell lines with 2-hydroxy palmitic acid correlated with an increased sensitivity of the cells to the anti-tumor drug PM02734 [272]. In addition, siRNA-FA2H-depleted major 3T3-L1 adipocytes exhibited reduced GLUT4 and insulin receptor protein levels and a

decreased basal and insulin-stimulated glucose uptake [273]. This context opens up the question, whether the metformin dependent increase in hydroxylated lipid species is associated with the observed impact of metformin on the cell number and the glucose household.

Analyzing the lipid profile of metformin treated Hep G2 cells; it is noteworthy that most of the phosphatidylcholines were found to be elevated. However, in metformin treated patients, the levels of a number of serum acylalkylphosphatidylcholines (PC ae 36:4, PC ae 28:5 and PC ae 38:6) were found to be decreased [106]. Quite strikingly, all three acylalkylphosphatidylcholines were found to be significantly increased in metformin treated Hep G2 cells. However, their levels were found to be decreased in the according cell culture supernatant. In addition, the levels of the sum of all phosphatidylcholines were found to be strongly decreased in the cell culture supernatant (**Table S-6**) and the sum of intracellular acylalkylphosphatidylcholines was significantly elevated (**Table S-5**). This indicates that the reduction of serum acylalkylphosphatidylcholine levels might be, in part, caused by an increased hepatocellular uptake of these metabolites. However, to verify this hypothesis, labeling experiments have to be conducted.

Among the hits of the enrichment analysis of metformin treated Hep G2 cells (**Table 28**) were: the glucose metabolism (e.g. glycolysis/gluconeogenesis and pentose phosphate pathway), the mitochondrial electron transport chain, the malate-aspartate shuttle, the alanine metabolism and the glucose-alanine cycle. Again, the gluconeogenesis precursor alanine [242] was found to be significantly increased, indicating a metformin-associated reduction in its conversion to glucose. In accordance, metformin has been shown to inhibit the glucose production from alanine [82]. Further, the reduction of gluconeogenesis is a hallmark of molecular metformin action [274], and metformin treatment was shown to correlate with elevated blood alanine levels in insulin resistant patients [218]. Interestingly, whereas an increase in exogenous glucose levels correlated with decreased cellular BCAA levels in Hep G2 cells, the application of metformin led to a significant increase in the intracellular leucine, valine and isoleucine levels. It should be noted, that the administration of BCAA granules led to a reduced prevalence of the cumulative reoccurrence of hepatocellular carcinoma in patients with pronounced insulin resistance [275]. Consequently, this metabolic response to metformin treatment might contribute to the reported anti-cancer [93] action of the drug. However, the drug associated dysregulation of the BCAA metabolism and its associated pathways appears to be quite complex. Whereas the BCAA levels are uniformly elevated, glutamate, a product of the first step of BCAA degradation [245], was not found to be significantly altered. Further, the acylcarnitines isobutyrylcarnitine and isovalerylcarnitine, which are via isobutyryl-CoA/isovaleryl-CoA [245] and the carnitine shuttle [265] linked to BCAA degradation [245], were found to be decreased. Interestingly, acetyl-CoA and acetylcarnitine and propionylcarnitine, which are transport forms of the BCAA degradation products acetyl-CoA and propionyl-CoA [245], [265], were found to be elevated. In addition, it should be considered that these metabolites partake in a number of pathways [241], [245], [265] and cannot be considered to be unique markers of the BCAA degradation. A clear elucidation of their fate and the implication of

their changed levels for the BCAA metabolism can only be obtained via flux studies. Next to the altered BCAA metabolism, the aromatic amino acids phenylalanine, tyrosine and tryptophan were elevated as well. In addition, the γ-glutamyl derivatives of valine, leucine, isoleucine, tyrosine and phenylalanine were found to be significantly elevated. γ-Glutamyltryptophane was not covered by the metabolomics analyses. It should be noted, that glycine, cysteine and GSH were found to be elevated (not significant), whereas, 5-oxoproline was found to be decreased (not significant). Although these observations were not significant, when the cells, which were subjected to metformin treatment, were cultivated at a physiological glucose concentration; this metformin-induced pattern became significant, when the cells were cultivated at an elevated glucose concentration. These results indicate that the impact of metformin on the glutathione metabolism adapts to the availability of glucose.

In addition to the BCAAs, a number of metabolites, belonging to the arginine and proline metabolism, the urea cycle, ammonia recycling and the one-carbon metabolism, were found to be altered in metformin treated Hep G2 cells. In detail, intracellular arginine as well as proline and ornithine levels were found to be significantly increased. However, citrulline and aspartate levels were not significantly altered. Regarding glycine, methionine, betaine and SAH (one-carbon metabolism), the levels were found to be increased, although, in case of most of them, not significantly so. Interestingly, creatinine (targeted: significant, non-targeted: not significant) and creatine phosphate were found to be significantly decreased. In case of creatinine, the type of dysreluation was the same for the targeted and non-targeted data set. Thus, the difference in their significance level can be explained by the different sample sizes. In accordance with these dysregulations, the creatine levels were found to be decreased as well (not significant). In summary, these results indicate a metformin-associated downregulation of the hepatocellular creatine synthesis. Further, taurine and hypotaurine levels were found to be elevated. However, the change in their respective levels did not pass the significance threshold. Serine was found to be significantly decreased in the targeted data set, but not in the non-targeted one. It should be noted, that serine was one of the metabolites, wich, when measured in Hep G2 cells, displayed a very low precision with the non-targeted metabolomics approach (**Figure 16B**). The precision, observed with targeted metabolomics, was found to be satisfactory (**Figure 11**). The serine levels in the cell culture supernatant were found to be strongly decreased, indicating a drain of the extra- and intracellular serine pool. In accordance, the levels of palmitoylcarnitine (significant), sphinganine (not significant), sphingosine (not significant) and the majority of sphingomyelins (not significant), measured with targeted metabolomics, were found to be decreased. In conclusion, the altered serine levels might be indicative of a decreased sphingolipid synthesis. Although most of the changes, discussed in this paragraph were not significant, they are of interest, as they will become more pronounced at high glucose conditions.

4.3.1. The impact of metformin on the hepatocellular metabolism at diabetic glucose conditions

Although, the impact of metformin on the hepatocellular glucose metabolism has been studied in detail [82], the knowledge presented in literature is still very one-dimensional: namely, metformin treatment alters the hepatocellular glucose metabolism [82]. However, whether the glucose concentration on its own plays a central role in the hepatocellular metabolic response to metformin has not yet been assessed. Only rather recently, Wahdan-Alaswad *et al.* demonstrated that the glucose concentration has a negative impact on the metformin efficacy in breast cancer cell lines [87]. Considering the fact, that the physiological glucose range is very dynamic, especially in patients with dysfunctional glucose homeostasis [221], and that the liver is of crucial importance to glucose metabolism [276], these results open the question, whether the molecular impact of this drug on the hepatocellular metabolism might be glucose dependent. Hence, the liver cell line THLE-2 and the hepatoma cell line Hep G2 were cultured at a high glucose condition and treated with metformin. Then, targeted and non-targeted metabolomics were performed.

THLE-2. In THLE-2 cells, the long chain acylcarnitines and acetylcarnitine, were (in part significantly) elevated upon metformin treatment. As the carnitine shuttle is closely linked to the mitochondrial β-oxidation [277], this elevation in acylcarnitine levels might indicate increased hepatocellular β-oxidation due to drug treatment. In this regard, Fulgencio *et al.* focused on the impact of metformin on the fatty acid and glucose metabolism in isolated rat hepatocytes [82]. They illustrated that metformin treatment (male Wistar rats, metformin concentrations: 5 and 50 mM, incubation time: 1 h) led to a dose-dependent decrease in hepatocellular glucose production from alanine, galactose, dihydroxyacetone and lactate/pyruvate. However, they did not observe any impact on the oxidation fatty acids (^{14}C oleate and octanoate) [82]. Interestingly, these results contradict the observations made by Zhou *et al.* [89]. Among a number of assessed parameters, they also used the consumption of ^{14}C oleate to evaluate the impact of metformin treatment on fatty acid oxidation in primary rat hepatocytes (male Sprague Dawley rats, concentration: 500 µM, incubation time: 4 h) and observed a significant increase. Based on their results, they proposed an AMPK mediated upregulation of the hepatocellular fatty acid oxidation [89]. The observed differences in their observations might originate from the different incubation times. In this study, an incubation time of 24 h was chosen to allow for the adjustment of the cellular metabolism to the drug. Hence, the acylcarnitine patterns, observed in human THLE-2 cells, are in accordance with the upregulation of the hepatocellular fatty acid oxidation proposed by Zhou *et al*. [89].

Regarding the impact of metformin treatment on the amino acid and biogenic amine profile and the free carnitine levels of THLE-2 cells, cultivated at a high glucose concentration, analytical issues had to be taken into consideration. Namely, a number of amino acids and biogenic amines, which were covered by both, targeted and non-targeted metabolomics analyses, exhibited significant changes in their levels, when measured with non-targeted metabolomics, but not, when measured with targeted metabolomics. This observation is counterintuitive, as the sample size was smaller and the number of assessed parameters was higher with non-targeted metabolomics. Further, the differences in significance for these

metabolites cannot be accounted for by the analytical performance of the targeted approach, since the analyte levels were above the LLOQ. To verify, whether the changes observed in the non-targeted data set are reliable, a different targeted approach has to be applied. Despite these analytical considerations, the potential biological implications of the observed patterns will be discussed below.

Spermidine levels were significantly decreased (**Table S-7**). In accordance, spermine levels were found to be decreased, indicating a metformin dependent downregulation of the polyamine pathway. In addition, methionine and betaine, intermediates of the methionine cycle, which is part of the one-carbon metabolism [255], were found to be significantly decreased, which correlated with significantly decreased GSH levels. Further, a number of γ-glutamyl amino acid derivatives were found to be significantly lowered. The methionine cycle is, via decarboxylated SAM, linked to the polyamine synthesis (**Figure 40**), which in turn results in the generation of hyposine [255]. The hyposine cascade has been linked to tumor growth and cancer progression [278]. Glutamine as well as glutamate levels were significantly decreased, which might indicate a reduction in hepatocellular glutamine utilization. Again, the glutaminolysis is very closely linked to GSH synthesis [279]. Consequently, the lowered glutamine and glutamate levels might contribute to the observed reduction in GSH and γ- glutamyl amino acid levels. In this regard, it has to be taken into consideration that glutamine and glucose are the major determinants of cancer cell proliferation [279] as the metabolism of malignant cells heavily relies on glutaminolysis and glycolysis [257]. Hence, the downregulation of glutaminolysis and the methionine cycle seem to lead to a downregulation of GSH and γ- glutamyl amino acid synthesis. In addition, the potential reduction in glutaminolysis, the methionine cycle and polyamine synthesis might contribute to the observed hepatocellular carcinoma-preventive effect of metformin [99], [100].

Hep G2. In case of Hep G2 cells, cultivated at a glucose concentration of 11 mM, the treatment with metformin vastly alters the metabolome. As to be expected, alanine was found to be strongly elevated. In addition, the metabolite profile mirrored quite extensive drug-associated dysregulations. In detail, all measured metabolites involved in the urea cycle (arginine, ornithine, aspartate and citrulline), were found to be elevated. This indicates a metformin-induced upregulation of the urea cycle. Interestingly, whereas ornithine and putrescine were found to be significantly increased, spermidine was significantly decreased (**Table S-5**) (**Figure 40**). Again, it should be considered that the polyamine pathway has been closely linked to cell growth and rapidly proliferating cell types and inhibitors and polyamine depletion have been shown to exhibit an anticancer effect [280]. The observed metformin-associated regulation of the polyamine pathway is quite characteristic as the rate limiting step is the generation of putrescine from ornithine by the ornithine decarboxylase [280]. This enzyme has been proposed as promising target for anticancer and cancer chemopreventive therapies since the 1980ies [280], [281]. However, the step, dowregulated by metformin treatment, is the conversion of putrescine and decarboxylated SAM to spermidine, which is catalyzed by the spermidine synthase [280]. Interestingly, in 2010, the spermidine synthase has been proposed as new therapeutic target for cancer

chemoprevention [282]. The spermidine synthase links the polyamine synthesis to the one-carbon metabolism (Decarboxylated SAM) [280] (**Figure 40**).

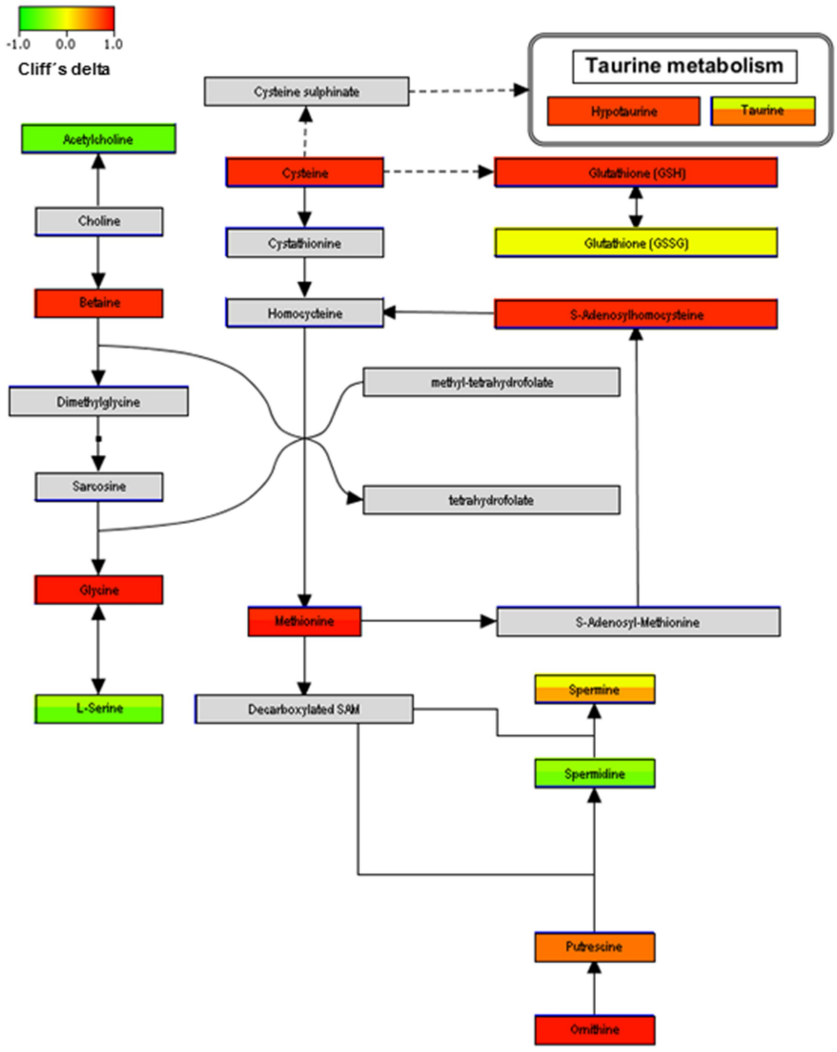

Figure 40: Impact of the metformin treatment on the one carbon metabolism of Hep G2 cells, cultivated at an elevated glucose concentration.
The figure shows a schematic overview of the one carbon donor metabolism. Regulations of measured metabolites are represented by the effect size (Cliff´s delta). In case the metabolite was present in the non-targeted and the targeted dataset, the respective box is horizontally parted. The upper part represents the effect size, obtained with non-targeted metabolomics, the lower part, the one, obtained with targeted metabolomics analysis.
The pathway was modified after wikipathways (http://www.wikipathways.org, [289]), Pathway: Yang L, Willighagen E, Hanspers K, Cirillo E, Kutmon M. One carbon donor (Homo sapiens). Accession date: 07/21/2016, http://www.wikipathways.org/index.php/Pathway:WP2190, [290].

Interestingly, intermediates of the one-carbon, the transulfuration/glutathione and the taurine metabolism were found to be elevated (**Figure 40** and **Figure 41**). In detail, betaine, methionine, SAH, cysteine, glycine, GSH, taurine and hypotaurine were found to be significantly elevated. Glutamate was found to be elevated as well, however, this elevation was only significant in the non-targeted data set. Further, all measured γ-glutamyl amino acids, except γ-glutamylglutamine, were found to be significantly elevated. 5-oxoproline, which is an intermediate of γ-glutamyl amino acid degradation [254], was found to be significantly decreased (**Figure 41**). Again, serine levels were found to be decreased. It should be noted, that carbamoylaspartate, an intermediate of pyrimidine synthesis [260], which is linked to the one-carbon metabolism [255], was found to be significantly decreased as well. Taken together, quite a complex picture of metformin action at high glucose conditions arises. The folate and methionine metabolism (one-carbon cycle) is increased. However, its associated pathways, the polyamine synthesis and the pyrimidine synthesis, are decreased, whereas the taurine, glutathione and γ-glutamyl metabolism are increased. In

addition, the impact of metformin treatment was, for the most part, more pronounced at high than at physiological glucose conditions. These results indicate, that, as shortly introduced in the previous chapter, the dimension of the metabolic metformin response is related to the available glucose concentration. In this regard, Wahdan-Alaswad *et al.* showed that the exogenous glucose concentration ameliorates the metformin action in breast cancer cell lines [87]. At first, this observation and the results, presented by the authors, seem to contradict the observations made with Hep G2 cells in course of this study. However, it becomes obvious that the dynamics of glucose and metformin action are more complex than assumed. In detail, Wahdan-Alaswad *et al.* focused on the impact of glucose on metformin action in regard to its anti-proliferatory and pro-apoptotic properties [87]. They showed that an elevation of the glucose concentration leads to a massive elevation of the EC_{50} for metformin induced cell growth inhibition in a wide range of breast cancer cell lines. Further, the percentage of metformin treated cells undergoing apoptosis was higher at low glucose conditions. Interestingly, the transciptomic analysis revealed that metformin-treatment of cells, cultivated at high glucose conditions, resulted in the expression of a far higher percentage of metabolism associated genes, than in cells, cultivated at a physiological glucose concentration [87]. Therefore, although the elevation of the exogenous glucose concentration correlated with an amelioration of the anti-proliferatory and pro-apoptotic impact of metformin [87], it might lead to a more pronounced metabolic response in cancer cell lines.

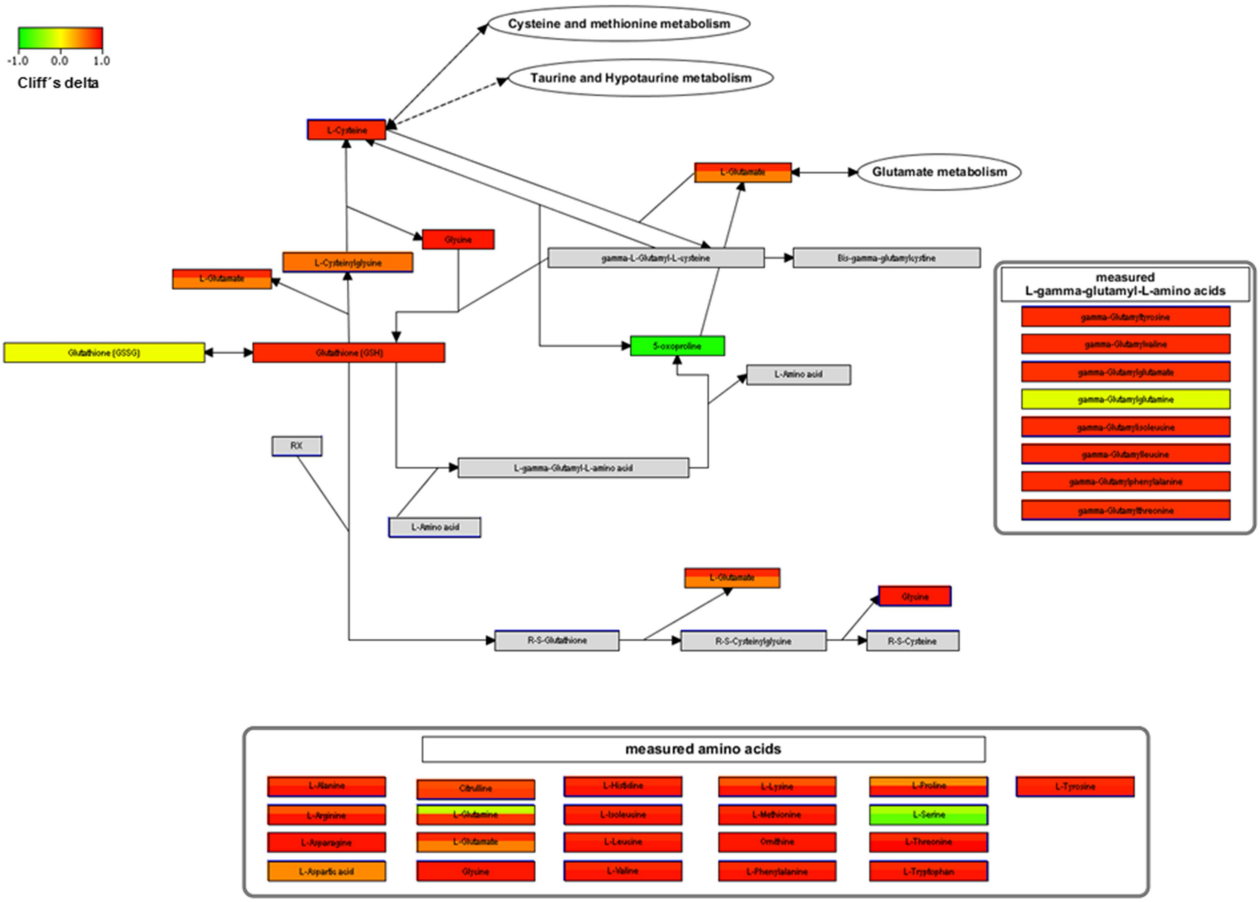

Figure 41: Impact of the metformin treatment on the glutathione metabolism and associated pathways and metabolites of Hep G2 cells, cultivated at an elevated glucose concentration.

The figure shows a schematic overview of the glutathione metabolism and selected associated pathways and metabolites. Regulations of measured metabolites are represented by the effect size (Cliff´s delta). In case the metabolite was present in the non-targeted and the targeted dataset, the respective box is horizontally divided. The upper part represents the effect size, obtained with non-targeted metabolomics, the lower part, the one, obtained with targeted metabolomics analysis.
This pathway was designed on basis of information provided by KEGG [252], [253].

Regarding the other significantly affected metabolites, a BCAA-acylcarnitine pattern can be observed. In detail, the intracellular BCAA, acetylcarnitine and propionylcarnitine levels were significantly elevated. However, isobutyrylcarnitine and isovalerylcarnitine were significantly decreased. The same pattern was present in THLE-2 cells. In case of Hep G2 cells, the non-hydroxylated long chain acylcarnitines were found to be decreased, while in THLE-2 cells, they were increased. This difference in the respective patterns might indicate that the characteristic changes in short chain acylcarnitine levels are not caused by a dysregulation of the β-oxidation/fatty acid synthesis – as the long chain acylcarnitine responses differ between the two cell lines – but by a complex, metformin-associated response of the BCAA metabolism. This dysregulation of the crossroads of BCAA and lipid metabolism represents a challenge for any interpretation. Further studies, such as flux analyses and the assessment of protein expression patterns of the according enzymes, have to be conducted.

Again, hydroxylated carnitines as well as the sum of hydroxylated sphinogmyelins were found to be increased. In addition to the lipid hydroxylation status, the saturation status was affected as well. In detail, the sum of polyunsaturated phosphatidylcholines and the sum of unsaturated sphingomyelins were significantly increased in metformin treated Hep G2 cells. Interestingly, those parameters were found to negatively correlate with elevated glucose levels. Consequently, metformin reversed this impact of glucose on the saturation status of the cellular lipidome. Long chain polyunsaturated fatty acids have been associated with beneficial effects on insulin resistance, the lipid profile and blood pressure [283]. Nonetheless, lipid and fatty acid desaturation patterns and their associations and implications are complex and not yet fully understood [283], [284]. Based on the data, presented in this study, it might be concluded that metformin counteracts the impact of elevated glucose levels on a part of the hepatocellular lipidome.

Conclusions. To elucidate the impact of glucose and metformin on the hepatocellular metabolism, the human liver cell line THLE-2 and the hepatoma cell line Hep G2 were cultivated at either a physiological or a diabetic glucose concentration and treated with metformin. Then, targeted and non-targeted metabolomics were performed.

The impact of both, glucose and metformin, was found to be strongly cell type dependent. In general, the hepatoma cell line displayed a more pronounced response to altered exogenous glucose levels and metformin treatment, which might be explained by the strong dependency of cancer cells on aerobic glycolysis [88]. Further, the affected pathways and the dysregulation of these pathways strongly differed between the two cell types. Hence, the observations indicate that the metabolic metformin action differs between liver cells and

hepatoma cells. Further, the interaction between the molecular glucose and metformin action was found to be bidirectional.

The next step should be the elucidation of the impact of glucose and metformin on the metabolome of primary cells, to verify, wether the results are indicative of a cell type dependent response in humans. Further, the therapeutic implications of these observations should be assessed *in vivo*.

5. References

[1] A. M. Ahmed, "History of diabetes mellitus," *Saudi Medical Journal*, vol. 23, no. 4. pp. 373–378, 2002.

[2] K. Laios, M. Karamanou, Z. Saridaki, and G. Androutsos, "Aretaeus of Cappadocia and the first description of diabetes," *Hormones*, vol. 11, no. 1, pp. 109–113, 2012.

[3] R. Lakhtakia, "The history of diabetes mellitus," *Sultan Qaboos University Medical Journal*, vol. 13, no. 3, pp. 368–370, 2013.

[4] C. Stylianou and C. Kelnar, "The introduction of successful treatment of diabetes mellitus with insulin," *Journal of the Royal Society of Medicine*, vol. 102, no. 7, pp. 298–303, 2009.

[5] J. von Mering and O. Minkowski, "Diabetes mellitus nach Pankreasexstirpation," *Archiv für experimentelle Pathologie und Pharmacologie*, vol. 26, no. 22, pp. 371–387, 1890.

[6] H. P. Himsworth, "Diabetes mellitus: its differentiation into insulin-sensitive and insulin-insensitive types," *The Lancet*, vol. 227, no. 5864, pp. 127–130, 1936.

[7] National Diabetes Data Group, "Classification and diagnosis of diabetes mellitus and other categories of glucose intolerance," *Diabetes*, vol. 28, no. 12, pp. 1039–1057, 1979.

[8] The Expert Committee on the Diagnosis and Classification of Diabetes Mellitus, "Report of the Expert Committee on the Diagnosis and Classification of Diabetes Mellitus," *Diabetes Care*, vol. 25, no. Supplement 1, pp. S5–S20, 2002.

[9] American Diabetes Association, "Diagnosis and classification of diabetes mellitus," *Diabetes Care*, vol. 33, no. Supplement 1, pp. S62–S69, 2010.

[10] G. M. Reaven, "Banting lecture 1988. Role of insulin resistance in human disease," *Diabetes*, vol. 37, no. 12, pp. 1595–1607, 1988.

[11] International Diabetes Federation, "IDF Diabetes Atlas," *Brussels, Belgium: International Diabetes Federation*, 2015. http://www.diabetesatlas.org (Accessed: 10/17/2016).

[12] F. B. Hu, T. Y. Li, G. A. Colditz, W. C. Willett, and J. E. Manson, "Television watching and other sedentary behaviors in relation to risk of obesity and type 2 diabetes mellitus in women," *The Journal of the American Medical Association*, vol. 289, no. 14, pp. 1785–1791, 2003.

[13] I. Shai, R. Jiang, J. E. Manson, M. J. Stampfer, W. C. Willett, G. A. Colditz, and F. B. Hu, "Ethnicity, obesity, and risk of type 2 diabetes in women," *Diabetes Care*, vol. 29, no. 7, pp. 1585–1590, 2006.

[14] E. van 't Riet, J. M. Dekker, Q. Sun, G. Nijpels, F. B. Hu, and R. M. van Dam, "Role of adiposity and lifestyle in the relationship between family history of diabetes and 20-year incidence of type 2 diabetes in U.S. women," *Diabetes Care*, vol. 33, no. 4, pp. 763–767, 2010.

[15] L. Bellamy, J.-P. Casas, A. D. Hingorani, and D. Williams, "Type 2 diabetes mellitus after gestational diabetes: a systematic review and meta-analysis," *The Lancet*, vol. 373, no. 9677, pp. 1773–1779, 2009.

[16] E. Giovannucci, D. M. Harlan, M. C. Archer, R. M. Bergenstal, S. M. Gapstur, L. A. Habel, M. Pollak, J. G. Regensteiner, and D. Yee, "Diabetes and cancer," *Diabetes Care*, vol. 33, no. 7, pp. 1674–1685, 2010.

[17] H. B. El-Serag, T. Tran, and J. E. Everhart, "Diabetes increases the risk of chronic liver disease and hepatocellular carcinoma," *Gastroenterology*, vol. 126, no. 2, pp. 460–468, 2004.

[18] H. B. El-Serag and K. L. Rudolph, "Hepatocellular carcinoma: epidemiology and

molecular carcinogenesis," *Gastroenterology*, vol. 132, no. 7, pp. 2557–2576, 2007.
[19] A. B. Evert, J. L. Boucher, M. Cypress, S. A. Dunbar, M. J. Franz, E. J. Mayer-Davis, J. J. Neumiller, R. Nwankwo, C. L. Verdi, P. Urbanski, and W. S. Yancy Jr., "Nutrition therapy recommendations for the management of adults with diabetes," *Diabetes Care*, vol. 37, no. Supplement 1, pp. S120–S143, 2014.
[20] A. B. Olokoba, O. A. Obateru, and L. B. Olokoba, "Type 2 diabetes mellitus: a review of current trends," *Oman Medical Journal*, vol. 27, no. 4, pp. 269–273, 2012.
[21] J. (Jim) Liu, T. Lee, and R. A. DeFronzo, "Why do SGLT2 inhibitors inhibit only 30-50% of renal glucose reabsorption in humans?," *Diabetes*, vol. 61, no. 9, pp. 2199–2204, 2012.
[22] L. C. Groop, "Sulfonylureas in NIDDM," *Diabetes Care*, vol. 15, no. 6, pp. 737–754, 1992.
[23] J. Fuhlendorff, P. Rorsman, H. Kofod, C. L. Brand, B. Rolin, P. MacKay, R. Shymko, and R. D. Carr, "Stimulation of insulin release by repaglinide and glibenclamide involves both common and distinct processes," *Diabetes*, vol. 47, no. 3, pp. 345–351, 1998.
[24] H. Yki-Järvinen, "Thiazolidinediones," *New England Journal of Medicine*, vol. 351, no. 11, pp. 1106–1118, 2004.
[25] S. Kalra, "Alpha glucosidase inhibitors," *The Journal of the Pakistan Medical Association*, vol. 64, no. 4, pp. 474–476, 2014.
[26] M. Nauck, "Incretin therapies: highlighting common features and differences in the modes of action of glucagon-like peptide-1 receptor agonists and dipeptidyl peptidase-4 inhibitors," *Diabetes, Obesity & Metabolism*, vol. 18, no. 3, pp. 203–216, 2016.
[27] D. Kawanami, K. Matoba, K. Sango, and K. Utsunomiya, "Incretin-Based Therapies for Diabetic Complications: Basic Mechanisms and Clinical Evidence," *International Journal of Molecular Sciences*, vol. 17, no. 8, p. 1223, 2016.
[28] E. Bosi, "Metformin - the gold standard in type 2 diabetes: what does the evidence tell us?," *Diabetes, Obesity & Metabolism*, vol. 11, no. Suppl. 2, pp. 3–8, 2009.
[29] C. J. Bailey, "Biguanides and NIDDM," *Diabetes Care*, vol. 15, no. 6, pp. 755–772, 1992.
[30] J. A. Dykens, J. Jamieson, L. Marroquin, S. Nadanaciva, P. A. Billis, and Y. Will, "Biguanide-induced mitochondrial dysfunction yields increased lactate production and cytotoxicity of aerobically-poised HepG2 cells and human hepatocytes in vitro," *Toxicology and Applied Pharmacology*, vol. 233, no. 2, pp. 203–210, 2008.
[31] M. Fung, A. Thornton, K. Mybeck, J. H. -h. Wu, K. Hornbuckle, and E. Muniz, "Evaluation of the characteristics of safety withdrawal of prescription drugs from worldwide pharmaceutical markets-1960 to 1999," *Drug Information Journal*, vol. 35, no. 1, pp. 293–317, 2001.
[32] M. Nattrass and K. G. M. M. Alberti, "Biguanides," *Diabetologia*, vol. 14, no. 2, pp. 71–74, 1978.
[33] G. Orgován and B. Noszál, "Electrodeless, accurate pH determination in highly basic media using a new set of 1H NMR pH indicators," *Journal of Pharmaceutical and Biomedical Analysis*, vol. 54, no. 5, pp. 958–964, 2011.
[34] B. Hernández, F. Pflüger, S. G. Kruglik, R. Cohen, and M. Ghomi, "Protonation – deprotonation and structural dynamics of antidiabetic drug metformin," *Journal of Pharmaceutical and Biomedical Analysis*, vol. 114, pp. 42–48, 2015.
[35] N. Vidon, S. Chaussade, M. Noel, C. Franchisseur, B. Huchet, and J. J. Bernier, "Metformin in the digestive tract," *Diabetes Research and Clinical Practice*, vol. 4, no. 3, pp. 223–229, 1988.
[36] N.-N. Song, Q.-S. Li, and C.-X. Liu, "Intestinal permeability of metformin using

single-pass intestinal perfusion in rats," *World Journal of Gastroenterology*, vol. 12, no. 25, pp. 4064–4070, 2006.
[37] R. Beckmann, "Resorption, Verteilung im Organismus und Ausscheidung von Metformin," *Diabetologia*, vol. 5, no. 5, pp. 318–324, 1969.
[38] P. J. Pentikäinen, P. J. Neuvonen, and A. Penttilä, "Pharmacokinetics of metformin after intravenous and oral administration to man," *European Journal of Clinical Pharmacology*, vol. 16, no. 3, pp. 195–202, 1979.
[39] G. T. Tucker, C. Casey, P. J. Phillips, H. Connor, J. D. Ward, and H. F. Woods, "Metformin kinetics in healthy subjects and in patients with diabetes mellitus," *British Journal of Clinical Pharmacology*, vol. 12, no. 2, pp. 235–246, 1981.
[40] Y. Sogame, A. Kitamura, M. Yabuki, and S. Komuro, "Liver uptake of biguanides in rats," *Biomedicine & Pharmacotherapy*, vol. 65, no. 6, pp. 451–455, 2011.
[41] C. Wilcock and C. J. Bailey, "Accumulation of metformin by tissues of the normal and diabetic mouse," *Xenobiotica*, vol. 24, no. 1, pp. 49–57, 1994.
[42] M. Zhou, L. Xia, and J. Wang, "Metformin transport by a newly cloned proton-stimulated organic cation transporter (plasma membrane monoamine transporter) expressed in human intestine," *Drug Metabolism and Disposition*, vol. 35, no. 10, pp. 1956–1962, 2007.
[43] M. Tsuda, T. Terada, T. Mizuno, T. Katsura, J. Shimakura, and K. Inui, "Targeted disruption of the multidrug and toxin extrusion 1 (mate1) gene in mice reduces renal secretion of metformin," *Molecular Pharmacology*, vol. 75, no. 6, pp. 1280–1286, 2009.
[44] A. T. Nies, U. Hofmann, C. Resch, E. Schaeffeler, M. Rius, and M. Schwab, "Proton pump inhibitors inhibit metformin uptake by organic cation transporters (OCTs)," *PLoS one*, vol. 6, no. 7, p. e22163, 2011.
[45] N. Nakamichi, H. Shima, S. Asano, T. Ishimoto, T. Sugiura, K. Matsubara, H. Kusuhara, Y. Sugiyama, Y. Sai, K.-I. Miyamoto, A. Tsuji, and Y. Kato, "Involvement of carnitine/organic cation transporter OCTN1/SLC22A4 in gastrointestinal absorption of metformin," *Journal of Pharmaceutical Sciences*, vol. 102, no. 9, pp. 3407–3417, 2013.
[46] M. V Tzvetkov, S. V Vormfelde, D. Balen, I. Meineke, T. Schmidt, D. Sehrt, I. Sabolić, H. Koepsell, and J. Brockmöller, "The effects of genetic polymorphisms in the organic cation transporters OCT1, OCT2, and OCT3 on the renal clearance of metformin," *Clinical Pharmacology & Therapeutics*, vol. 86, no. 3, pp. 299–306, 2009.
[47] Y. Shu, S. A. Sheardown, C. Brown, R. P. Owen, S. Zhang, R. A. Castro, A. G. Ianculescu, L. Yue, J. C. Lo, E. G. Burchard, C. M. Brett, and K. M. Giacomini, "Effect of genetic variation in the organic cation transporter 1 (OCT1) on metformin action," *The Journal of Clinical Investigation*, vol. 117, no. 5, pp. 1422–1431, 2007.
[48] X. Liang, H.-C. Chien, S. W. Yee, M. M. Giacomini, E. C. Chen, M. Piao, J. Hao, J. Twelves, E.-I. Lepist, A. S. Ray, and K. M. Giacomini, "Metformin is a substrate and inhibitor of the human thiamine transporter, THTR-2 (SLC19A3)," *Molecular Pharmaceutics*, vol. 12, no. 12, pp. 4301–4310, 2015.
[49] H. Koepsell, K. Lips, and C. Volk, "Polyspecific organic cation transporters: structure, function, physiological roles, and biopharmaceutical implications," *Pharmaceutical Research*, vol. 24, no. 7, pp. 1227–1251, 2007.
[50] H. Koepsell and H. Endou, "The SLC22 drug transporter family," *Pflügers Archiv - European Journal of Physiology*, vol. 447, no. 5, pp. 666–676, 2004.
[51] K. Engel and J. Wang, "Interaction of organic cations with a newly identified plasma membrane monoamine transporter," *Molecular Pharmacology*, vol. 68, no. 5, pp.

1397–1407, 2005.
[52] H. Yabuuchi, I. Tamai, J.-I. Nezu, K. Sakamoto, A. Oku, M. Shimane, Y. Sai, and A. Tsuji, “Novel membrane transporter OCTN1 mediates multispecific, bidirectional, and pH-dependent transport of organic cations,” *The Journal of Pharmacology and Experimental Therapeutics*, vol. 289, no. 2, pp. 768–773, 1999.
[53] Y. Tanihara, S. Masuda, T. Sato, T. Katsura, O. Ogawa, and K. Inui, “Substrate specificity of MATE1 and MATE2-K, human multidrug and toxin extrusions/H(+)-organic cation antiporters,” *Biochemical Pharmacology*, vol. 74, no. 2, pp. 359–371, 2007.
[54] R. Kekuda, P. D. Prasad, X. Wu, H. Wang, Y.-J. Fei, F. H. Leibach, and V. Ganapathy, “Cloning and functional characterization of a potential-sensitive, polyspecific organic cation transporter (OCT3) most abundantly expressed in placenta,” *The Journal of Biological Chemistry*, vol. 273, no. 26, pp. 15971–15979, 1998.
[55] N. Kimura, S. Masuda, Y. Tanihara, H. Ueo, M. Okuda, T. Katsura, and K. Inui, “Metformin is a superior substrate for renal organic cation transporter OCT2 rather than hepatic OCT1,” *Drug Metabolism and Pharmacokinetics*, vol. 20, no. 5, pp. 379–386, 2005.
[56] T. K. Han, W. R. Proctor, C. L. Costales, H. Cai, R. S. Everett, and D. R. Thakker, “Four cation-selective transporters contribute to apical uptake and accumulation of metformin in Caco-2 cell monolayers,” *The Journal of Pharmacology and Experimental Therapeutics*, vol. 352, no. 3, pp. 519–528, 2015.
[57] T. F. Solbach, M. Grube, M. F. Fromm, and O. Zolk, “Organic cation transporter 3: expression in failing and nonfailing human heart and functional characterization,” *Journal of Cardiovascular Pharmacology*, vol. 58, no. 4, pp. 409–417, 2011.
[58] D.-S. Wang, J. W. Jonker, Y. Kato, H. Kusuhara, A. H. Schinkel, and Y. Sugiyama, “Involvement of organic cation transporter 1 in hepatic and intestinal distribution of metformin,” *The Journal of Pharmacology and Experimental Therapeutics*, vol. 302, no. 2, pp. 510–515, 2002.
[59] D.-S. Wang, H. Kusuhara, Y. Kato, J. W. Jonker, A. H. Schinkel, and Y. Sugiyama, “Involvement of organic cation transporter 1 in the lactic acidosis caused by metformin,” *Molecular Pharmacology*, vol. 63, no. 4, pp. 844–848, 2003.
[60] D. Gründemann, V. Gorboulev, S. Gambaryan, M. Veyhl, and H. Koepsell, “Drug excretion mediated by a new prototype of polyspecific transporter,” *Nature*, vol. 372, no. 6506, pp. 549–552, 1994.
[61] L. Chen, B. Pawlikowski, A. Schlessinger, S. S. More, D. Stryke, S. J. Johns, M. A. Portman, E. Chen, T. E. Ferrin, A. Sali, and K. M. Giacomini, “Role of organic cation transporter 3 (SLC22A3) and its missense variants in the pharmacologic action of metformin,” *Pharmacogenetics and Genomics*, vol. 20, no. 11, pp. 687–699, 2010.
[62] C. Hilgendorf, G. Ahlin, A. Seithel, P. Artursson, A.-L. Ungell, and J. Karlsson, “Expression of thirty-six drug transporter genes in human intestine, liver, kidney, and organotypic cell lines,” *Drug Metabolism and Disposition*, vol. 35, no. 8, pp. 1333–1340, 2007.
[63] M. Nishimura and S. Naito, “Tissue-specific mRNA expression profiles of human ATP-binding cassette and solute carrier transporter superfamilies,” *Drug Metabolism and Pharmacokinetics*, vol. 20, no. 6, pp. 452–477, 2005.
[64] L. Pochini, M. Scalise, M. Galluccio, G. Pani, K. A. Siminovitch, and C. Indiveri, “The human OCTN1 (SLC22A4) reconstituted in liposomes catalyzes acetylcholine transport which is defective in the mutant L503F associated to the Crohn’s disease,” *Biochimica et Biophysica Acta (BBA) - Biomembranes*, vol. 1818, no. 3, pp. 559–565,

2012.
[65] K. Engel, M. Zhou, and J. Wang, “Identification and characterization of a novel monoamine transporter in the human brain,” *The Journal of Biological Chemistry*, vol. 279, no. 48, pp. 50042–50049, 2004.
[66] B. A. Davis, A. Nagarajan, L. R. Forrest, and S. K. Singh, “Mechanism of paroxetine (Paxil) inhibition of the serotonin transporter,” *Scientific Reports*, vol. 6, p. 23789, 2016.
[67] M. Tsuda, T. Terada, M. Ueba, T. Sato, S. Masuda, T. Katsura, and K. Inui, “Involvement of human multidrug and toxin extrusion 1 in the drug interaction between cimetidine and metformin in renal epithelial cells,” *The Journal of Pharmacology and Experimental Therapeutics*, vol. 329, no. 1, pp. 185–191, 2009.
[68] M. Otsuka, T. Matsumoto, R. Morimoto, S. Arioka, H. Omote, and Y. Moriyama, “A human transporter protein that mediates the final excretion step for toxic organic cations,” *Proceedings of the National Academy of Sciences of the United States of America*, vol. 102, no. 50, pp. 17923–17928, 2005.
[69] H. R. Bridges, A. J. Y. Jones, M. N. Pollak, and J. Hirst, “Effects of metformin and other biguanides on oxidative phosphorylation in mitochondria,” *Biochemical Journal*, vol. 462, no. 3, pp. 475–487, 2014.
[70] S. Larsen, R. Rabøl, C. N. Hansen, S. Madsbad, J. W. Helge, and F. Dela, “Metformin-treated patients with type 2 diabetes have normal mitochondrial complex I respiration,” *Diabetologia*, vol. 55, no. 2, pp. 443–449, 2012.
[71] M. R. Owen, E. Doran, and A. P. Halestrap, “Evidence that metformin exerts its anti-diabetic effects through inhibition of complex 1 of the mitochondrial respiratory chain,” *Biochemical Journal*, vol. 348, no. 3, pp. 607–614, 2000.
[72] J. Ouyang, R. A. Parakhia, and R. S. Ochs, “Metformin activates AMP kinase through inhibition of AMP deaminase,” *The Journal of Biological Chemistry*, vol. 286, no. 1, pp. 1–11, 2011.
[73] B. Salani, C. Marini, A. Del Rio, S. Ravera, M. Massollo, A. M. Orengo, A. Amaro, M. Passalacqua, S. Maffioli, U. Pfeffer, R. Cordera, D. Maggi, and G. Sambuceti, “Metformin impairs glucose consumption and survival in Calu-1 cells by direct inhibition of hexokinase-II,” *Scientific Reports*, vol. 3, p. 2070, 2013.
[74] C. Marini, B. Salani, M. Massollo, A. Amaro, A. I. Esposito, A. M. Orengo, S. Capitanio, L. Emionite, M. Riondato, G. Bottoni, C. Massara, S. Boccardo, M. Fabbi, C. Campi, S. Ravera, G. Angelini, S. Morbelli, M. Cilli, R. Cordera, M. Truini, D. Maggi, U. Pfeffer, and G. Sambuceti, “Direct inhibition of hexokinase activity by metformin at least partially impairs glucose metabolism and tumor growth in experimental breast cancer,” *Cell Cycle*, vol. 12, no. 22, pp. 3490–3499, 2013.
[75] D. Voet, J. G. Voet, and C. W. Pratt, *Lehrbuch der Biochemie*. Weinheim: WILEY-VCH Verlag GmbH & Co. KGaA, ISBN: 978-3-527-30519-3, p. 408, 2002.
[76] X. Stephenne, M. Foretz, N. Taleux, G. C. van der Zon, E. Sokal, L. Hue, B. Viollet, and B. Guigas, “Metformin activates AMP-activated protein kinase in primary human hepatocytes by decreasing cellular energy status,” *Diabetologia*, vol. 54, no. 12, pp. 3101–3110, 2011.
[77] M. C. Towler and D. G. Hardie, “AMP-activated protein kinase in metabolic control and insulin signaling,” *Circulation Research*, vol. 100, no. 3, pp. 328–341, 2007.
[78] A. Woods, K. Dickerson, R. Heath, S.-P. Hong, M. Momcilovic, S. R. Johnstone, M. Carlson, and D. Carling, “Ca2+/calmodulin-dependent protein kinase kinase-beta acts upstream of AMP-activated protein kinase in mammalian cells,” *Cell Metabolism*, vol. 2, no. 1, pp. 21–33, 2005.
[79] S. A. Hawley, D. A. Pan, K. J. Mustard, L. Ross, J. Bain, A. M. Edelman, B. G.

Frenguelli, and D. G. Hardie, “Calmodulin-dependent protein kinase kinase-β is an alternative upstream kinase for AMP-activated protein kinase,” *Cell Metabolism*, vol. 2, no. 1, pp. 9–19, 2005.

[80] M. Foretz, S. Hébrard, J. Leclerc, E. Zarrinpashneh, M. Soty, G. Mithieux, K. Sakamoto, F. Andreelli, and B. Viollet, “Metformin inhibits hepatic gluconeogenesis in mice independently of the LKB1/AMPK pathway via a decrease in hepatic energy state,” *The Journal of Clinical Investigation*, vol. 120, no. 7, pp. 2355–2369, 2010.

[81] B. Viollet, B. Guigas, N. Sanz Garcia, J. Leclerc, M. Foretz, and F. Andreelli, “Cellular and molecular mechanisms of metformin: an overview,” *Clinical Science*, vol. 122, no. 6, pp. 253–270, 2012.

[82] J.-P. Fulgencio, C. Kohl, J. Girard, and J.-P. Pégorier, “Effect of metformin on fatty acid and glucose metabolism in freshly isolated hepatocytes and on specific gene expression in cultured hepatocytes,” *Biochemical Pharmacology*, vol. 62, no. 4, pp. 439–446, 2001.

[83] J. E. Gunton, P. J. D. Delhanty, S.-I. Takahashi, and R. C. Baxter, “Metformin rapidly increases insulin receptor activation in human liver and signals preferentially through insulin-receptor substrate-2,” *The Journal of Clinical Endocrinology & Metabolism*, vol. 88, no. 3, pp. 1323–1332, 2003.

[84] S. Rice, L. J. Pellatt, S. J. Bryan, S. A. Whitehead, and H. D. Mason, “Action of metformin on the insulin-signaling pathway and on glucose transport in human granulosa cells,” *The Journal of Clinical Endocrinology & Metabolism*, vol. 96, no. 3, pp. E427–E435, 2011.

[85] J. M. Lord, S. I. White, C. J. Bailey, T. W. Atkins, R. F. Fletcher, and K. G. Taylor, “Effect of metformin on insulin receptor binding and glycaemic control in type II diabetes,” *British Medical Journal (Clinical Research Ed.)*, vol. 286, no. 6368, pp. 830–831, 1983.

[86] E. J. Meuillet, N. Wiernsperger, B. Mania-Farnell, P. Hubert, and G. Cremel, “Metformin modulates insulin receptor signaling in normal and cholesterol-treated human hepatoma cells (HepG2),” *European Journal of Pharmacology*, vol. 377, no. 2–3, pp. 241–252, 1999.

[87] R. Wahdan-Alaswad, Z. Fan, S. M. Edgerton, B. Liu, X.-S. Deng, S. Salling Arnadottir, J. K. Richer, S. M. Anderson, and A. D. Thor, “Glucose promotes breast cancer aggression and reduces metformin efficacy,” *Cell Cycle*, vol. 12, no. 24, pp. 3759–3769, 2013.

[88] M. G. Vander Heiden, L. C. Cantley, and C. B. Thompson, “Understanding the Warburg effect: the metabolic requirements of cell proliferation,” *Science*, vol. 324, no. 5930, pp. 1029–1033, 2009.

[89] G. Zhou, R. Myers, Y. Li, Y. Chen, X. Shen, J. Fenyk-Melody, M. Wu, J. Ventre, T. Doebber, N. Fujii, N. Musi, M. F. Hirshman, L. J. Goodyear, and D. E. Moller, “Role of AMP-activated protein kinase in mechanism of metformin action,” *The Journal of Clinical Investigation*, vol. 108, no. 8, pp. 1167–1174, 2001.

[90] R. Pryor and F. Cabreiro, “Repurposing metformin: an old drug with new tricks in its binding pockets,” *Biochemical Journal*, vol. 471, no. 3, pp. 307–322, 2015.

[91] Diabetes Prevention Program Research Group, “Reduction in the incidence of type 2 diabetes with lifestyle intervention or metformin,” *The New England Journal of Medicine*, vol. 346, no. 6, pp. 393–403, 2002.

[92] J. A. Jara and R. López-Muñoz, “Metformin and cancer: between the bioenergetic disturbances and the antifolate activity,” *Pharmacological Research*, vol. 101, pp. 102–108, 2015.

[93] B. Petrushev, C. Tomuleasa, O. Soritau, M. Aldea, T. Pop, S. Susman, G. Kacso, I.

Berindan, A. Irimie, and V. Cristea, “Metformin plus PIAF combination chemotherapy for hepatocellular carcinoma,” *Experimental Oncology*, vol. 34, no. 1, pp. 17–24, 2012.

[94] T. V. Kourelis and R. D. Siegel, “Metformin and cancer: new applications for an old drug,” *Medical Oncology*, vol. 29, no. 2, pp. 1314–1327, 2012.

[95] H.-P. Chen, J.-J. Shieh, C.-C. Chang, T.-T. Chen, J.-T. Lin, M.-S. Wu, J.-H. Lin, and C.-Y. Wu, “Metformin decreases hepatocellular carcinoma risk in a dose-dependent manner: population-based and in vitro studies,” *Gut*, vol. 62, no. 4, pp. 606–615, 2013.

[96] N. Sadeghi, J. L. Abbruzzese, S.-C. J. Yeung, M. Hassan, and D. Li, “Metformin use is associated with better survival of diabetic patients with pancreatic cancer,” *Clinical Cancer Research*, vol. 18, no. 10, pp. 2905–2912, 2012.

[97] X.-X. He, S. M. Tu, M.-H. Lee, and S.-C. J. Yeung, “Thiazolidinediones and metformin associated with improved survival of diabetic prostate cancer patients,” *Annals of Oncology*, vol. 22, no. 12, pp. 2640–2645, 2011.

[98] M. Bodmer, C. Meier, S. Krähenbühl, S. S. Jick, and C. R. Meier, “Long-term metformin use is associated with decreased risk of breast cancer,” *Diabetes Care*, vol. 33, no. 6, pp. 1304–1308, 2010.

[99] V. Donadon, M. Balbi, M. Dal Mas, P. Casarin, and G. Zanette, “Metformin and reduced risk of hepatocellular carcinoma in diabetic patients with chronic liver disease,” *Liver International*, vol. 30, no. 5, pp. 750–758, 2010.

[100] H. Zhang, C. Gao, L. Fang, H.-C. Zhao, and S.-K. Yao, “Metformin and reduced risk of hepatocellular carcinoma in diabetic patients: a meta-analysis,” *Scandinavian Journal of Gastroenterology*, vol. 48, no. 1, pp. 78–87, 2012.

[101] M. Oldiges, S. Lütz, S. Pflug, K. Schroer, N. Stein, and C. Wiendahl, “Metabolomics: current state and evolving methodologies and tools,” *Applied Microbiology and Biotechnology*, vol. 76, no. 3, pp. 495–511, 2007.

[102] O. Fiehn, “Metabolomics – the link between genotypes and phenotypes,” *Plant Molecular Biology*, vol. 48, no. 1, pp. 155–171, 2002.

[103] J. Adamski, “Genome-wide association studies with metabolomics,” *Genome Medicine*, vol. 4, no. 4, p. 34, 2012.

[104] A. M. Evans, C. D. DeHaven, T. Barrett, M. Mitchell, and E. Milgram, “Integrated, nontargeted ultrahigh performance liquid chromatography/electrospray ionization tandem mass spectrometry platform for the identification and relative quantification of the small-molecule complement of biological systems.,” *Analytical Chemistry*, vol. 81, no. 16, pp. 6656–6667, 2009.

[105] S. Zukunft, M. Sorgenfrei, C. Prehn, G. Möller, and J. Adamski, “Targeted metabolomics of dried blood spot extracts,” *Chromatographia*, vol. 76, no. 19, pp. 1295–1305, 2013.

[106] T. Xu, S. Brandmaier, A. C. Messias, C. Herder, H. H. M. Draisma, A. Demirkan, Z. Yu, J. S. Ried, T. Haller, M. Heier, M. Campillos, G. Fobo, R. Stark, C. Holzapfel, J. Adam, S. Chi, M. Rotter, T. Panni, A. S. Quante, Y. He, C. Prehn, W. Roemisch-Margl, G. Kastenmüller, G. Willemsen, R. Pool, K. Kasa, K. W. van Dijk, T. Hankemeier, C. Meisinger, B. Thorand, A. Ruepp, M. Hrabě de Angelis, Y. Li, H.-E. Wichmann, B. Stratmann, K. Strauch, A. Metspalu, C. Gieger, K. Suhre, J. Adamski, T. Illig, W. Rathmann, M. Roden, A. Peters, C. M. van Duijn, D. I. Boomsma, T. Meitinger, and R. Wang-Sattler, “Effects of metformin on metabolite profiles and LDL cholesterol in patients with type 2 diabetes,” *Diabetes Care*, vol. 38, no. 10, pp. 1858–1867, 2015.

[107] C. Menni, E. Fauman, I. Erte, J. R. B. Perry, G. Kastenmüller, S.-Y. Shin, A.-K. Petersen, C. Hyde, M. Psatha, K. J. Ward, W. Yuan, M. Milburn, C. N. A. Palmer, T.

M. Frayling, J. Trimmer, J. T. Bell, C. Gieger, R. P. Mohney, M. J. Brosnan, K. Suhre, N. Soranzo, and T. D. Spector, "Biomarkers for type 2 diabetes and impaired fasting glucose using a nontargeted metabolomics approach," *Diabetes*, vol. 62, no. 12, pp. 4270–4276, 2013.

[108] R. Wang-Sattler, Z. Yu, C. Herder, A. C. Messias, A. Floegel, Y. He, K. Heim, M. Campillos, C. Holzapfel, B. Thorand, H. Grallert, T. Xu, E. Bader, C. Huth, K. Mittelstrass, A. Döring, C. Meisinger, C. Gieger, C. Prehn, W. Roemisch-Margl, M. Carstensen, L. Xie, H. Yamanaka-Okumura, G. Xing, U. Ceglarek, J. Thiery, G. Giani, H. Lickert, X. Lin, Y. Li, H. Boeing, H.-G. Joost, M. Hrabě de Angelis, W. Rathmann, K. Suhre, H. Prokisch, A. Peters, T. Meitinger, M. Roden, H.-E. Wichmann, T. Pischon, J. Adamski, and T. Illig, "Novel biomarkers for pre-diabetes identified by metabolomics," *Molecular Systems Biology*, vol. 8, no. 1, p. 615, 2012.

[109] M. Rottenkolber, C. Muschet, M. Breier, M. Fugmann, V. Sacco, M. Weise, S. Heinrich, C. Prehn, H. Grallert, M. Bidlingmaier, M. Hrabě de Angelis, J. Seissler, M. Reincke, J. Adamski, U. Ferrari, and A. Lechner, "Targeted metabolomics to predict the primary success of metformin monotherapy in type 2 diabetes," *Scientific Reports (Submitted)*.

[110] A. Scalbert, L. Brennan, O. Fiehn, T. Hankemeier, B. S. Kristal, B. van Ommen, E. Pujos-Guillot, E. Verheij, D. Wishart, and S. Wopereis, "Mass-spectrometry-based metabolomics: limitations and recommendations for future progress with particular focus on nutrition research," *Metabolomics*, vol. 5, no. 4, pp. 435–458, 2009.

[111] European Medicines Agency (EMA) Committee for Medicinal Products for Human Use (CHMP), "Guideline on bioanalytical method validation. EMEA/CHMP/EWP/192217/2009 Rev. 1 Corr. 2**," *21 July 2011, Effective 1 February 2012*. http://www.ema.europa.eu/docs/en_GB/document_library/Scientific_guideline/2011/08/WC500109686.pdf (Accessed: 08/13/2016).

[112] M. Breier, S. Wahl, C. Prehn, M. Fugmann, U. Ferrari, M. Weise, F. Banning, J. Seissler, H. Grallert, J. Adamski, and A. Lechner, "Targeted metabolomics identifies reliable and stable metabolites in human serum and plasma samples," *PLoS one*, vol. 9, no. 2, p. e89728, 2014.

[113] US Department of Health and Human Services Food and Drug Administration (CDER) and (CVM), "Guidance for industry. Bioanalytical method validation.," *May 2001*. http://www.fda.gov/downloads/Drugs/Guidance/ucm070107.pdf (Accessed: 08/13/2016).

[114] O. Fiehn, D. Robertson, J. Griffin, M. van der Werf, B. Nikolau, N. Morrison, L. W. Sumner, R. Goodacre, N. W. Hardy, C. Taylor, J. Fostel, B. Kristal, R. Kaddurah-Daouk, P. Mendes, B. van Ommen, J. C. Lindon, and S.-A. Sansone, "The metabolomics standards initiative (MSI)," *Metabolomics*, vol. 3, no. 3, pp. 175–178, 2007.

[115] A. Halama, "Metabolomics in cell culture-a strategy to study crucial metabolic pathways in cancer development and the response to treatment," *Archives of Biochemistry and Biophysics*, vol. 564, pp. 100–109, 2014.

[116] Q. Teng, W. Huang, T. W. Collette, D. R. Ekman, and C. Tan, "A direct cell quenching method for cell-culture based metabolomics," *Metabolomics*, vol. 5, no. 2, pp. 199–208, 2009.

[117] C. Muschet, G. Möller, C. Prehn, M. Hrabě de Angelis, J. Adamski, and J. Tokarz, "Removing the bottlenecks of cell culture metabolomics: fast normalization procedure, correlation of metabolites to cell number, and impact of the cell harvesting method," *Metabolomics*, vol. 12, no. 10, p. 151, 2016.

[118] H. Bi, K. W. Krausz, S. K. Manna, F. Li, C. H. Johnson, and F. J. Gonzalez, "Optimization of harvesting, extraction, and analytical protocols for UPLC-ESI-MS-based metabolomic analysis of adherent mammalian cancer cells," *Analytical and Bioanalytical Chemistry*, vol. 405, no. 15, pp. 5279–5289, 2013.
[119] Z. Ser, X. Liu, N. N. Tang, and J. W. Locasale, "Extraction parameters for metabolomics from cultured cells," *Analytical Biochemistry*, vol. 475, pp. 22–28, 2015.
[120] K. Dettmer, N. Nürnberger, H. Kaspar, M. A. Gruber, M. F. Almstetter, and P. J. Oefner, "Metabolite extraction from adherently growing mammalian cells for metabolomics studies: optimization of harvesting and extraction protocols," *Analytical and Bioanalytical Chemistry*, vol. 399, no. 3, pp. 1127–1139, 2011.
[121] L. P. Silva, P. L. Lorenzi, P. Purwaha, V. Yong, D. H. Hawke, and J. N. Weinstein, "Measurement of DNA concentration as a normalization strategy for metabolomic data from adherent cell lines," *Analytical Chemistry*, vol. 85, no. 20, pp. 9536–9542, 2013.
[122] A. Hutschenreuther, A. Kiontke, G. Birkenmeier, and C. Birkemeyer, "Comparison of extraction conditions and normalization approaches for cellular metabolomics of adherent growing cells with GC-MS," *Analytical Methods*, vol. 4, no. 7, pp. 1953–1963, 2012.
[123] G.-Y. Chen, H.-W. Liao, I.-L. Tsai, Y. J. Tseng, and C.-H. Kuo, "Using the matrix-induced ion suppression method for concentration normalization in cellular metabolomics studies," *Analytical Chemistry*, vol. 87, no. 19, pp. 9731–9739, 2015.
[124] B. Cao, J. Aa, G. Wang, X. Wu, L. Liu, M. Li, J. Shi, X. Wang, C. Zhao, T. Zheng, S. Guo, and J. Duan, "GC-TOFMS analysis of metabolites in adherent MDCK cells and a novel strategy for identifying intracellular metabolic markers for use as cell amount indicators in data normalization," *Analytical and Bioanalytical Chemistry*, vol. 400, no. 9, pp. 2983–2993, 2011.
[125] M. Wabitsch, R. E. Brenner, I. Melzner, M. Braun, P. Möller, E. Heinze, K.-M. Debatin, and H. Hauner, "Characterization of a human preadipocyte cell strain with high capacity for adipose differentiation," *International Journal of Obesity*, vol. 25, no. 1, pp. 8–15, 2001.
[126] R Core Team, "R: A language and environment for statistical computing." R Foundation for Statistical Computing (http://www.R-project.org/), Vienna, Austria, 2014.
[127] M. P. van Iersel, T. Kelder, A. R. Pico, K. Hanspers, S. Coort, B. R. Conklin, and C. Evelo, "Presenting and exploring biological pathways with PathVisio," *BMC Bioinformatics*, vol. 9, p. 399, 2008.
[128] M. Kutmon, M. P. van Iersel, A. Bohler, T. Kelder, N. Nunes, A. R. Pico, and C. T. Evelo, "PathVisio 3: An Extendable Pathway Analysis Toolbox," *PLoS Computational Biology*, vol. 11, no. 2, p. e1004085, 2015.
[129] J. Ye, G. Coulouris, I. Zaretskaya, I. Cutcutache, S. Rozen, and T. L. Madden, "Primer-BLAST: a tool to design target-specific primers for polymerase chain reaction," *BMC Bioinformatics*, vol. 13, p. 134, 2012.
[130] C. L. Muschet, "Cell culture based assay for metabolic changes caused by nutrients and anti-diabetic substances," (Master´s thesis), Munich: Technical University Munich, 2012.
[131] J. J. Tokarz, "Catabolism of glucocorticoids – novel pathways for stress reduction in zebrafish," (PhD thesis), Munich: Technical University Munich, 2012.
[132] W. Römisch-Margl, C. Prehn, R. Bogumil, C. Röhring, K. Suhre, and J. Adamski, "Procedure for tissue sample preparation and metabolite extraction for high-throughput targeted metabolomics," *Metabolomics*, vol. 8, no. 1, pp. 133–142, 2012.

[133] J. Xia, N. Psychogios, N. Young, and D. S. Wishart, “MetaboAnalyst: a web server for metabolomic data analysis and interpretation,” *Nucleic Acids Research*, vol. 37, no. suppl 2, pp. W652–W660, 2009.
[134] R. A. van den Berg, H. C. J. Hoefsloot, J. A. Westerhuis, A. K. Smilde, and M. J. van der Werf, “Centering, scaling, and transformations: improving the biological information content of metabolomics data,” *BMC Genomics*, vol. 7, p. 142, 2006.
[135] J. Xia and D. S. Wishart, “Metabolomic data processing, analysis, and interpretation using MetaboAnalyst,” *Current Protocols in Bioinformatics*, p. 14.10.1-14.10.48, 2011.
[136] J. Xia, R. Mandal, I. V Sinelnikov, D. Broadhurst, and D. S. Wishart, “MetaboAnalyst 2.0 - a comprehensive server for metabolomic data analysis,” *Nucleic Acids Research*, vol. 40, no. W1, pp. W127–W133, 2012.
[137] J. Xia, I. V. Sinelnikov, B. Han, and D. S. Wishart, “MetaboAnalyst 3.0 - making metabolomics more meaningful,” *Nucleic Acids Research*, vol. 43, no. W1, pp. W251–W257, 2015.
[138] J. Xia and D. S. Wishart, “Web-based inference of biological patterns, functions and pathways from metabolomic data using MetaboAnalyst,” *Nature Protocols*, vol. 6, no. 6, pp. 743–760, 2011.
[139] W. R. Proctor, D. L. Bourdet, and D. Thakker, “Mechanisms underlying saturable intestinal absorption of metformin,” *Drug Metabolism and Disposition*, vol. 36, no. 8, pp. 1650–1658, 2008.
[140] A. Halama, G. Möller, and J. Adamski, “Metabolic signatures in apoptotic human cancer cell lines,” *Omics A Journal of Integrative Biology*, vol. 15, no. 5, pp. 325–335, 2011.
[141] A. M. Halama, “Analyses of metabolic pathways of cellular processes in apoptosis and adipogenesis,” (PhD thesis), Munich: Technical University Munich, 2013.
[142] K. N. Diakopoulos, M. Lesina, S. Wörmann, L. Song, M. Aichler, L. Schild, A. Artati, W. Römisch-Margl, T. Wartmann, R. Fischer, Y. Kabiri, H. Zischka, W. Halangk, I. E. Demir, C. Pilsak, A. Walch, C. S. Mantzoros, J. M. Steiner, M. Erkan, R. M. Schmid, H. Witt, J. Adamski, and H. Algül, “Impaired autophagy induces chronic atrophic pancreatitis in mice via sex- and nutrition-dependent processes,” *Gastroenterology*, vol. 148, no. 3, p. 626–638.e17, 2015.
[143] M. Torchiano, “effsize: efficient effect size computation. R package version 0.6.4,” 2016. https://cran.r-project.org/package=effsize (Accessed: 08/13/2016).
[144] R. Scherer, “samplesize: sample size calculation for Various t-Tests and Wilcoxon-Test. R package version 0.2-2.,” 2015. https://cran.r-project.org/package=samplesize (Accessed: 08/13/2016).
[145] T. Hothorn, K. Hornik, M. A. van de Wiel, and A. Zeileis, “A Lego system for conditional inference,” *The American Statistician*, vol. 60, no. 3, pp. 257–263, 2006.
[146] T. Hothorn, K. Hornik, M. A. van de Wiel, and A. Zeileis, “Implementing a class of permutation tests: the coin package,” *Journal of Statistical Software*, vol. 28, no. 8, pp. 1–23, 2008.
[147] T. Hothorn and K. Hornik, “exactRankTests: exact distributions for rank and permutation tests. R package version 0.8-28,” 2015. http://cran.r-project.org/package=exactRankTests (Accessed: 08/13/2016).
[148] A. I. McLeod, “Kendall: Kendall rank correlation and Mann-Kendall trend test. R package version 2.2,” 2011. http://cran.r-project.org/package=Kendall (Accessed: 08/13/2016).
[149] A. Henningsen and O. Toomet, “miscTools: miscellaneous tools and utilities. R package version 0.6-16,” 2013. https://cran.r-project.org/package=miscTools

(Accessed: 08/13/2016).
[150] H. Wickham, “The split-apply-combine strategy for data analysis,” *Journal of Statistical Software*, vol. 40, no. 1, pp. 1–29, 2011.
[151] J. L. Gastwirth, Y. R. Gel, W. W. L. Hui, W. Miao, and K. Noguchi, “lawstat: tools for biostatistics, public policy, and law. R package version 3.0,” 2015. https://cran.r-project.org/package=lawstat (Accessed: 08/13/2016).
[152] H. Wickham, *ggplot2: elegant graphics for data analysis*. Springer-Verlag New York, ISBN: 978-0-387-98140-6, 2009.
[153] G. Grothendieck, “nls2: non-linear regression with brute force. R package version 0.2,” 2013. https://cran.r-project.org/package=nls2 (Accessed: 08/13/2016).
[154] Y. Cao, A. Charisi, L.-C. Cheng, T. Jiang, and T. Girke, “ChemmineR: a compound mining framework for R,” *Bioinformatics*, vol. 24, no. 15, pp. 1733–1734, 2008.
[155] Y. Wang, T. W. H. Backman, K. Horan, and T. Girke, “fmcsR: mismatch tolerant maximum common substructure searching in R,” *Bioinformatics*, vol. 29, no. 21, pp. 2792–2794, 2013.
[156] R. Suzuki and H. Shimodaira, “pvclust: hierarchical clustering with p-values via multiscale bootstrap resampling. R package version 2.0-0,” 2015. https://cran.r-project.org/package=pvclust (Accessed: 08/13/2016).
[157] R. Kolde, “pheatmap: pretty heatmaps. R package version 1.0.8,” 2015. http://cran.r-project.org/package=pheatmap (Accessed: 08/13/2016).
[158] D. Voet, J. G. Voet, and C. W. Pratt, *Lehrbuch der Biochemie*. Weinheim: WILEY-VCH Verlag GmbH & Co. KGaA, ISBN: 978-3-527-30519-3, 2002.
[159] L. Michaelis and M. L. Menten, “Die Kinetik der Invertinwirkung,” *Biochemische Zeitschrift*, vol. 49, pp. 333–369, 1913.
[160] K. A. Johnson and R. S. Goody, “The original Michaelis constant: translation of the 1913 Michaelis–Menten paper,” *Biochemistry*, vol. 50, no. 39, pp. 8264–8269, 2011.
[161] H. Lineweaver and D. Burk, “The determination of enzyme dissociation constants,” *Journal of the American Chemical Society*, vol. 56, no. 3, pp. 658–666, 1934.
[162] R. J. Leatherbarrow, “Using linear and non-linear regression to fit biochemical data,” *Trends in Biochemical Sciences*, vol. 15, no. 12, pp. 455–458, 1990.
[163] D. S. Wishart, D. Tzur, C. Knox, R. Eisner, A. C. Guo, N. Young, D. Cheng, K. Jewell, D. Arndt, S. Sawhney, C. Fung, L. Nikolai, M. Lewis, M.-A. Coutouly, I. Forsythe, P. Tang, S. Shrivastava, K. Jeroncic, P. Stothard, G. Amegbey, D. Block, D. D. Hau, J. Wagner, J. Miniaci, M. Clements, M. Gebremedhin, N. Guo, Y. Zhang, G. E. Duggan, G. D. MacInnis, A. M. Weljie, R. Dowlatabadi, F. Bamforth, D. Clive, R. Greiner, L. Li, T. Marrie, B. D. Sykes, H. J. Vogel, and L. Querengesser, “HMDB: the Human Metabolome Database,” *Nucleic Acids Research*, vol. 35, no. Database issue, pp. D521–D526, 2007.
[164] D. S. Wishart, C. Knox, A. C. Guo, R. Eisner, N. Young, B. Gautam, D. D. Hau, N. Psychogios, E. Dong, S. Bouatra, R. Mandal, I. Sinelnikov, J. Xia, L. Jia, J. A. Cruz, E. Lim, C. A. Sobsey, S. Shrivastava, P. Huang, P. Liu, L. Fang, J. Peng, R. Fradette, D. Cheng, D. Tzur, M. Clements, A. Lewis, A. De Souza, A. Zuniga, M. Dawe, Y. Xiong, D. Clive, R. Greiner, A. Nazyrova, R. Shaykhutdinov, L. Li, H. J. Vogel, and I. Forsythe, “HMDB: a knowledgebase for the human metabolome,” *Nucleic Acids Research*, vol. 37, no. Database issue, pp. D603–D610, 2009.
[165] D. S. Wishart, T. Jewison, A. C. Guo, M. Wilson, C. Knox, Y. Liu, Y. Djoumbou, R. Mandal, F. Aziat, E. Dong, S. Bouatra, I. Sinelnikov, D. Arndt, J. Xia, P. Liu, F. Yallou, T. Bjorndahl, R. Perez-Pineiro, R. Eisner, F. Allen, V. Neveu, R. Greiner, and A. Scalbert, “HMDB 3.0 - The Human Metabolome Database in 2013,” *Nucleic Acids Research*, vol. 41, no. Database issue, pp. D801–D807, 2013.

[166] D. S. Wishart, C. Knox, A. C. Guo, S. Shrivastava, M. Hassanali, P. Stothard, Z. Chang, and J. Woolsey, "DrugBank: a comprehensive resource for in silico drug discovery and exploration," *Nucleic Acids Research*, vol. 34, no. Database issue, pp. D668–D672, 2006.
[167] D. R. Flower, "On the properties of bit string-based measures of chemical similarity," *Journal of Chemical Information and Modeling*, vol. 38, no. 3, pp. 379–386, 1998.
[168] X. Chen and C. H. Reynolds, "Performance of similarity measures in 2D fragment-based similarity searching: comparison of structural descriptors and similarity coefficients," *Journal of Chemical Information and Computer Sciences*, vol. 42, no. 6, pp. 1407–1414, 2002.
[169] S. S. Shapiro and M. B. Wilk, "An analysis of variance test for normality (complete samples)," *Biometrika*, vol. 52, no. 3/4, pp. 591–611, 1965.
[170] H. Levene, "Robust tests for equality of variances," in *Contributions to Probability and Statistics: Essays in Honor of Harold Hotelling*, I. Olkin, S. G. Ghurye, W. Hoeffding, W. G. Madow, and H. B. Mann, Eds. Stanford: Stanford University Press, ISBN: 978-0804705967, 1960, pp. 278–292.
[171] B. Everitt and T. Hothorn, *An introduction to applied multivariate analysis with R*. New York: Springer Science+Business Media, ISBN: 978-1-4419-9649-7, pp. 18-19, 2011.
[172] F. Wilcoxon, "Individual comparisons by ranking methods," *Biometrics Bulletin*, vol. 1, no. 6, pp. 80–83, 1945.
[173] H. B. Mann and D. R. Whitney, "On a test of whether one of two random variables is stochastically larger than the other," *The Annals of Mathematical Statistics*, vol. 18, no. 1, pp. 50–60, 1947.
[174] W. H. Kruskal and W. A. Wallis, "Use of ranks in one-criterion variance analysis," *Journal of the American Statistical Association*, vol. 47, no. 260, pp. 583–621, 1952.
[175] J. M. Bland and D. G. Altman, "Multiple significance tests: the Bonferroni method," *British Medical Journal*, vol. 310, no. 6973, p. 170, 1995.
[176] Y. Benjamini and Y. Hochberg, "Controlling the false discovery rate: a practical and powerful approach to multiple testing," *Journal of the Royal Statistical Society. Series B (Methological)*, vol. 57, no. 1, pp. 289–300, 1995.
[177] J. Romano, J. D. Kromrey, J. Coraggio, J. Skowronek, and L. Devine, "Exploring methods for evaluating group differences on the NSSE and other surveys: are the t-test and Cohen's d indices the most appropriate choices?," *Annual meeting of the Southern Association for Institutional Research*, pp. 1–51, 2006.
[178] G. MacBeth, E. Razumiejczyk, and R. Ledsema, "Cliff 's Delta Calculator: a non-parametric effect size program for two groups of observations," *Universitas Psychologica*, vol. 10, no. 2, pp. 545–555, 2011.
[179] A. Ly, M. F. Scheerer, S. Zukunft, C. Muschet, J. Merl, J. Adamski, M. Hrabě de Angelis, S. Neschen, S. M. Hauck, and M. Ueffing, "Retinal proteome alterations in a mouse model of type 2 diabetes," *Diabetologia*, vol. 57, no. 1, pp. 192–203, 2014.
[180] S. Zukunft, "Metabolomic analysis of antidiabetic drug action," (PhD thesis) (Submitted), Munich: Technical University Munich.
[181] M. A. S. Marques, A. de S. Soares, O. W. Pinto, P. T. W. Barroso, D. P. Pinto, M. Ferreira-Filho, and E. Werneck-Barroso, "Simple and rapid method determination for metformin in human plasma using high performance liquid chromatography tandem mass spectrometry: Application to pharmacokinetic studies," *Journal of Chromatography B*, vol. 852, no. 1–2, pp. 308–316, 2007.
[182] Y. Wang, Y. Tang, J. Gu, J. P. Fawcett, and X. Bai, "Rapid and sensitive liquid chromatography-tandem mass spectrometric method for the quantitation of metformin

in human plasma," *Journal of Chromatography B*, vol. 808, no. 2, pp. 215–219, 2004.
[183] V. Rizzatti, F. Boschi, M. Pedrotti, E. Zoico, A. Sbarbati, and M. Zamboni, "Lipid droplets characterization in adipocyte differentiated 3T3-L1 cells: Size and optical density distribution," *European Journal of Histochemistry*, vol. 57, no. 3, p. e24, 2013.
[184] M. Vogeser and C. Seger, "Pitfalls associated with the use of liquid chromatography–tandem mass spectrometry in the clinical laboratory," *Clinical Chemistry*, vol. 56, no. 8, pp. 1234–1244, 2010.
[185] W. Müller and F. Gautier, "Interactions of heteroaromatic compounds with nucleic acids. A · T-specific non-intercalating DNA ligands," *European Journal of Biochemistry*, vol. 54, no. 2, pp. 385–394, 1975.
[186] A. Böhm, A. Halama, T. Meile, M. Zdichavsky, R. Lehmann, C. Weigert, A. Fritsche, N. Stefan, A. Königsrainer, H.-U. Häring, M. Hrabě de Angelis, J. Adamski, and H. Staiger, "Metabolic signatures of cultured human adipocytes from metabolically healthy versus unhealthy obese individuals," *PLoS one*, vol. 9, no. 4, p. e93148, 2014.
[187] C. Leys, C. Ley, O. Klein, P. Bernard, and L. Licata, "Detecting outliers: Do not use standard deviation around the mean, use absolute deviation around the median," *Journal of Experimental Social Psychology*, vol. 49, no. 4, pp. 764–766, 2013.
[188] C. Jourdan, A.-K. Petersen, C. Gieger, A. Döring, T. Illig, R. Wang-Sattler, C. Meisinger, A. Peters, J. Adamski, C. Prehn, K. Suhre, E. Altmaier, G. Kastenmüller, W. Römisch-Margl, F. J. Theis, J. Krumsiek, H.-E. Wichmann, and J. Linseisen, "Body fat free mass is associated with the serum metabolite profile in a population-based study," *PLoS one*, vol. 7, no. 6, p. e40009, 2012.
[189] M. Morrison, C. Klein, N. Clemann, D. A. Collier, J. Hardy, B. Heißerer, M. Z. Cader, M. Graf, and J. Kaye, "StemBANCC: governing access to material and data in a large stem cell research consortium," *Stem Cell Reviews and Reports*, vol. 11, no. 5, pp. 681–687, 2015.
[190] A. M. Zivkovic, M. M. Wiest, U. T. Nguyen, R. Davis, S. M. Watkins, and B. J. German, "Effects of sample handling and storage on quantitative lipid analysis in human serum," *Metabolomics*, vol. 5, no. 4, pp. 507–516, 2009.
[191] P. M. Abuja, F. Ehrhart, U. Schoen, T. Schmidt, F. Stracke, G. Dallmann, T. Friedrich, H. Zimmermann, and K. Zatloukal, "Alterations in human liver metabolome during prolonged cryostorage," *Journal of Proteome Research*, vol. 14, no. 7, pp. 2758–2768, 2015.
[192] P. L. Yeagle, "Lipid regulation of cell membrane structure and function," *The FASEB Journal*, vol. 3, no. 7, pp. 1833–1842, 1989.
[193] Y. Sogame, A. Kitamura, M. Yabuki, S. Komuro, and M. Takano, "Transport of biguanides by human organic cation transporter OCT2," *Biomedicine & Pharmacotherapy*, vol. 67, no. 5, pp. 425–430, 2013.
[194] J.-Y. Chung, S. K. Cho, T. H. Kim, K. H. Kim, G. H. Jang, C. O. Kim, E.-M. Park, J.-Y. Cho, I.-J. Jang, and J. H. Choi, "Functional characterization of MATE2-K genetic variants and their effects on metformin pharmacokinetics," *Pharmacogenetics and Genomics*, vol. 23, no. 7, pp. 365–373, 2013.
[195] H. Yoon, H.-Y. Cho, H.-D. Yoo, S.-M. Kim, and Y.-B. Lee, "Influences of organic cation transporter polymorphisms on the population pharmacokinetics of metformin in healthy subjects," *The AAPS Journal*, vol. 15, no. 2, pp. 571–580, 2013.
[196] "Gebrauchsinformation: Information für Anwender, Glycophage® 500 mg Filmtabletten," 2015. https://www.bfarm.de/SharedDocs/Downloads/DE/Arzneimittel/Pharmakovigilanz/Risikoinformationen/RI_rhb/2015/Glucophage500mg_Packungsbeilage.pdf?__blob=publicationFile&v=3 (Accessed: 08/08/2016).

[197] G. Gusler, J. Gorsline, G. Levy, S. Z. Zhang, I. E. Weston, D. Naret, and B. Berner, "Pharmacokinetics of metformin gastric-retentive tablets in healthy volunteers," *The Journal of Clinical Pharmacology*, vol. 41, no. 6, pp. 655–661, 2001.

[198] L. Blonde, G. E. Dailey, S. A. Jabbour, C. A. Reasner, and D. J. Mills, "Gastrointestinal tolerability of extended-release metformin tablets compared to immediate-release metformin tablets: results of a retrospective cohort study," *Current Medical Research and Opinion*, vol. 20, no. 4, pp. 565–572, 2004.

[199] Y. Sogame, A. Kitamura, M. Yabuki, and S. Komuro, "A comparison of uptake of metformin and phenformin mediated by hOCT1 in human hepatocytes," *Biopharmaceutics & Drug Disposition*, vol. 30, no. 8, pp. 476–484, 2009.

[200] T. Mehrens, S. Lelleck, Ç. Ibrahim, M. Knollmann, H. Hohage, V. Gorboulev, P. Bokník, H. Koepsell, and E. Schlatter, "The affinity of the organic cation transporter rOCT1 is increased by protein kinase C-dependent phosphorylation," *Journal of the American Society of Nephrology*, vol. 11, no. 7, pp. 1216–1224, 2000.

[201] G. Pietig, T. Mehrens, J. R. Hirsch, Ç. Ibrahim, H. Piechota, and E. Schlatter, "Properties and regulation of organic cation transport in freshly isolated human proximal tubules," *The Journal of Biological Chemistry*, vol. 276, no. 36, pp. 33741–33746, 2001.

[202] K. Hacker, R. Maas, J. Kornhuber, M. F. Fromm, and O. Zolk, "Substrate-dependent inhibition of the human organic cation transporter OCT2: a comparison of metformin with experimental substrates," *PLoS one*, vol. 10, no. 9, p. e0136451, 2015.

[203] K.-I. Umehara, T. Iwatsubo, K. Noguchi, T. Usui, and H. Kamimura, "Effect of cationic drugs on the transporting activity of human and rat OCT/Oct 1-3 in vitro and implications for drug-drug interactions," *Xenobiotica*, vol. 38, no. 9, pp. 1203–1218, 2008.

[204] M. L. Beckman, A. B. Pramod, D. Perley, and L. K. Henry, "Stereoselective inhibition of serotonin transporters by antimalarial compounds," *Neurochemistry International*, vol. 73, pp. 98–106, 2014.

[205] X. Zhang, N. J. Cherrington, and S. H. Wright, "Molecular identification and functional characterization of rabbit MATE1 and MATE2-K," *American journal of physiology. Renal physiology*, vol. 293, no. 1, pp. F360-370, 2007.

[206] M. Zhou, K. Engel, and J. Wang, "Evidence for significant contribution of a newly identified monoamine transporter (PMAT) to serotonin uptake in the human brain," *Biochemical Pharmacology*, vol. 73, no. 1, pp. 147–154, 2007.

[207] W. Xuan, A.-M. Lamhonwah, C. Librach, K. Jarvi, and I. Tein, "Characterization of organic cation/carnitine transporter family in human sperm," *Biochemical and Biophysical Research Communications*, vol. 306, no. 1, pp. 121–128, 2003.

[208] A. M. A. Pfeifer, K. E. Cole, D. T. Smoot, A. Weston, J. D. Groopman, P. G. Shields, J.-M. Vignaud, M. Juillerat, M. M. Lipsky, B. F. Trump, J. F. Lechner, and C. C. Harris, "Simian virus 40 large tumor antigen-immortalized normal human liver epithelial cells express hepatocyte characteristics and metabolize chemical carcinogens," *Proceedings of the National Academy of Sciences*, vol. 90, no. 11, pp. 5123–5127, 1993.

[209] S. J. Kwon, D. W. Lee, D. A. Shah, B. Ku, S. Y. Jeon, K. Solanki, J. D. Ryan, D. S. Clark, J. S. Dordick, and M.-Y. Lee, "High-throughput and combinatorial gene expression on a chip for metabolism-induced toxicology screening," *Nature Communications*, vol. 5, p. 3739, 2014.

[210] J. V Castell, R. Jover, C. P. Martnez-Jimnez, and M. J. Gmez-Lechn, "Hepatocyte cell lines: their use, scope and limitations in drug metabolism studies," *Expert Opinion on Drug Metabolism & Toxicology*, vol. 2, no. 2, pp. 183–212, 2006.

[211] D.-S. Kim, S.-K. Jeong, H.-R. Kim, D.-S. Kim, S.-W. Chae, and H.-J. Chae, "Metformin regulates palmitate-induced apoptosis and ER stress response in HepG2 liver cells," *Immunopharmacology and Immunotoxicology*, vol. 32, no. 2, pp. 251–257, 2010.

[212] D. P. Aden, A. Fogel, S. Plotkin, I. Damjanov, and B. B. Knowles, "Controlled synthesis of HBsAg in a differentiated human liver carcinoma-derived cell line," *Nature*, vol. 282, pp. 615–616, 1979.

[213] B. B. Knowles, C. C. Howe, and D. P. Aden, "Human hepatocellular carcinoma cell lines secrete the major plasma proteins and hepatitis B surface antigen," *Science*, vol. 209, no. 4455, pp. 497–499, 1980.

[214] L. Guo, S. Dial, L. Shi, W. Branham, J. Liu, J.-L. Fang, B. Green, H. Deng, J. Kaput, and B. Ning, "Similarities and differences in the expression of drug-metabolizing enzymes between human hepatic cell lines and primary human hepatocytes," *Drug Metabolism and Disposition*, vol. 39, no. 3, pp. 528–538, 2011.

[215] L. He, A. Sabet, S. Djedjos, R. Miller, X. Sun, M. A. Hussain, S. Radovick, and F. E. Wondisford, "Metformin and insulin suppress hepatic gluconeogenesis through phosphorylation of CREB binding protein," *Cell*, vol. 137, no. 4, pp. 635–646, 2009.

[216] A. Anedda, E. Rial, and M. M. González-Barroso, "Metformin induces oxidative stress in white adipocytes and raises uncoupling protein 2 levels," *Journal of Endocrinology*, vol. 199, no. 1, pp. 33–40, 2008.

[217] D. Argaud, H. Roth, N. Wiernsperger, and X. M. Levere, "Metformin decreases gluconeogenesis by enhancing the pyruvate kinase flux in isolated rat hepatocytes," *European Journal of Biochemistry*, vol. 213, no. 3, pp. 1341–1348, 1993.

[218] C. Cadeddu, M. Deidda, S. Nocco, E. Locci, E. Cossu, M. G. Baroni, L. Atzori, and G. Mercuro, "Effects of metformin treatment on myocardial and endothelial function in insulin resistance patients: a metabolomic study," *Journal of Diabetes & Metabolism*, vol. 4, no. 6, p. 279, 2013.

[219] Y. Jenkins, T.-Q. Sun, Y. Li, V. Markovtsov, G. Uy, L. Gross, D. A. Goff, S. J. Shaw, L. Boralsky, R. Singh, D. G. Payan, and Y. Hitoshi, "Global metabolite profiling of mice with high-fat diet-induced obesity chronically treated with AMPK activators R118 or metformin reveals tissue-selective alterations in metabolic pathways," *BMC Research Notes*, vol. 7, p. 674, 2014.

[220] K. D. Pagana and T. J. Pagana, *Mosby's manual of diagnostic and laboratory tests*, 5th ed. St. Louis: Elsevier Mosby, ISBN: 978-0-323-08949-4, 2013.

[221] World Health Organization. Department of Noncommunicable Disease Surveillance, "Definition, diagnosis and classification of diabetes mellitus and its complications. Report of a WHO consultation. Part 1: diagnosis and classification of diabetes mellitus," Geneva, 1999.

[222] H. P. Chhetri, P. Thapa, and A. Van Schepdael, "Simple HPLC-UV method for the quantification of metformin in human plasma with one step protein precipitation," *Saudi Pharmaceutical Journal*, vol. 22, no. 5, pp. 483–487, 2014.

[223] L. Chen, Z. Zhou, M. Shen, and A. Ma, "Simultaneous determination and pharmacokinetic study of metformin and rosiglitazone in human plasma by HPLC-ESI-MS," *Journal of Chromatographic Science*, vol. 49, no. 2, pp. 94–100, 2011.

[224] A. Liu and S. P. Coleman, "Determination of metformin in human plasma using hydrophilic interaction liquid chromatography–tandem mass spectrometry," *Journal of Chromatography B*, vol. 877, no. 29, pp. 3695–3700, 2009.

[225] L. K. Sørensen, "Determination of metformin and other biguanides in forensic whole blood samples by hydrophilic interaction liquid chromatography-electrospray tandem mass spectrometry," *Biomedical Chromatography*, vol. 26, no. 1, pp. 1–5, 2012.

[226] A. Ruiz-Aracama, A. Peijnenburg, J. Kleinjans, D. Jennen, J. van Delft, C. Hellfrisch, and A. Lommen, "An untargeted multi-technique metabolomics approach to studying intracellular metabolites of HepG2 cells exposed to 2,3,7,8-tetrachlorodibenzo-p-dioxin," *BMC Genomics*, vol. 12, p. 251, 2011.

[227] L. Chen, M. Takizawa, E. Chen, A. Schlessinger, J. Segenthelar, J. H. Choi, A. Sali, M. Kubo, S. Nakamura, Y. Iwamoto, N. Iwasaki, and K. M. Giacomini, "Genetic polymorphisms in organic cation transporter 1 (OCT1) in chinese and japanese populations exhibit altered function," *The Journal of Pharmacology and Experimental Therapeutics*, vol. 335, no. 1, pp. 42–50, 2010.

[228] M. L. Becker, L. E. Visser, R. H. N. van Schaik, A. Hofman, A. G. Uitterlinden, and B. H. C. Stricker, "Genetic variation in the organic cation transporter 1 is associated with metformin response in patients with diabetes mellitus," *The Pharmacogenomics Journal*, vol. 9, no. 4, pp. 242–247, 2009.

[229] Y. Chen, S. Li, C. Brown, S. Cheatham, R. A. Castro, M. K. Leabman, T. J. Urban, L. Chen, S. W. Yee, J. H. Choi, Y. Huang, C. M. Brett, E. G. Burchard, and K. M. Giacomini, "Effect of genetic variation in the organic cation transporter 2, OCT2, on the renal elimination of metformin," *Pharmacogenetics and Genomics*, vol. 19, no. 7, pp. 497–504, 2009.

[230] K. Sugano, M. Kansy, P. Artursson, A. Avdeef, S. Bendels, L. Di, G. F. Ecker, B. Faller, H. Fischer, G. Gerebtzoff, H. Lennernaes, and F. Senner, "Coexistence of passive and carrier-mediated processes in drug transport," *Nature Reviews Drug Discovery*, vol. 9, no. 8, pp. 597–614, 2010.

[231] Y. Liang, S. Li, and L. Chen, "The physiological role of drug transporters," *Protein & Cell*, vol. 6, no. 5, pp. 334–350, 2015.

[232] L. Chen, Y. Shu, X. Liang, E. C. Chen, S. W. Yee, A. A. Zur, S. Li, L. Xu, K. R. Keshari, M. J. Lin, H.-C. Chien, Y. Zhang, K. M. Morrissey, J. Liu, J. Ostrem, N. S. Younger, J. Kurhanewicz, K. M. Shokat, K. Ashrafi, and K. M. Giacomini, "OCT1 is a high-capacity thiamine transporter that regulates hepatic steatosis and is a target of metformin," *Proceedings of the National Academy of Sciences of the United States of America*, vol. 111, no. 27, pp. 9983–9988, 2014.

[233] N. A. Khan, N. Wiernsperger, V. Quemener, R. Havouis, and J. P. Moulinoux, "Characterization of metformin transport system in NIH 3T3 cells," *Journal of Cellular Physiology*, vol. 152, no. 2, pp. 310–316, 1992.

[234] A. Schlessinger, N. Khuri, K. M. Giacomini, and A. Sali, "Molecular modeling and ligand docking for solute carrier (SLC) transporters," *Current Topics in Medicinal Chemistry*, vol. 13, no. 7, pp. 843–856, 2013.

[235] C. Zhu, K. B. Nigam, R. C. Date, K. T. Bush, S. A. Springer, M. H. J. Saier, W. Wu, and S. K. Nigam, "Evolutionary analysis and classification of OATs, OCTs, OCTNs, and Other SLC22 transporters: structure-function implications and analysis of sequence motifs," *PLoS one*, vol. 10, no. 11, p. e0140569, 2015.

[236] V. Vallon, S. A. Eraly, S. R. Rao, M. Gerasimova, M. Rose, M. Nagle, N. Anzai, T. Smith, K. Sharma, S. K. Nigam, and T. Rieg, "A role for the organic anion transporter OAT3 in renal creatinine secretion in mice," *American journal of physiology. Renal physiology*, vol. 302, no. 10, pp. F1293-1299, 2012.

[237] J. Strobel, F. Müller, O. Zolk, B. Endreß, J. König, M. F. Fromm, and R. Maas, "Transport of asymmetric dimethylarginine (ADMA) by cationic amino acid transporter 2 (CAT2), organic cation transporter 2 (OCT2) and multidrug and toxin extrusion protein 1 (MATE1)," *Amino Acids*, vol. 45, no. 4, pp. 989–1002, 2013.

[238] W. H. Bestermann, Jr., "The ADMA-metformin hypothesis: linking the cardiovascular consequences of the metabolic syndrome and type 2 diabetes," *Cardiorenal Medicine*,

vol. 1, no. 4, pp. 211–219, 2011.
[239] T. Ishida, Z. Chap, J. Chou, R. Lewis, C. Hartley, M. Entman, and J. B. Field, "Differential effects of oral, peripheral intravenous, and intraportal glucose on hepatic glucose uptake and insulin and glucagon extraction in conscious dogs," *The Journal of Clinical Investigation*, vol. 72, no. 2, pp. 590–601, 1983.
[240] D. Voet, J. G. Voet, and C. W. Pratt, *Lehrbuch der Biochemie*. Weinheim: WILEY-VCH Verlag GmbH & Co. KGaA, ISBN: 978-3-527-30519-3, pp. 601-606, 2002.
[241] D. Voet, J. G. Voet, and C. W. Pratt, *Lehrbuch der Biochemie*. Weinheim: WILEY-VCH Verlag GmbH & Co. KGaA, ISBN: 978-3-527-30519-3, p. 493, 2002.
[242] B. D. Ross, R. Hems, and H. A. Krebs, "The rate of gluconeogenesis from various precursors in the perfused rat liver," *Biochemical Journal*, vol. 102, no. 3, pp. 942–951, 1967.
[243] J. M. Argilés and F. J. López-Soriano, "Oxidation of branched-chain amino acids in tumour-bearing rats," *Biochemical Society transactions*, vol. 17, no. 6, pp. 1044–1045, 1989.
[244] A. Watanabe, T. Higashi, T. Sakata, and H. Nagashima, "Serum amino acid levels in patients with hepatocellular carcinoma," *Cancer*, vol. 54, no. 9, pp. 1875–1882, 1984.
[245] D. Voet, J. G. Voet, and C. W. Pratt, *Lehrbuch der Biochemie*. Weinheim: WILEY-VCH Verlag GmbH & Co. KGaA, ISBN: 978-3-527-30519-3, p.666, 2002.
[246] K. Paxton, L. C. Ward, and P. A. Wilce, "Amino acid oxidation in the tumor-bearing rat," *Cancer biochemistry biophysics*, vol. 9, no. 4, pp. 343–351, 1988.
[247] N. Katunuma, M. Okada, and Y. Nishii, "Regulation of the urea cycle and TCA cycle by ammonia," *Advances in Enzyme Regulation*, vol. 4, pp. 317–335, 1966.
[248] D. Voet, J. G. Voet, and C. W. Pratt, *Lehrbuch der Biochemie*. Weinheim: WILEY-VCH Verlag GmbH & Co. KGaA, ISBN: 978-3-527-30519-3, pp. 652-656, 2002.
[249] J. T. Brosnan, "Glutamate, at the interface between amino acid and carbohydrate metabolism," *The Journal of nutrition*, vol. 130, no. 4, p. 988S–990S, 2000.
[250] M. Wyss and R. Kaddurah-Daouk, "Creatine and creatinine metabolism," *Physiological Reviews*, vol. 80, no. 3, pp. 1107–1213, 2000.
[251] S. Zhao, W. Xu, W. Jiang, W. Yu, Y. Lin, T. Zhang, J. Yao, L. Zhou, Y. Zeng, H. Li, Y. Li, J. Shi, W. An, S. M. Hancock, F. He, L. Qin, J. Chin, P. Yang, X. Chen, Q. Lei, Y. Xiong, and K.-L. Guan, "Regulation of cellular metabolism by protein lysine acetylation," *Science*, vol. 327, no. 5968, pp. 1000–1004, 2010.
[252] M. Kanehisa and S. Goto, "KEGG: kyoto encyclopedia of genes and genomes," *Nucleic Acids Research*, vol. 28, no. 1, pp. 27–30, 2000.
[253] M. Kanehisa, Y. Sato, M. Kawashima, M. Furumichi, and M. Tanabe, "KEGG as a reference resource for gene and protein annotation," *Nucleic Acids Research*, vol. 44, no. Database issue, pp. D457-462, 2016.
[254] S. C. Lu, "Glutathione synthesis," *Biochimica et Biophysica Acta*, vol. 1830, no. 5, pp. 3143–3153, 2013.
[255] J. W. Locasale, "Serine, glycine and one-carbon units: cancer metabolism in full circle," *Nature Reviews Cancer*, vol. 13, no. 8, pp. 572–583, 2013.
[256] K. K. Tsuboi, H. N. Edmunds, and L. K. Kwong, "Selective inhibition of pyrimidine biosynthesis and effect on proliferative growth of colonic cancer cells," *Cancer Research*, vol. 37, no. 9, pp. 3080–3087, 1977.
[257] W. W. Souba, "Glutamine and cancer," *Annals of Surgery*, vol. 218, no. 6, pp. 715–728, 1993.
[258] D. Voet, J. G. Voet, and C. W. Pratt, *Lehrbuch der Biochemie*. Weinheim: WILEY-VCH Verlag GmbH & Co. KGaA, ISBN: 978-3-527-30519-3, pp. 439-445, 2002.
[259] D. G. Roth, E. Shelton, and T. F. Deuel, "Purification and Properties of

Phosphoribosyl Pyrophosphate Synthetase from Rat Liver," *The Journal of Biological Chemistry*, vol. 249, no. 1, pp. 291–296, 1974.
[260] D. Voet, J. G. Voet, and C. W. Pratt, *Lehrbuch der Biochemie*. Weinheim: WILEY-VCH Verlag GmbH & Co. KGaA, ISBN: 978-3-527-30519-3, pp. 735-738, 2002.
[261] K. D. Corbin and S. H. Zeisel, "Choline metabolism provides novel insights into nonalcoholic fatty liver disease and its progression," *Current Opinion in Gastroenterology*, vol. 28, no. 2, pp. 159–165, 2012.
[262] A. K. Ghoshal and E. Farber, "The induction of liver cancer by dietary deficiency of choline and methionine without added carcinogens," *Carcinogenesis*, vol. 5, no. 10, pp. 1367–1370, 1984.
[263] S. Kubo, A. Tamori, H. Tanaka, S. Takemura, T. Shuto, K. Hirohashi, H. Kinoshita, and S. Nishiguchi, "Polyamine metabolism and recurrence after resection for hepatocellular carcinoma," *Hepato-gastroenterology*, vol. 51, no. 55, pp. 208–210, 2004.
[264] C. Batandier, B. Guigas, D. Detaille, M.-Y. El-Mir, E. Fontaine, M. Rigoulet, and X. M. Leverve, "The ROS production induced by a reverse-electron flux at respiratory-chain complex 1 is hampered by metformin," *Journal of Bioenergetics and Biomembranes*, vol. 38, no. 1, pp. 33–42, 2006.
[265] D. Voet, J. G. Voet, and C. W. Pratt, *Lehrbuch der Biochemie*. Weinheim: WILEY-VCH Verlag GmbH & Co. KGaA, ISBN: 978-3-527-30519-3, pp. 600-601, 2002.
[266] D. G. Cotter, R. C. Schugar, and P. A. Crawford, "Ketone body metabolism and cardiovascular disease," *American journal of physiology. Heart and circulatory physiology*, vol. 304, no. 8, pp. H1060–H1076, 2013.
[267] T. J. Wang, D. Ngo, N. Psychogios, A. Dejam, M. G. Larson, R. S. Vasan, A. Ghorbani, J. O'Sullivan, S. Cheng, E. P. Rhee, S. Sinha, E. McCabe, C. S. Fox, C. J. O'Donnell, J. E. Ho, J. C. Florez, M. Magnusson, K. A. Pierce, A. L. Souza, Y. Yu, C. Carter, P. E. Light, O. Melander, C. B. Clish, and R. E. Gerszten, "2-Aminoadipic acid is a biomarker for diabetes risk," *The Journal of Clinical Investigation*, vol. 123, no. 10, pp. 4309–4317, 2013.
[268] J. Yaligar, W. W. Teoh, R. Othman, S. K. Verma, B. H. Phang, S. S. Lee, W. W. Wang, H. C. Toh, V. Gopalan, K. Sabapathy, and S. S. Velan, "Longitudinal metabolic imaging of hepatocellular carcinoma in transgenic mouse models identifies acylcarnitine as a potential biomarker for early detection," *Scientific Reports*, vol. 6, p. 20299, 2016.
[269] H. Hama, "Fatty acid 2-hydroxylation in mammalian sphingolipid biology," *Biochimica et Biophysica Acta*, vol. 1801, no. 4, pp. 405–414, 2010.
[270] N. L. Alderson and H. Hama, "Fatty acid 2-hydroxylase regulates cAMP-induced cell cycle exit in D6P2T schwannoma cells," *Journal of Lipid Research*, vol. 50, no. 6, pp. 1203–1208, 2009.
[271] R. Bansal and S. E. Pfeiffer, "Regulated galactolipid synthesis and cell surface expression in Schwann cell line D6P2T," *Journal of Neurochemistry*, vol. 49, no. 6, pp. 1902–1911, 1987.
[272] A. B. Herrero, A. M. Astudillo, M. A. Balboa, C. Cuevas, J. Balsinde, and S. Moreno, "Levels of SCS7/FA2H-mediated fatty acid 2-hydroxylation determine the sensitivity of cells to antitumor PM02734," *Cancer Research*, vol. 68, no. 23, pp. 9779–9787, 2008.
[273] L. Guo, D. Zhou, K. M. Pryse, A. L. Okunade, and X. Su, "Fatty acid 2-hydroxylase mediates diffusional mobility of Raft-associated lipids, GLUT4 level, and lipogenesis in 3T3-L1 adipocytes," *The Journal of Biological Chemistry*, vol. 285, no. 33, pp. 25438–25447, 2010.

[274] R. S. Hundal, M. Krssak, S. Dufour, D. Laurent, V. Lebon, V. Chandramouli, S. E. Inzucchi, W. C. Schumann, K. F. Petersen, B. R. Landau, and G. I. Shulman, "Mechanism by which metformin reduces glucose production in type 2 diabetes," *Diabetes*, vol. 49, no. 12, pp. 2063–2069, 2000.
[275] H. Yoshiji, R. Noguchi, T. Namisaki, K. Moriya, M. Kitade, Y. Aihara, A. Douhara, J. Yamao, M. Fujimoto, M. Toyohara, A. Mitoro, M. Sawai, M. Yoshida, C. Morioka, M. Uejima, M. Uemura, and H. Fukui, "Branched-chain amino acids suppress the cumulative recurrence of hepatocellular carcinoma under conditions of insulin-resistance," *Oncology Reports*, vol. 30, no. 2, pp. 545–552, 2013.
[276] R. C. Nordlie, J. D. Foster, and A. J. Lange, "Regulation of glucose production by the liver," *Annual Review of Nutrition*, vol. 19, pp. 379–406, 1999.
[277] M. E. Rubio-Gozalbo, J. A. Bakker, H. R. Waterham, and R. J. A. Wanders, "Carnitine–acylcarnitine translocase deficiency, clinical, biochemical and genetic aspects," *Molecular Aspects of Medicine*, vol. 25, no. 5–6, pp. 521–532, 2004.
[278] T. Muramatsu, K. Kozaki, S. Imoto, R. Yamaguchi, H. Tsuda, T. Kawano, N. Fujiwara, M. Morishita, S. Miyano, and J. Inazawa, "The hypusine cascade promotes cancer progression and metastasis through the regulation of RhoA in squamous cell carcinoma," *Oncogene*, vol. 35, no. 40, pp. 5304–5316, 2016.
[279] C. Gorrini, I. S. Harris, and T. W. Mak, "Modulation of oxidative stress as an anticancer strategy," *Nature Reviews Drug Discovery*, vol. 12, no. 12, pp. 931–947, 2013.
[280] H. Olle, "Putrescine, spermidine, and spermine," *Physiology*, vol. 1, no. 1, pp. 12–15, 1986.
[281] E. W. Gerner, "Cancer chemoprevention locks onto a new polyamine metabolic target," *Cancer Prevention Research*, vol. 3, no. 2, pp. 125–127, 2010.
[282] T. P. Forshell, S. Rimpi, and J. A. Nilsson, "Chemoprevention of B-cell lymphomas by inhibition of the Myc target spermidine synthase," *Cancer Prevention Research*, vol. 3, no. 2, pp. 140–147, 2010.
[283] J. A. Nettleton and R. Katz, "n-3 long-chain polyunsaturated fatty acids in type 2 diabetes: A review," *Journal of the American Dietetic Association*, vol. 105, no. 3, pp. 428–440, 2005.
[284] J. Delarue, C. LeFoll, C. Corporeau, and D. Lucas, "n-3 long chain polyunsaturated fatty acids: a nutritional tool to prevent insulin resistance associated to type 2 diabetes and obesity?," *Reproduction Nutrition Development*, vol. 44, no. 3, pp. 289–299, 2004.
[285] B. F. McBride, T. Yang, K. Liu, T. J. Urban, K. M. Giacomini, R. B. Kim, and D. M. Roden, "The organic cation transporter, OCTN1, expressed in the human heart, potentiates antagonism of the HERG potassium channel," *Journal of Cardiovascular Pharmacology*, vol. 54, no. 1, pp. 63–71, 2009.
[286] D. Voet, J. G. Voet, and C. W. Pratt, *Lehrbuch der Biochemie*. Weinheim: WILEY-VCH Verlag GmbH & Co. KGaA, ISBN: 978-3-527-30519-3, p. 657, 2002.
[287] F. Murtagh and P. Legendre, "Ward's Hierarchical Agglomerative Clustering Method: Which Algorithms Implement Ward's Criterion?," *Journal of Classification*, vol. 31, no. 3, pp. 274–295, 2014.
[288] P. Legendre and L. Legendre, *Developments in environmental modelling, 20. numerical ecology*, Second Eng. Amsterdam: Elsevier Science B.V., ISBN: 0-444-89249-4; pp.282, 1998.
[289] A. R. Pico, T. Kelder, M. P. van Iersel, K. Hanspers, B. R. Conklin, and C. Evelo, "WikiPathways: pathway editing for the people," *PLoS Biology*, vol. 6, no. 7, p. e184, 2008.
[290] L. Yang, E. Willighagen, K. Hanspers, E. Cirillo, and M. Kutmon, "One carbon donor

(Homo sapiens).” http://www.wikipathways.org/index.php/Pathway:WP2190 (Accessed: 07/27/2016).

Acknowledgements

My sincere and very heartfelt thanks to all who have contributed to the realization of this project and the thesis!

Very cordial thanks to Prof. Dr. Adamski for giving me the great chance to work in his group, for offering me the possibility to pursue this topic, for all the conferences, for all his help and input and for being a fantastic supervisor. Further, I want to thank Prof. Dr. med. Susanna Hofmann for her supervision. Great thanks to Dr. Cornelia Prehn for being my supervisor, for her scientific input and constant support. Also, very heartfelt thanks to Dr. Janina Tokarz, for her fantastic tutorship, for always having an open door, for believing in my ideas and for lots and lots of feedback, input and proofreading. In addition, my sincere thanks to Dr. Gabriele Möller, for her help and scientific input and for a massive amount of proofreading. My cordial thanks to Dr. Anna Artati, who taught me all I know about non-targeted metabolomics, and who let me join in on so many fascinating projects – Thank you for broadening my horizon. Very big thanks to Mark Haid, for opening up the world of R and multivariate analysis to me, for constant support in any situation, for letting me join his fascinating project, for lots (and lots and lots) of brainstorming sessions, for lending me his laptop, when mine broke down during the final stages of writing up, and for so much more. Cordial thanks to PD Dr. med. Andreas Lechner for our collaboration. Further, I want to kindly thank Prof. Dr. med. Wabitsch and Dr. Michaela Keuper for the provision of SGBS cells. Many thanks to Susanne Weber for offering her expertise. Cordial thanks to Marina Rudisch for all her fantastic, diligent work. Very big thanks to Sven Zukunft for introducing the world of cell culture metabolomics to me, for being my tutor, for your constant help, input and feedback; even long after you had finished your own project. Thanks also to Dr. Anna Halama, for helping me with my first steps in cell culture and the trust you placed in me as a scientist. In addition, I want to thank Jannis Bröker, Birgit Meßner and Ivana Ristovski for their dedicated work during their internsips. Last, but for sure not least, very sincere thanks to: Katharina Faschinger, Andrea Kraume, Gabriele Zieglmeier, Bianca Eichner, Silke Becker, Maria Kugler and Marion Schieweg for all your help – without it, there would be no thesis.

Further, I want to seize this opportunity to thank my family, for their help and their support, for always being there and so much more. In addition, I want to give very special thanks to my brother - Alexander - for all those things; for countless hours of (me) talking, for always listening, for explaining lots of math and physics to me and most importantly, for being my best friend.

THANK YOU!

Index of figures

Figure 1: Metformin and its monoprotonated forms. 4
Figure 2: Metformin transport into the cell and action inside the cell. 9
Figure 3: Histograms of the number of non-detected (N. D.) values in samples with different cell numbers. 30
Figure 4: Multiple reaction monitoring (MRM) chromatogram of the optimized LC-MS/MS metformin quantification method using treated Hep G2 cells. 41
Figure 5: Optimization of the incubation time and incubation temperature of the DNA based cell number quantification method. 50
Figure 6: Optimization of the Hoechst 33342 concentration and the sample volume. 51
Figure 7: Impact of the methanol content of the extraction solvent on the fluorescent signal of the optimized DNA quantification method. 53
Figure 8: Standard curves for mammalian cell lines with different properties, culturing conditions and organisms and tissues of origin. 54
Figure 9: Linear correlation of the metabolite concentration to the cell number for Hep G2, HK-2, SGBS and THLE-2 cells. 56
Figure 10: Precision of the analyte concentrations of targeted cell culture metabolomics (1 x 10^6 cells). 57
Figure 11: Precision of the analyte signals of targeted cell culture metabolomics. 60
Figure 12: Optimization of the sample volume for targeted cell culture metabolomics. 62
Figure 13: Impact of the extraction solvent composition on non-targeted cell culture metabolomics. 64
Figure 14: HEK293 and Hep G2 cells exhibit different metabolite profiles. 65
Figure 15: Within-run precision of the non-targeted metabolomics analysis. 66
Figure 16: Precision of the harvesting protocol in combination with non-targeted cell culture metabolomics. 68
Figure 17: Time course analysis of metformin uptake for the determination of the metformin incubation time. 71
Figure 18: Impact of the FBS withdrawal on the cell number. 71
Figure 19: Hepatocellular metformin uptake. 72
Figure 20: Hepatocellular metformin transport kinetics. 73
Figure 21: Inhibition of metformin uptake by ASP^+. 75
Figure 22: Inhibition of metformin uptake by quinidine. 76
Figure 23: Expression of the organic cation transporters OCT1-3 in human cell lines. 76
Figure 24: Expression of the novel organic carnitine/cation/zwitterion transporters OCTN1 and OCTN2 in human cell lines. 77
Figure 25: Expression of the plasma membrane monoamine (PMAT) and the serotonine transporter (SERT) in human cell lines. 78
Figure 26: Expression of the multidrug and toxin extrusion protein 1 (MATE1) in human cell lines. 79
Figure 27: Expression of the thiamine transporter 2 (THTR-2) in human cell lines. 80
Figure 28: THLE-2 and Hep G2 cells were cultivated at physiological (6 mM) or diabetic (11 mM) glucose concentrations and treated with metformin or H_2O. 83
Figure 29: Metformin concentration dependent regulation of intracellular metabolite concentrations. 86
Figure 30: Impact of metformin and glucose concentration on the cell number of Hep G2 and THLE-2 cells in samples for targeted metabolomics. 87
Figure 31: Impact of metformin and glucose concentration on the hepatocellular metabolite profile in samples for targeted metabolomics. 87
Figure 32: Impact of metformin and glucose concentration on the cell number of Hep G2 and THLE-2 cells in samples fo non-targeted metabolomics. 88
Figure 33: Impact of metformin and glucose concentration on the hepatocellular metabolite profile in samples for non-targeted metabolomics. 88
Figure 34: Metabolic profile of metformin- and vehicle-treated THLE-2 and Hep G2 cells cultivated at different glucose conditions, analyzed with targeted metabolomics. 89
Figure 35: Metabolic profile of metformin- and vehicle-treated THLE-2 and Hep G2 cells cultivated at different glucose conditions, analyzed with non-targeted metabolomics. 90
Figure 36: Metabolic profiles of the culture media of metformin- and vehicle-treated Hep G2 and THLE-2 cells cultivated at different glucose concentrations and analyzed with targeted metabolomics. 91
Figure 37: Expression of the cationic amino acid transporter 2 (CAT2) in human cell lines. 107
Figure 38: Impact of the glucose concentration on the urea cycle and associated pathways of Hep G2 cells. 111
Figure 39: Impact of the glucose concentration on the glutathione metabolism and associated pathways and metabolites of Hep G2 cells. 113
Figure 40: Impact of the metformin treatment on the one carbon metabolism of Hep G2 cells cultivated at an elevated glucose concentration. 120
Figure 41: Impact of the metformin treatment on the glutathione metabolism and associated pathways and metabolites of Hep G2 cells cultivated at an elevated glucose concentration. 121

Index of tables

Table 1: List of reported (potential) human metformin transporters and their K_M values for metformin. 6
Table 2: List of spiked amino acids and their respective concentrations. 22
Table 3: List of inhibitors, their concentrations and the according vehicle. 24
Table 4: PCR mastermix composition for a single reaction. 26
Table 5: PCR conditions used in transporter expression analyses. 26
Table 6: Metformin concentrations used for the evaluation of the linear range and as standard curves for the quantification of metformin in cell culture samples. 31
Table 7: Parameter settings of the mass spectrometer for the metformin quantification method. 32
Table 8: Nomenclature of the metabolites covered by the Absolute*IDQ* p180 Kit. 40
Table 9: Determination of the linear range of the LC-MS/MS based metformin quantification method. 43
Table 10: LOD, LLOQ, accuracy and precision of the LC-MS/MS based metformin quantification method. 44
Table 11: Injection precision of the LC-MS/MS based metformin quantification method. 45
Table 12: Short term and long term stability of prepared calibrators. 45
Table 13: Precision (CV) of the LC-MS/MS based metformin quantification method in cell homogenates and cell culture supernatants. 46
Table 14: Accuracy of the LC-MS/MS based metformin quantification method in cell homogenates and cell culture supernatants. 47
Table 15: Matrix factors of the LC-MS/MS based metformin quantification in cell homogenates and cell culture supernatants. 47
Table 16: Precision of the fluorometric DNA quantification method for cell number determination in combination with the optimized harvesting protocol for targeted metabolomics. 52
Table 17: Percentage of metabolites, which display a linear correlation ($R^2 > 0.9$) of their concentration to the cell number. 55
Table 18: Precision of the analyte concentrations of targeted cell culture metabolomics (1×10^6 cells). 58
Table 19: Accuracy of targeted cell culture metabolomics. 59
Table 20: Matrix factors of targeted metabolomics analysis of seven amino acids in cell homogenates. 60
Table 21: Precision of the analyte signals of targeted cell culture metabolomics. 61
Table 22: Precision of the non-targeted metabolomics analysis. 66
Table 23: Precision of non-targeted cell culture metabolomics. 67
Table 24: List of compounds relevant for the elucidation of transporter-mediated hepatic metformin transport. 74
Table 25: Inhibition of potential metformin transporters involved in the hepatocellular metformin uptake. 78
Table 26: Enriched pathways of Hep G2 cells cultivated at physiological and high glucose concentrations. 92
Table 27: Enriched pathways of THLE-2 cells cultivated at a physiological glucose concentration, and treated with metformin. 93
Table 28: Enriched pathways of Hep G2 cells cultivated at a physiological glucose concentration and treated with metformin. 94
Table 29: Enriched pathways of THLE-2 cells cultivated at a diabetic glucose concentration and treated with metformin. 95
Table 30: Enriched pathways of Hep G2 cells cultivated at a diabetic glucose concentration and treated with metformin. 96
Table 31: List of relative hepatic expression levels of reported human metformin transporters. 106

Appendix

Expression analysis of potential metformin transporters in mammalian cell lines

Table S-1: Primers for the expression analysis of potential metformin transporters in human cell lines.

Primers						
Name	**Gene**	**NCBI reference sequence**	**Internal number**	**Primer type**	**Sequence (5' - 3')**	**T_m**
β-Actin	*ACTB*	See comment*	2244 (3042)	Forward	GGA TTC CTA TGT GGG CGA CGA GG	68
			2245 (3043)	Reverse	CAC GGA GTA CTT GCG CTC AGG AGG	70
OCT1	*SLC22A1*	NM_003057.2	3146	Forward	ATGTACCTGTGGTTCACGGAC	61
			3147	Reverse	GGGGTACAGCTCAGCATTCA	60
OCT2	*SLC22A2*	NM_003058.3	2834	Forward	CCTGGTATGTGCCAACTCCT	58
			2835	Reverse	AGGCAGCTGGGAATTCAACC	60
OCT3	*SLC22A3*	NM_021977.3	3152	Forward	TCACAAGCGCAGTGGTGTAT	58
			3153	Reverse	AGGAATGTGGACTGCCAAGT	58
OCTN1	*SLC22A4*	See comment**	3004	Forward	TTCTTATCCATTGGTCTGGTCATGC	64
			3005	Reverse	TGGGAACAACGAATTTCTCCACA	61
OCTN2	*SLC22A5*	NM_003060.3	2986	Forward	TATGTGGCAGCATTTGTCCTG	59
			2987	Reverse	TACAAGTCTGGGGGTACCAG	60
PMAT	*SLC29A4*	NM_153247.2	3051	Forward	CGGGCGTAGTGATGAGCTTC	63
			3052	Reverse	TAAGAGGTAGCCTGCGGTGA	60
SERT	*SLC6A4*	NM_001045.5	3055	Forward	AATTTTACACGCGCCACGTC	58
			3056	Reverse	CTTCACGTCCCTGCAGAACT	60
CAT2	*SLC7A2*	NM_003046.5	3110	Forward	TTCCTAGCTTTCCTCGTGTTGG	62
			3111	Reverse	CAGCAAACCCATGACAACCC	60
THTR-2	*SLC19A3*	NM_025243.3	3208	Forward	CCTGACCAGTGCAGAGATAACA	62
			3209	Reverse	CAGCATAGCACGCCCAGATA	60

* These primers were designed and kindly provided by Susanne Weber.

** The primers used for amplification of the human OCTN1 transcript have been adopted from McBride *et al.* [285]. Their accuracy was double-checked using the Primer-BLAST tool [129] (http://www.ncbi.nlm.nih.gov/tools/primer-blast/). *SLC22A4* mRNA (NM_003059.2) and two predicted transcript variants of *SLC22A4* (XM_011543589.1 and XM_006714675.2) were identified as hits. No off-targets were found.

Precision of the analyte concentration of targeted cell culture metabolomics (5 x 10^5 cells)

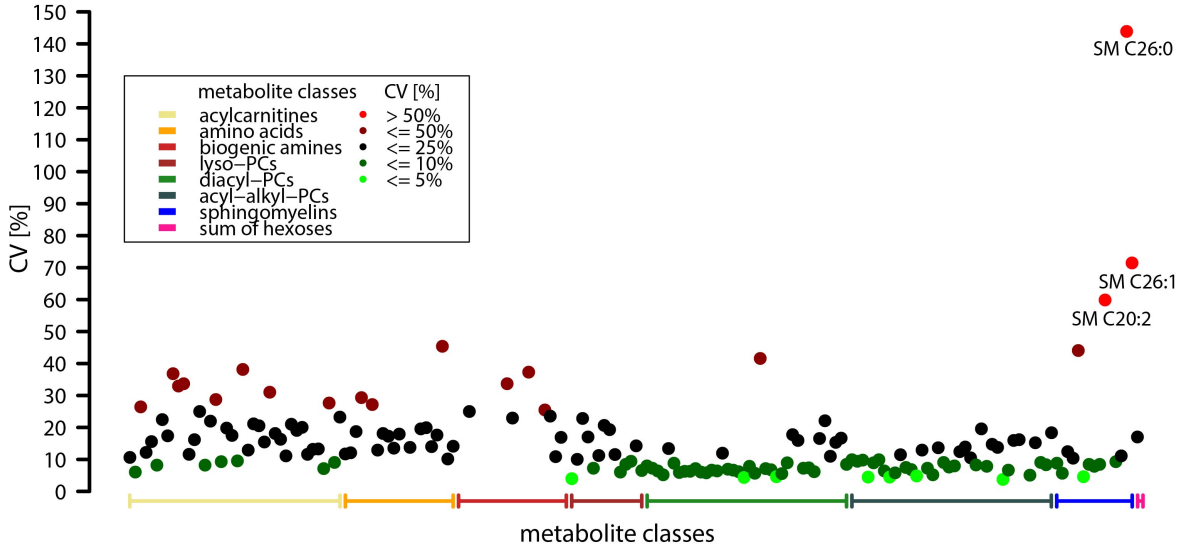

Figure S-1: Precision the analyte concentrations of targeted cell culture metabolomics (5 x 10^5 cells).
5 x 10^5 Hep G2 cells were scraped and processed according to the adapted protocol for targeted cell culture metabolomics (n = 6). Then, targeted metabolomics analysis of 188 metabolites was performed. Analyte concentrations, normalized to the respective internal standards, were used for the calculation of the CVs. The plot shows the distribution of the CVs of all metabolites, assigned to their respective metabolite classes. Metabolites, which show a CV of above 50%, are named.

Table S-2: Precision of the analyte concentrations of targeted cell culture metabolomics (5 x 10^5 cells).
5 x 10^5 Hep G2 cells were harvested and processed according to the adapted protocol for targeted cell culture metabolomics (n = 6) and targeted metabolomics of 188 metabolites, belonging to different metabolite classes, was performed. Analyte concentrations, normalized to the respective internal standards, were used for the calculation of the CVs. The table shows the means of the CVs ± standard deviations of the metabolite classes and lists the median of the CVs in brackets.

Precision

Metabolite class (number of measured metabolites in the metabolite class)	**CV [%]**
Acylcarnitines (40)	18.51 ± 8.47 (17.50)
Amino acids (21)	18.51 ± 8.41 (17.43)
Biogenic amines (21)	24.48 ± 8.41 (24.28)
Lyso-phosphatidylcholines (14)	12.02 ± 5.90 (10.61)
Diacyl-phosphatidylcholines (38)	9.69 ± 6.82 (7.17)
Acyl-alkylphosphatidylcholines (38)	9.80 ± 4.11 (9.04)
Sphingomyelins (15)	29.04 ± 39.57 (9.88)
Sum of hexoses (1)	16.98

Impact of metformin and glucose concentration on the hepatocellular metabolism

List of metabolites above the LOD and/or the LLOQ for cells and cell culture supernatant, measured with targeted metabolomics

Table S-3: List of metabolites, which were above the determined LOD and/or LLOQ.
The LOD was defined as three times the median of the signal intensity of the according zero (cells: 87.5% methanol; media: PBS). The LLOQ was defined as five times the median signal intensity of the according zeros. Metabolites of which ≥ 60% of the samples were found to be ≥ this threshold were regarded as being above the LOD or LLOQ, respectively. The nomenclature of the metabolites is based on the one provided by BIOCRATES LIFE SCIENCES AG (Absolute*IDQ*® Kit. Analytical Specifications p180. AS-P180-3. BIOCRATES LIFE SCIENCES AG) and Römisch-Margl *et al.*[132] and is listed in **Table 8**.

Metabolites above the LOD and/or the LLOQ

Cells		Media	
LOD (3 x zero)	**LLOQ (5 x zero)**	**LOD (3 x zero)**	**LLOQ (5 x zero)**
C0			
C16	C16		
C18			
C18:1	C18:1		
C2	C2	C2	C2
C3	C3	C3	C3
C4	C4	C4	
		C5	
		C5-OH/C3-DC-M (Methylmalonylcarnitine)	C5-OH/C3-DC-M (Methylmalonylcarnitine)
Ala	Ala	Ala	Ala
Arg	Arg	Arg	Arg
Asn	Asn	Asn	Asn
Asp	Asp	Asp	Asp
Cit	Cit	Cit	Cit
Gln	Gln	Gln	Gln
Glu	Glu	Glu	Glu
Gly	Gly	Gly	Gly
His	His	His	His
Ile	Ile	Ile	Ile
Leu	Leu	Leu	Leu
Lys	Lys	Lys	Lys
Met	Met	Met	Met
Orn	Orn	Orn	Orn
Phe	Phe	Phe	Phe
Pro	Pro	Pro	Pro
Ser	Ser	Ser	Ser
Thr	Thr	Thr	Thr
Trp	Trp	Trp	Trp
Tyr	Tyr	Tyr	Tyr
Val	Val	Val	Val
Acetylornithine	Acetylornithine	Acetylornithine	Acetylornithine
ADMA	ADMA	ADMA	ADMA
α-AAA	α-AAA	α-AAA	α-AAA

Metabolites above the LOD and/or the LLOQ

Cells		Media	
LOD (3 x zero)	**LLOQ (5 x zero)**	**LOD (3 x zero)**	**LLOQ (5 x zero)**
		c4 Hydroxyproline	c4 Hydroxyproline
Carnosine	Carnosine	Carnosine	Carnosine
		Kynurenine	
Methioninesulfoxide	Methioninesulfoxide	Methioninesulfoxide	Methioninesulfoxide
Phenylethylamine	Phenylethylamine		
Putrescine	Putrescine	Putrescine	
		SDMA	SDMA
Serotonin	Serotonin	Serotonin	Serotonin
Spermidine	Spermidine	Spermidine	Spermidine
Spermine	Spermine	Spermine	Spermine
t4 Hydroxyproline	t4 Hydroxyproline	t4 Hydroxyproline	t4 Hydroxyproline
Taurine	Taurine	Taurine	Taurine
Total DMA	Total DMA	Total DMA	Total DMA
lysoPC a C16:0	lysoPC a C16:0	lysoPC a C16:0	lysoPC a C16:0
lysoPC a C16:1	lysoPC a C16:1		
lysoPC a C17:0	lysoPC a C17:0		
		lysoPC a C18:0	
lysoPC a C18:1	lysoPC a C18:1	lysoPC a C18:1	lysoPC a C18:1
lysoPC a C18:2	lysoPC a C18:2	lysoPC a C18:2	
lysoPC a C20:4	lysoPC a C20:4	lysoPC a C20:4	
lysoPC a C26:0		lysoPC a C26:0	lysoPC a C26:0
lysoPC a C26:1	lysoPC a C26:1		
lysoPC a C28:0			
lysoPC a C28:1	lysoPC a C28:1	lysoPC a C28:1	
PC aa C24:0			
PC aa C28:1	PC aa C28:1		
PC aa C30:0	PC aa C30:0	PC aa C30:0	PC aa C30:0
PC aa C30:2	PC aa C30:2	PC aa C30:2	PC aa C30:2
PC aa C32:0	PC aa C32:0	PC aa C32:0	PC aa C32:0
PC aa C32:1	PC aa C32:1	PC aa C32:1	PC aa C32:1
PC aa C32:2	PC aa C32:2	PC aa C32:2	PC aa C32:2
PC aa C32:3	PC aa C32:3	PC aa C32:3	PC aa C32:3
PC aa C34:1	PC aa C34:1	PC aa C34:1	PC aa C34:1
PC aa C34:2	PC aa C34:2	PC aa C34:2	PC aa C34:2
PC aa C34:3	PC aa C34:3	PC aa C34:3	PC aa C34:3
PC aa C34:4	PC aa C34:4	PC aa C34:4	PC aa C34:4
PC aa C36:1	PC aa C36:1	PC aa C36:1	PC aa C36:1
PC aa C36:2	PC aa C36:2	PC aa C36:2	PC aa C36:2
PC aa C36:3	PC aa C36:3	PC aa C36:3	PC aa C36:3
PC aa C36:4	PC aa C36:4	PC aa C36:4	PC aa C36:4
PC aa C36:5	PC aa C36:5	PC aa C36:5	PC aa C36:5
PC aa C36:6	PC aa C36:6	PC aa C36:6	PC aa C36:6

Metabolites above the LOD and/or the LLOQ

Cells		Media	
LOD (3 x zero)	**LLOQ (5 x zero)**	**LOD (3 x zero)**	**LLOQ (5 x zero)**
PC aa C38:0	PC aa C38:0	PC aa C38:0	
PC aa C38:1	PC aa C38:1	PC aa C38:1	PC aa C38:1
PC aa C38:3	PC aa C38:3	PC aa C38:3	PC aa C38:3
PC aa C38:4	PC aa C38:4	PC aa C38:4	PC aa C38:4
PC aa C38:5	PC aa C38:5	PC aa C38:5	PC aa C38:5
PC aa C38:6	PC aa C38:6	PC aa C38:6	PC aa C38:6
PC aa C40:2	PC aa C40:2		
PC aa C40:3	PC aa C40:3	PC aa C40:3	PC aa C40:3
PC aa C40:4	PC aa C40:4	PC aa C40:4	PC aa C40:4
PC aa C40:5	PC aa C40:5	PC aa C40:5	PC aa C40:5
PC aa C40:6	PC aa C40:6	PC aa C40:6	PC aa C40:6
PC aa C42:1	PC aa C42:1	PC aa C42:1	PC aa C42:1
PC aa C42:2			
PC aa C42:4	PC aa C42:4	PC aa C42:4	PC aa C42:4
PC aa C42:5	PC aa C42:5	PC aa C42:5	
PC ae C30:0	PC ae C30:0		
PC ae C30:1	PC ae C30:1		
PC ae C32:1	PC ae C32:1	PC ae C32:1	PC ae C32:1
PC ae C32:2	PC ae C32:2		
PC ae C34:0	PC ae C34:0	PC ae C34:0	PC ae C34:0
PC ae C34:1	PC ae C34:1	PC ae C34:1	PC ae C34:1
PC ae C34:2	PC ae C34:2	PC ae C34:2	PC ae C34:2
PC ae C34:3	PC ae C34:3	PC ae C34:3	PC ae C34:3
PC ae C36:0	PC ae C36:0		
PC ae C36:1	PC ae C36:1	PC ae C36:1	PC ae C36:1
PC ae C36:2	PC ae C36:2	PC ae C36:2	PC ae C36:2
PC ae C36:3	PC ae C36:3	PC ae C36:3	PC ae C36:3
PC ae C36:4	PC ae C36:4	PC ae C36:4	PC ae C36:4
PC ae C36:5	PC ae C36:5	PC ae C36:5	PC ae C36:5
PC ae C38:0	PC ae C38:0		
PC ae C38:1	PC ae C38:1	PC ae C38:1	PC ae C38:1
PC ae C38:2	PC ae C38:2	PC ae C38:2	PC ae C38:2
PC ae C38:3	PC ae C38:3	PC ae C38:3	PC ae C38:3
PC ae C38:4	PC ae C38:4	PC ae C38:4	PC ae C38:4
PC ae C38:5	PC ae C38:5	PC ae C38:5	PC ae C38:5
PC ae C38:6	PC ae C38:6	PC ae C38:6	PC ae C38:6
PC ae C40:1	PC ae C40:1	PC ae C40:1	
PC ae C40:2	PC ae C40:2	PC ae C40:2	PC ae C40:2
PC ae C40:3	PC ae C40:3	PC ae C40:3	PC ae C40:3
PC ae C40:4	PC ae C40:4		
PC ae C40:5	PC ae C40:5	PC ae C40:5	PC ae C40:5
PC ae C40:6	PC ae C40:6	PC ae C40:6	PC ae C40:6
PC ae C42:1			

Metabolites above the LOD and/or the LLOQ

Cells		Media	
LOD (3 x zero)	**LLOQ (5 x zero)**	**LOD (3 x zero)**	**LLOQ (5 x zero)**
PC ae C42:2	PC ae C42:2	PC ae C42:2	
PC ae C42:3	PC ae C42:3	PC ae C42:3	PC ae C42:3
PC ae C42:4	PC ae C42:4		
SM-OH C14:1	SM-OH C14:1		
SM-OH C16:1	SM-OH C16:1	SM-OH C16:1	SM-OH C16:1
SM-OH C22:1	SM-OH C22:1	SM-OH C22:1	SM -OH C22:1
SM-OH C22:2	SM-OH C22:2	SM-OH C22:2	SM-OH C22:2
SM-OH C24:1	SM-OH C24:1	SM-OH C24:1	SM-OH C24:1
SM C16:0	SM C16:0	SM C16:0	SM C16:0
SM C16:1	SM C16:1	SM C16:1	SM C16:1
SM C18:0	SM C18:0	SM C18:0	SM C18:0
SM C18:1	SM C18:1	SM C18:1	SM C18:1
SM C20:2	SM C20:2	SM C20:2	SM C20:2
SM C24:0	SM C24:0	SM C24:0	SM C24:0
SM C24:1	SM C24:1	SM C24:1	SM C24:1
SM C26:0	SM C26:0	SM C26:0	SM C26:0
SM C26:1	SM C26:1	SM C26:1	SM C26:1
		H1	H1
metformin	metformin	N.D. *	N.D. *

* not determined

List of compounds and their HMDB IDs, covered by non-targeted metabolomics

Table S-4: List of the compounds, detected with non-targeted metabolomics, and, if available their HMDB IDs. Compounds starting with and "X – ", followed by a numerical value were not identified. The "*" indicates compounds, which were identified but not yet confirmed based on a standard.

Compound	HMDB ID
1-(1-enyl-palmitoyl)-GPE (P-16:0)*	
1-arachidonoyl-GPE (20:4n6)*	HMDB11517
1-arachidonoyl-GPI (20:4)*	HMDB61690
1-dihomo-linoleoyl-GPC (20:2)*	HMDB10392
1-eicosenoyl-GPC (20:1)*	
1-linoleoyl-GPC (18:2)	HMDB10386
1-linoleoyl-GPE (18:2)*	HMDB11507
1-myristoyl-GPC (14:0)	HMDB10379
1-oleoyl-GPC (18:1)	HMDB02815
1-oleoyl-GPE (18:1)	HMDB11506
1-oleoyl-GPG (18:1)*	
1-oleoyl-GPI (18:1)*	
1-oleoyl-GPS (18:1)	
1-oleoylglycerol (18:1)	HMDB11567
1-palmitoleoyl-GPC (16:1)*	HMDB10383
1-palmitoyl-GPC (16:0)	HMDB10382
1-palmitoyl-GPE (16:0)	HMDB11503
1-pentadecanoyl-GPC (15:0)*	
1-stearoyl-GPC (18:0)	HMDB10384
1-stearoyl-GPE (18:0)	HMDB11130
1-stearoyl-GPG (18:0)	
1-stearoyl-GPI (18:0)	HMDB61696
1-stearoyl-GPS (18:0)*	
10-heptadecenoate (17:1n7)	HMDB60038
17-methylstearate	
2-deoxyuridine	HMDB00012
2-aminoadipate	HMDB00510
2-arachidonoyl-GPC (20:4)*	HMDB61699
2-arachidonoyl-GPE (20:4)*	
2-docosahexaenoyl-GPE (22:6)*	
2-docosapentaenoyl-GPC (22:5n3)*	
2-eicosapentaenoyl-GPE (20:5)*	
2-linoleoyl-GPC (18:2)*	
2-methylbutyrylcarnitine (C5)	HMDB00378
2-myristoyl-GPC (14:0)*	
2-oleoyl-GPC (18:1)*	HMDB61701
2-oleoyl-GPE (18:1)*	
2-oleoyl-GPG (18:1)*	
2-palmitoleoyl-GPC (16:1)*	
2-palmitoleoyl-GPE (16:1)*	
2-palmitoyl-GPC (16:0)*	HMDB61702
2-palmitoyl-GPE (16:0)*	

Compound	HMDB ID
2-stearoyl-GPC (18:0)*	
3-(4-hydroxyphenyl)lactate	HMDB00755
3-hydroxybutyrylcarnitine (1)	HMDB13127
3-methyl-2-oxovalerate	HMDB03736
3-phosphoglycerate (isobar with 2-phosphoglycerate)	
4-guanidinobutanoate	HMDB03464
4-methyl-2-oxopentanoate	HMDB00695
4-methylglutamate	
5-methylthioadenosine (MTA)	HMDB01173
5-oxoproline	HMDB00267
6-phosphogluconate	HMDB01316
acetyl CoA	HMDB01206
acetylcarnitine	HMDB00201
acetylcholine	
adenosine	HMDB00050
adenosine 5'-diphosphate (ADP)	HMDB01341
adenosine 5'-diphosphoribose (ADP-ribose)	HMDB01178
adenosine 5'-monophosphate (AMP)	HMDB00045
adenosine 5'-triphosphate (ATP)	HMDB00538
alanine	HMDB00161
alanylleucine	HMDB28691
arachidonate (20:4n6)	HMDB01043
arginine	HMDB00517
benzoylcarnitinex	
beta-hydroxyisovaleroylcarnitine	
betaine	HMDB00043
butyrylcarnitine	HMDB02013
C-glycosyltryptophan	
carnitine	HMDB00062
choline phosphate	HMDB01565
citrate	HMDB00094
citrulline	HMDB00904
coenzyme A	HMDB01423
creatine	HMDB00064
creatine phosphate	HMDB01511
creatinine	HMDB00562
cysteine	HMDB00574
cysteinylglycine	HMDB00078
cytidine	HMDB00089
cytidine 5'-monophosphate (5'-CMP)	HMDB00095
cytidine triphosphate	HMDB00082
cytidine-5'-diphosphoethanolamine	HMDB01564
deoxycarnitine	HMDB01161
dihomo-linolenate (20:3n3 or n6)	HMDB02925
docosahexaenoate (DHA, 22:6n3)	HMDB02183
eicosenoate (20:1)	HMDB02231

Compound	HMDB ID
erucate (22:1n9)	HMDB02068
flavin adenine dinucleotide (FAD)	HMDB01248
flavin mononucleotide (FMN)	HMDB01520
gamma-glutamylglutamate	HMDB11737
gamma-glutamylglutamine	HMDB11738
gamma-glutamylisoleucinex	HMDB11170
gamma-glutamylleucine	HMDB11171
gamma-glutamylphenylalanine	HMDB00594
gamma-glutamylthreoninex	HMDB29159
gamma-glutamyltyrosine	HMDB11741
gamma-glutamylvaline	HMDB11172
glutamate	HMDB00148
glutamate, gamma-methyl ester	
glutamine	HMDB00641
glutathione, oxidized (GSSG)	HMDB03337
glutathione, reduced (GSH)	HMDB00125
glycerophosphoethanolamine	HMDB00114
glycerophosphorylcholine (GPC)	HMDB00086
glycylleucine	HMDB00759
guanine	HMDB00132
guanosine	HMDB00133
guanosine 5-diphospho-fucose	
HEPES	
hexanoylcarnitine	HMDB00705
hippurate	HMDB00714
histidine	HMDB00177
hypotaurine	HMDB00965
imidazole propionate	HMDB02271
inosine	HMDB00195
inosine 5-monophosphate (IMP)	HMDB00175
Isobar: fructose 1,6-diphosphate, glucose 1,6-diphosphate, myo-inositol 1,4 or 1,3-diphosphate	
isobutyrylcarnitine	HMDB00736
isoleucine	HMDB00172
isoleucylglycine	
isovalerylcarnitine	HMDB00688
kynurenine	HMDB00684
laurylcarnitine	HMDB02250
leucine	HMDB00687
leucylglycine	
lysine	HMDB00182
malate	HMDB00156
maltotetraose	HMDB01296
mead acid (20:3n9)	HMDB10378
metformin	HMDB01921
methionine	HMDB00696
myristoylcarnitine	HMDB05066

Compound	HMDB ID
N(1)-acetylspermine	HMDB01186
N-acetyl-aspartyl-glutamate (NAAG)	HMDB01067
N-acetylaspartate (NAA)	HMDB00812
N-acetylglutamate	HMDB01138
N-acetylmethionine	HMDB11745
N-acetylserine	HMDB02931
N-acetylthreonine	
N-acetyltyrosine	HMDB00866
N-carbamoylaspartate	HMDB00828
N-delta-acetylornithinex	
N-formylmethionine	HMDB01015
nicotinamide	HMDB01406
nicotinamide adenine dinucleotide (NAD+)	HMDB00902
nicotinamide adenine dinucleotide reduced (NADH)	HMDB01487
octanoylcarnitine	HMDB00791
oleoylcarnitine	HMDB05065
ophthalmate	HMDB05765
palmitoleate (16:1n7)	HMDB03229
palmitoyl ethanolamide	HMDB02100
palmitoylcarnitine	HMDB00222
pantothenate	HMDB00210
penicillin G	HMDB15186
phenol red	
phenylalanine	HMDB00159
phosphate	HMDB01429
pipecolate	HMDB00070
pro-hydroxy-pro	HMDB06695
proline	HMDB00162
propionylcarnitine	HMDB00824
pyridoxal	HMDB01545
pyridoxate	HMDB00017
pyridoxine (Vitamin B6)	HMDB02075
pyroglutaminex	
S-adenosylhomocysteine (SAH)	HMDB00939
S-lactoylglutathione	HMDB01066
S-methylglutathione	
S-nitrosoglutathione (GSNO)	HMDB04645
serine	HMDB00187
spermidine	HMDB01257
spermine	HMDB01256
sphinganine	HMDB00269
sphingosine	HMDB00252
stearoylcarnitine	HMDB00848
streptomycin	
succinylcarnitine	
taurine	HMDB00251

Compound	HMDB ID
taurochenodeoxycholate	HMDB00951
thiamin (Vitamin B1)	HMDB00235
threonine	HMDB00167
trans-4-hydroxyproline	HMDB00725
tryptophan	HMDB00929
tyrosine	HMDB00158
UDP-glucuronate	HMDB00935
uridine	HMDB00296
uridine 5'-diphosphate (UDP)	HMDB00295
uridine 5'-triphosphate (UTP)	HMDB00285
uridine monophosphate (5' or 3')	HMDB00288
valerylcarnitine	HMDB13128
valine	HMDB00883
X - 08893	
X - 11272	
X - 11277	
X - 11323	
X - 11564	
X - 11569	
X - 11583	
X - 11586	
X - 11616	
X - 11787	
X - 12411	
X - 12443	
X - 12676	
X - 12748	
X - 12776	
X - 12855	
X - 12944	
X - 12948	
X - 13396	
X - 13505	
X - 13511	
X - 13528	
X - 13530	
X - 13556	
X - 13832	
X - 13871	
X - 14057	
X - 14255	
X - 15192	
X - 15220	
X - 15303	
X - 15306	
X - 15352	

Compound	HMDB ID
X - 15458	
X - 15472	
X - 15474	
X - 15497	
X - 15558	
X - 15559	
X - 15562	
X - 15563	
X - 15591	
X - 15678	
X - 16439	
X - 17101	
X - 17254	
X - 17638	
X - 18341	
X - 18739	
X - 19363	
X - 19365	
X - 19524	
X - 19561	
X - 19807	
X - 19808	
X - 20051	
X - 21004	
X - 21027	
X - 21031	
X - 21365	

Elucidation of the impact of glucose and metformin in the hepatocellular metabolism: Statistics

Table S-5: List of p-values for the pairwise comparisons of the tested conditions of the cell homogenates for targeted metabolomics.
THLE-2 and Hep G2 cells were either cultivated at a physiological or a diabetic glucose concentration and treated with vehicle or 2 mM metformin. Then, the cells were harvested via scraping and targeted metabolomics, LC-MS/MS based metformin quantification and DNA based cell number determination was performed (n per group = 12). For the pairwise comparison of conditions the U-Test was used. The p-values, listed in the table, are Benjamini-Hochberg corrected.

Cells: Targeted metabolomics

Condition	**Low vs. high glucose**		**Low glucose: Controls vs. metformin treatment**		**High glucose: Controls vs. metformin treatment**	
Cell line	**THLE-2**	**Hep G2**	**THLE-2**	**Hep G2**	**THLE-2**	**Hep G2**
C0	8.26E-01	2.03E-01	3.54E-01	4.13E-01	4.62E-01	3.34E-01
C10	4.48E-01	8.79E-03	4.52E-01	5.39E-01	2.56E-01	1.28E-02
C10:1	9.22E-01	7.98E-02	7.30E-01	8.58E-02	9.54E-01	2.69E-02
C10:2	4.48E-01	3.77E-01	3.54E-01	1.81E-03	3.22E-01	6.57E-03
C12	4.53E-01	4.81E-01	3.71E-01	1.54E-03	3.28E-01	8.39E-02
C12-DC	6.44E-01	5.23E-03	1.81E-01	9.01E-04	2.19E-01	4.57E-04
C12:1	7.11E-01	6.40E-02	6.67E-01	4.01E-02	3.28E-01	6.38E-01
C14	8.26E-01	8.89E-01	4.43E-02	4.64E-04	1.39E-01	3.33E-03
C14:1	4.52E-01	2.88E-01	1.62E-01	4.64E-04	4.45E-02	3.50E-02
C14:1-OH	3.60E-01	5.69E-02	7.85E-02	3.66E-01	6.51E-02	3.97E-03
C14:2	6.44E-01	1.35E-01	2.07E-01	9.64E-01	3.70E-01	5.65E-01
C14:2-OH	4.48E-01	7.98E-02	6.96E-01	8.80E-01	3.22E-01	6.62E-02
C16	7.93E-01	8.09E-01	4.86E-02	2.13E-03	3.28E-01	1.28E-02
C16-OH	5.96E-01	7.28E-02	3.65E-03	2.04E-01	1.62E-03	4.68E-03
C16:1	4.48E-01	8.89E-01	4.86E-02	3.84E-01	4.45E-02	3.34E-01
C16:1-OH	5.33E-01	2.88E-01	3.50E-02	1.73E-02	2.04E-02	1.07E-01
C16:2	4.48E-01	1.00E+00	1.94E-01	2.90E-01	1.83E-01	9.54E-01
C16:2-OH	4.48E-01	6.73E-03	5.58E-01	1.51E-02	1.83E-01	6.29E-04
C18	5.87E-01	9.64E-01	4.86E-02	9.01E-04	1.88E-01	5.12E-02
C18:1	7.66E-01	7.30E-01	4.62E-02	2.21E-01	1.88E-01	8.34E-01
C18:1-OH	4.53E-01	4.51E-02	1.62E-01	3.33E-03	2.04E-02	9.47E-04
C18:2	4.62E-01	5.48E-01	9.47E-02	8.51E-01	1.03E-01	6.03E-01
C2	5.21E-01	2.44E-01	3.65E-03	3.86E-03	2.04E-02	6.57E-03
C3	7.66E-01	6.19E-04	9.47E-02	2.47E-03	3.28E-01	5.56E-03
C5-OH/C3-DC-M	7.11E-01	1.60E-03	9.59E-01	1.00E+00	5.51E-01	9.47E-02
C3-OH	4.53E-01	1.49E-01	3.71E-01	6.75E-02	2.83E-01	6.29E-04
C3:1	9.41E-01	2.30E-02	1.81E-01	5.21E-02	4.93E-01	2.81E-03
C4	9.73E-01	1.74E-02	9.26E-02	6.12E-01	1.14E-01	1.30E-01
C3-DC/C4-OH	9.03E-01	6.59E-01	2.15E-03	4.64E-04	1.62E-03	1.22E-04
C4 1	6.43E-01	1.60E-03	1.81E-01	3.33E-03	3.70E-01	1.22E-04
C5	5.33E-01	6.19E-04	2.15E-03	1.33E-03	1.62E-03	1.75E-01
C5-DC/C6-OH	9.73E-01	5.80E-01	9.26E-02	7.56E-03	6.38E-01	3.72E-04
C5-M-DC	6.44E-01	2.44E-01	3.98E-01	1.34E-02	6.59E-01	8.39E-02
C5:1	6.44E-01	2.28E-03	6.30E-01	8.51E-01	3.61E-01	5.12E-02
C5:1-DC	4.48E-01	9.85E-02	4.52E-01	3.38E-01	5.22E-01	1.70E-02

Cells: Targeted metabolomics

Condition	Low vs. high glucose		Low glucose: Controls vs. metformin treatment		High glucose: Controls vs. metformin treatment	
Cell line	**THLE-2**	**Hep G2**	**THLE-2**	**Hep G2**	**THLE-2**	**Hep G2**
C6 /C4:1-DC	4.60E-01	9.85E-02	7.67E-01	6.49E-03	4.62E-01	1.44E-01
C6:1	4.60E-01	1.65E-01	6.67E-01	5.91E-02	2.65E-01	4.68E-03
C7-DC	4.75E-01	9.78E-03	7.30E-01	1.99E-02	2.83E-01	3.33E-03
C8	3.60E-01	3.19E-03	8.43E-01	2.28E-02	1.96E-01	7.82E-03
C9	6.90E-01	3.19E-03	4.52E-01	1.73E-02	7.04E-01	2.48E-04
Ala	8.57E-01	3.19E-03	8.90E-02	4.64E-04	1.54E-01	1.22E-04
Arg	4.62E-01	8.51E-01	5.86E-02	4.64E-04	4.14E-01	1.22E-04
Asn	4.75E-01	6.19E-04	1.47E-01	3.84E-01	6.59E-01	1.22E-04
Asp	4.53E-01	6.19E-04	3.65E-03	6.49E-01	3.47E-03	7.50E-02
Cit	1.00E+00	6.73E-03	8.80E-01	3.66E-01	2.83E-01	2.81E-03
Gln	5.96E-01	7.71E-01	8.05E-01	6.89E-01	8.56E-01	1.99E-03
Glu	4.62E-01	9.78E-03	8.90E-02	2.21E-01	8.56E-01	5.12E-02
Gly	5.33E-01	6.19E-04	4.62E-02	2.04E-01	1.54E-01	1.64E-04
His	7.66E-01	6.19E-04	2.07E-01	2.47E-03	6.21E-01	1.22E-04
Ile	7.93E-01	6.43E-04	9.47E-02	4.64E-04	3.48E-01	1.22E-04
Leu	6.90E-01	9.25E-04	1.94E-01	8.20E-04	3.28E-01	1.22E-04
Lys	4.75E-01	2.66E-01	5.86E-02	1.20E-03	5.22E-01	1.22E-04
Met	6.43E-01	6.19E-04	1.26E-01	8.79E-03	4.62E-01	1.22E-04
Orn	8.73E-01	9.78E-03	3.09E-01	5.56E-03	2.65E-01	1.41E-04
Phe	6.90E-01	6.19E-04	9.47E-02	1.20E-03	3.28E-01	1.22E-04
Pro	5.96E-01	5.14E-01	1.02E-01	1.54E-03	3.61E-01	4.57E-04
Ser	4.48E-01	7.98E-02	2.07E-01	4.64E-04	7.09E-01	1.70E-02
Thr	4.53E-01	1.44E-03	6.47E-02	1.73E-02	3.48E-01	1.64E-04
Trp	5.96E-01	6.89E-04	2.59E-01	2.47E-03	3.61E-01	1.22E-04
Tyr	6.90E-01	6.43E-04	9.47E-02	1.99E-02	1.88E-01	6.29E-04
Val	4.62E-01	6.19E-04	1.79E-01	2.83E-03	3.28E-01	1.22E-04
Acetylornithine	4.48E-01	3.73E-03	9.26E-02	4.58E-02	3.28E-01	2.39E-03
ADMA	6.43E-01	9.49E-01	NA	2.61E-01	5.50E-01	7.97E-01
α-AAA	4.37E-01	2.24E-01	3.74E-02	2.28E-02	3.70E-01	1.16E-01
Carnosine	4.48E-01	8.09E-01	1.81E-01	1.87E-01	7.09E-01	2.37E-01
Creatinine	5.59E-01	1.09E-01	1.38E-01	1.01E-02	3.61E-01	6.29E-04
Histamine	5.87E-01	1.00E+00	5.94E-01	5.21E-02	6.55E-01	6.38E-01
Kynurenine	4.48E-01	5.85E-03	3.71E-01	1.09E-01	1.54E-01	2.39E-03
Methioninesulfoxide	4.52E-01	6.89E-04	9.47E-02	3.84E-01	6.38E-01	4.68E-03
Phenylethylamine	1.50E-01	1.29E-02	8.43E-01	4.41E-01	5.37E-02	1.41E-04
Putrescine	6.90E-01	2.88E-01	3.71E-01	8.80E-01	8.56E-01	3.50E-02
Serotonin	6.90E-01	9.13E-01	6.89E-01	5.06E-01	4.93E-01	9.54E-01
Spermidine	1.00E+00	4.51E-02	5.27E-01	9.63E-02	9.54E-01	3.50E-02
Spermine	7.33E-01	1.49E-01	8.80E-01	2.90E-01	2.49E-01	1.75E-01
t4 Hydroxyproline	4.53E-01	3.53E-02	4.26E-01	5.06E-01	3.70E-01	4.24E-01
Taurine	7.49E-01	2.68E-02	5.86E-02	3.12E-01	2.56E-01	3.50E-02
Total DMA	8.26E-01	2.03E-01	5.58E-01	6.49E-01	8.84E-01	9.22E-01

Cells: Targeted metabolomics

Condition	Low vs. high glucose		Low glucose: Controls vs. metformin treatment		High glucose: Controls vs. metformin treatment	
Cell line	**THLE-2**	**Hep G2**	**THLE-2**	**Hep G2**	**THLE-2**	**Hep G2**
lysoPC a C14:0	5.59E-01	1.97E-02	2.59E-01	2.13E-03	1.54E-01	1.64E-04
lysoPC a C16:0	4.48E-01	1.21E-01	3.71E-01	8.58E-02	3.48E-01	7.50E-02
lysoPC a C16:1	5.96E-01	8.79E-03	1.81E-01	1.71E-01	9.54E-01	8.39E-02
lysoPC a C17:0	4.75E-01	1.29E-02	2.44E-01	4.01E-02	4.14E-01	1.16E-01
lysoPC a C18:0	4.48E-01	5.48E-01	3.71E-01	1.54E-01	3.28E-01	5.84E-02
lysoPC a C18:1	4.48E-01	5.23E-03	2.59E-01	4.41E-01	4.93E-01	8.34E-01
lysoPC a C18:2	6.44E-01	7.98E-02	1.62E-01	2.90E-01	9.54E-01	2.15E-01
lysoPC a C20:3	5.21E-01	5.85E-03	1.81E-01	8.79E-03	3.08E-01	1.99E-03
lysoPC a C20:4	9.41E-01	8.79E-03	8.34E-02	2.83E-03	7.32E-01	2.81E-03
lysoPC a C24:0	8.73E-01	9.78E-03	5.94E-01	3.11E-02	6.38E-01	1.75E-01
lysoPC a C26:0	9.03E-01	4.01E-02	1.94E-01	2.04E-01	6.38E-01	1.16E-01
lysoPC a C26:1	8.26E-01	1.97E-02	1.81E-01	2.28E-02	6.59E-01	4.00E-02
lysoPC a C28:0	7.66E-01	7.65E-03	2.22E-01	1.01E-02	3.98E-01	1.67E-03
lysoPC a C28:1	8.26E-01	6.73E-03	1.47E-01	1.34E-02	7.92E-01	3.33E-03
PC aa C24:0	8.26E-01	1.50E-02	1.94E-01	2.83E-03	7.62E-01	1.13E-03
PC aa C26:0	1.00E+00	1.11E-02	2.07E-01	4.01E-02	4.48E-01	1.48E-02
PC aa C28:1	8.19E-01	1.29E-03	1.38E-01	1.87E-01	7.04E-01	2.81E-03
PC aa C30:0	3.60E-01	6.59E-01	8.34E-02	8.58E-02	6.55E-01	1.16E-01
PC aa C30:2	7.49E-01	6.19E-04	1.62E-01	1.18E-02	7.09E-01	1.22E-04
PC aa C32:0	6.81E-01	1.35E-01	7.67E-01	5.91E-02	7.92E-01	5.56E-03
PC aa C32:1	4.53E-01	4.51E-02	3.54E-01	5.39E-01	7.32E-01	1.16E-01
PC aa C32:2	6.81E-01	7.96E-04	7.85E-02	2.83E-03	7.04E-01	1.22E-04
PC aa C32:3	9.03E-01	6.19E-04	5.86E-02	4.64E-04	2.56E-01	1.22E-04
PC aa C34:1	4.53E-01	9.85E-02	3.35E-01	4.76E-01	7.32E-01	5.65E-01
PC aa C34:2	6.44E-01	5.85E-03	1.02E-01	1.87E-01	7.32E-01	1.10E-02
PC aa C34:3	9.22E-01	1.44E-03	4.86E-02	1.54E-03	5.91E-01	1.22E-04
PC aa C34:4	8.26E-01	6.89E-04	4.43E-02	4.64E-04	2.65E-01	1.22E-04
PC aa C36:0	3.60E-01	6.92E-01	4.26E-01	1.71E-01	2.65E-01	7.97E-01
PC aa C36:1	3.60E-01	6.92E-01	3.71E-01	2.04E-01	7.62E-01	4.53E-02
PC aa C36:2	4.60E-01	2.66E-01	1.47E-01	1.99E-02	6.59E-01	3.11E-02
PC aa C36:3	7.33E-01	8.79E-03	7.85E-02	7.26E-01	6.59E-01	3.62E-01
PC aa C36:4	8.73E-01	1.60E-03	9.19E-02	2.13E-03	8.56E-01	1.64E-04
PC aa C36:5	8.73E-01	9.25E-04	7.85E-02	4.64E-04	6.38E-01	1.22E-04
PC aa C36:6	7.49E-01	1.11E-02	7.85E-02	4.64E-04	1.96E-01	1.22E-04
PC aa C38:0	9.73E-01	1.29E-02	7.85E-02	9.01E-04	3.28E-01	2.48E-04
PC aa C38:1	4.60E-01	1.97E-02	6.96E-01	4.64E-04	6.95E-01	1.41E-04
PC aa C38:3	6.43E-01	5.05E-02	1.62E-01	8.58E-02	6.59E-01	6.74E-01
PC aa C38:4	8.57E-01	3.73E-03	7.85E-02	1.51E-02	3.28E-01	1.13E-03
PC aa C38:5	9.22E-01	1.29E-03	4.62E-02	5.99E-04	3.08E-01	1.22E-04
PC aa C38:6	9.41E-01	3.73E-03	7.85E-02	4.64E-04	5.51E-01	1.22E-04
PC aa C40:1	7.66E-01	5.80E-01	2.81E-01	7.56E-03	3.48E-01	3.72E-04
PC aa C40:2	3.60E-01	5.80E-01	2.81E-01	3.12E-01	7.62E-01	2.31E-02

Cells: Targeted metabolomics

Condition	Low vs. high glucose		Low glucose: Controls vs. metformin treatment		High glucose: Controls vs. metformin treatment	
Cell line	**THLE-2**	**Hep G2**	**THLE-2**	**Hep G2**	**THLE-2**	**Hep G2**
PC aa C40:3	9.03E-01	6.40E-02	5.58E-01	9.22E-01	3.98E-01	1.75E-01
PC aa C40:4	6.43E-01	3.05E-02	1.47E-01	2.21E-01	4.93E-01	1.70E-02
PC aa C40:5	9.22E-01	1.97E-02	1.02E-01	1.51E-02	3.28E-01	3.72E-04
PC aa C40:6	8.73E-01	9.78E-03	9.47E-02	4.64E-04	3.98E-01	1.22E-04
PC aa C42:0	7.33E-01	8.96E-02	1.47E-01	1.33E-03	7.09E-01	1.41E-04
PC aa C42:1	3.60E-01	7.30E-01	7.30E-01	8.79E-03	9.27E-01	5.46E-04
PC aa C42:2	9.41E-01	6.92E-01	4.52E-01	4.01E-02	6.38E-01	6.29E-04
PC aa C42:4	8.26E-01	9.85E-02	3.98E-01	3.38E-01	4.62E-01	1.70E-02
PC aa C42:5	9.41E-01	5.05E-02	9.22E-01	4.01E-02	3.28E-01	9.47E-04
PC aa C42:6	8.57E-01	5.05E-02	9.19E-02	9.01E-04	3.28E-01	1.41E-04
PC ae C30:0	4.48E-01	1.44E-03	4.62E-02	9.01E-04	3.22E-01	1.22E-04
PC ae C30:1	7.49E-01	7.96E-04	2.07E-01	3.86E-03	5.22E-01	3.06E-04
PC ae C30:2	8.26E-01	1.10E-03	1.62E-01	1.05E-03	2.49E-01	1.64E-04
PC ae C32:1	5.05E-01	6.19E-04	1.81E-01	7.34E-04	6.55E-01	1.22E-04
PC ae C32:2	8.19E-01	6.43E-04	1.94E-01	1.05E-03	7.04E-01	1.22E-04
PC ae C34:0	7.11E-01	9.78E-03	2.22E-01	7.56E-03	6.55E-01	1.67E-03
PC ae C34:1	4.60E-01	1.60E-03	1.62E-01	1.81E-03	7.04E-01	2.48E-04
PC ae C34:2	5.33E-01	6.19E-04	1.38E-01	8.20E-04	7.09E-01	1.22E-04
PC ae C34:3	6.44E-01	6.89E-04	9.19E-02	4.64E-04	6.59E-01	1.22E-04
PC ae C36:0	7.33E-01	7.65E-03	1.02E-01	1.51E-02	4.48E-01	1.13E-03
PC ae C36:1	4.52E-01	1.11E-02	1.62E-01	3.33E-03	4.14E-01	7.77E-04
PC ae C36:2	5.96E-01	5.85E-03	1.12E-01	1.01E-02	6.21E-01	5.46E-04
PC ae C36:3	6.81E-01	1.10E-03	9.19E-02	1.54E-03	5.51E-01	1.22E-04
PC ae C36:4	6.90E-01	6.19E-04	8.34E-02	4.64E-04	7.04E-01	1.22E-04
PC ae C36:5	6.43E-01	5.85E-03	9.26E-02	1.51E-02	3.70E-01	1.38E-03
PC ae C38:0	8.73E-01	6.19E-04	4.86E-02	4.64E-04	1.96E-01	1.22E-04
PC ae C38:1	4.62E-01	1.11E-02	3.54E-01	2.47E-03	7.92E-01	1.13E-03
PC ae C38:2	5.05E-01	5.69E-02	2.44E-01	3.12E-01	6.59E-01	1.60E-01
PC ae C38:3	8.19E-01	1.88E-03	1.81E-01	1.34E-02	6.59E-01	5.46E-04
PC ae C38:4	8.19E-01	7.96E-04	9.47E-02	5.45E-04	4.14E-01	1.22E-04
PC ae C38:5	5.87E-01	6.19E-04	8.90E-02	5.45E-04	3.22E-01	1.22E-04
PC ae C38:6	8.57E-01	6.19E-04	9.26E-02	1.20E-03	4.62E-01	1.22E-04
PC ae C40:1	7.49E-01	1.29E-03	9.26E-02	4.64E-04	2.29E-01	1.22E-04
PC ae C40:2	4.37E-01	7.65E-03	1.62E-01	1.34E-02	4.62E-01	6.29E-04
PC ae C40:3	7.11E-01	4.49E-03	2.59E-01	1.73E-02	3.70E-01	6.29E-04
PC ae C40:4	8.73E-01	6.89E-04	2.07E-01	1.33E-03	3.61E-01	1.22E-04
PC ae C40:5	7.93E-01	6.43E-04	7.85E-02	8.20E-04	4.14E-01	1.22E-04
PC ae C40:6	7.93E-01	6.19E-04	1.12E-01	4.64E-04	4.62E-01	1.22E-04
PC ae C42:0	6.32E-01	6.73E-03	1.62E-01	8.20E-04	3.28E-01	1.22E-04
PC ae C42:1	6.90E-01	9.78E-03	1.62E-01	4.64E-04	2.56E-01	1.22E-04
PC ae C42:2	9.22E-01	3.05E-02	4.86E-02	4.64E-04	3.28E-01	1.22E-04
PC ae C42:3	8.19E-01	4.01E-02	1.12E-01	5.99E-04	1.72E-01	1.22E-04

Cells: Targeted metabolomics

Condition	Low vs. high glucose		Low glucose: Controls vs. metformin treatment		High glucose: Controls vs. metformin treatment	
Cell line	**THLE-2**	**Hep G2**	**THLE-2**	**Hep G2**	**THLE-2**	**Hep G2**
PC ae C42:4	7.66E-01	5.05E-02	7.80E-01	4.58E-02	3.28E-01	1.10E-02
PC ae C42:5	5.21E-01	9.25E-04	1.81E-01	1.20E-03	2.29E-01	1.22E-04
PC ae C44:3	7.33E-01	1.21E-01	9.19E-02	5.99E-04	5.91E-01	1.22E-04
PC ae C44:4	5.21E-01	7.65E-03	1.62E-01	4.64E-04	1.26E-01	1.22E-04
PC ae C44:5	7.49E-01	4.01E-02	3.98E-01	5.99E-04	4.14E-01	1.22E-04
PC ae C44:6	9.41E-01	1.60E-03	2.22E-01	3.86E-03	3.28E-01	1.41E-04
SM-OH C14:1	4.48E-01	1.11E-02	6.47E-02	6.49E-03	6.59E-01	3.97E-03
SM-OH C16:1	3.60E-01	5.85E-03	4.86E-02	2.83E-03	6.55E-01	1.99E-03
SM-OH C22:1	4.48E-01	1.44E-03	2.59E-01	1.01E-02	8.84E-01	2.48E-04
SM-OH C22:2	6.44E-01	1.88E-03	1.81E-01	1.18E-02	6.55E-01	1.22E-04
SM-OH C24:1	7.93E-01	6.19E-04	1.00E+00	3.86E-03	3.70E-01	1.22E-04
SM C16:0	4.37E-01	7.98E-02	8.90E-02	1.22E-01	7.32E-01	2.59E-01
SM C16:1	4.48E-01	1.44E-03	4.86E-02	6.49E-03	8.31E-01	5.46E-04
SM C18:0	7.66E-01	2.44E-01	3.35E-01	3.12E-01	7.62E-01	5.34E-01
SM C18:1	5.87E-01	1.97E-02	1.47E-01	8.80E-01	6.21E-01	4.53E-02
SM C20:2	6.21E-01	1.21E-01	9.51E-02	4.41E-01	3.28E-01	1.48E-02
SM C22:3	5.59E-01	4.90E-01	3.36E-01	8.73E-01	3.61E-01	2.65E-01
SM C24:0	7.11E-01	1.49E-01	9.59E-01	2.21E-01	7.92E-01	2.80E-01
SM C24:1	6.32E-01	7.65E-03	6.30E-01	5.74E-01	7.09E-01	9.54E-01
SM C26:0	9.22E-01	1.03E-01	4.26E-01	3.84E-01	8.84E-01	4.10E-01
SM C26:1	6.44E-01	6.40E-02	1.94E-01	3.84E-01	7.04E-01	4.00E-02
H1	6.49E-03	6.19E-04	3.54E-01	1.34E-02	2.29E-01	3.06E-04
metformin	5.33E-01	9.85E-02	2.15E-03	4.64E-04	1.62E-03	1.22E-04
sum BCAAs	5.21E-01	6.19E-04	1.62E-01	1.81E-03	3.28E-01	1.22E-04
sum aromatic AAs	7.11E-01	6.19E-04	9.19E-02	1.33E-03	3.28E-01	1.22E-04
fischer ratio	5.59E-01	1.09E-01	6.96E-01	4.01E-02	8.56E-01	1.48E-02
sum glucogenic AAs	4.53E-01	3.19E-03	1.62E-01	1.33E-03	6.38E-01	1.64E-04
sum ketogenic AAs	4.53E-01	6.43E-04	4.86E-02	1.33E-03	6.55E-01	1.22E-04
sum total PCs	5.05E-01	4.51E-02	1.79E-01	4.13E-01	7.04E-01	1.44E-01
sum total SMs	5.33E-01	1.74E-02	8.34E-02	7.26E-01	8.31E-01	2.80E-01
sum total lysoPCs	1.00E+00	5.23E-03	2.22E-01	9.63E-02	7.09E-01	3.50E-02
sum total PC aa	4.75E-01	5.69E-02	1.62E-01	5.74E-01	7.09E-01	2.59E-01
sum total PC ae	5.96E-01	1.60E-03	9.26E-02	1.05E-03	6.21E-01	1.22E-04
sum saturated SMs	4.48E-01	8.96E-02	1.26E-01	5.06E-01	7.09E-01	6.74E-01
sum unsaturated SMs	7.49E-01	3.19E-03	2.22E-01	1.00E+00	8.84E-01	4.53E-02
sum SM-OHs	4.52E-01	1.88E-03	9.26E-02	4.64E-03	6.95E-01	2.06E-04
sum saturated PCs	6.43E-01	9.64E-01	2.59E-01	3.84E-01	7.32E-01	7.59E-01
sum monounsaturated PCs	4.48E-01	7.98E-02	2.81E-01	8.13E-01	7.09E-01	5.65E-01
sum unsaturated PCs	4.62E-01	3.05E-02	1.81E-01	3.84E-01	7.04E-01	1.16E-01
sum polyunsaturated PCs	7.33E-01	1.50E-02	7.85E-02	2.44E-01	6.95E-01	2.31E-02

Glucogenic AAs: Amino acids used for the calculation of the sum of glucogenic amino acids were: Arg, Glu, Gln, His, Pro, Ile, Met, Val, Asp, Phe, Tyr, Asn, Ala, Cys, Gly, Ser, Thr and Trp. The selection of glucogenic amino acids was based on Voet *et al.* [286].

Ketogenic AAs: Amino acids used for the calculation of the sum of ketogenic amino acids were: Ile, Leu, Lys, Thr, Phe, Trp and Tyr. The selection of glucogenic amino acids was based on Voet *et al.* [286].

Table S-6: List of p-values for the pairwise comparisons of the tested conditions of the cell culture supernatants for targeted metabolomics.
THLE-2 and Hep G2 cells were either cultivated at a physiological or a diabetic glucose concentration and treated with vehicle or 2 mM metformin. Then, the cell culture supernatant was collected and targeted metabolomics was performed (n per group = 6). For the pairwise comparison of conditions the U-Test was used. The p-values, listed in the table, are Benjamini-Hochberg corrected.

Cell culture supernatant: Targeted metabolomics

Condition	Low vs. high glucose		Low glucose: Control vs. metformin treatment		High glucose: Control vs. metformin treatment	
Cell line	**THLE-2**	**Hep G2**	**THLE-2**	**Hep G2**	**THLE-2**	**Hep G2**
C0	7.86E-01	9.32E-01	1.34E-01	5.01E-02	1.34E-01	1.88E-01
C10	3.02E-01	8.15E-01	5.67E-01	6.66E-01	6.73E-01	4.62E-01
C10:1	9.05E-01	8.99E-01	7.72E-01	2.12E-01	9.27E-01	9.04E-01
C10:2	8.96E-01	8.83E-01	9.05E-01	5.38E-01	9.27E-01	8.14E-01
C12	8.26E-01	8.99E-01	8.26E-01	2.22E-01	6.73E-01	4.62E-01
C12-DC	3.90E-01	8.99E-01	7.72E-01	5.38E-01	6.73E-01	9.04E-01
C12:1	8.96E-01	7.22E-01	7.72E-01	1.49E-01	7.51E-01	9.04E-01
C14	7.50E-01	5.23E-01	8.26E-01	1.49E-01	6.73E-01	9.04E-01
C14:1	7.50E-01	2.76E-01	9.23E-01	1.81E-01	1.00E+00	9.04E-01
C14:1-OH	8.96E-01	6.90E-01	8.26E-01	8.47E-01	7.51E-01	9.04E-01
C14:2	3.90E-01	8.99E-01	1.34E-01	9.23E-01	1.34E-01	9.04E-01
C14:2-OH	7.86E-01	8.99E-01	5.28E-01	5.86E-01	6.73E-01	8.83E-01
C16	8.96E-01	5.23E-01	7.72E-01	6.66E-01	7.48E-01	9.04E-01
C16-OH	8.96E-01	9.32E-01	9.05E-01	3.47E-01	9.27E-01	8.43E-01
C16:1	1.00E+00	8.99E-01	7.72E-01	6.66E-01	8.32E-01	8.83E-01
C16:1-OH	5.01E-01	8.83E-01	2.35E-01	9.74E-01	6.73E-01	6.59E-01
C16:2	7.50E-01	8.99E-01	5.67E-01	6.66E-01	6.73E-01	8.68E-01
C16:2-OH	6.61E-01	5.23E-01	5.67E-01	1.81E-01	8.32E-01	8.68E-01
C18	9.05E-01	6.46E-01	9.05E-01	3.47E-01	6.73E-01	1.00E+00
C18:1	6.61E-01	4.96E-01	6.16E-01	7.81E-01	6.73E-01	8.68E-01
C18:1-OH	7.23E-01	9.32E-01	2.62E-01	4.84E-01	8.99E-01	9.04E-01
C18:2	8.54E-01	7.22E-01	4.40E-01	6.66E-01	6.73E-01	6.89E-01
C2	6.61E-01	4.96E-01	1.34E-01	1.18E-01	1.34E-01	2.35E-01
C3	7.23E-01	3.62E-01	2.35E-01	1.18E-01	1.89E-01	9.04E-01
C5-OH/C3-DC-M	7.50E-01	6.90E-01	1.00E+00	1.81E-01	6.73E-01	9.04E-01
C3-OH	8.54E-01	9.32E-01	8.92E-01	7.26E-01	6.73E-01	5.16E-01
C3:1	2.00E-01	9.32E-01	2.73E-01	5.38E-01	5.08E-01	7.40E-01
C4	7.23E-01	8.99E-01	1.34E-01	5.01E-02	2.36E-01	3.38E-01
C3-DC/C4-OH	2.00E-01	4.80E-01	9.05E-01	9.60E-02	8.32E-01	4.62E-01
C4 1	7.23E-01	7.22E-01	8.26E-01	7.81E-01	6.73E-01	7.40E-01
C5	7.50E-01	9.32E-01	1.34E-01	5.01E-02	1.34E-01	1.34E-01
C5-DC/C6-OH	7.23E-01	4.96E-01	8.26E-01	6.58E-02	6.73E-01	9.04E-01
C5-M-DC	7.50E-01	7.22E-01	9.05E-01	1.18E-01	8.99E-01	9.04E-01
C5:1	8.26E-01	6.90E-01	2.73E-01	7.81E-01	8.70E-01	9.04E-01
C5:1-DC	9.05E-01	1.00E+00	8.26E-01	6.66E-01	6.73E-01	8.83E-01
C6 /C4:1-DC	8.26E-01	5.23E-01	7.72E-01	9.23E-01	8.99E-01	6.59E-01
C6:1	9.05E-01	7.22E-01	3.82E-01	6.66E-01	8.70E-01	9.04E-01
C7-DC	8.96E-01	9.32E-01	9.05E-01	2.22E-01	8.32E-01	9.04E-01

Cell culture supernatant: Targeted metabolomics

Condition	Low vs. high glucose		Low glucose: Control vs. metformin treatment		High glucose: Control vs. metformin treatment	
Cell line	**THLE-2**	**Hep G2**	**THLE-2**	**Hep G2**	**THLE-2**	**Hep G2**
C8	9.05E-01	9.32E-01	9.74E-01	4.84E-01	5.08E-01	7.40E-01
C9	7.50E-01	7.22E-01	7.72E-01	4.84E-01	6.73E-01	9.04E-01
Ala	9.05E-01	5.81E-01	9.05E-01	6.58E-02	6.73E-01	5.16E-01
Arg	9.47E-01	2.76E-01	8.26E-01	1.81E-01	6.73E-01	3.01E-01
Asn	9.47E-01	1.00E-01	8.98E-01	6.10E-01	7.51E-01	1.34E-01
Asp	8.54E-01	1.00E-01	9.05E-01	3.47E-01	9.27E-01	3.38E-01
Cit	9.47E-01	5.23E-01	7.23E-01	2.22E-01	6.73E-01	8.68E-01
Gln	8.54E-01	6.74E-01	9.05E-01	8.74E-01	6.73E-01	8.83E-01
Glu	8.26E-01	1.00E-01	6.16E-01	1.81E-01	6.73E-01	4.62E-01
Gly	7.50E-01	3.62E-01	8.98E-01	7.26E-01	6.73E-01	4.62E-01
His	9.05E-01	5.23E-01	8.26E-01	7.81E-01	8.32E-01	5.16E-01
Ile	9.05E-01	5.81E-01	1.00E+00	4.84E-01	9.27E-01	5.16E-01
Leu	9.47E-01	4.96E-01	9.05E-01	2.22E-01	6.73E-01	3.38E-01
Lys	7.86E-01	4.96E-01	5.28E-01	7.81E-01	2.36E-01	5.95E-01
Met	9.47E-01	4.96E-01	7.23E-01	1.00E+00	8.32E-01	5.95E-01
Orn	8.54E-01	5.23E-01	5.67E-01	3.47E-01	5.08E-01	8.68E-01
Phe	1.00E+00	4.96E-01	9.05E-01	3.47E-01	8.99E-01	4.62E-01
Pro	8.26E-01	6.90E-01	9.23E-01	7.26E-01	8.70E-01	8.68E-01
Ser	9.47E-01	6.90E-01	8.26E-01	5.01E-02	6.73E-01	1.34E-01
Thr	8.96E-01	5.23E-01	7.72E-01	7.26E-01	8.99E-01	6.89E-01
Trp	8.96E-01	4.96E-01	9.23E-01	9.23E-01	9.27E-01	5.16E-01
Tyr	7.86E-01	5.81E-01	8.26E-01	3.47E-01	9.27E-01	8.68E-01
Val	9.05E-01	5.23E-01	7.72E-01	9.23E-01	6.73E-01	5.16E-01
Acetylornithine	1.00E+00	5.23E-01	7.72E-01	2.22E-01	6.73E-01	8.68E-01
ADMA	1.00E+00	7.22E-01	7.23E-01	1.81E-01	4.63E-01	1.00E+00
α-AAA	8.26E-01	4.21E-01	8.98E-01	6.58E-02	1.00E+00	8.83E-01
c4 Hydroxyproline	8.96E-01	6.90E-01	6.16E-01	5.01E-02	6.73E-01	1.34E-01
Carnosine	8.54E-01	5.23E-01	6.16E-01	1.49E-01	6.73E-01	8.68E-01
Creatinine	2.00E-01	5.81E-01	1.34E-01	5.01E-02	1.34E-01	1.34E-01
Dihydroxyphenylalanine	7.86E-01	8.15E-01	NA	9.23E-01	9.53E-01	9.04E-01
Dopamine	NA	6.90E-01	8.26E-01	6.10E-01	6.73E-01	NA
Histamine	3.90E-01	8.83E-01	7.72E-01	6.66E-01	6.73E-01	8.43E-01
Kynurenine	7.86E-01	7.22E-01	5.28E-01	4.84E-01	7.51E-01	8.83E-01
Methioninesulfoxide	8.96E-01	6.90E-01	8.26E-01	5.38E-01	6.73E-01	8.83E-01
Nitrotyrosine	NA	NA	NA	NA	NA	8.14E-01
Phenylethylamine	1.00E+00	1.00E+00	7.23E-01	1.00E+00	9.27E-01	8.14E-01
Putrescine	8.54E-01	6.90E-01	9.05E-01	1.49E-01	1.00E+00	8.43E-01
SDMA	1.00E+00	9.32E-01	8.26E-01	4.40E-01	5.08E-01	8.68E-01
Serotonin	8.26E-01	7.22E-01	9.23E-01	6.10E-01	9.27E-01	7.40E-01
Spermidine	1.00E+00	5.23E-01	7.72E-01	6.66E-01	6.73E-01	8.83E-01
Spermine	8.96E-01	9.85E-01	9.05E-01	2.22E-01	9.27E-01	4.62E-01
t4 Hydroxyproline	1.00E+00	8.15E-01	8.98E-01	2.22E-01	8.99E-01	8.14E-01

Cell culture supernatant: Targeted metabolomics

Condition	Low vs. high glucose		Low glucose: Control vs. metformin treatment		High glucose: Control vs. metformin treatment	
Cell line	**THLE-2**	**Hep G2**	**THLE-2**	**Hep G2**	**THLE-2**	**Hep G2**
Taurine	7.86E-01	8.83E-01	8.26E-01	3.47E-01	6.73E-01	9.04E-01
Total DMA	7.86E-01	6.74E-01	8.98E-01	1.18E-01	6.73E-01	9.04E-01
lysoPC a C14:0	9.05E-01	5.23E-01	1.00E+00	5.38E-01	8.99E-01	8.83E-01
lysoPC a C16:0	6.61E-01	1.00E-01	8.26E-01	7.81E-01	9.27E-01	2.35E-01
lysoPC a C16:1	7.50E-01	4.21E-01	9.23E-01	9.74E-01	8.70E-01	9.04E-01
lysoPC a C17:0	7.50E-01	1.00E-01	4.83E-01	2.99E-01	5.59E-01	9.04E-01
lysoPC a C18:0	3.02E-01	2.76E-01	8.26E-01	9.23E-01	6.73E-01	7.40E-01
lysoPC a C18:1	7.50E-01	1.00E-01	1.00E+00	6.10E-01	8.70E-01	3.01E-01
lysoPC a C18:2	7.50E-01	4.21E-01	6.16E-01	5.86E-01	8.70E-01	6.89E-01
lysoPC a C20:3	8.54E-01	6.74E-01	8.26E-01	5.86E-01	6.73E-01	8.68E-01
lysoPC a C20:4	8.26E-01	4.03E-01	9.05E-01	6.66E-01	9.27E-01	5.16E-01
lysoPC a C24:0	9.05E-01	9.32E-01	9.74E-01	8.74E-01	8.70E-01	9.04E-01
lysoPC a C26:0	8.26E-01	7.22E-01	6.16E-01	1.00E+00	8.70E-01	5.16E-01
lysoPC a C26:1	7.23E-01	7.22E-01	5.28E-01	3.47E-01	8.12E-01	8.83E-01
lysoPC a C28:0	7.23E-01	1.00E+00	8.26E-01	6.66E-01	9.27E-01	7.40E-01
lysoPC a C28:1	9.05E-01	8.99E-01	7.72E-01	7.81E-01	8.12E-01	8.83E-01
PC aa C24:0	3.90E-01	9.85E-01	5.67E-01	4.40E-01	6.73E-01	9.04E-01
PC aa C26:0	6.61E-01	7.22E-01	7.23E-01	7.26E-01	9.27E-01	8.83E-01
PC aa C28:1	7.23E-01	7.22E-01	9.23E-01	7.81E-01	9.27E-01	9.04E-01
PC aa C30:0	7.23E-01	6.74E-01	5.67E-01	6.58E-02	6.73E-01	5.16E-01
PC aa C30:2	7.86E-01	5.23E-01	9.05E-01	6.66E-01	8.70E-01	8.83E-01
PC aa C32:0	8.96E-01	8.99E-01	9.05E-01	5.01E-02	8.32E-01	5.16E-01
PC aa C32:1	9.05E-01	9.32E-01	1.00E+00	5.01E-02	6.73E-01	5.16E-01
PC aa C32:2	7.50E-01	4.96E-01	9.05E-01	6.10E-01	8.70E-01	7.40E-01
PC aa C32:3	8.26E-01	5.81E-01	8.26E-01	6.10E-01	7.51E-01	7.40E-01
PC aa C34:1	7.50E-01	8.99E-01	9.05E-01	5.01E-02	6.73E-01	4.62E-01
PC aa C34:2	8.96E-01	8.83E-01	9.23E-01	5.01E-02	7.51E-01	5.95E-01
PC aa C34:3	1.00E+00	6.90E-01	9.05E-01	4.84E-01	1.00E+00	1.00E+00
PC aa C34:4	4.36E-01	1.00E+00	7.72E-01	7.26E-01	6.73E-01	9.04E-01
PC aa C36:0	9.47E-01	8.83E-01	8.26E-01	2.99E-01	6.20E-01	8.68E-01
PC aa C36:1	7.86E-01	7.22E-01	9.05E-01	7.26E-01	7.51E-01	8.43E-01
PC aa C36:2	9.05E-01	8.15E-01	9.23E-01	5.01E-02	6.73E-01	5.16E-01
PC aa C36:3	1.00E+00	8.99E-01	1.00E+00	1.18E-01	6.73E-01	5.95E-01
PC aa C36:4	1.00E+00	8.99E-01	9.23E-01	7.26E-01	7.51E-01	9.04E-01
PC aa C36:5	9.47E-01	5.81E-01	9.23E-01	5.38E-01	6.73E-01	8.14E-01
PC aa C36:6	9.05E-01	8.99E-01	9.05E-01	9.23E-01	6.73E-01	8.83E-01
PC aa C38:0	9.47E-01	5.23E-01	9.05E-01	7.26E-01	6.73E-01	4.62E-01
PC aa C38:1	9.05E-01	4.96E-01	9.23E-01	8.74E-01	6.73E-01	9.04E-01
PC aa C38:3	9.05E-01	8.99E-01	9.23E-01	5.38E-01	6.73E-01	9.04E-01
PC aa C38:4	8.96E-01	9.32E-01	9.23E-01	3.47E-01	6.73E-01	8.68E-01
PC aa C38:5	8.54E-01	8.83E-01	9.05E-01	7.26E-01	6.73E-01	8.43E-01
PC aa C38:6	8.54E-01	1.00E+00	9.05E-01	8.74E-01	6.73E-01	8.83E-01

Cell culture supernatant: Targeted metabolomics

Condition	Low vs. high glucose		Low glucose: Control vs. metformin treatment		High glucose: Control vs. metformin treatment	
Cell line	**THLE-2**	**Hep G2**	**THLE-2**	**Hep G2**	**THLE-2**	**Hep G2**
PC aa C40:1	6.53E-01	5.81E-01	6.16E-01	6.66E-01	8.99E-01	7.40E-01
PC aa C40:2	7.86E-01	5.23E-01	9.05E-01	8.74E-01	8.12E-01	5.16E-01
PC aa C40:3	8.26E-01	8.15E-01	9.05E-01	8.74E-01	6.73E-01	8.14E-01
PC aa C40:4	9.05E-01	6.90E-01	7.72E-01	4.84E-01	8.99E-01	9.04E-01
PC aa C40:5	8.54E-01	8.15E-01	9.23E-01	5.38E-01	9.27E-01	8.68E-01
PC aa C40:6	8.96E-01	8.83E-01	9.05E-01	1.00E+00	6.73E-01	6.89E-01
PC aa C42:0	6.61E-01	6.90E-01	5.28E-01	6.66E-01	1.00E+00	9.04E-01
PC aa C42:1	7.86E-01	6.90E-01	7.72E-01	3.47E-01	6.73E-01	7.40E-01
PC aa C42:2	1.00E+00	6.90E-01	8.92E-01	7.26E-01	8.70E-01	8.14E-01
PC aa C42:4	7.23E-01	6.74E-01	5.67E-01	9.23E-01	8.70E-01	8.68E-01
PC aa C42:5	8.26E-01	5.81E-01	8.98E-01	2.99E-01	9.84E-01	3.38E-01
PC aa C42:6	6.53E-01	5.23E-01	9.05E-01	9.23E-01	6.73E-01	8.14E-01
PC ae C30:0	3.90E-01	6.90E-01	5.28E-01	4.40E-01	8.99E-01	9.04E-01
PC ae C30:1	9.47E-01	8.15E-01	9.74E-01	7.26E-01	9.27E-01	8.83E-01
PC ae C30:2	7.23E-01	6.90E-01	7.72E-01	6.66E-01	8.99E-01	8.14E-01
PC ae C32:1	7.50E-01	5.81E-01	8.26E-01	9.23E-01	6.73E-01	5.95E-01
PC ae C32:2	7.86E-01	9.32E-01	8.98E-01	3.98E-01	8.99E-01	9.04E-01
PC ae C34:0	7.23E-01	1.00E+00	9.05E-01	9.23E-01	6.73E-01	8.43E-01
PC ae C34:1	7.50E-01	6.74E-01	8.26E-01	7.81E-01	9.27E-01	1.00E+00
PC ae C34:2	9.47E-01	8.83E-01	9.23E-01	1.00E+00	6.73E-01	8.83E-01
PC ae C34:3	7.50E-01	8.99E-01	9.05E-01	5.38E-01	8.32E-01	8.14E-01
PC ae C36:0	7.23E-01	8.99E-01	7.72E-01	7.26E-01	8.70E-01	9.04E-01
PC ae C36:1	8.54E-01	8.99E-01	9.05E-01	9.23E-01	6.73E-01	9.04E-01
PC ae C36:2	8.26E-01	8.83E-01	9.05E-01	1.49E-01	6.73E-01	9.04E-01
PC ae C36:3	9.47E-01	8.83E-01	9.05E-01	7.81E-01	6.73E-01	5.95E-01
PC ae C36:4	8.96E-01	8.99E-01	9.23E-01	5.38E-01	8.99E-01	8.43E-01
PC ae C36:5	9.05E-01	8.99E-01	8.26E-01	6.66E-01	6.73E-01	7.40E-01
PC ae C38:0	8.26E-01	7.22E-01	8.26E-01	4.84E-01	7.51E-01	8.83E-01
PC ae C38:1	9.05E-01	5.23E-01	9.05E-01	7.81E-01	8.99E-01	5.95E-01
PC ae C38:2	9.47E-01	5.23E-01	6.16E-01	7.81E-01	6.73E-01	6.89E-01
PC ae C38:3	9.47E-01	6.90E-01	1.00E+00	1.81E-01	9.27E-01	8.68E-01
PC ae C38:4	9.47E-01	1.00E+00	7.72E-01	9.23E-01	8.70E-01	9.04E-01
PC ae C38:5	8.26E-01	8.83E-01	9.23E-01	1.00E+00	6.73E-01	8.68E-01
PC ae C38:6	7.86E-01	8.15E-01	7.72E-01	6.10E-01	8.99E-01	7.40E-01
PC ae C40:1	8.54E-01	4.96E-01	9.05E-01	4.40E-01	1.00E+00	8.43E-01
PC ae C40:2	7.50E-01	7.22E-01	7.23E-01	6.66E-01	6.73E-01	8.83E-01
PC ae C40:3	6.61E-01	8.15E-01	9.05E-01	9.23E-01	8.70E-01	9.04E-01
PC ae C40:4	9.47E-01	9.32E-01	9.05E-01	8.74E-01	1.00E+00	9.04E-01
PC ae C40:5	7.23E-01	5.81E-01	7.72E-01	8.74E-01	1.00E+00	8.83E-01
PC ae C40:6	1.00E+00	8.99E-01	9.23E-01	6.10E-01	6.73E-01	9.04E-01
PC ae C42:0	7.50E-01	7.22E-01	7.72E-01	5.38E-01	8.99E-01	9.04E-01
PC ae C42:1	2.63E-01	9.32E-01	8.26E-01	7.26E-01	6.20E-01	8.43E-01

Cell culture supernatant: Targeted metabolomics

Condition	Low vs. high glucose		Low glucose: Control vs. metformin treatment		High glucose: Control vs. metformin treatment	
Cell line	**THLE-2**	**Hep G2**	**THLE-2**	**Hep G2**	**THLE-2**	**Hep G2**
PC ae C42:2	8.54E-01	6.46E-01	8.26E-01	7.81E-01	8.32E-01	5.16E-01
PC ae C42:3	8.54E-01	5.23E-01	9.05E-01	5.38E-01	8.70E-01	8.14E-01
PC ae C42:4	9.74E-01	NA	8.26E-01	NA	7.51E-01	NA
PC ae C42:5	8.96E-01	8.99E-01	7.72E-01	5.86E-01	6.73E-01	8.68E-01
PC ae C44:3	8.96E-01	6.90E-01	9.05E-01	9.60E-02	8.99E-01	8.83E-01
PC ae C44:4	9.05E-01	5.23E-01	7.72E-01	4.84E-01	8.32E-01	8.43E-01
PC ae C44:5	7.23E-01	6.90E-01	9.05E-01	3.47E-01	8.99E-01	9.04E-01
PC ae C44:6	3.90E-01	8.83E-01	8.26E-01	7.81E-01	8.99E-01	9.04E-01
SM-OH C14:1	7.50E-01	1.00E+00	8.92E-01	6.10E-01	9.27E-01	8.43E-01
SM-OH C16:1	8.54E-01	7.22E-01	9.23E-01	9.74E-01	1.00E+00	5.16E-01
SM-OH C22:1	8.26E-01	2.76E-01	8.98E-01	4.84E-01	8.70E-01	5.95E-01
SM-OH C22:2	8.54E-01	8.99E-01	7.72E-01	4.84E-01	7.51E-01	1.00E+00
SM-OH C24:1	7.23E-01	7.22E-01	8.26E-01	4.84E-01	9.27E-01	9.04E-01
SM C16:0	7.50E-01	8.83E-01	8.26E-01	9.23E-01	8.70E-01	9.04E-01
SM C16:1	9.05E-01	9.85E-01	9.23E-01	5.38E-01	6.73E-01	9.04E-01
SM C18:0	7.50E-01	5.81E-01	9.05E-01	7.26E-01	8.70E-01	8.68E-01
SM C18:1	9.05E-01	5.23E-01	9.05E-01	1.81E-01	6.73E-01	1.00E+00
SM C20:2	1.00E+00	9.32E-01	8.98E-01	9.23E-01	6.73E-01	1.00E+00
SM C22:3	9.47E-01	7.22E-01	9.23E-01	7.81E-01	9.27E-01	9.04E-01
SM C24:0	8.96E-01	9.32E-01	9.23E-01	1.00E+00	6.73E-01	8.14E-01
SM C24:1	8.54E-01	8.15E-01	9.05E-01	7.81E-01	6.73E-01	9.04E-01
SM C26:0	7.86E-01	6.90E-01	1.00E+00	8.74E-01	1.00E+00	8.43E-01
SM C26:1	7.50E-01	8.99E-01	9.05E-01	5.38E-01	6.73E-01	8.43E-01
H1	2.00E-01	1.00E-01	2.35E-01	5.01E-02	1.34E-01	1.34E-01
sum BCAAs	9.47E-01	5.23E-01	7.72E-01	7.81E-01	6.73E-01	5.16E-01
sum aromatic AAs	1.00E+00	5.23E-01	8.98E-01	1.00E+00	8.99E-01	5.16E-01
fischer ratio	9.05E-01	4.96E-01	8.26E-01	4.84E-01	3.33E-01	7.40E-01
sum glucogenic AAs	9.47E-01	5.23E-01	8.26E-01	9.23E-01	6.73E-01	6.89E-01
sum ketogenic AAs	9.05E-01	4.96E-01	7.72E-01	9.23E-01	6.73E-01	5.16E-01
sum total PCs	7.50E-01	9.32E-01	9.05E-01	5.01E-02	7.51E-01	8.43E-01
sum total SMs	8.26E-01	8.83E-01	9.05E-01	7.26E-01	6.73E-01	9.04E-01
sum total lysoPCs	7.23E-01	1.00E-01	9.05E-01	5.38E-01	8.99E-01	5.16E-01
sum total PC aa	7.50E-01	9.32E-01	9.05E-01	5.01E-02	6.73E-01	8.43E-01
sum total PC ae	7.50E-01	8.15E-01	8.26E-01	7.26E-01	6.73E-01	9.04E-01
sum saturated SMs	7.86E-01	1.00E+00	8.98E-01	7.81E-01	8.99E-01	8.83E-01
sum unsaturated SMs	8.54E-01	6.74E-01	9.23E-01	4.84E-01	6.73E-01	9.04E-01
sum SM-OHs	7.23E-01	5.23E-01	8.26E-01	4.84E-01	6.73E-01	8.68E-01
sum saturated PCs	7.50E-01	5.81E-01	8.26E-01	1.18E-01	6.73E-01	8.43E-01
sum monounsaturated PCs	7.50E-01	1.00E+00	9.05E-01	5.01E-02	8.70E-01	8.43E-01
sum unsaturated PCs	7.50E-01	9.32E-01	9.05E-01	5.01E-02	6.73E-01	8.43E-01
sum polyunsaturated PCs	8.54E-01	9.32E-01	9.23E-01	1.49E-01	6.73E-01	8.83E-01

Glucogenic AAs: Amino acids used for the calculation of the sum of glucogenic amino acids were: Arg, Glu, Gln, His, Pro, Ile, Met, Val, Asp, Phe, Tyr, Asn, Ala, Cys, Gly, Ser, Thr and Trp. The selection of glucogenic amino acids was based on Voet *et al.* [286].

Ketogenic AAs: Amino acids used for the calculation of the sum of ketogenic amino acids were: Ile, Leu, Lys, Thr, Phe, Trp and Tyr. The selection of glucogenic amino acids was based on Voet *et al.* [286].

Table S-7: List of p-values for the pairwise comparisons of the tested conditions of the cell homogenates for non-targeted metabolomics.
THLE-2 and Hep G2 cells were either cultivated at a physiological or a diabetic glucose concentration and treated with vehicle or 2 mM metformin. Then, the cells were harvested via scraping and non-targeted metabolomics and DNA based cell number determination was performed (n per group = 6). For the pairwise comparison of conditions the U-Test was used. The p-values, listed in the table, are Benjamini-Hochberg corrected. Compounds starting with and "X – ", followed by a numerical value were not identified. The "*" indicates compounds, which were identified but not yet confirmed based on a standard.

Cells: Non-targeted metabolomics

Condition	Low vs. high glucose		Low glucose: Control vs. metformin treatment		High glucose: Control vs. metformin treatment	
Cell line	**THLE-2**	**Hep G2**	**THLE-2**	**Hep G2**	**THLE-2**	**Hep G2**
1-(1-enyl-palmitoyl)-GPE (P-16:0)*	8.20E-01	2.60E-01	4.35E-01	6.51E-01	1.00E+00	NA
1-arachidonoyl-GPE (20:4n6)*	8.20E-01	1.35E-01	7.43E-01	5.87E-01	4.22E-01	5.38E-01
1-arachidonoyl-GPI (20:4)*	1.00E+00	1.67E-01	8.86E-01	3.29E-01	6.36E-01	3.79E-01
1-dihomo-linoleoyl-GPC (20:2)*	NA	1.67E-01	NA	5.07E-01	NA	9.18E-01
1-eicosenoyl-GPC (20:1)*	7.19E-01	6.31E-01	NA	8.16E-01	4.56E-01	6.24E-01
1-linoleoyl-GPC (18:2)	NA	4.34E-02	NA	4.48E-01	NA	6.24E-01
1-linoleoyl-GPE (18:2)*	7.19E-01	1.67E-01	4.84E-01	8.16E-01	7.02E-01	5.38E-01
1-myristoyl-GPC (14:0)	NA	1.67E-01	NA	7.44E-01	NA	8.27E-01
1-oleoyl-GPC (18:1)	8.20E-01	2.08E-01	8.22E-01	2.27E-01	6.36E-01	9.18E-01
1-oleoyl-GPE (18:1)	1.00E+00	6.31E-01	4.35E-01	7.44E-01	4.59E-01	1.00E+00
1-oleoyl-GPG (18:1)*	9.54E-01	8.20E-01	1.49E-01	6.74E-01	9.32E-01	6.24E-01
1-oleoyl-GPI (18:1)*	9.20E-01	7.31E-01	6.35E-01	7.44E-01	4.59E-01	7.19E-01
1-oleoyl-GPS (18:1)	7.19E-01	4.34E-02	8.89E-01	3.29E-01	4.22E-01	4.46E-01
1-oleoylglycerol (18:1)	NA	6.31E-01	NA	1.65E-01	NA	1.95E-01
1-palmitoleoyl-GPC (16:1)*	7.19E-01	1.35E-01	4.84E-01	4.48E-01	4.56E-01	7.19E-01
1-palmitoyl-GPC (16:0)	9.54E-01	8.20E-01	4.35E-01	5.87E-01	8.25E-01	3.00E-01
1-palmitoyl-GPE (16:0)	9.54E-01	7.31E-01	4.84E-01	3.82E-01	1.41E-01	2.50E-01
1-pentadecanoyl-GPC (15:0)*	NA	1.35E-01	NA	8.99E-01	NA	2.85E-01
1-stearoyl-GPC (18:0)	9.20E-01	8.91E-01	6.35E-01	6.74E-01	1.80E-01	7.19E-01
1-stearoyl-GPE (18:0)	7.57E-01	8.20E-01	3.82E-01	3.82E-01	6.00E-02	1.50E-01
1-stearoyl-GPG (18:0)	9.54E-01	8.06E-02	9.42E-01	1.07E-01	4.56E-01	3.00E-01
1-stearoyl-GPI (18:0)	7.19E-01	1.00E+00	8.89E-01	2.75E-01	2.85E-01	1.95E-01
1-stearoyl-GPS (18:0)*	7.57E-01	1.05E-01	5.74E-01	1.07E-01	8.34E-02	3.79E-01
10-heptadecenoate (17:1n7)	9.76E-01	1.05E-01	6.35E-01	1.00E+00	9.24E-01	8.85E-02
17-methylstearate	9.54E-01	5.51E-01	4.35E-01	8.16E-01	9.32E-01	3.00E-01
2'-deoxyuridine	7.19E-01	NA	NA	NA	4.56E-01	NA
2-aminoadipate	7.57E-01	3.78E-01	6.35E-01	3.32E-02	1.41E-01	3.21E-02
2-arachidonoyl-GPC (20:4)*	7.19E-01	1.35E-01	6.35E-01	8.16E-01	NA	1.95E-01
2-arachidonoyl-GPE (20:4)*	7.19E-01	2.87E-01	6.35E-01	4.16E-01	5.60E-01	4.42E-01
2-docosahexaenoyl-GPE (22:6)*	9.20E-01	1.35E-01	6.79E-01	8.99E-01	9.58E-01	1.11E-01
2-docosapentaenoyl-GPC (22:5n3)*	NA	1.05E-01	NA	6.74E-01	NA	2.85E-01
2-eicosapentaenoyl-GPE (20:5)*	9.54E-01	5.51E-01	5.74E-01	3.82E-01	2.66E-01	1.95E-01
2-linoleoyl-GPC (18:2)*	7.19E-01	3.13E-01	NA	4.48E-01	6.40E-01	1.00E+00
2-methylbutyrylcarnitine (C5)	7.19E-01	3.49E-02	6.53E-02	3.32E-02	2.68E-02	1.78E-02
2-myristoyl-GPC (14:0)*	9.54E-01	2.08E-01	6.35E-01	8.99E-01	4.56E-01	1.11E-01
2-oleoyl-GPC (18:1)*	8.68E-01	3.78E-01	9.48E-01	3.29E-01	6.63E-01	8.27E-01

Cells: Non-targeted metabolomics

Condition	Low vs. high glucose		Low glucose: Control vs. metformin treatment		High glucose: Control vs. metformin treatment	
Cell line	**THLE-2**	**Hep G2**	**THLE-2**	**Hep G2**	**THLE-2**	**Hep G2**
2-oleoyl-GPE (18:1)*	8.68E-01	5.51E-01	8.89E-01	7.44E-01	7.28E-01	9.18E-01
2-oleoyl-GPG (18:1)*	NA	6.31E-01	NA	1.00E+00	NA	3.00E-01
2-palmitoleoyl-GPC (16:1)*	7.19E-01	2.60E-01	NA	5.07E-01	7.62E-01	1.00E+00
2-palmitoleoyl-GPE (16:1)*	NA	1.35E-01	6.35E-01	8.99E-01	NA	1.11E-01
2-palmitoyl-GPC (16:0)*	9.54E-01	1.67E-01	1.00E+00	4.48E-01	7.02E-01	2.50E-01
2-palmitoyl-GPE (16:0)*	7.19E-01	1.00E+00	NA	8.16E-01	9.32E-01	3.00E-01
2-stearoyl-GPC (18:0)*	7.19E-01	3.78E-01	6.79E-01	1.25E-01	NA	9.18E-01
3-(4-hydroxyphenyl)lactate	NA	4.34E-02	NA	6.74E-01	NA	3.79E-01
3-hydroxybutyrylcarnitine (1)	8.68E-01	2.08E-01	6.53E-02	3.32E-02	2.68E-02	1.78E-02
3-methyl-2-oxovalerate	7.19E-01	5.51E-01	NA	8.84E-02	4.56E-01	2.51E-02
3-phosphoglycerate (isobar with 2-phosphoglycerate)	9.04E-01	4.34E-02	3.31E-01	6.51E-02	5.78E-01	1.78E-02
4-guanidinobutanoate	7.19E-01	2.58E-02	7.43E-01	1.65E-01	5.60E-01	5.38E-01
4-methyl-2-oxopentanoate	9.20E-01	2.60E-01	5.74E-01	8.84E-02	5.60E-01	2.51E-02
4-methylglutamate	7.57E-01	1.05E-01	5.38E-01	8.16E-01	4.56E-01	2.50E-01
5-methylthioadenosine (MTA)	1.00E+00	8.06E-02	4.84E-01	3.29E-01	8.25E-01	6.41E-02
5-oxoproline	7.19E-01	1.35E-01	7.43E-01	1.25E-01	4.22E-01	3.21E-02
6-phosphogluconate	NA	2.58E-02	NA	5.64E-02	2.73E-01	1.11E-01
acetyl CoA	9.54E-01	3.13E-01	6.35E-01	3.09E-01	4.56E-01	6.72E-01
acetylcarnitine	7.19E-01	3.13E-01	6.53E-02	3.32E-02	1.41E-01	3.21E-02
acetylcholine	7.19E-01	2.08E-01	8.89E-01	8.99E-01	1.41E-01	1.47E-01
adenosine	1.00E+00	8.91E-01	6.35E-01	4.48E-01	8.34E-02	3.00E-01
adenosine 5'-diphosphate (ADP)	9.20E-01	3.78E-01	1.92E-01	1.65E-01	1.41E-01	1.78E-02
adenosine 5'-diphosphoribose (ADP-ribose)	NA	3.44E-01	NA	8.75E-01	NA	9.76E-02
adenosine 5'-monophosphate (AMP)	9.54E-01	8.91E-01	9.30E-02	8.84E-02	6.36E-01	1.78E-02
adenosine 5'-triphosphate (ATP)	7.19E-01	6.33E-01	7.43E-01	3.30E-01	2.40E-01	7.65E-01
alanine	9.54E-01	2.58E-02	9.48E-01	3.32E-02	3.41E-01	6.41E-02
alanylleucine	9.20E-01	7.31E-01	9.48E-01	3.82E-01	2.69E-01	6.24E-01
arachidonate (20:4n6)	7.57E-01	1.05E-01	6.35E-01	3.29E-01	4.43E-02	1.50E-01
arginine	7.19E-01	6.31E-01	7.43E-01	3.32E-02	2.68E-02	1.11E-01
benzoylcarnitine*	7.19E-01	3.49E-02	8.89E-01	3.32E-02	2.73E-01	3.21E-02
beta-hydroxyisovaleroylcarnitine	8.20E-01	4.34E-02	6.79E-01	8.84E-02	2.69E-01	1.00E+00
betaine	7.57E-01	2.58E-02	7.43E-01	6.74E-01	4.43E-02	1.78E-02
butyrylcarnitine	7.57E-01	4.63E-01	8.22E-01	5.87E-01	4.43E-02	1.50E-01
C-glycosyltryptophan	7.19E-01	6.07E-02	6.79E-01	4.48E-01	3.43E-02	4.52E-02
carnitine	7.19E-01	3.13E-01	1.92E-01	3.29E-01	2.68E-02	1.00E+00
choline phosphate	7.19E-01	2.58E-02	9.48E-01	3.32E-02	3.43E-02	1.78E-02
citrate	7.19E-01	2.58E-02	6.53E-02	7.44E-01	2.68E-02	1.78E-02
citrulline	7.19E-01	4.34E-02	7.43E-01	3.29E-01	1.00E+00	8.85E-02
coenzyme A	7.57E-01	3.13E-01	4.84E-01	5.07E-01	2.68E-02	4.52E-02
creatine	7.19E-01	2.58E-02	6.53E-02	3.82E-01	2.68E-02	3.21E-02
creatine phosphate	7.19E-01	1.35E-01	6.53E-02	3.32E-02	2.68E-02	1.78E-02

Cells: Non-targeted metabolomics

Condition	Low vs. high glucose		Low glucose: Control vs. metformin treatment		High glucose: Control vs. metformin treatment	
Cell line	**THLE-2**	**Hep G2**	**THLE-2**	**Hep G2**	**THLE-2**	**Hep G2**
creatinine	9.20E-01	8.91E-01	6.79E-01	1.65E-01	4.43E-02	2.50E-01
cysteine	9.54E-01	2.60E-01	6.79E-01	8.84E-02	6.17E-01	1.78E-02
cysteinylglycine	9.54E-01	8.91E-01	6.35E-01	2.75E-01	4.56E-01	1.95E-01
cytidine	7.78E-01	4.63E-01	9.96E-01	5.87E-01	7.62E-01	8.85E-02
cytidine 5'-monophosphate (5'-CMP)	7.19E-01	1.05E-01	8.22E-01	5.10E-02	6.00E-02	9.18E-01
cytidine triphosphate	7.19E-01	6.09E-01	6.79E-01	7.44E-01	2.68E-02	3.79E-01
cytidine-5'-diphosphoethanolamine	8.10E-01	1.86E-01	9.96E-01	3.32E-02	4.59E-01	1.78E-02
deoxycarnitine	8.68E-01	8.91E-01	2.51E-01	3.32E-02	2.68E-02	1.78E-02
dihomo-linolenate (20:3n3 or n6)	8.10E-01	7.31E-01	6.79E-01	3.82E-01	1.49E-01	1.00E+00
docosahexaenoate (DHA; 22:6n3)	7.78E-01	2.60E-01	4.84E-01	4.48E-01	2.89E-01	4.46E-01
eicosenoate (20:1)	7.57E-01	8.06E-02	6.35E-01	4.48E-01	1.00E+00	8.27E-01
erucate (22:1n9)	8.68E-01	1.05E-01	8.22E-01	5.07E-01	6.36E-01	6.24E-01
flavin adenine dinucleotide (FAD)	7.19E-01	3.78E-01	1.75E-01	5.07E-01	8.25E-01	3.21E-02
flavin mononucleotide (FMN)	7.57E-01	4.54E-01	6.35E-01	3.30E-01	2.73E-01	4.42E-01
gamma-glutamylglutamate	7.19E-01	1.67E-01	8.89E-01	1.25E-01	2.68E-02	2.51E-02
gamma-glutamylglutamine	9.54E-01	1.35E-01	6.35E-01	5.00E-01	9.24E-01	8.27E-01
gamma-glutamylisoleucine*	NA	3.78E-01	6.35E-01	3.32E-02	NA	1.78E-02
gamma-glutamylleucine	7.19E-01	4.34E-02	6.79E-01	3.32E-02	4.43E-02	1.78E-02
gamma-glutamylphenylalanine	7.19E-01	3.49E-02	6.35E-01	3.32E-02	5.43E-01	1.78E-02
gamma-glutamylthreonine*	7.19E-01	3.49E-02	9.48E-01	4.48E-01	2.68E-02	2.51E-02
gamma-glutamyltyrosine	NA	1.05E-01	NA	3.32E-02	NA	1.78E-02
gamma-glutamylvaline	9.54E-01	1.67E-01	4.35E-01	2.27E-01	1.80E-01	1.78E-02
glutamate	7.19E-01	4.34E-02	1.00E+00	6.74E-01	2.68E-02	4.52E-02
glutamate, gamma-methyl ester	7.19E-01	2.58E-02	9.48E-01	1.07E-01	9.24E-01	3.21E-02
glutamine	7.19E-01	2.58E-02	6.35E-01	3.82E-01	3.43E-02	6.24E-01
glutathione, oxidized (GSSG)	7.57E-01	6.07E-02	9.48E-01	3.82E-01	1.41E-01	9.18E-01
glutathione, reduced (GSH)	7.19E-01	2.08E-01	6.79E-01	1.07E-01	3.43E-02	1.78E-02
glycerophosphoethanolamine	7.19E-01	6.31E-01	4.35E-01	1.25E-01	2.68E-02	1.78E-02
glycerophosphorylcholine (GPC)	8.68E-01	8.06E-02	1.00E+00	2.75E-01	6.00E-02	1.78E-02
glycylleucine	1.00E+00	7.31E-01	8.67E-01	8.99E-01	7.62E-01	1.00E+00
guanine	8.68E-01	3.49E-02	7.43E-01	5.87E-01	6.36E-01	3.00E-01
guanosine	8.68E-01	3.13E-01	6.79E-01	7.44E-01	4.43E-02	9.18E-01
guanosine 5'-diphospho-fucose	9.54E-01	1.67E-01	3.82E-01	1.25E-01	5.32E-02	1.78E-02
HEPES	9.20E-01	3.78E-01	8.22E-01	5.87E-01	2.68E-02	1.78E-02
hexanoylcarnitine	8.10E-01	3.13E-01	1.00E+00	3.32E-02	3.77E-01	4.46E-01
hippurate	NA	4.34E-02	4.84E-01	3.82E-01	NA	6.24E-01
histidine	7.19E-01	2.58E-02	8.89E-01	8.99E-01	6.00E-02	1.78E-02
hypotaurine	9.54E-01	2.08E-01	4.35E-01	5.10E-02	1.07E-01	4.52E-02
imidazole propionate	7.57E-01	6.07E-02	6.35E-01	1.25E-01	9.24E-01	8.85E-02
inosine	7.19E-01	8.91E-01	3.18E-01	7.44E-01	3.23E-01	5.16E-01
inosine 5'-monophosphate (IMP)	7.19E-01	6.31E-01	1.00E+00	5.07E-01	1.13E-01	5.38E-01
Isobar: fructose 1,6-diphosphate, glucose	7.19E-01	1.43E-01	2.51E-01	NA	1.41E-01	2.15E-01

Cells: Non-targeted metabolomics

Condition	Low vs. high glucose		Low glucose: Control vs. metformin treatment		High glucose: Control vs. metformin treatment	
Cell line	**THLE-2**	**Hep G2**	**THLE-2**	**Hep G2**	**THLE-2**	**Hep G2**
1,6-diphosphate, myo-inositol 1,4 or 1,3-diphosphate						
isobutyrylcarnitine	8.20E-01	2.58E-02	6.53E-02	3.32E-02	2.68E-02	1.78E-02
isoleucine	7.19E-01	8.06E-02	6.79E-01	8.84E-02	6.36E-01	1.78E-02
isoleucylglycine	9.76E-01	2.08E-01	1.00E+00	1.17E-01	4.53E-01	5.38E-01
isovalerylcarnitine	7.19E-01	2.58E-02	6.53E-02	3.32E-02	2.68E-02	1.78E-02
kynurenine	9.54E-01	2.58E-02	7.43E-01	2.75E-01	6.36E-01	1.11E-01
laurylcarnitine	8.24E-01	6.31E-01	1.49E-01	1.07E-01	6.35E-01	2.51E-02
leucine	7.19E-01	2.58E-02	1.00E+00	6.51E-02	1.80E-01	1.78E-02
leucylglycine	7.19E-01	1.47E-01	9.48E-01	4.16E-01	6.36E-01	1.66E-01
lysine	8.20E-01	5.51E-01	6.35E-01	4.48E-01	1.00E+00	1.11E-01
malate	7.57E-01	2.58E-02	6.53E-02	3.29E-01	1.00E+00	3.00E-01
maltotetraose	7.19E-01	NA	NA	NA	2.73E-01	NA
mead acid (20:3n9)	NA	1.67E-01	NA	6.74E-01	NA	3.00E-01
metformin	NA	NA	6.53E-02	3.32E-02	2.68E-02	1.78E-02
methionine	7.19E-01	2.58E-02	6.79E-01	6.74E-01	4.43E-02	1.78E-02
myristoylcarnitine	7.57E-01	8.20E-01	4.84E-01	1.07E-01	6.35E-01	3.21E-02
N(1)-acetylspermine	NA	4.63E-01	6.35E-01	3.29E-01	NA	4.52E-02
N-acetyl-aspartyl-glutamate (NAAG)	7.19E-01	8.91E-01	3.59E-01	3.82E-01	4.22E-01	8.85E-02
N-acetylaspartate (NAA)	7.19E-01	5.51E-01	1.00E+00	6.74E-01	8.34E-02	1.78E-02
N-acetylglutamate	7.19E-01	8.20E-01	8.89E-01	2.75E-01	2.68E-02	1.78E-02
N-acetylmethionine	7.19E-01	8.06E-02	1.92E-01	8.99E-01	4.22E-01	1.50E-01
N-acetylserine	7.19E-01	8.06E-02	7.43E-01	5.87E-01	4.59E-01	5.38E-01
N-acetylthreonine	7.19E-01	3.13E-01	NA	8.99E-01	4.56E-01	1.95E-01
N-acetyltyrosine	NA	3.49E-02	NA	8.16E-01	NA	7.19E-01
N-carbamoylaspartate	7.19E-01	2.58E-02	7.43E-01	5.87E-01	1.41E-01	1.78E-02
N-delta-acetylornithine*	1.00E+00	6.07E-02	8.22E-01	3.29E-01	3.56E-01	4.46E-01
N-formylmethionine	9.20E-01	2.60E-01	7.43E-01	8.99E-01	3.56E-01	1.78E-02
nicotinamide	9.54E-01	2.08E-01	3.18E-01	7.44E-01	1.41E-01	2.50E-01
nicotinamide adenine dinucleotide (NAD+)	8.20E-01	6.31E-01	8.22E-01	3.32E-02	4.22E-01	8.85E-02
nicotinamide adenine dinucleotide reduced (NADH)	7.57E-01	2.58E-02	6.53E-02	3.82E-01	2.68E-02	1.11E-01
octanoylcarnitine	7.19E-01	3.13E-01	4.84E-01	2.75E-01	NA	3.21E-02
oleoylcarnitine	7.19E-01	5.51E-01	2.42E-01	7.44E-01	4.22E-01	5.38E-01
ophthalmate	7.19E-01	3.13E-01	8.89E-01	3.32E-02	2.68E-02	3.21E-02
palmitoleate (16:1n7)	NA	6.12E-01	NA	8.16E-01	NA	4.18E-01
palmitoyl ethanolamide	8.68E-01	4.63E-01	1.92E-01	5.87E-01	6.89E-01	6.41E-02
palmitoylcarnitine	7.19E-01	8.20E-01	6.35E-01	1.25E-01	6.36E-01	1.78E-02
pantothenate	1.00E+00	2.60E-01	3.82E-01	6.51E-02	2.68E-02	1.78E-02
penicillin G	7.19E-01	NA	NA	NA	4.56E-01	NA
phenol red	NA	1.67E-01	NA	8.16E-01	NA	3.21E-02
phenylalanine	7.19E-01	2.58E-02	9.48E-01	2.75E-01	1.13E-01	1.78E-02
phosphate	7.19E-01	4.34E-02	5.74E-01	3.32E-02	2.68E-02	1.78E-02

Cells: Non-targeted metabolomics

Condition	Low vs. high glucose		Low glucose: Control vs. metformin treatment		High glucose: Control vs. metformin treatment	
Cell line	**THLE-2**	**Hep G2**	**THLE-2**	**Hep G2**	**THLE-2**	**Hep G2**
pipecolate	NA	2.60E-01	NA	6.74E-01	NA	3.79E-01
pro-hydroxy-pro	7.19E-01	6.31E-01	7.43E-01	3.67E-01	6.00E-02	3.00E-01
proline	7.19E-01	1.05E-01	8.22E-01	8.16E-01	2.68E-02	3.00E-01
propionylcarnitine	7.57E-01	2.58E-02	1.32E-01	3.32E-02	2.68E-02	1.78E-02
pyridoxal	NA	8.20E-01	NA	5.07E-01	NA	1.50E-01
pyridoxate	NA	5.51E-01	NA	3.82E-01	NA	2.51E-02
pyridoxine (Vitamin B6)	NA	3.13E-01	NA	8.99E-01	NA	1.11E-01
pyroglutamine*	8.20E-01	2.58E-02	3.18E-01	8.16E-01	3.56E-01	6.24E-01
S-adenosylhomocysteine (SAH)	7.19E-01	2.58E-02	6.35E-01	3.29E-01	1.00E+00	1.78E-02
S-lactoylglutathione	7.19E-01	6.07E-02	9.48E-01	9.51E-01	7.28E-01	7.19E-01
S-methylglutathione	NA	2.58E-02	NA	5.87E-01	NA	1.78E-02
S-nitrosoglutathione (GSNO)	7.19E-01	8.91E-01	8.89E-01	6.74E-01	3.43E-02	4.46E-01
serine	8.10E-01	8.62E-01	7.43E-01	8.02E-01	3.97E-01	4.08E-01
spermidine	9.54E-01	2.08E-01	6.35E-01	5.87E-01	3.43E-02	3.79E-01
spermine	1.00E+00	1.00E+00	4.35E-01	7.44E-01	8.34E-02	9.18E-01
sphinganine	NA	1.00E+00	NA	1.25E-01	NA	1.78E-02
sphingosine	9.54E-01	6.31E-01	6.35E-01	1.07E-01	8.80E-01	3.21E-02
stearoylcarnitine	9.04E-01	2.08E-01	4.84E-01	6.51E-02	1.71E-01	1.11E-01
streptomycin	7.19E-01	NA	NA	NA	4.56E-01	NA
succinylcarnitine	7.19E-01	1.35E-01	6.35E-01	1.65E-01	NA	3.21E-02
taurine	7.19E-01	2.58E-02	4.35E-01	1.25E-01	7.28E-01	7.19E-01
taurochenodeoxycholate	NA	2.08E-01	NA	2.75E-01	NA	3.00E-01
thiamin (Vitamin B1)	9.54E-01	5.51E-01	8.22E-01	1.65E-01	7.28E-01	1.00E+00
threonine	7.19E-01	2.58E-02	9.48E-01	2.75E-01	2.68E-02	1.78E-02
trans-4-hydroxyproline	7.19E-01	4.63E-01	4.84E-01	2.75E-01	2.64E-01	3.00E-01
tryptophan	7.19E-01	2.58E-02	9.48E-01	1.07E-01	2.40E-01	1.78E-02
tyrosine	8.20E-01	2.58E-02	6.35E-01	3.82E-01	1.80E-01	1.78E-02
UDP-glucuronate	7.19E-01	2.58E-02	7.43E-01	3.32E-02	6.00E-02	4.52E-02
uridine	7.19E-01	8.91E-01	4.84E-01	8.16E-01	3.43E-02	6.24E-01
uridine 5'-diphosphate (UDP)	7.19E-01	8.71E-01	1.92E-01	1.07E-01	7.62E-01	3.00E-01
uridine 5'-triphosphate (UTP)	9.20E-01	4.63E-01	8.89E-01	1.00E+00	8.34E-02	1.11E-01
uridine monophosphate (5' or 3')	7.19E-01	3.78E-01	3.18E-01	5.87E-01	3.43E-02	6.24E-01
valerylcarnitine	7.19E-01	8.06E-02	7.47E-01	8.16E-01	5.78E-01	2.78E-02
valine	7.57E-01	2.58E-02	8.89E-01	1.25E-01	4.43E-02	1.78E-02
X - 08893	7.19E-01	1.67E-01	9.48E-01	8.16E-01	8.25E-01	8.27E-01
X - 11272	9.20E-01	2.60E-01	6.35E-01	5.07E-01	1.41E-01	8.85E-02
X - 11277	9.20E-01	2.08E-01	4.35E-01	5.07E-01	4.43E-02	4.46E-01
X - 11323	8.20E-01	8.91E-01	3.82E-01	6.51E-02	4.22E-01	6.24E-01
X - 11564	NA	2.58E-02	NA	3.32E-02	NA	3.21E-02
X - 11569	7.19E-01	2.60E-01	9.48E-01	7.44E-01	1.80E-01	4.52E-02
X - 11583	9.54E-01	3.13E-01	2.51E-01	4.48E-01	8.25E-01	1.95E-01
X - 11586	9.20E-01	2.58E-02	8.89E-01	5.07E-01	2.68E-02	1.78E-02

Cells: Non-targeted metabolomics

Condition	Low vs. high glucose		Low glucose: Control vs. metformin treatment		High glucose: Control vs. metformin treatment	
Cell line	**THLE-2**	**Hep G2**	**THLE-2**	**Hep G2**	**THLE-2**	**Hep G2**
X - 11616	NA	8.20E-01	NA	6.51E-02	NA	6.41E-02
X - 11787	7.19E-01	3.13E-01	1.00E+00	8.16E-01	7.28E-01	1.95E-01
X - 12411	NA	3.49E-02	NA	8.16E-01	NA	4.52E-02
X - 12443	7.19E-01	6.33E-01	6.35E-01	5.07E-01	3.77E-01	6.29E-01
X - 12676	1.00E+00	NA	1.00E+00	5.07E-01	4.22E-01	NA
X - 12748	7.19E-01	2.58E-02	8.22E-01	7.44E-01	2.68E-02	8.85E-02
X - 12776	7.19E-01	4.34E-02	1.92E-01	3.32E-02	2.68E-02	1.78E-02
X - 12855	7.19E-01	2.08E-01	6.53E-02	3.32E-02	2.68E-02	1.78E-02
X - 12944	8.68E-01	6.31E-01	1.32E-01	3.32E-02	4.59E-01	1.78E-02
X - 12948	8.68E-01	8.20E-01	6.79E-01	8.99E-01	4.59E-01	2.50E-01
X - 13396	9.76E-01	5.51E-01	9.96E-01	3.29E-01	8.80E-01	9.18E-01
X - 13505	8.68E-01	3.78E-01	8.22E-01	3.32E-02	5.60E-01	2.51E-02
X - 13511	7.19E-01	3.78E-01	1.92E-01	1.25E-01	2.73E-01	2.51E-02
X - 13528	7.19E-01	2.58E-02	6.53E-02	6.51E-02	4.43E-02	6.41E-02
X - 13530	7.19E-01	4.34E-02	6.79E-01	3.29E-01	4.22E-01	1.11E-01
X - 13556	7.57E-01	NA	6.35E-01	NA	2.73E-01	NA
X - 13832	9.20E-01	NA	9.48E-01	NA	2.40E-01	NA
X - 13871	7.19E-01	4.34E-02	6.35E-01	1.25E-01	1.99E-01	2.51E-02
X - 14057	9.04E-01	2.58E-02	1.00E+00	1.07E-01	9.32E-01	1.78E-02
X - 14255	7.19E-01	8.91E-01	6.35E-01	1.25E-01	6.00E-02	9.18E-01
X - 15192	8.68E-01	3.13E-01	8.89E-01	1.25E-01	9.24E-01	1.78E-02
X - 15220	9.54E-01	NA	9.75E-01	NA	4.56E-01	4.42E-01
X - 15303	9.54E-01	2.58E-02	6.35E-01	4.48E-01	9.32E-01	7.19E-01
X - 15306	7.19E-01	9.17E-01	1.00E+00	9.25E-01	4.59E-01	4.18E-01
X - 15352	7.19E-01	8.62E-01	4.84E-01	7.44E-01	2.68E-02	1.00E+00
X - 15458	7.19E-01	1.35E-01	5.74E-01	1.00E+00	1.41E-01	9.18E-01
X - 15472	7.19E-01	3.49E-02	9.30E-02	7.44E-01	4.59E-01	3.00E-01
X - 15474	7.19E-01	2.60E-01	1.92E-01	5.07E-01	2.40E-01	2.45E-01
X - 15497	NA	6.07E-02	NA	2.75E-01	NA	6.24E-01
X - 15558	7.57E-01	1.67E-01	6.79E-01	5.87E-01	2.85E-01	4.46E-01
X - 15559	7.19E-01	1.35E-01	6.79E-01	5.07E-01	1.13E-01	1.95E-01
X - 15562	7.57E-01	1.05E-01	8.22E-01	4.48E-01	1.41E-01	1.11E-01
X - 15563	8.20E-01	1.67E-01	6.35E-01	2.75E-01	1.80E-01	2.50E-01
X - 15591	9.54E-01	8.62E-01	6.35E-01	6.09E-01	4.56E-01	8.14E-01
X - 15678	7.19E-01	7.31E-01	6.35E-01	5.87E-01	NA	6.41E-02
X - 16439	8.68E-01	3.13E-01	7.43E-01	5.07E-01	2.85E-01	4.46E-01
X - 17101	7.19E-01	6.78E-01	8.22E-01	4.99E-01	3.43E-02	2.78E-02
X - 17254	8.68E-01	4.63E-01	6.79E-01	1.07E-01	1.13E-01	7.17E-01
X - 17638	8.68E-01	3.78E-01	3.18E-01	7.44E-01	3.56E-01	6.41E-02
X - 18341	NA	2.58E-02	NA	5.07E-01	NA	4.52E-02
X - 18739	7.19E-01	3.78E-01	6.35E-01	1.07E-01	2.73E-01	1.78E-02
X - 19363	9.54E-01	NA	6.35E-01	NA	4.56E-01	NA

Cells: Non-targeted metabolomics

Condition	Low vs. high glucose		Low glucose: Control vs. metformin treatment		High glucose: Control vs. metformin treatment	
Cell line	**THLE-2**	**Hep G2**	**THLE-2**	**Hep G2**	**THLE-2**	**Hep G2**
X - 19365	9.04E-01	NA	6.35E-01	1.74E-01	2.73E-01	4.42E-01
X - 19524	9.54E-01	8.06E-02	5.74E-01	7.44E-01	1.13E-01	1.11E-01
X - 19561	NA	2.58E-02	NA	3.82E-01	NA	1.11E-01
X - 19807	9.20E-01	6.07E-02	3.82E-01	1.25E-01	1.13E-01	1.78E-02
X - 19808	8.68E-01	1.05E-01	4.84E-01	1.65E-01	1.80E-01	1.78E-02
X - 20051	8.68E-01	8.06E-02	9.48E-01	7.44E-01	9.24E-01	1.00E+00
X - 21004	9.54E-01	8.20E-01	6.79E-01	1.00E+00	1.80E-01	1.11E-01
X - 21027	7.19E-01	2.60E-01	1.00E+00	1.65E-01	3.56E-01	1.50E-01
X - 21031	8.68E-01	8.20E-01	6.79E-01	5.07E-01	2.68E-02	1.00E+00
X - 21365	7.19E-01	8.20E-01	7.43E-01	2.75E-01	8.34E-02	1.00E+00

Publications and presentations

Publications

C. Muschet, G. Möller, C. Prehn, M. Hrabě de Angelis, J. Adamski, and J. Tokarz, "Removing the bottlenecks of cell culture metabolomics: fast normalization procedure, correlation of metabolites to cell number, and impact of the cell harvesting method," *Metabolomics*, vol. 12, no. 10, p. 151, 2016.

A. Ly, M. F. Scheerer, S. Zukunft, **C. Muschet**, J. Merl, J. Adamski, M. Hrabě de Angelis, S. Neschen, S. M. Hauck, and M. Ueffing, "Retinal proteome alterations in a mouse model of type 2 diabetes," *Diabetologia*, vol. 57, no. 1, pp. 192–203, 2014.

Submitted publications

M. Rottenkolber, **C. Muschet**, M. Breier, M. Fugmann, V. Sacco, M. Weise, S. Heinrich, C. Prehn, H. Grallert, M. Bidlingmaier, M. Hrabě de Angelis, J. Seissler, M. Reincke, J. Adamski, U. Ferrari, and A. Lechner, "Targeted metabolomics to predict the primary success of metformin monotherapy in type 2 diabetes," *Scientific Reports (Submitted)*.

Master´s Thesis

C. L. Muschet, "Cell culture based assay for metabolic changes caused by nutrients and anti-diabetic substances," (Master´s thesis), Munich: Technical University Munich, 2012.

Presentations

M. Rottenkolber (presenter), **C. Muschet**, M. Breier, M. Fugmann, V. Sacco, M. Weise, C. Prehn, H. Grallert, M. Bidlingmaier, M. Hrabě de Angelis, J. Seissler, M. Reincke, J. Adamski, U. Ferrari, and A. Lechner, "Targeted metabolomics to predict the primary success of metformin monotherapy in type 2 diabetes," *52nd EASD Annual Meeting*, Munich (Germany), September 12th - 16th 2016.

Poster presentations

This section cites the posters as listed in the abstract booklets and programmes of the conferences. In some cases, the titles or author lists were modified after the submission of the abstract. In these cases, the citations of the presented posters are listed in the according footnotes.

C. Muschet, C. Prehn, A. Artati, G. Möller, M. Hrabě de Angelis and J. Adamski, "Impact of metformin and glucose on the hepatocellular metabolism," *12th Annual Conference of the Metabolomics Society*, Dublin (Ireland), June 27th - 30th 2016.

M. Haid, M. Rudisch, **C. Muschet** and J. Adamski, "Targeted metabolomics assay for absolute quantification of omega-3 and omega-6 oxylipins in human plasma," *12th Annual Conference of the Metabolomics Society*, Dublin (Ireland), June 27th - 30th 2016.

A. Artati, A. Wilmes, A. Cecil, P. Jennings and J. Adamski, "Metabolome changes during differentiation of induced pluripotent stem (iPS) cell into renal lineages," *12th Annual Conference of the Metabolomics Society*, Dublin (Ireland), June 27th - 30th 2016[1].

C. Muschet, M. Hrabě de Angelis, J. Adamski and J. Tokarz, "Novel high-throughput DNA quantification method for normalization of cell culture metabolomics data," *11th Annual International Conference of the Metabolomics Society*, San Francisco (U.S.A), June 29th - July 2nd 2015[2].

A. Artati , **C. Muschet**, J. Tokarz, M. Hrabě de Angelis and J. Adamski, "Optimizing the harvesting and extraction method of adherently growing cells for non-targeted metabolomics analysis," *11th Annual International Conference of the Metabolomics Society*, San Francisco (U.S.A), June 29th - July 2nd 2015[3].

M. Haid, **C. Muschet**, T. Friedrich, W. Roemisch-Margl, C. Prehn, M. Hrabě de Angelis and J. Adamski, "Long-term stability of plasma metabolites stored at -80°C," *11th Annual International Conference of the Metabolomics Society*, San Francisco (U.S.A), June 29th - July 2nd 2015[4].

C. Muschet, S. Zukunft, G. Möller, C. Prehn, M. Hrabě de Angelis and J. Adamski, "Impact of metformin and hexoses on the lipid profile of HepG2, Hepa1-6 and differentiated 3T3-L1 cells," *5th International Singapore Lipid Symposium*, Singapore (Singapore), March 18th - 21st 2014.

C. Muschet, S. Zukunft, G. Möller, C. Prehn, M. Hrabě de Angelis and J. Adamski, „Impact of metformin on HepG2, Hepa1-6 and differentiated 3T3-L1 cells under glucose and galactose conditions," *9th Annual Conference of the Metabolomics Society*, Glasgow (Scotland), July 1st - 4th 2013.

---

[1] The author (C. Muschet) is only listed on the final poster, presented at the 12th Annual Conference of the Metabolomics Society, as she was added to the author´s list after the submission of the abstract.

A. Artati, A. Wilmes, A. Cecil, **C. Muschet**, P. Jennings and J. Adamski, "Metabolome changes during differentiation of induced pluripotent stem (iPS) cells into renal lineages," *12th Annual Conference of the Metabolomics Society*, Dublin (Ireland), June 27th - 30th 2016

[2] **C. Muschet**, M. Hrabě de Angelis, J. Adamski and J. Tokarz, "Novel high-throughput DNA quantification method for normalization of metabolomics data from cell culture," *11th Annual International Conference of the Metabolomics Society*, San Francisco (U.S.A), June 29th - July 2nd 2015.

[3] A. Artati , **C. Muschet**, J. Tokarz, M. Hrabě de Angelis and J. Adamski, "Optimizing the harvesting and extraction method of adherently growing cells for non-targeted metabolomics analyses," *11th Annual International Conference of the Metabolomics Society*, San Francisco (U.S.A), June 29th - July 2nd 2015.

[4] M. Haid, S. Wahl, **C. Muschet**, C. Prehn, W. Römisch-Margl, M. Hrabě de Angelis and J. Adamski[4], "Long-term stability of plasma metabolites stored at -80 °C," *11th Annual International Conference of the Metabolomics Society*, San Francisco (U.S.A), June 29th - July 2nd 2015.

C. Prehn, S. Zukunft, M. Haid, **C. Muschet**, M. Waldenberger, B. Thorand, A. Peters and J. Adamski, "Implementation of a multiple steroid quantification in the KORA F4 Study," *2nd Congress on Steroid Research*, Chicago (U.S.A), March 10th - 12th 2013.